UNIVERSIDAD DE BARCELONA
Departamento de Bioquímica y Biología Molecular
Facultad de Farmacia

IMPLICATION OF LONG-CHAIN FATTY ACIDS IN GLUCOSE-INDUCED INSULIN SECRETION IN THE PANCREATIC β-CELL

LAURA HERRERO RODRÍGUEZ

2004

Memoria presentada por Laura Herrero Rodríguez, Licenciada en Química por la Universidad de Barcelona, para optar al grado de Doctora en la Universidad de Barcelona.

Esta tesis ha sido realizada bajo la dirección de la Doctora Guillermina Asins y el Doctor Fausto García Hegardt, en el Departamento de Bioquímica y Biología Molecular de la Facultad de Farmacia de la Universidad de Barcelona.

Laura Herrero

Dra. Guillermina Asins

Dr. Fausto G. Hegardt

Barcelona, octubre de 2004

Programa de doctorado: Biomedicina

Bienio 1999-2001

A mis padres

LAS RANITAS EN LA NATA

Había una vez dos ranas que cayeron en un recipiente de nata. Inmediatamente se dieron cuenta de que se hundían: era imposible nadar o flotar demasiado tiempo en esa masa espesa como arenas movedizas. Al principio, las dos ranas patalearon en la nata para llegar al borde del recipiente. Pero era inútil; sólo conseguían chapotear en el mismo lugar y hundirse. Sentían que cada vez era más difícil salir a la superficie y respirar.

Una de ellas dijo en voz alta: "No puedo más. Es imposible salir de aquí. En esta materia no se puede nadar. Ya que voy a morir, no veo por qué prolongar este sufrimiento. No entiendo qué sentido tiene morir agotada por un esfuerzo estéril".

Dicho esto, dejó de patalear y se hundió con rapidez, siendo literalmente tragada por el espeso líquido blanco.

La otra rana, más persistente o quizá más tozuda se dijo: "¡No hay manera! Nada se puede hacer para avanzar en esta cosa. Sin embargo, aunque se acerque la muerte, prefiero luchar hasta mi último aliento. No quiero morir ni un segundo antes de que llegue mi hora".

Siguió pataleando y chapoteando siempre en el mismo lugar, sin avanzar ni un centímetro, durante horas y horas.

Y de pronto, de tanto patalear y batir las ancas, agitar y patalear, la nata se convirtió en mantequilla.

Sorprendida, la rana dio un salto y, patinando, llegó hasta el borde del recipiente. Desde allí, pudo regresar a casa croando alegremente.

JORGE BUCAY

Déjame que te cuente…

GRACIAS, GRÀCIES, THANKS, MERCI

En primer lugar quiero mostrar mi más profundo agradecimiento a mis directores de tesis. Al Prof. Fausto García Hegardt por abrirme las puertas al mundo de la ciencia y permitirme realizar la tesis en su grupo, por su dedicación plena y entusiasmo en la investigación. A Guillermina Asins, por su dinamismo y buen humor y por darme grandes dosis de energía cuando lo necesitaba. Y a Dolors Serra que ha estado de manera constante a mi lado, por su paciencia y amabilidad.

Especialmente quisiera dar las gracias a todos los compañeros del grupo con los que he pasado tantas horas, por dar el mejor ambiente al laboratorio que hubiera podido desear, por tratar los problemas con una sonrisa y por apoyarme en todo. A ti Montse, que me contagiaste de ilusión por hacer el doctorado, a Blanca que me has enseñado tanto, a David por ser el compañero ideal para compartir problemas, risas, limpieza y orden en el laboratorio y a Assia, Irene, Guillem y Toni, porque juntos hemos hecho un gran equipo. Muchas gracias a Núria Casals que me ha mostrado siempre su ayuda e interés por la tesis. Gracias también a Rosa Aledo por sus comentarios y nuestra página web.

Agradecer también a todos los demás grupos del Departamento, por su ayuda en un momento u otro de la tesis. Mil gracias también a Mari Carmen, Jordi, Tina y especialmente a Silvia porque el Departamento entero ha cambiado de color a tu lado. También a Ana y a Teresa por darme ánimos y recibirme siempre con una sonrisa.

I would like to express my heartfelt thanks to Prof. Marc Prentki for giving me the opportunity to stay in his lab, for his scientific enthusiasm, hepful suggestions and optimism. Many thanks, Jean for showing me the best people and places in Montreal. Johane, je te remercie beaucoup pour ton aide avec les cellules, pour faire de cette thèse un peut plus facile. Thanks also to the other members of Prentki's lab: Raphaël, Ewa, Marie-Line, Eric, Serge and Wissal. Finally, thanks to Alix and Diane.

I am very grateful to Prof. CB. Wollheim for accepting me during my three months' stay in his lab. Many thanks also to Pierre Maechler, Haiyan Wang, Victor, Marina, Mariella, Thierry, Yan and Anneli.

Mil gracias a los mejores haciendo reuniones y comilonas y sobretodo por llenar de risas los fines de semana. A Jordi, Isabel, Gisela, Judith, Riad, Jose Luís, Ruth, Evaristo (y el peque), Damian, Vero y Juan. También a mis grandes compañeros de "química": Marta, Jordi, Lucrecia, Marisa, Mar, Roger, Javi, David, Ana, Igor, Silvia, JuanFra, Jorge, Raquel, Isabel, Ignacio, Oriol y Belén, porque sigamos manteniendo el contacto. Gracias también a mis amigas de toda la vida: Mª Pilar, Núria y Berta.

Agradecer con infinito cariño a mis padres y a mi hermana porque se han desvivido siempre por mí dándome la mejor educación, ayuda y apoyo incondicional en todo momento. ¡Os lo debo todo a vosotros! Quisiera dar las gracias también al resto de mi familia: mis abuelos, tíos y primos, por quererme tanto y estar siempre a mi lado.

Finalmente a ti Rubén, gracias por tu cariño, infinita paciencia y comprensión. Por tus acertados consejos y por estar siempre ahí, para lo bueno y para lo malo.

Este trabajo ha sido realizado con la ayuda de las becas de Formación de Personal Universitario del Ministerio de Educación y Ciencia y la Universidad de Barcelona. I am also very grateful to Robin Rycroft of the Language Service for valuable assistance in the preparation of the manuscript.

Laura

ABBREVIATIONS

ABBREVIATIONS

Ab	antibody
Abs	absorbance
A.C.	autoclaved
ACC	acetyl-CoA carboxylase
ADD1	adipocyte determination and differentiation factor-1 (or SREBP-1)
AICAR	5-aminoimidazole-4-carboxamide ribonucleoside
AMPK	AMP-activated protein kinase
amp^r	ampicillin-resistance
ASP	Acid-Soluble Products
bd.	bidistilled water
bp	base pair
BSA	Bovine Serum Albumin
CACT	carnitine:acylcarnitine translocase
cDNA	complimentary DNA
CE	Cholesterol Ester
Ci	curie
CIP	Calf Instestinal alkaline Phosphatase
ChAT	choline acetyltransferase
CL	citrate lyase
CMV	cytomegalovirus
CoA	Coenzyme A
COT	Carnitine Octanoyltransferase
cpm	counts per minute
CPT	Carnitine Palmitoyltransferase
DAG	diacylglycerol
DEPC	diethylpyrocarbonate
DHB	dihydroxybenzoic acid
DIO	diet-induced obese
DMF	dimethyl formamide
DMSO	dimethyl sulfoxide

DNA	deoxyribonucleic acid
DNase	deoxyribonuclease
dNTPs	2'-deoxynucleosides 5'-triphosphate
dox	doxycycline
DTE	dithioeritrol
DTT	dithiothreitol
EDTA	ethylenediamine-tetraacetic acid
EGTA	ethylene glycol-bis (aminoethyl ether)- N,N,N',N'- tetraacetic acid
ER	endoplasmic reticulum
FA-CoA	fatty acyl-CoA
FAS	Fatty Acid Synthase
FBS	Fetal Bovine Serum
FCCP	carbonyl cyanide 4-trifluoromethoxyphenylhydrazone
FFA	free fatty acids
for	forward
GAD	glutamate decarboxylase
GK	glucokinase
GLUT-2	glucose transporter-2
GSH	glutathione (reduced form)
GSIS	glucose-stimulated insulin secretion
h	hour
HBSS	Hanks Balanced Salt Solution
hCMV	human cytomegalovirus
HEK	Human Embryo Kidney
HEPES	N-2-hydroxyethylpiperazine-N'-2-ethanesulfonic acid
HNF	hepatocyte nuclear factor
HRP	horseradish peroxidase
ICV	intracerebroventricular
I.D.	Internal Diameter
IDDM	insulin-dependent diabetes mellitus
IGF	insulin-like growth factor
ip	intraperitoneal
IRS	insulin receptor substrate

IU	insulin units
K_m	Michaelis constant
kDa	kiloDalton
KO	knock-out
KRBH buffer	Krebs-Ringer Bicarbonate Hepes buffer
LCAS	long-chain acyl-CoA synthetase
LC-CoA	long-chain fatty acyl-CoA
LXR	liver X receptor
M	molar (mol/l)
mA	milliamps
MCD	malonyl-CoA decarboxylase
MCS	Multiple Cloning Site
MIDD	Maternally Inherited Diabetes and Deafness
MIM	Mitochondria Inner Membrane
min	minute
ml	millilitre
MODY	Maturity-Onset Diabetes of the Young
MOM	Mitochondria Outer Membrane
MOPS	3-(N-Morpholino)propanesulfonic acid
MTT	3-(4,5-dimethylthiazol-2-yl)-2,5-diphenyltetrazolium bromide
MW	Molecular Weight
NADPH	Nicotinamide Adenine Dinucleotide Phosphate (reduced form)
naSREBP-1c	nuclear active form of SREBP-1c
NEFA	non-esterified fatty acids
NE palm	Non-Esterified Palmitate
NIDDM	non-insulin-dependent diabetes mellitus
NPY	neuropeptide Y
OD	optical density
o/n	over night
PAGE	polyacrylamide gel electrophoresis
PBS	Phosphate-Buffered Saline
PC	pyruvate carboxylase
PCR	Polymerase Chain Reaction
PDH	pyruvate dehydrogenase

PEG	polyethylene glycol
pfu	adenovirus plaque forming units
PKC	protein kinase C
PL	phospholipid
PMA	phorbol myristate acetate
PMSF	phenylmethylsulfonyl fluoride
PPAR	peroxisomal proliferator-activated receptor
PPRE	peroxisome proliferator response element
ppt.	pellet
PS	phosphatidylserine
rev	reverse
Rf	rate factor
RIA	radioimmunoassay
RIP	Rat Insulin Promoter
RNA	ribonucleic acid
RNase	ribonuclease
rpm	revolutions per minute
r.t.	room temperature
rtTA	reverse tTA
S.A.	Specific Activity
SCAP	SREBP cleavage-activating protein
SDS	Sodium Dodecyl Sulphate
sec	seconds
sp.	species
S.R.	Specific Radioactivity
SRE	Sterol regulatory element
SREBP	Sterol Regulatory Element Binding Protein
SSC	sodium chloride and sodium citrate solution
sup.	supernatant
TCA	tricarboxylic acid cycle
TEMED	N,N,N'N'-tetramethyl-ethylenediamine
tet	tetracycline
tetO	tetracycline operator
TetR	tetracycline repressor

tet^{r}	tetracycline-resistance
TG	triacylglycerol
TLC	Thin Layer Chromatography
Tm	melting temperature
TNFα	tumor-necrosis factorα
TOFA	5-(tetradecyloxy)-2-furoic acid
tTA	tetracycline transactivator protein
TRE	Tetracycline-Response Element
TZD	thiazolidinedione
U	Units
UCP	uncoupling protein
UV	Ultraviolet
V	volts
ZDF	Zucker diabetic fatty

INDEX

INDEX

INTRODUCTION

RESULTS

INTRODUCTION

INTRODUCTION

1. DIABETES

Diabetes mellitus is a disease characterized by uncontrolled hyperglycemia, the result of either the failure of insulin production, or a combined defect in insulin production and action. This leads to the dysregulation of glucose metabolism.

Concurrent with the spread of the western lifestyle, which is linked with an increasingly overweight and sedentary population, the prevalence of diabetes is rising dramatically. It is estimated to affect 4% of the world's population, with the number of diabetics increasing by 4-5% per year[1]. The statistics are alarming: the global figure of people with diabetes is set to rise from about 118 million in 1995 to 220 million in 2010 and 300 million in 2025[2].

Diabetes is characterized by fasting hyperglycemia as a consequence of the lack of insulin or of its correct action in the liver and in peripheral tissues, accompanied by increased levels of glucagon. In addition, free fatty acids (FFA) from the adipose tissue are abnormally mobilized, promoting the stimulation of hepatic ketogenesis. These metabolic disorders lead to the typical symptoms of diabetes: polyuria, polyphagia, polydipsia and loss of weight. Diabetes is associated with neuropathy, nephropathy, retinopathy, coronary heart disease and early death. The result is disability, impact on the quality of life of the patients and shortened life expectancy; which have a serious impact on both the social and economic costs of diabetes to the health care system in the developed and developing world.

Clinical diabetes is considered to be attained when fasting plasma glucose levels exceed 126 mg/dl. Maintaining a healthy diet and an active exercise program are important components in the prevention and treatment of diabetes. Even while maintaining a healthy lifestyle, most patients need pharmacological intervention which might consist of one or a combination of the following oral medications: sulfonylureas,

[1] Wagman A, Nuss JM. Current therapies and emerging targets for the treatment of Diabetes. *Curr. Pharm. Des.* 7:417-450, 2001

[2] King H, Aubert RE, Herman WH. Global burden of Diabetes, 1995-2025. Prevalence, numerical estimates and projections. *Diabetes Care.* 21:1414-1431, 1998

metformin or thiazolidinediones. However 30-40% of patients are not adequately controlled by these therapies and require subcutaneous insulin injections intended to restore normoglycemia, but they can inadvertently lead to hypoglycemia, a potentially fatal consequence. Thus, new drugs and novel methods of treatment such as gene therapy are needed.

Diabetes mellitus has been known since the time of Aristotle. In 1889 Oskar Minkowski observed that the urine from pancreatectomized dogs attracted an unusual number of flies. Intrigued, he tasted the urine and was struck by its sweetness. From this simple but astute observation, he established for the first time that the pancreas produced some entity essential for control of the blood sugar concentration, which, when absent, resulted in diabetes mellitus. Several decades later, in 1921 Frederick Banting identified the active pancreatic principle as insulin. Thus, the concept of an insulin-glucose axis as a central component of fuel homeostasis came into being. In keeping with its etymological derivation, diabetes mellitus has been viewed ever since as a disorder primarily associated with abnormal glucose metabolism. However, it is now clear that glucose metabolism and lipid metabolism are intimately interrelated. McGarry[3] postulated that if Minkowski had focused on the smell of acetone in the diabetic urine, generated from fatty acid metabolism, instead of the taste of the sugar, perhaps we would have advanced our understanding of the disease more rapidly.

1.1 TYPE 1 DIABETES

Among diabetic patients, 10-25% fall into the category of insulin-dependent diabetes mellitus (IDDM) or Type 1 diabetes, which generally appears before age 40, frequently in adolescence, and results from autoimmune destruction of insulin-producing pancreatic β-cells. Type 1 diabetic patients dramatically depend on insulin administration for their survival.

1.1 TYPE 2 DIABETES

Non-insulin-dependent diabetes mellitus (NIDDM) or Type 2 diabetes is far more common than IDDM, affecting 75-90% of diabetic patients. It is characterized by a combination of genetic and environmental factors that affect the organism's ability to respond to insulin. The condition has two hallmark features: 1) insulin resistance,

[3] McGarry JD. What if Minkowski had been ageusic? An alternative angle of Diabetes. *Science*. 258:766-770, 1992

defined as an impaired ability of the hormone to suppress hepatic glucose output and to promote peripheral glucose disposal and 2) compromised function of the pancreatic β-cell such that insulin secretion is insufficient to match the degree of insulin resistance.

The early stages of Type 2 diabetes are characterized by a conjunction of metabolic and hormonal abnormalities including insulin resistance, hyperinsulinemia, hyperlipidemia, glucose intolerance and, in some instances, hypertension. These symptoms are often collectively referred to as syndrome X[4]. The temporal sequence in which these component derangements appear and how they relate to one another has been extensively debated[5].

Despite the gaps in our knowledge, there is general agreement that Type 2 diabetes, unlike IDDM, is tightly associated with obesity[6]. Over 80% of individuals with Type 2 diabetes are obese. However, only 10% of obese individuals are diabetic. In the prediabetic phase, when insulin resistance has already begun, the β-cell actually hypersecretes insulin despite normal blood glucose levels. What has defied explanation is precisely what causes this insulin resistance in the first place and how it relates in a temporal sense to the accompanying hyperinsulinemia. Type 2 diabetes is related almost invariably to a serious breakdown in lipid dynamics, often reflected by elevated levels of circulating FFA and triglycerides, together with excessive deposition of fat in various tissues including the muscle bed[7]. Less clear has been whether this breakdown in lipid homeostasis is a result of the diabetic state or is in fact instrumental in its development.

1.2.1 Monogenic forms of Type 2 diabetes

A minority of Type 2 diabetic patients (2-5%) have a form of diabetes that results from mutations in a single gene, which might result in either β-cell dysfunction or, less frequently, insulin resistance. The most common genetic subtypes are the dominantly inherited maturity-onset diabetes of the young (MODY) and maternally inherited diabetes and deafness (MIDD). MODY is a genetically heterogeneous monogenic form of Type 2 diabetes mellitus, characterized by early onset, usually

[4] Reaven GM. The role of insulin resistance and hyperinsulinemia in coronary heart disease. *Metabolism.* 41:16-19, 1992

[5] McGarry JD. Glucose-fatty acid interactions in health and disease. *Am. J. Clin. Nutr*. 67:500S-504S, 1998

[6] Nadler ST, Stoehr JP, Schueler KL, Tanimoto G, Yandell BS, Attie AD. The expression of adipogenic genes is decreased in obesity and Diabetes mellitus. *Proc. Natl. Acad. Sci.* USA. 97:11371-11376, 2000

[7] Reaven GM. The fourth musketeer-from Alexadre Dumas to Claude Bernard. *Diabetologia*. 38:3-13, 1995

before 25 years of age and often in adolescence or childhood and by autosomal dominant inheritance[8]. Mutations in five different genes allow the classification of the different types of MODY: hepatocyte nuclear factor (HNF)-4α (MODY 1), glucokinase (MODY 2), HNF-1α in chromosomal 12q (MODY 3), insulin promoter factor-1α (MODY 4) and HNF-1α in chromosomal 17q (MODY 5). MIDD is characterized by maternally inherited mitochondrial gene mutations. This causes a reduced oxidative phosphorylation capacity, resulting in a lower ATP/ADP ratio and therefore, a reduced capacity to secrete insulin (see Section 4.1). Patients with MIDD have early onset Type 2 diabetes that frequently progresses to insulin requirement owing to progressive β-cell loss[9].

2. STRUCTURE AND FUNCTION OF THE PANCREAS

The pancreas consists of acinar (exocrine) cells and islets of endocrine cells embedded within the much larger mass of the exocrine pancreas. These hormone-secreting islets are called islets of Langerhans in honor of the scientist who first described them in 1869. Each islet of Langerhans is composed of about 2,000 cells, they are ductless, have a rich blood supply, and are innervated in many species. An adult human has roughly 1 g of islet tissue constituted by approximately 1 to 2 million islets, but they represent only about 1 to 2% of pancreatic tissue. Each islet is composed of distinct α, β, δ and PP cells (Fig. 1), which constitute 25%, 60%, 10% and 5% of the total islet cells, respectively. The α, β, δ and PP cells secrete glucagon, insulin, somatostatin and pancreatic polypeptide, respectively. Glucagon and insulin are inhibited reciprocally while somatostatin inhibits both glucagon and insulin.

[8] Frayling T. Maturity-onset Diabetes of the young: a monogenic model of Diabetes. In Type 2 Diabetes: Prediction and Prevention. *Hitman G. ed*. John Wiley & Sons. 107-126, 1999

[9] Permutt MA, Hattersley AT. Searching for Type 2 Diabetes Genes in the post-genome Era. *Trends in endocrinology and metabolism.* 11: 383-393, 2000

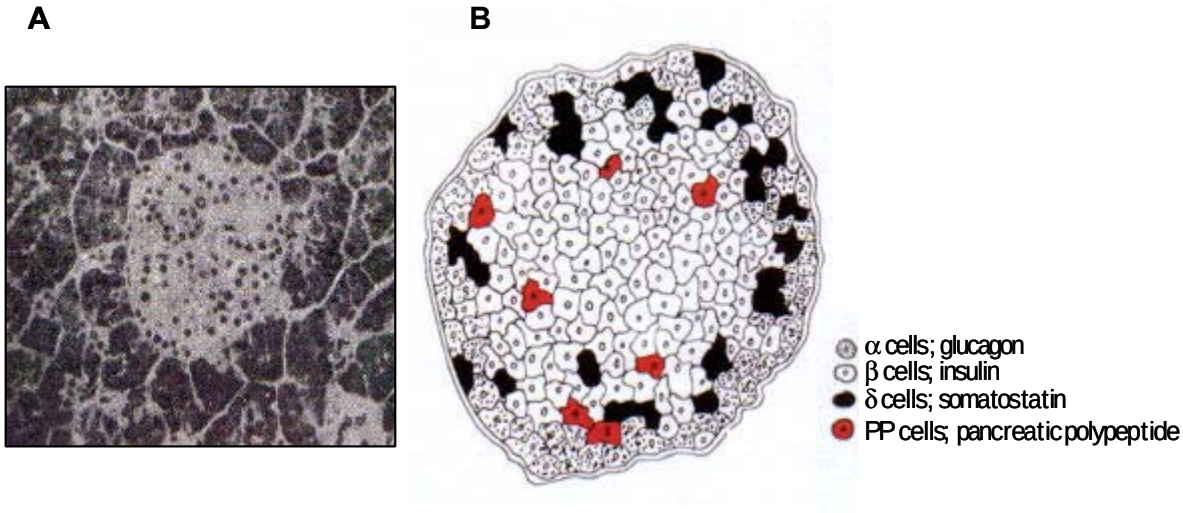

Fig. 1. Islet of Langerhans. (A) Photomicrograph of a human pancreatic islet. (B) Diagrammatic representation of the endocrine cell distribution in a typical mammalian islet of Langerhans.

In addition to the pancreatic enzyme secretion by the exocrine cells, the pancreas has an important endocrine role: to maintain a constant blood glucose level, to facilitate cellular storage of nutrients following a meal, and to provide for the mobilization of these depot metabolic substrates during periods of fasting. The underproduction or overproduction of insulin or glucagon therefore can profoundly affect the storage and use of carbohydrates, fats and proteins within the different tissues and thus severely affect cellular metabolic processes.

Glucose homeostasis involves a push-pull system that controls glucose flux into and out of the extracellular space. By their actions on the liver, adipose tissue, and muscle, glucagon and insulin maintain a balance of glucose production and utilization, respectively, that requires a coordinated action of both hormones under the guidance of a perceptive glucose sensor.

2.1 INSULIN

Insulin is one of a number of hormones that is required for normal growth and development. In addition, it is the only hormone that directly lowers blood glucose levels, therefore it is a dominant metabolic regulatory factor. Absolute insulin deficiency results in unrestrained glucose production, lipolysis, ketogenesis, proteolysis and, ultimately, death. Insulin excess results in hypoglycemia with consequent brain

failure and again, ultimately, death. Clearly, insulin is a potent and critically important hormone[10].

Insulin is a member of a gene family which includes insulin-like growth factor (IGF)-I, IGF-II and relaxin. However, unlike the other members of this gene family, expression of insulin is restricted exclusively to the β-cells of the pancreas. The insulin gene is transcribed and translated as preproinsulin. This contains a 24-amino acid signal sequence which is cleaved during transit through the rough endoplasmic reticulum to yield the 81-amino acid proinsulin molecule (Fig. 2). This is a single polypeptide chain with three internal disulphide bonds. From the trans-Golgi network proinsulin is sorted into vesicles destined for secretion. These vesicles undergo a process of maturation, during which a series of specific endopeptidases sequentially cleave the proinsulin. The processing of proinsulin to insulin is thought to be largely effected by Ca^{2+} dependent soluble proteases that specifically cleave proinsulin in the low pH environment of the maturing insulin storage granule. The insulin granules are 300 nm in diameter.

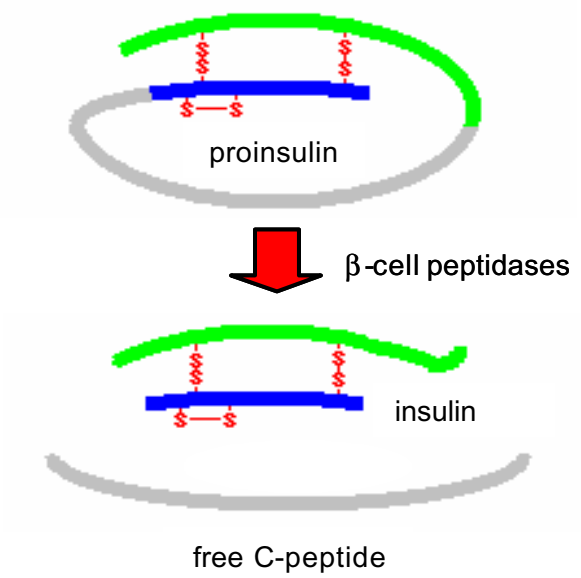

Fig. 2. Insulin maturation. Proinsulin is cleaved specifically by β-cell peptidases producing the mature insulin and the C-peptide.

Fully processed insulin consists of two chains, the 30-amino acid chain and the 21-amino acid chain, which are linked by two disulphide bonds. The central portion of the proinsulin molecule which is released is known as the C-peptide and is largely

[10] Hadley Mac E. Endocrinology. Prentice Hall Ed. 2000

retained in the mature storage granule and secreted along with insulin. There is some evidence that this C-peptide may serve some function(s), along with insulin, in glucose homeostasis[10].

3. GLUCOSE-SENSING IN THE β-CELL

Insulin secretion is accurately linked to blood glucose levels in the physiological range, and the mechanism by which the pancreatic β-cells sense changes in glucose concentrations has been a major focus of research efforts. Therefore, the rate-limiting steps regulating glucose influx and metabolism in the β-cell are likely to function as glucose sensors.

The role of the β-cell is to sense an increase in the concentration of nutrients in the blood and to synthesize, package and release insulin to control blood glucose homeostasis. The metabolism of glucose is an absolute requirement for the stimulation of insulin release. This conclusion is based on the evidence that the insulinotropic effect of glucose is inhibited by agents that interfere with its cellular metabolism and is mimicked only by metabolized sugars. Various agents such as amino acids (particularly arginine and leucine) and fatty acids can increase the secretion of insulin but only in the presence of facilitating concentrations of glucose (above 3 mM), whilst non-metabolizable analogues of glucose such as galactose or fructose are largely inactive as secretagogues[11]. This effect, mediated by the metabolism of the sugar, was dubbed the "fuel hypothesis"[12].

The above fuel secretagogues are true "initiators" of secretion, but there are also other agents including neurotransmitters (such acetylcholine), and enteric factors (e.g. glucagon-like peptide, GLP-1, gastric inhibitory peptide, GIP, and pituitary adenylate cyclase-activating polypeptide, PACAP) that act as "potentiators", enhancing secretion only at permissive concentrations of fuel secretagogues. These molecules usually act *via* G-protein coupled receptors and the generation of classical second messengers such as cAMP and Ca^{2+}[13].

[11] Hedeskov CJ. Mechanisms of glucose-induced insulin secretion. *Physiol. Rev*. 60:442-509, 1980

[12] Coore HG, Randle PJ. Inhibition of glucose phosphorylation by mannoheptulose. *Biochem. J*. 91:56-59, 1964

[13] Rutter GA. Nutrient-secretion coupling in the pancreatic islet β-cell: recent advances. *Molecular Aspects of Medicine*. 22:247-284, 2001

3.1 GLUCOSE TRANSPORT IN THE β-CELL

Islet β-cells are equipped with high-capacity glucose transporters located at the plasma membrane that are known as GLUT-2 in rodents. Whether this or another GLUT isoform (GLUT-1 or GLUT-3) is present in human β-cells is unclear[14]. GLUT-2 has a relatively high V_{max}. The K_m for glucose is also high, and so the rate of glucose transport into the cell will vary as the concentration of glucose fluctuates over the physiological range. GLUT-2 is required for efficient glucose-stimulated insulin secretion (GSIS), as demonstrated by studies in transgenic mice in which antisense RNA reduced GLUT-2 levels in β-cells by 80%[15]. These mice develop impaired insulin secretion and elevated blood glucose levels. Studies performed in knockout mice of GLUT-2[16] showed that homozygous (-/-), but not heterozygous (-/+), mice deficient in GLUT-2 are hyperglycemic and relatively hypoinsulinemic and have elevated plasma levels of glucagon, free fatty acids and beta-hydroxybutyrate. *In vivo*, their glucose tolerance is abnormal while *in vitro*, β-cells display loss of control of insulin gene expression by glucose and impaired GSIS. This is accompanied by alterations in the postnatal development of pancreatic islets, evidenced by an inversion of the alpha- to beta-cell ratio. As its absence leads to symptoms characteristic of NIDDM, it was suggested that GLUT-2 is thus required to maintain normal glucose homeostasis and normal function and development of the endocrine pancreas. However, as glucose transport across the β-cell membrane is rapid, it is thus unlikely that GLUT-2 is a strong controller of glucose metabolism.

3.2 GLUCOSE PHOSPHORYLATION IN THE β-CELL

The glucose-phosphorylating hexokinase enzyme called glucokinase (GK) has also been considered to be a crucial step in the control of glucose metabolism in pancreatic β-cells. β-cells contain a high K_m glucokinase, which displays strongly

[14] Schuit FC. Is GLUT2 required for glucose sensing? *Diabetologia*. 40:104-111, 1997

[15] Valera A, Solanes G, Fernández-Alvarez J, Pujol A, Ferrer J, Asins G, Gomis R, Bosch F. Expression of GLUT-2 antisense RNA in β cells of transgenic mice leads to Diabetes. *J. Biol. Chem.* 269:28543-28546, 1994

[16] Guillam MT, Hummler E, Schaerer E, Yeh JI, Birnbaum MJ, Beermann F, Schmidt A, Deriaz N, Thorens B, Wu JY. Early diabetes and abnormal postnatal pancreatic islet development in mice lacking Glut-2. *Nat. Genet.* 17:327-330, 1997

cooperative kinetics and has thus been termed the β-cell "glucose sensor"[17]. This high K_m (approximately 10 mM for glucose) explains the concentration dependence of the β-cell response to glucose in the physiological range, which stimulates insulin release. The importance of GK in this regulation is highlighted by transgenic approaches using β-cell-specific antisense RNA[18] and homologous recombination to knockout the GK gene[19], where the reduction in β-cell GK levels was associated with reduced capacity to secrete insulin in response to glucose. However, the most convincing evidence for the role of GK comes from the finding that mutations which reduce GK function in humans are associated with impaired GSIS[20] and the development of a subclass of NIDDM, MODY 2[21]. Overall, GK has been proposed as the rate-limiting enzyme in glycolysis that acts as a glucose-sensor. Nevertheless, it is now evident that subsequent metabolic steps, in the lower glycolytic pathway, may also play an important role in determining the fate of glucose carbon atoms[22], and that β-cells display a highly unusual range of glucose-sensing enzymes.

4. SIGNAL TRANSDUCTION IN INSULIN SECRETION

The study of stimulus-secretion coupling in β-cells began in the 1960s and rapidly led to three key discoveries: glucose must be metabolized by β-cells to induce insulin secretion; Ca^{2+} has an essential role in insulin secretion; and pancreatic β-cells are electrically excitable.

---

[17] Meglasson MD, Matschinsky FM. Pancreatic islet glucose metabolism and regulation of insulin secretion. *Diabetes/Metab. Rev*. 2:163-214, 1986

[18] Efrat S, Leiser M, Wu Y-J, FuscoDeMane D, Emran OA, Surana M, Jetton TL, Magnuson MA, Weir G, Fleischer N. Ribozyme-mediated attenuation of pancreatic beta-cell glucokinase expression in transgenic mice results in impaired glucose-induced insulin secretion. *Proc. Natl. Acad. Sci. USA*. 91:2051-2055, 1994

[19] Grupe A, Hultgren B, Ryan A, Ma YH, Bauer M, Stewart TA. Transgenic mice knockouts reveal a critical requirement for pancreatic beta cell glucokinase in maintaining glucose homeostasis. *Cell*. 83:69-78, 1995

[20] Byrne MM, Sturis J, Clement K, Vionnet N, Pueyo ME, Stoffel M, Takeda J, Passa P, Cohen D, Bell GI, et al. Insulin secretory abnormalities in subjects with hyperglycemia due to glucokinase mutations. *J. Clin. Invest.* 93:1120-1130, 1994

[21] Frogel P, Vaxillaire M, Sun F, Vehlo G, Zouali H, Butel MO, Lesage S, Vionnet N, Clement K, Fougerousse F. Close linkage of glucokinase locus on chromosome 7p to early-onset non-insulin-dependent diabetes mellitus. *Nature*. 356:162-164, 1992.

[22] Berman HK, Newgard CB. Fundamental metabolic differences between hepatocytes and islet beta-cells revealed by glucokinase overexpression. *Biochemistry*. 37:4543-4552, 1998

Glucose stimulation of insulin secretion involves two pathways: the triggering or K_{ATP} channel-dependent pathway, and the amplifying or K_{ATP} channel-independent pathway.

4.1 K_{ATP} CHANNEL-DEPENDENT PATHWAY

The demonstration in isolated β-cells of ATP-inhibitable K^+ currents[23] and their closure in intact cells by glucose[24] provided the first evidence that changes in intracellular ATP concentrations, [ATP], may be critical for the response to glucose. An ATP-sensitive K^+ channel was later cloned[25] and shown to be made of four Kir 6.2 subunits (forming the ionic pore) and four regulatory SUR1 subunits (containing the site to which antidiabetic sulfonylureas bind). The K_{ATP} channel is closed by the oral hypoglycemic sulfonylureas such as tolbutamide and glibenclamide while it is opened by diazoxide[26]. SUR1 also mediates the opening action of Mg^{2+}-ADP, whereas the closing action of ATP is on Kir 6.2 itself. Kir 6.2 also possesses a near-consensus phosphorylation site for AMP-activated protein kinase (AMPK)[27].

Glucose enters the β-cell through the high-capacity GLUT-2, which allows for rapid equilibration of glucose across the β-cell plasma membrane (Fig. 3). Glucose is then phosphorylated by GK, the first enzyme in the glycolytic pathway in the β-cell, which acts as a glucose sensor. The production of ATP from glycolysis and the Krebs cycle results in oscillations in the ATP/ADP ratio. These oscillations are thought to lead to oscillations in membrane potential through modulation of the K_{ATP} channel. Thus, elevated extracellular glucose concentrations increase the ATP/ADP ratio and therefore close K_{ATP} channels. This, in turn, suppresses efflux of K^+ ions, leading to progressive

---

[23] Cook DL, Hales CN. Intracellular ATP directly blocks K^+ channels in pancreatic β-cells. *Nature.* 311:271-273, 1984

[24] Ashcroft FM, Harrison DE, Ashcroft SJH. Glucose induces closure of single potassium channels in isolated rat pancreatic β-cells. *Nature.* 312:446-448, 1984

[25] Inagaki N, Gonoi T, Clement IV, Namba N, Inazawa J, Gonzalez G, AguilarBryan L, Seino S, Bryan J. Reconstitution of I(KATP): an inward rectifier subunit plus the sulfonylurea receptor. *Scienc*e. 270:1166-1170, 1995

[26] Henquin JC. Triggering and amplifying pathways of regulation of insulin secretion by glucose. *Diabetes*. 49:1751-1760, 2000

[27] Woods A, Salt I, Scott J, Hardie DG, Carling D. The alpha 1 and alpha 2 isoforms of the AMP-activated protein kinase have similar activities in rat liver but exhibit differences in substrate specificity in vitro. *FEBS Lett.* 397:347-351, 1996

depolarization of the plasma membrane (resting potential of about -70mV)[28]. The drop in voltage leads to the opening of voltage-sensitive L-type Ca^{2+} channels and the influx of Ca^{2+} ions. The resulting increase in intracellular free Ca^{2+} concentration $[Ca^{2+}]_i$ modulates kinases or other effector systems involved in secretion, triggering the movement of dense-core secretory vesicles to the cell surface, prompting their fusion with the plasma membrane and finally releasing stored insulin. However, the precise connection between elevated intracellular $[Ca^{2+}]_i$ and triggering of the insulin exocytotic mechanism remains unknown.

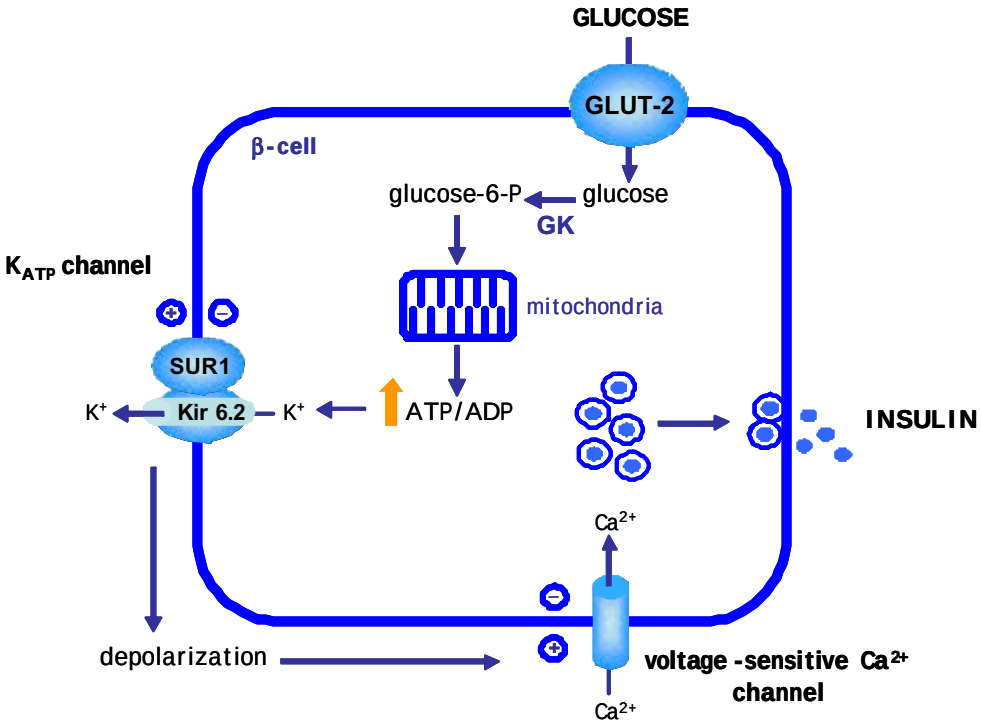

Fig. 3. K_{ATP} channel-dependent pathway of glucose sensing in the β-cell. Glucose enters the β-cell through the glucose transporter GLUT-2 and is phosphorylated by glucokinase (GK), the first enzyme in the glycolytic pathway in the β-cell, which acts as a glucose sensor. Mitochondrial metabolism increases the cytosolic ATP/ADP ratio. This leads to closure of K_{ATP} channels and depolarization of the plasma membrane. As a consequence, the cytosolic Ca^{2+} concentration is raised by the opening of voltage-sensitive Ca^{2+} channels. This increase in the cytosolic Ca^{2+} concentration is the main trigger for exocytosis, fusion of the insulin-containing secretory granules with the plasma membrane and insulin secretion.

[28] Henquin JC, Meissner HP. Significance of ionic fluxes and changes in membrane potential for stimulus-secretion coupling in pancreatic β-cells. *Experientia*. 40:1043-1052, 1984

4.2 K_{ATP} CHANNEL-INDEPENDENT PATHWAY

During the past decade, a substantial amount of new evidence has emerged which indicates that other mechanisms, apart from the closure of K_{ATP} channels, are involved in the stimulation of insulin release at high glucose concentrations. This was first demonstrated by the finding that glucose can stimulate insulin release under conditions of fixed, high $[Ca^{2+}]_c$[29]. Under maximal activation of the K_{ATP} channel-dependent pathway, glucose still increases insulin secretion in a concentration-dependent manner. This increase in secretion is highly sensitive to glucose (produced by as little as 1-6 mM glucose) and requires glucose metabolism. More recently, knockout mouse models lacking either of the two functional subunits of the K_{ATP} channel showed marked reductions, albeit not eliminations, of GSIS[30]. These β-cells show a partial secretory response to glucose without changes in $[Ca^{2+}]_c$, which is already elevated at low glucose concentration. Taken together, all these studies suggest the existence of metabolic coupling factors generated by glucose. Thus, the Ca^{2+} signal in the cytosol is necessary, but not sufficient, for the full development of insulin secretion. This second mechanism was called the amplifying pathway or K_{ATP} channel-independent pathway (Fig. 4).

[29] Gembal M, Gilon P, Henquin JC. Evidence that glucose can control insulin release independently from its action on ATP-sensitive K^+ channels in mouse β-cells. *J. Clin. Invest.* 89:1288-1295, 1992

[30] Seghers V, Nakazaki M, DeMayo F, Aguilar-Bryan L, Bryan J. SUR1 knockout mice: a model for K(ATP) channel-independent regulation of insulin secretion. *J. Biol. Chem*. 275:9270-9277, 2000

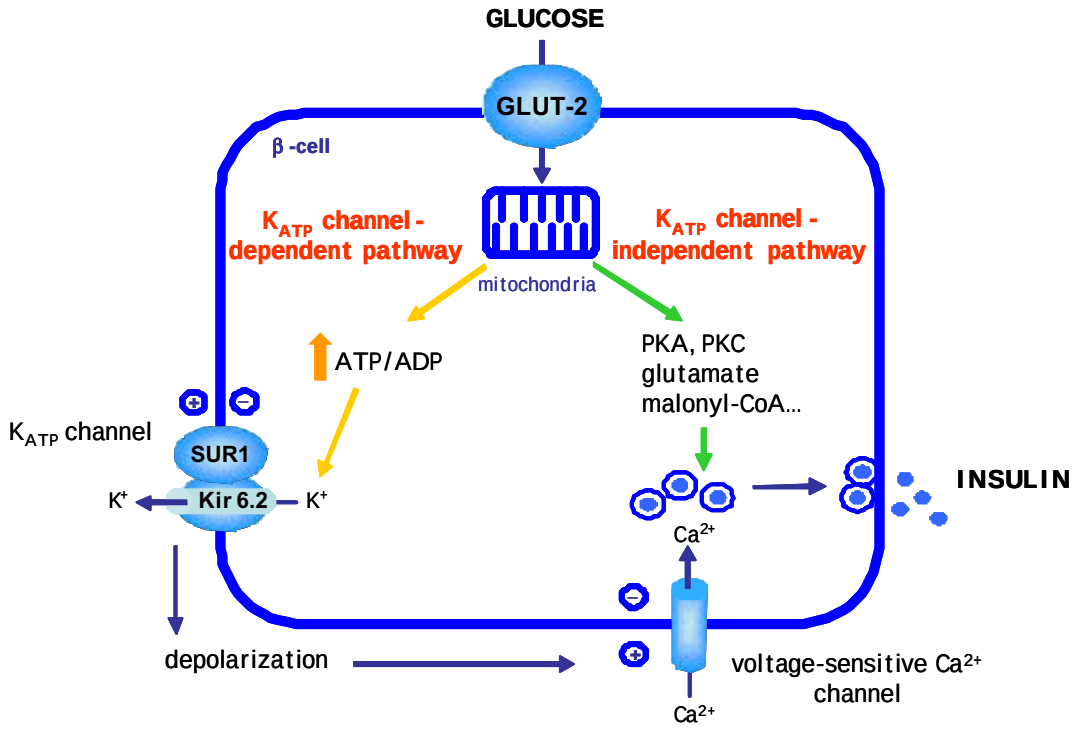

Fig. 4. Schematic representation of the K_{ATP} channel-dependent and -independent pathways of glucose sensing in the β-cell. Glucose metabolism produces an increase in the ATP/ADP ratio. Subsequently, closure of the K_{ATP} channels depolarizes the cytosolic membrane, which opens voltage-sensitive Ca^{2+}-channels, raising $[Ca^{2+}]_i$ and triggering insulin exocytosis (K_{ATP} channel-dependent pathway, yellow arrows). Under high $[Ca^{2+}]_c$, glucose metabolism produces other factors that still increase insulin secretion. These other metabolic coupling factors such as protein kinase A (PKA), PKC, glutamate and/or malonyl-CoA are believed to stimulate insulin secretion *via* a K_{ATP} channel-independent pathway (green arrows).

The molecular mechanisms involved in the K_{ATP} channel-independent pathway are still under discussion. The aim of this thesis is to gain more insight into the metabolic coupling factors implicated in the K_{ATP} channel-independent pathway of glucose sensing.

4.3 HIERARCHY BETWEEN THE K_{ATP} CHANNEL-DEPENDENT AND -INDEPENDENT PATHWAYS

Glucose-stimulated insulin release from human and rat islets is markedly biphasic *in vitro*[31], with an initial peak after approximately 5 min followed by a trough, and a second, more sustained phase. It now seems likely that the fast increase in $[Ca^{2+}]_i$ induced by the K_{ATP} channel-dependent pathway is responsible for the first phase and that the second phase involves the activation by glucose of mechanisms which are at least in part K_{ATP} channel-independent[32]. The first phase is thought to be due to a small pool of readily releasable granules and the second phase to granules that have translocated from reserve pools to a releasable pool at the membrane. Therefore, in the presence of elevated $[Ca^{2+}]_i$, the K_{ATP} channel-independent pathway is responsible for the selection and translocation of insulin-containing granules from the reserve pools to the cell membrane, their assembly at the plasma membrane, priming to achieve fusion competence, and finally exocytosis.

Low concentrations of glucose (1-6 mM) can influence insulin secretion, but only when a triggering signal has been produced[26]. This establishes a clear hierarchy between the two pathways: the K_{ATP} channel-independent pathway remains functionally silent as long as the K_{ATP} channel-dependent pathway has not depolarized the membrane and raised $[Ca^{2+}]_i$; i.e., as long as glucose has not reached its threshold concentration. The K_{ATP} channel-independent pathway serves to optimize the secretory response induced by the K_{ATP} channel-dependent signal. This hierarchy between the two pathways ensures that no insulin is inappropriately secreted in the presence of low glucose concentrations.

4.4 USE OF K^+ AND DIAZOXIDE TO DISCERN BETWEEN THE TWO PATHWAYS

Elevated K^+ and diazoxide can be used to discern between the K_{ATP} channel-dependent and -independent pathways of glucose sensing. When K_{ATP} channels are opened by diazoxide, the stimulation of insulin secretion by glucose is abrogated

[31] Curry DL, Bennett LL, Grodsky GM. Dynamics of insulin secretion by the perfused rat pancreas. *Endocrinology*. 83:572-584, 1968

[32] Komatsu M, Schermerhorn T, Noda M, Straub SG, Aizawa T, Sharp GW. Augmentation of insulin release by glucose in the absence of extracellular Ca^{2+}: new insights into stimulus-secretion coupling. *Diabetes*. 46:1928-1938, 1997

because the β-cell membrane does not depolarize and $[Ca^{2+}]_i$ does not increase. But β-cells could be depolarized by increasing the concentration of extracellular K^+, a manoeuvre that simply shifts the equilibrium potential for K^+ to more positive values. Under these conditions, elevated K^+ plus diazoxide, Ca^{2+} influx and insulin secretion are stimulated, and neither of these effects is inhibited by diazoxide[33]. Moreover, glucose still increases insulin secretion from islets depolarized with high K^+, although it does not close K_{ATP} channels in the presence of diazoxide. This effect of glucose is concentration-dependent, requires glucose metabolism, and does not involve any change in membrane potential or $[Ca^{2+}]_i$[29].

Using the same paradigm of K^+-induced depolarization in the presence of diazoxide, many laboratories have confirmed that glucose can increase insulin secretion independently of its action on K_{ATP} channels in rodent islets[34], human islets[35], perfused rat pancreas[36] and insulin-secreting cell lines[37].

5. MITOCHONDRIAL ANAPLEROSIS

Signals generated from glucose metabolism in the β-cell modulate the relative rates of glucose and FFA oxidation. At low glucose levels the mitochondria fill the energy needs of the β-cell by FFA oxidation. When the glucose level rises, FFA oxidation is decreased and glucose oxidation fulfils a larger part of the cellular energy needs. The first step in glucose-induced inhibition of FFA oxidation is an increase in mitochondrial Krebs cycle intermediates known as anaplerosis, resulting in citrate formation. The citrate content of insulin-secreting cells increases rapidly and precedes the increase in insulin release, consistent with a role for elevated citrate levels in

[33] Henquin JC, Charles S, Nenquin M, Mathot F, Tamagawa TD. Diazoxide and D600 inhibition of insulin release: distinct mechanisms explain the specificity for different stimuli. *Diabetes*. 31:776-783, 1982

[34] Fujimoto S, Ishida H, Kato S, Okamoto Y, Tsuji K, Mizuno N, Ueda S, Mukai E, Seino Y. The novel insulinotropic mechanism of pimobendan: direct enhancement of the exocytotic process of insulin secretory granules by increased Ca^{2+} sensitivity in β-cells. *Endocrinology*. 139:1133-1140, 1998

[35] Straub SG, James RFL, Dunne MJ, Sharp GWG. Glucose activates both K_{ATP} channel-dependent and K_{ATP} channel-independent signaling pathways in human islets. *Diabetes*. 47:758-763, 1998

[36] Abdel-Halim SM, Guenifi A, Khan A, Larsson O, Berggren PO, Östenson CG, Efendic S. Impaired coupling of glucose signal to the exocytotic machinery in diabetic GK rats: a defect ameliorated by cAMP. *Diabetes*. 45:934-940, 1996

[37] Hohmeier HE, Mulder H, Chen G, Henkel-Rieger R, Prentki M, Newgard CB. Isolation of INS-1-derived cell lines with robust ATP-sensitive K^+ channel-dependent and -independent glucose-stimulated insulin secretion. *Diabetes*. 49(3):424-430, 2000

nutrient-induced insulin secretion[38]. Mitochondrial citrate production leads to increased cytosolic citrate that is converted to malonyl-CoA by the combined enzymatic actions of citrate lyase (CL) and acetyl-CoA carboxylase (ACC) (Fig. 5). Malonyl-CoA is a potent inhibitor of carnitine palmitoyltransferase I (CPTI), which controls the transport of long-chain fatty acyl-coenzyme A (LC-CoA) into the mitochondria to be oxidized. Thus, malonyl-CoA switches β-cell metabolism from fatty acid oxidation to glucose oxidation. An important consequence of this switch is an increase in cytosolic LC-CoA, which is believed to act as an effector molecule in the β-cell[39] (Section 7).

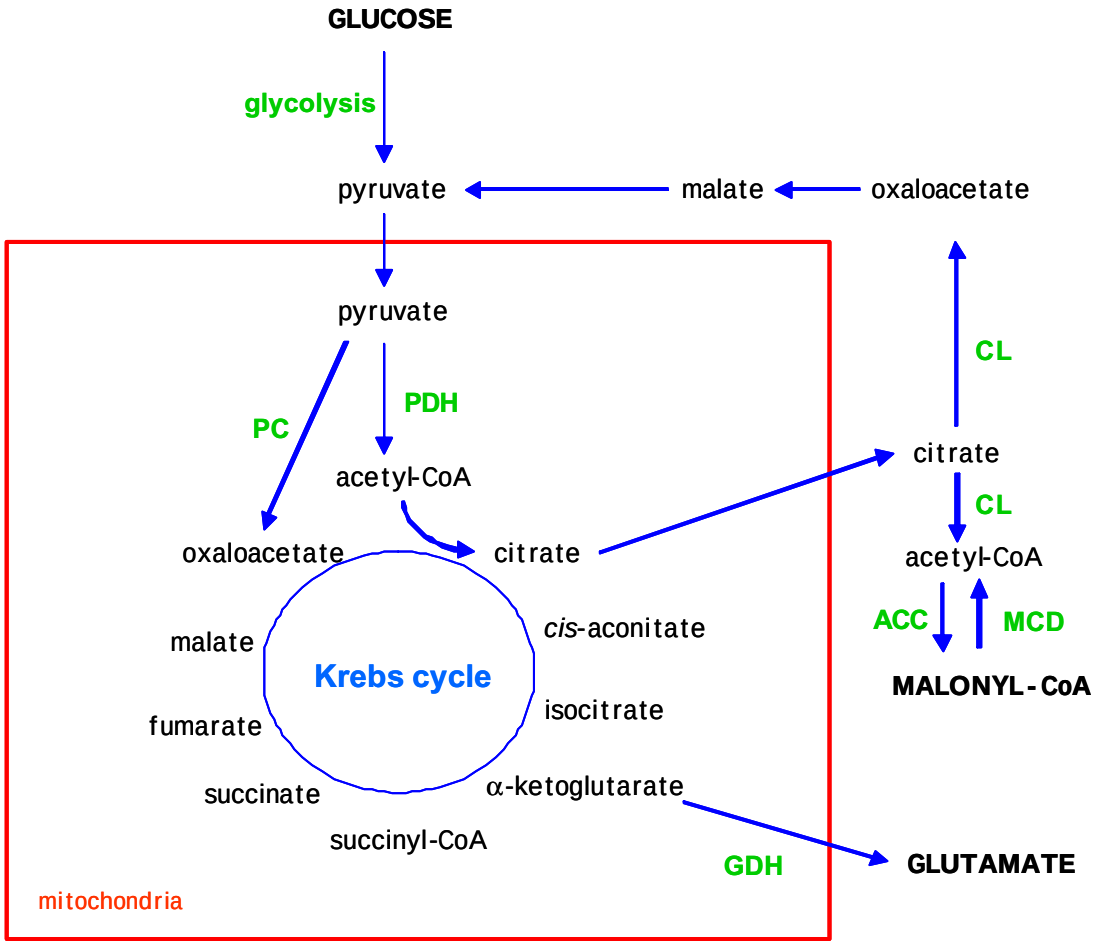

Fig. 5. Mitochondrial anaplerosis in the β-cell. PC: pyruvate carboxylase, PDH: pyruvate dehydrogenase, GDH: glutamate dehydrogenase, CL: citrate lyase, ACC: acetyl-CoA carboxy lase, MCD: malonyl-CoA decarboxylase.

[38] Brun T, Roche E, Assimacopoulos-Jeannet F, Corkey BE, Kim KH, Prentki M. Evidence for anaplerotic/malonyl-CoA pathway in pancreatic β-cell nutrient signalling. *Diabetes*. 45:190-198, 1996

[39] Prentki M, Corkey BE. Are the β-cell signaling molecules malonyl-CoA and cytosolic long-chain acyl-CoA implicated in multiple tissue defects of obesity and NIDDM? *Diabetes*. 45: 273-283, 1996

Anaplerosis is likely to be important in β-cell activation for several reasons. Firstly, it is required for the efficient operation of either a pyruvate/malate or pyruvate/citrate shuttle allowing the production of cytosolic malonyl-CoA and NADPH. Secondly, the dose dependence of anaplerosis, citrate, malate and malonyl-CoA accumulation in response to glucose correlate well with secretion in β-cells[40,41]. Thirdly, methylsuccinate is a potent secretagogue in intact β-cells[42] and succinate directly promotes exocytosis of insulin in permeabilized pancreatic β-cells[43]. Fourthly, phenylacetic acid reduces anaplerosis and insulin secretion in clonal INS β-cells and rat islets[40] by inhibition of pyruvate carboxylase.

An interesting feature of the β-cell is not only the tight link between glycolysis and mitochondrial oxidative metabolism, but also the extremely high proportion of glucose-derived carbons oxidized in the mitochondria. β-cell glucose metabolism is remarkably aerobic: more than 80% of the glucose carbons are converted to CO_2 and H_2O[41]. As a result, pyruvate produced from glucose by glycolysis enters mitochondria, rather than exiting the cell across the plasma membrane, whilst NADH generated at the glyceraldehyde phosphate dehydrogenase step of glycolysis is oxidised by the mitochondrial respiratory chain. In the mitochondria, pyruvate is a substrate for both pyruvate dehydrogenase (PDH) and pyruvate carboxylase (PC). The latter forms oxaloacetate, providing anaplerotic input to the tricarboxylic acid (TCA) cycle. Reducing equivalents generated by the TCA cycle activate the electron transport chain, resulting in hyperpolarization of the mitochondrial membrane and formation of ATP.

Mitochondrial metabolism plays a pivotal role in the pancreatic β-cell by generating signals that couple glucose sensing to insulin secretion. As explained above, the Ca^{2+} signal alone is not sufficient to reproduce the complete and sustained secretion elicited by glucose. Therefore, glucose metabolism must generate other factors to

[40] Farfari S, Schulz V, Corkey B, Prentki M. Glucose-regulated anaplerosis and cataplerosis in pancreatic β-cells: possible implication of a pyruvate/citrate shuttle in insulin secretion. *Diabetes*. 49:718-726, 2000

[41] Schuit F, De Bos A, Farfai S, Moens K, Pipeleers D, Brun T, Prentki M. Metabolic fate of glucose in purified islet cells: glucose-regulated anaplerosis in beta cells. *J. Biol. Chem*. 272:18572-18579, 1997

[42] MacDonald MJ, Fahien LA. Insulin release in pancreatic islets by a glycolytic and a Krebs cycle intermediate: contrasting patterns of glyceraldehyde phosphate and succinate. *Arch. Biochem. Biophys*. 279:104-108, 1990

[43] Maechler P, Kennedy ED, Pozzan T, Wollheim CB. Mitochondrial activation directly triggers the exocytosis of insulin in permeabilized pancreatic β-cells. *EMBO J*. 16:3833-3841, 1997

stimulate insulin secretion. Such metabolites may be generated in different compartments, the mitochondrion being the most likely source.

Ultrastructural examination of the β-cell has shown that mitochondria are often in close proximity to the secretory insulin granules (Fig. 6), suggesting that this may facilitate metabolism-secretion coupling.

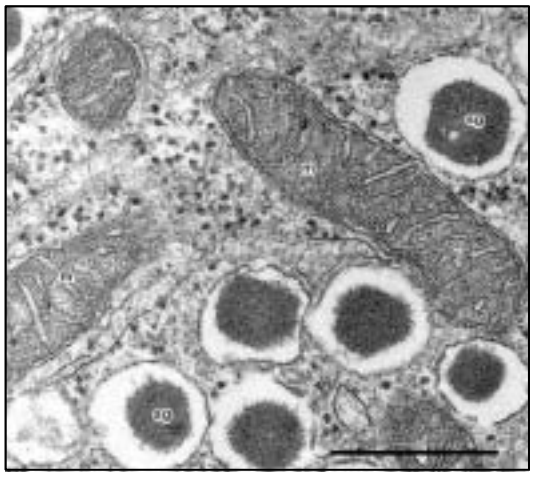

Fig. 6. β-cell cytoplasm. Electron micrograph of the rat β-cell cytoplasm showing mitochondria (m) and insulin-containing secretory granules (sg). The mitochondrial outer and inner membranes are visible. The scale bar represents 0.5 µm. Picture obtained from[44].

In permeabilized INS-1 cells, mitochondrial activation is associated with a marked stimulation of insulin release, which depends both on activation of the mitochondrial respiratory chain and on provision of carbons for the TCA cycle[44]. Glucose, glyceraldehyde and dihydroxyacetone, which feed directly into glycolysis, are all secretagogues[11]. However, glucose, which provides anaplerosis, is required for fatty acid- and ketone body-induced insulin release[45]. Leucine (acetyl-CoA production) and glutamine (anaplerosis) synergize to promote secretion[45].

In conclusion, all these features of β-cell fuel stimuli favour the concept that acetyl-CoA production and anaplerosis are the earliest mitochondrial events synergizing to promote the production of coupling factors activating the β-cell secretory process. This secretory response requires a factor(s) generated by mitochondrial metabolism

[44] Maechler P, Wollheim CB. Mitochondrial glutamate acts as a messenger in glucose-induced insulin exocytosis. *Nature*. 402:685-689, 1999

[45] Malaisse WJ, Malaisse-Lagae F, Rasschaert J, Zahner D, Sener A, Davies DR, Van Schaftingen E. The fuel concept for insulin release: regulation of glucose phosphorylation in pancreatic islets. *Biochem. Soc. Trans*. 18:107-108, 1990

distinct from ATP. There have been proposed several candidates for the metabolic coupling factors generated by glucose, such as citrate[40], glutamate[44], AMPK[46], protein kinases A and C[47], and malonyl-CoA/LC-CoA[48]. The present thesis will focus on malonyl-CoA/LC-CoA as a metabolic coupling factor in insulin secretion.

6. METABOLIC COUPLING FACTORS IN INSULIN SECRETION

6.1 GLUTAMATE

In 1999 Maechler and Wollheim demonstrated that glutamate could trigger insulin secretion in permeabilized clonal β-cells, and that the concentration of this molecule increases in INS-1 cells in response to elevated glucose concentration[44]. Thus, glutamate, which can be produced from the TCA cycle intermediate α-ketoglutarate or by transamination reactions, would seem to satisfy the criteria for an important signalling molecule in the β-cell. Glutamate is believed to act on the secretory vesicle, by undefined mechanisms which may involve uptake of the molecule, and which enhance the competence of the vesicle for fusion with the plasma membrane. It is most likely to affect the second phase of insulin secretion.

This hypothesis has met with some resistance, since it has been pointed out that increases in the islet content of glutamate do not always occur in response to glucose, under conditions in which insulin secretion is robustly stimulated[49]. However, transgenic over-expression of glutamate decarboxylase (GAD65) in mouse β-cells leads to an inhibition of insulin release, and glucose intolerance, *in vivo*[50]. Further studies in INS-1E cells and rat islets overexpressing GAD65 using an adenoviral vector showed

[46] daSilvaXavier G, Leclerc I, Salt IP, Doiron B, Hardie DG, Kahn A, Rutter GA. Role of AMP-activated protein kinase in the regulation by glucose of islet beta-cell gene expression. *Proc. Natl. Acad. Sci. USA*. 97:4023-4028, 2000

[47] Aizawa T, Komatsu M, Asanuma N, Sato Y, Sharp GG. Glucose action 'beyond ionic events' in the pancreatic beta cell. *Trends Pharmacol. Sci.* 19:496-499, 1998

[48] Prentki M, Vischer S, Glennon MC, Regazzi R, Deeney JT, Corkey BE. Malonyl-CoA and long chain acyl-CoA esters as metabolic coupling factors in nutrient-induced insulin secretion. *J. Biol. Chem*. 267:5802-5810, 1992

[49] MacDonald MJ, Fahien LA. Glutamate is not a Messenger in insulin secretion. *J. Biol. Chem*. 275:34025-34027, 2000

[50] Shi Y, Kanaani J, Menard-Rose V, Ma YH, Chang PY, Hanahan D, Tobin A, Grodsky G, Baekkeskov S. Increased expression of GAD65 and GABA in pancreatic beta-cells impairs first-phase insulin secretion. *Am. J. Physiol. Endocrinol. Metab*. 279:E684-E694, 2000

reduced glutamate levels and impaired GSIS, demonstrating a positive correlation between cellular glutamate concentrations and the secretory response to glucose[51].

Overall, data both for and against the "glutamate hypothesis" have emerged, although the precise mechanism of glutamate action on exocytosis is unknown. Further investigation is needed to clarify the role of glutamate as an intracellular messenger or cofactor in insulin secretion.

6.2 AMPK

AMP-activated protein kinase (AMPK) is a heterotrimer containing α-, β- and γ-subunits. The α-subunit contains the catalytic site; the β-subunit, a glycogen-binding domain; and the γ-subunit the AMP-binding site. Increases in the ratio of AMP/ATP activate AMPK by AMPK kinase phosphorylation. AMPK acts as a "fuel gauge", such that when it detects a "low fuel" situation it protects the cell by regulating processes that generate and utilize ATP. Therefore, activation of AMPK leads to the phosphorylation of a number of target molecules that result in increases in fatty acid oxidation (to generate more ATP) and in the decrease of their esterification and use in other non-β-oxidative pathways[52]. AMPK phosphorylates and activates malonyl-CoA decarboxylase (MCD) and suppresses the synthesis of ACC, fatty acid synthetase (FAS), glycerol-3-phosphate acyltransferase (GPAT) and other enzymes of lipid biogenesis by inhibiting the generation of the transcription factor sterol regulatory element binding protein-1c (SREBP-1c)[53].

AMPK is expressed in β-cells and it is acutely inhibited by elevated glucose concentrations[46]. AMPK has been suggested to be a key regulator of both insulin secretion and insulin gene expression[46]. The effects of AMPK may result, at least in part, from changes in the rate of insulin release. Thus, increases in AMPK activity can block GSIS in rat islets and clonal MIN6 β-cells without affecting the basal secretory

[51] Rubi B, Ishihara H, Hegardt FG, Wollheim CB, Maechler P. GAD65-mediated glutamate decarboxylation reduces glucosa-stimulated insulin secretion in pancreatic beta cells. *J. Biol. Chem*. 276:36391-36396, 2001

[52] Ruderman N, Prentki M. AMP kinase and malonyl-CoA: targets for therapy of the metabolic syndrome. *Nature.* 3:340-351, 2004

[53] Ferre P, Azzout-Marniche D, Foufelle F. AMP-activated protein kinase and hepatic genes involved in glucose metabolism. *Biochem. Soc. Trans*. 31:220-223, 2003

machinery[54]. Therefore, AMPK could be involved as a metabolic coupling factor in insulin secretion. AMPK has also been proposed as a target, along with malonyl-CoA, for therapy of the metabolic syndrome[52], a state of metabolic dysregulation characterized by insulin resistance, hyperinsulinemia, central obesity and a predisposition to Type 2 diabetes, dyslipidemia, hypertension, premature atherosclerosis and other diseases.

6.3 PKC

Protein kinase C (PKC) isoforms are reasonable candidates to either initiate secretion or augment GSIS, as they respond to both energy excess (lipid signals) and Ca^{2+}.

PKC is a family of different isozymes which are divided into three classes, based on structure and co-factor requirements. The conventional class (cPKC: α, β and γ) requires phosphatidylserine (PS), diacylglycerol (DAG) and Ca^{2+}, while the novel class (nPKC: ε, η, θ and δ) does not require Ca^{2+}. The atypical class (aPKC: ζ, λ, τ) requires only an acidic phospholipid like PS. PKCμ can be considered a separate class of kinase or an nPKC isoform with a modified phorbol ester binding site (C1 domain) and a putative transmembrane leader sequence. The β-cell expresses seven isoforms of PKC: α, β, δ, ε, τ, ζ and μ[55]. Unlike many enzymes, cPKC and nPKC isozymes require intracellular translocation and targeting to membrane surfaces for their activation. The mechanism of this targeting involves both lipid (C1) and Ca^{2+} binding domains (C2) as well as protein-protein interactions with adaptor molecules contained in the cytosol.

The stimulus-secretion coupling of some non-nutrient secretagogues occurs *via* PKC in receptor-mediated events linked to phospholipase C. Phospholipase C activation generates DAG, which translocates and activates PKC isoforms to phosphorylate endogenous substrates. In pancreatic β-cells PKC is activated by glucose[56] and by lipids (DAG and LC-CoA)[55]. A follow-up study showed that palmitate translocated PKC

[54] daSilvaXavier G, Leclerc I, Varadi A, Tsuboi T, Moule SK, Rutter GA. Role for AMP-activated protein kinase in glucose-stimulated insulin secretion and preproinsulin gene expression. *Biochem. J.* 371:761-774, 2003

[55] Yaney GC, Korchak HM, Corkey BE. Long-chain acyl-CoA regulation of protein kinase C and fatty acid potentiation of glucose-stimulated insulin secretion. *Endocrinology*. 141:1989-1998, 2000

[56] Ganesan S, Calle R, Zawalich K, Smallwood JI, Zawalich WS, Rasmussen H. Glucose-induced translocation of protein kinase C in rat pancreatic islets. *Proc Natl Acad Sci U S A*. 87:9893–9897, 1990

activity to a membrane fraction only in the presence of stimulating glucose[57]. Significantly, blocking the metabolism of these non-esterified fatty acids (NEFA), i.e., activation to LC-CoA, also blocked their ability to translocate PKC activity and stimulate insulin secretion. This suggests that either the LC-CoA or its esterification into a complex lipid such as DAG or phosphatidate was required for this effect. In addition, the activity of cPKC has been enhanced by palmitoylation through increased targeting to cell membranes[58].

However, the role of PKC in glucose-induced insulin secretion is unresolved, with several arguments for and against its involvement. Glucose causes a rise in DAG and promotes the translocation of PKCα in the β-cell. This is consistent with the observation that the mass of PKCα correlates with the ability of phorbol myristate acetate (PMA), a high affinity surrogate for DAG, to stimulate secretion[59]. Therefore, the short-term activation of PKC is thought to be a positive signal for insulin secretion. However, down-regulation of PKC activity by chronic phorbol ester stimulation led to the differential loss of PKC isoforms in HIT cells, and after down-regulation GSIS was not only preserved but enhanced, while the absolute potentiation due to exogenous NEFA did not change[55]. Overall, PKC seems most likely to stimulate insulin secretion through a K_{ATP} channel-independent mechanism.

7. THE MALONYL-CoA/LC-CoA MODEL OF GSIS

Malonyl-CoA is both an intermediate in the *de novo* synthesis of fatty acids and an allosteric inhibitor of CPTI, the enzyme that controls the transfer of LC-CoA molecules from the cytosol to the mitochondria, where they are oxidized. However, in pancreatic β-cells the level of FAS is very low[38], therefore the physiological role of malonyl-CoA in the endocrine pancreas, unlike many other tissues, is not *de novo* synthesis of fatty acids but rather the regulation of CPTI activity. By virtue of this, malonyl-CoA is a key physiological regulator of cellular fatty acid oxidation and lipid partitioning.

---

[57] Alcázar O, Qiu-yue Z, Giné E, Tamarit-Rodriguez J. Stimulation of islet protein kinase C translocation by palmitate requires metabolism of the fatty acid. *Diabetes*. 46:1153-1158, 1997

[58] Ford DA, Horner CC, Gross RW. Protein kinase C acylation by palmitoyl coenzyme A facilitates its translocation to membranes. *Biochemistry.* 37:11953-11961, 1998

[59] Yaney GC, Fairbanks JM, Deeney JT, Korchak HM, Tornheim K, Corkey BE. Potentiation of insulin secretion by phorbol esters is mediated by PKCα and nPKC isoforms. *Am. J. Physiol*. 283:E880-E888, 2002

Prentki and Corkey[48] were the first to propose that malonyl-CoA, besides its metabolic actions, acts as a coupling factor and signal of plenty that controls insulin secretion. They proposed a model that links β-cell nutrient sensing to insulin secretion in which, in addition to the K_{ATP} channel-dependent pathway, a parallel anaplerotic/lipid signalling pathway exists wherein malonyl-CoA acts as a coupling factor. The malonyl-CoA/LC-CoA model of GSIS holds that during glucose stimulation, anaplerosis increases citrate[41], which is exported to the cytosol (cataplerosis) and finally converted to malonyl-CoA, resulting in inhibition of CPTI and fatty acid oxidation. Therefore, the increase in malonyl-CoA may be responsible for the accumulation of LC-CoAs in the cytosol[60], which signal directly or indirectly *via* fatty acid esterification and/or protein acylation processes to augment insulin release[48] (Fig. 7). This model does not oppose, but rather complements, other candidate mechanisms of metabolic signal transduction, such as the cataplerotic output of glutamate, etc.

[60] Liang Y, Matschinsky FM. Content of CoA-esters in perifused rat islets stimulated by glucose and other fuels. *Diabetes*. 40:327-333, 1991

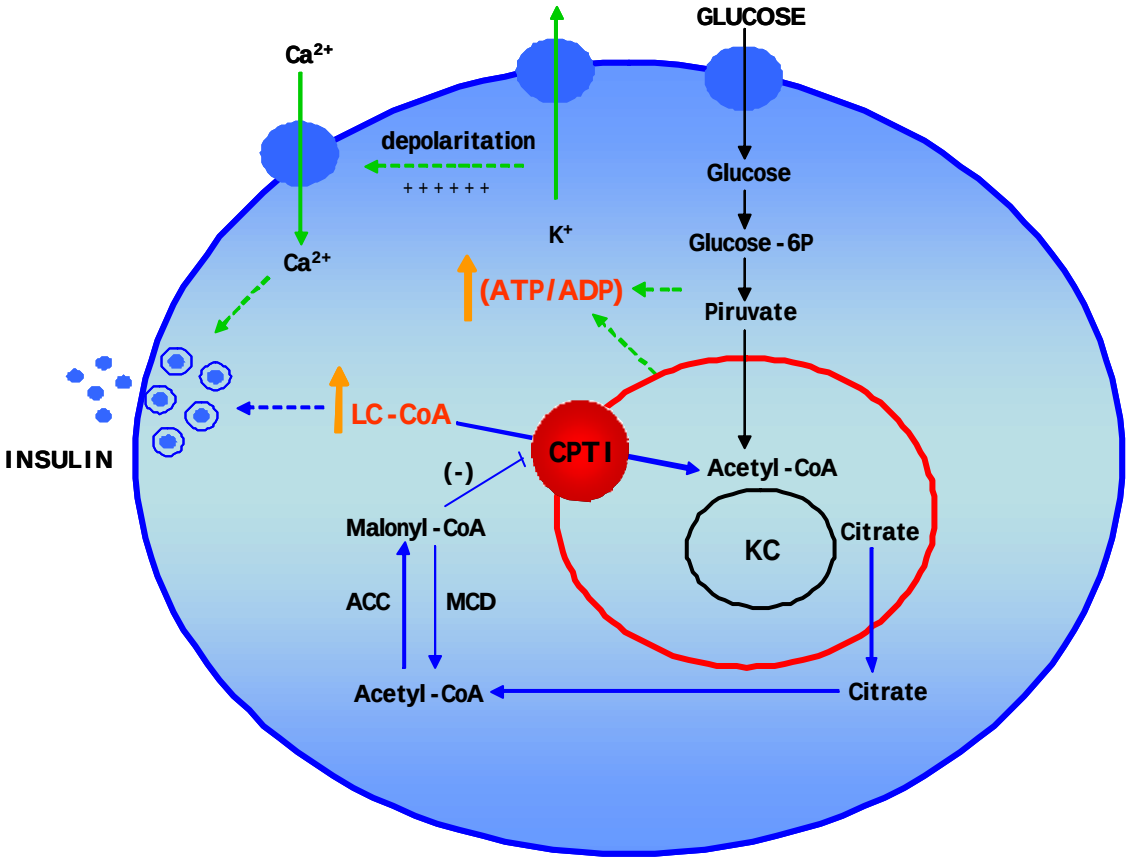

Fig. 7. The malonyl-CoA/LC-CoA model of GSIS in the β-cell. The malonyl-CoA/LC-CoA model acts as a K_{ATP} channel-independent pathway (blue arrows) in parallel to the K_{ATP} channel-dependent pathway (green arrows). At elevated glucose, anaplerosis-derived malonyl-CoA inhibits CPTI which modulates the partitioning of exogenous fatty acids *via* LC-CoA from fatty acid oxidation to lipid signaling involved in insulin vesicle exocytosis. CK: Krebs cycle, CPTI: carnitine palmitoyltransferase I, ACC: acetyl-CoA carboxylase, MCD: malonyl-CoA decarboxylase.

Many lines of evidences[61] supporting the malonyl-CoA/LC-CoA model of an anaplerotic/lipid signalling pathway of insulin secretion have been verified by different groups:

1- Pyruvate carboxylase is abundant in the islet, yet it is neither a gluconeogenic nor a lipogenic tissue; anaplerosis is very active in islet tissue because 50% of β-cell pyruvate is carboxylated to oxaloacetate[62].

[61] Prentki M. New insights into pancreatic β-cell metabolic signaling in insulin secretion. *European J. Endocrinology*. 134:272-286, 1996

2- Citrate rises markedly in response to glucose before secretion occurs[38].

3- Glucose activates ACC, which is abundant in the β-cell, and basal insulin secretion correlates with the content of the ACC protein[63].

4- Malonyl-CoA rises rapidly and markedly in response to glucose before secretion occurs[64].

5- Fatty acids potentiate glucose-induced insulin secretion. There is a correlation between the level of fatty acyl-CoA (FA-CoA) in response to different nutrients, and insulin secretion[48].

6- Elevated glucose inhibits fatty acid oxidation in β-cells[65] and increases esterified lipids such as DAG[48].

7- Inhibition of the pathway with hydroxy-citrate, an inhibitor of citrate lyase, curtails glucose-induced insulin secretion[66].

8- Inhibition of CPTI by pharmacological agents promotes the release of insulin[48,66].

10- Diacylglycerol[64] and phosphatidic acid[67], which can be formed *de novo via* esterification of FA-CoA to α-glycerophosphate, rise upon glucose stimulation of β-cells.

11- 2-Bromopalmitate, an inhibitor of CPTI, restores glucose sensitivity to islets from fasted animals[68], and allows foetal pancreas and islets from very young rats to become much more responsive to glucose[69].

---

[62] MacDonald MJ. Glucose enters mitochondrial metabolism via both carboxylation and decarboxylation of pyruvate in pancreatic islets. *Metabolism*. 42:1229-1231, 1993

[63] Brun T, Roche E, Kim KH, Prentki M. Glucose regulates acetyl-CoA carboxylase gene expression in a pancreatic beta-cell line (INS-1). *J Biol Chem*. 268:18905-18911, 1993

[64] Corkey BE, Glennon MC, Chen KS, Deeney JT, Matschinsky FM, Prentki M. A role for malonyl-CoA in glucose-stimulated insulin secretion from clonal pancreatic beta-cells. *J. Biol. Chem*. 264:21608-21612, 1989

[65] Segall L, Lameloise N, Assimacopoulos-Jeannet F, Roche E, Corkey P, Thumelin S, Corkey BE, Prentki M. Lipid rather than glucose metabolism is implicated in altered insulin secretion caused by oleate in INS-1 cells. *Am. J. Physiol*. 277:E521-528, 1999

[66] Chen S, Ogawa A, Ohneda M, Unger RH, Foster DW, McGarry JD. More direct evidence for a malonyl-CoA-carnitine palmitoyltransferase I interaction as a key event in pancreatic beta-cell signaling. *Diabetes*. 43:878-883, 1994

[67] Farese RV, DiMarco PE, Barnes DE, Sabir MA, Larson RE, Davis JS, Morrison AD. Rapid glucose-dependent increases in phosphatidic acid and phosphoinositides in rat pancreatic islets. *Endocrinology*. 118:1498-1503, 1986

[68] Vara E, Fernandez-Martin O, Garcia C, Tamarit-Rodriguez J. Palmitate dependence of insulin secretion, "de novo" phospholipid synthesis and $^{45}Ca^{2+}$-turnover in glucose stimulated rat islets. *Diabetologia*. 31:687-693, 1988

[69] Bliss CR, Sharp GW. Glucose-induced insulin release in islets of young rats: time-dependent potentiation and effects of 2-bromostearate. *Am. J. Physiol*. 263:E890-E896, 1992

12- Islets incubated in the absence of bicarbonate, a substrate for pyruvate carboxylase and ACC, show a marked decrease in glucose-induced secretion[70].

13- Sulfonylureas, which inhibit CPTI and curtail fatty acid oxidation[71], have been proposed to promote insulin release both *via* K_{ATP} channel closure and by CPTI inhibition[61].

14- Islets from hormone sensitive lipase-deficient mice do not release insulin in response to glucose either *in vivo* or *in vitro*[72], and pharmacological inhibition of islet lipase with 3,5-dimethylpyrazole curtails GSIS[73].

15- A patient with a mutation in the fat oxidation gene L-3-hydroxyacyl-CoA dehydrogenase showed hyperinsulinism[74].

16- Stable expression of an ACC-antisense construct in INS-1 cells decreased malonyl-CoA levels, increased LC-CoA oxidation and decreased insulin secretion[75].

17- The overexpression of native LCPTI in clonal INS-1E β-cells increased beta oxidation of fatty acids and decreased insulin secretion (40%) at high glucose[76]. The effect of LCPTI was reverted by etomoxir, an irreversible inhibitor of CPTI, and by the exogenous addition of fatty acids.

18- MCD overexpression in rat islets and β-cell stable clones curtailed GSIS (50%), only in the presence of fatty acids[77].

---

[70] Henquin JC, Lambert AE. Extracellular bicarbonate ions and insulin secretion. *Biochim Biophys Acta*. 381:437-442, 1975

[71] Cook GA. The hypoglycemic sulfonylureas glyburide and tolbutamide inhibit fatty acid oxidation by inhibiting carnitine palmitoyltransferase. *J. Biol. Chem*. 262:4968-4972, 1987

[72] Roduit R, Masiello P, Wang SP, Li H, Mitchell GA, Prentki M. A role for hormone-sensitive lipase in glucose-stimulated insulin secretion: a study in hormone-sensitive lipase-deficient mice. *Diabetes*. 50:1970-1975, 2001

[73] Masiello P, Novelli M, Bombara M, Fierabracci V, Vittorini S, Prentki M, Bergamini E. The antilipolytic agent 3,5-dimethylpyrazole inhibits insulin release in response to both nutrient secretagogues and cyclic adenosine monophosphate agonists in isolated rat islets. *Metabolism*. 51:110-114, 2002

[74] Clayton PT, Eaton S, Aynsley-Green A, Edginton M, Hussain K, Krywawych S, Datta V, Malingre HE, Berger R, van den Berg IE. Hyperinsulinism in short-chain L-3-hydroxyacyl-CoA dehydrogenase deficiency reveals the importance of beta-oxidation in insulin secretion. *J. Clin. Invest.* 108:457-465, 2001

[75] Zhang S, Kim K H. Essential role of acetyl-CoA carboxylase in the glucose-induced insulin secretion in a β-cell line. *Cell Signal.* 10:35-42, 1998

[76] Rubi B, Antinozzi PA, Herrero L, Ishihara H, Asins G, Serra D, Wollheim CB, Maechler P, Hegardt FG. Adenovirus-mediated overexpression of liver carnitine palmitoyltransferase I in INS1E cells: effects on cell metabolism and insulin secretion. *Biochem. J.* 364:219-226, 2002

[77] Roduit R, Nolan C, Alarcon C, Moore P, Barbeau A, Delghingaro-Augusto V, Przybykowski E, Morin J, Masse F, Massie B, Ruderman N, Rhodes C, Poitout V, Prentki M. A Role for the Malonyl-CoA/Long-Chain Acyl-CoA

On the other hand, the malonyl-CoA/LC-CoA hypothesis has been challenged by other authors. In a recent study[78] where pancreatic β-cells were chronically exposed to high FFA concentrations, the overexpression of MCD did not improve the lipid-induce impairment in GSIS. Instead, GSIS was partially restored with the addition of a pyruvate cycling intermediate. The authors propose that impaired GSIS is not a simple result of saturation of lipid storage pathways and that chronic exposure of islet β-cells to fatty acids grossly alters a mitochondrial pathway of pyruvate metabolism that is important for GSIS. The same authors had previously reported unimpaired secretion of insulin in β-cells overexpressing MCD in the cytoplasm[79]. However, this apparent discrepancy with the malonyl-CoA/LC-CoA hypothesis has been reconciled by a recent study demonstrating the importance of the availability of fatty acids for lipid signalling in the β-cell[77]. In this study, MCD overexpression in rat islets and β-cell stable clones curtailed GSIS, but only in the presence of exogenous fatty acids.

Overall, both malonyl-CoA and LC-CoA are thought to participate in the signal transduction for insulin secretion: the former as a regulator and the latter as an effector[80]. Systems that regulate both malonyl-CoA and LC-CoA appear to be involved in insulin secretion. Accordingly, ACC, which controls the synthesis of malonyl-CoA, MCD, which catalyzes malonyl-CoA degradation, and CPTI, which is regulated by malonyl-CoA, are components of a metabolic signalling network that senses the level of fuel stimuli. The metabolism of several nutrients that converge to form malonyl-CoA and increase LC-CoA esters (carbohydrate, amino acids and ketoacids) might play a key role in fuel regulated-insulin secretion in the β-cell[81]. To further investigate the implication of LC-CoA in insulin release, the present thesis will examine the hypothesis

---

Pathway of Lipid Signaling in the Regulation of Insulin Secretion in Response to Both Fuel and Nonfuel Stimuli. *Diabetes*. 53:1007-1019, 2004

[78] Boucher A, Lu D, Burgess SC, Telemaque-Potts S, Jensen MV, Mulder H, Wang MY, Unger RH, Sherry AD, Newgard CB. Biochemical mechanism of lipid-induced impairment of glucose-stimulated insulin secretion and reversal with a malate analogue. *J. Biol. Chem*. 279:27263-27271, 2004

[79] Mulder H, Lu D, Finley IV J, An J, Cohen J, Antinozzi PA, McGarry JD, Newgard CB. Overexpression of a modified human malonyl-CoA decarboxylase blocks the glucose-induced increase in malonyl-CoA level but has no impact on insulin secretion in INS-1-derived (832/13) β-cells. *J. Biol. Chem*. 276: 6479-6484, 2001

[80] Corkey BE, Deeney JT, Yaney GC, Torheim, Prentki M. The role of long-chain fatty acyl-CoA esters in β-cell signal transduction. *J. Nutr*. 130:299S-304S, 2000

[81] Yaney GC, Corkey BE. Fatty acid metabolism and insulin secretion in pancreatic beta cells. *Diabetologia*. 46:1297-1312, 2003

that the CPTI/malonyl-CoA interaction is involved in GSIS, supporting the malonyl-CoA/LC-CoA model.

7.1 EFFECTOR MOLECULES IN INSULIN SECRETION

It is generally accepted that exogenous NEFA increases LC-CoA and potentiates GSIS and that this action is physiologically relevant. What is missing is a signalling cascade linking changes in LC-CoA to changes in insulin release. Malonyl-CoA, as a nutrient-derived coupling factor, regulates the partitioning of fatty acid into effector molecules of the insulin secretory pathway important for all classes of secretagogues. The precise nature of these effector molecules and their mechanisms of action on insulin secretion are poorly understood. Possible candidates for these effector molecules are non-esterified palmitate, LC-CoA, phospholipids and/or DAG. PKC isoforms are also reasonable candidates to either initiate secretion or augment GSIS as they respond to both lipid signals and Ca^{2+}.

Insulin exocytosis is a complex sequential process involving many steps, including vesicle movement, docking, priming, fusion with the plasma membrane and ultimately dissociation and recycling of exocytotic components. This is a likely site for regulation by fatty acid moieties, acting directly on signal transducing effectors of secretion or indirectly *via* activation of some kinases, in particular the PKC enzymes by DAG and LC-CoA. Possibilities of more direct distal effects include LC-CoA acylation of proteins. Protein acylation is a post-translational event, which usually links palmitate in the form of a fatty acyl-CoA, as the preferred substrate, to a cysteine residue through a thioester linkage in a variety of proteins. Because it is a reversible modification with dynamic cycles of acylation and deacylation, it may have a role in signal transduction. This was supported by a study with rat islets in which the protein acylation inhibitor cerulenin inhibited GSIS[82]. Moreover, in the presence of KCl and diazoxide (conditions which allow us to differentiate the K_{ATP} channel-dependent from K_{ATP} channel-independent pathways of glucose sensing), cerulenin powerfully inhibited the augmentation of insulin release by glucose and palmitate, thus implicating protein acylation in the K_{ATP} channel-independent pathway. PKC has been suggested as one possible target for acylation, because its translocation to membrane bilayers was

[82] Yajima H, Komatsu M, Yamada S, Straub SG, Kaneko T, Sato Y, Yamauchi K, Hashizume K, Sharp GWG, Aizawa T. Cerulenin, an inhibitor of protein acylation, selectively attenuates nutrient stimulation of insulin release. *Diabetes*. 49:712-717, 2000

facilitated upon palmitoylation[58]. Moreover, acylation also occurs on proteins directly linked to exocytosis such as the synaptosomal-associated protein-25 (SNAP-25)[83] and synaptogamin[84], which can enhance their association with target membranes. Another possibility of a distal effect in secretion is DAG modulation of exocytotic machinery proteins such as the synaptic vesicle priming protein Munc-13[85]. Of potential importance, Munc-13 has a C1 domain binding site for DAG, and it is direct binding to this site, rather than PKC activation, by which β-phorbol esters and DAG mediate augmentation of neurotransmitter release from neurons. Munc-13 is present in β-cells[86] and therefore could be an important site for fatty acid induction/augmentation of insulin secretion.

In addition, three recent reports suggested that exogenous FFAs could also act directly on β-cells as a ligand for the orphan G-protein receptor GPR40[87,88,89]. These reports are preliminary, and, in particular, the secretory action of the FFA was tested in the absence of BSA. Thus, the real importance of this pathway of FFA-signalling in physiological insulin secretion is uncertain. It remains an attractive possibility that both FFA metabolism and direct effects *via* GPR40 are involved in the regulation of insulin secretion.

---

[83] Gonzalo S, Linder ME. SNAP-25 palmitoylation and plasma membrane targeting require a functional secretory pathway. *Mol. Biol. Cell*. 9:585-597, 1998

[84] Chapman ER, Blasi J, An S, Brose N, Johnston PA, Sudhof TC, Jahn R. Fatty acylation of synaptotagmin in PC12 cells and synaptosomes. *Biochem. Biophys. Res. Commun*. 225:326-332, 1996

[85] Rhee JS, Betz A, Pyott S, Reim K, Varoqueaux F, Augustin I, Hesse D, Sudhof TC, Takahashi M, Rosenmund C, Brose N. Beta phorbol ester- and diacylglycerol-induced augmentation of transmitter release is mediated by Munc13s and not by PKCs. *Cell*. 108:121-133, 2002

[86] Sheu L, Pasyk EA, Ji J, Huang X, Gao X, Varoqueaux F, Brose N, Gaisano HY. Regulation of insulin exocytosis by Munc13-1. *J. Biol. Chem*. 278:27556-27563, 2003

[87] Itoh Y, Kawamata Y, Harada M, Kobayashi M, Fujii R, Fukusumi S, Ogi K, Hosoya M, Tanaka Y, Uejima H, Tanaka H, Maruyama M, Satoh R, Okubo S, Kizawa H, Komatsu H, Matsumura F, Noguchi Y, Shinohara T, Hinuma S, Fujisawa Y, Fujino M. Free fatty acids regulate insulin secretion from pancreatic beta cells through GPR40. *Nature*. 422:173-176, 2003

[88] Kotarsky K, Nilsson NE, Flodgren E, Owman C, Olde B. A human cell surface receptor activated by free fatty acids and thiazolidinedione drugs. *Biochem Biophys Res Commun*. 301:406-410, 2003

[89] Briscoe CP, Tadayyon M, Andrews JL, Benson WG, Chambers JK, Eilert MM, Ellis C, Elshourbagy NA, Goetz AS, Minnick DT, Murdock PR, Sauls HR Jr, Shabon U, Spinage LD, Strum JC, Szekeres PG, Tan KB, Way JM, Ignar DM, Wilson S, Muir AI. The orphan G protein-coupled receptor GPR40 is activated by medium and long chain fatty acids. *J. Biol. Chem*. 278:11303-11311, 2003

Further investigation on these novel lipid-signalling processes will have many implications for the understanding of the link between fat and β-cell adaptation and failure in the cause of diabetes.

8. GLUCOLIPOTOXICITY

The roles of glucose and FFA as "toxic" factors of the (pre)diabetic milieu influencing β-cell function and the etiology of diabetes are controversial. It was first proposed that chronic hyperglycemia is progressively deleterious to the islet, which led to the concept of "glucotoxicity"[90]. However, more recent evidence suggests that elevated circulating and intracellular lipids, in addition to glucose, play an important role in the etiology of adipogenic diabetes[39]. Diabetes may therefore be considered as much a lipid disorder as a disease of glucose tolerance.

Lipid metabolism in the β-cell is critical for the regulation of insulin secretion[81]. Interestingly, glucose-induced insulin secretion by the perfused pancreas isolated from starved rats is absolutely dependent on the prior provision of exogenous fatty acid, whereas that by the pancreas isolated from fed animals is not[91, 92]. Similarly, inhibition of adipose tissue lipolysis in starved rats prevents the insulin secretory response that normally accompanies re-feeding, and this is restored by simultaneous infusion of triglyceride and heparin[93]. Long-term exposure of β-cells to NEFAs *in vitro* has several effects: 1) it increases basal insulin release and decreases secretion in response to glucose[94]; 2) it alters the coupling of glucose metabolism to insulin secretion by acting on the expression of specific genes, such as uncoupling protein-2 (UCP-2)[95,96]; 3) it

[90] Unger RH, Grundy S. Hyperglycaemia as an inducer as well as a consequence of impaired islet cell function and insulin resistance: implications for the management of diabetes. *Diabetologia*. 28:119-121, 1985

[91] Stein DT, Stevenson BE, Chester MW, Basit M, Daniels MB, Turley SD, McGarry JD. The insulinotropic potency of fatty acids is influenced profoundly by their chain length and degree of saturation. *J. Clin. Invest.* 100:398-403, 1997

[92] Dobbins RL, Chester MW, Daniels MB, McGarry JD, Stein DT. Circulating fatty acids are essential for efficient glucose-stimulated insulin secretion after prolonged fasting in humans. *Diabetes*. 47:1613-1618, 1998

[93] Stein DT, Esser V, Stevenson BE, Lane KE, Whiteside JH, Daniels MB, Chen S, McGarry JD. Essentiality of circulating fatty acids for glucose-stimulated insulin secretion in the fasted rat. *J. Clin. Invest.* 97:2728-2735, 1996

[94] Zhou YP, Grill V. Long-term exposure of rat pancreatic islets to fatty acids inhibits glucose-induced insulin secretion and biosynthesis through a glucose fatty acid cycle. *J. Clin. Invest.* 93:870-876, 1994

[95] Lameloise N, Muzzin P, Prentki M, Assimacopoulos-Jeannet F. Uncoupling protein 2: a possible link between fatty acid excess and impaired glucose-induced insulin secretion? *Diabetes*. 50:803-809, 2001

increases the expression of CPTI[97]. CPTI upregulation following chronic NEFA exposure of the β-cell may contribute to reduced GSIS.

In addition, the effects of nutrients on the β-cell can be quite different depending on whether the exposure is acute or chronic. Elevated levels of glucose and FFA stimulate insulin release acutely while chronic exposure, as is the case in NIDDM, can lead to deleterious effects described as "glucotoxicity" and "lipotoxicity". Chronic increases in the concentration of glucose and saturated FFA cause dysfunction and damage to the β-cell, and ultimately result in apoptosis[98,99]. This β-cell apoptosis resulting from the increased circulating free fatty acids and cellular lipid accumulation has been called lipotoxicity[100]. But, this is a confusing concept, since other authors have suggested that glucotoxicity is the prerequisite for lipotoxicity[101,102].

Nevertheless, recent studies demonstrate that even moderately elevated concentrations of glucose synergize with saturated FFAs to cause β-cell apopotosis, a phenomenon named "glucolipotoxicity"[98]. The authors propose[103] that when both glucose and FFA levels are high, cytosolic FA-CoA increases because the ability of fatty acids to increase their oxidation is diminished due to decreased PPARα activation, enhanced SREBP-1c expression, reduced AMPK activity and increased malonyl-CoA levels caused by the rise in glucose. This, in turn, increases FA-CoA partitioning toward potentially toxic cellular products, including possibly DAG, ceramide and lipid

---

[96] Zhang CY, Baffy G, Perret P, Krauss S, Peroni O, Grujic D, Hagen T, Vidal-Puig AJ, Boss O, Kim YB, Zheng XX, Wheeler MB, Shulman GI, Chan CB, Lowell BB. Uncoupling protein-2 negatively regulates insulin secretion and is a major link between obesity, beta cell dysfunction and type 2 diabetes. *Cell.* 105:745-755, 2001

[97] Assimacopoulos-Jeannet F, Thumelin S, Roche E, Esser V, McGarry JD, Prentki M. Fatty acids rapidly induce the carnitine palmitoyltransferase I gene in the pancreatic β-cell line INS-1. *J. Biol. Chem*. 272:1659-1664, 1997

[98] El-Assaad W, Buteau J, Peyot ML, Nolan C, Roduit R, Hardy S, Joly E, Dbaibo G, Rosenberg L, Prentki M. Saturated fatty acids synergize with elevated glucose to cause pancreatic beta-cell death. *Endocrinology*. 144:4154-4163, 2003

[99] Shimabukuro M, Higa M, Zhou YT, Wang MY, Newgard CB, Unger RH. Lipoapoptosis in beta-cells of obese prediabetic fa/fa rats. Role of serine palmitoyltransferase overexpression. *J. Biol. Chem*. 273:32487-90, 1998

[100] Unger RH. Lipotoxic diseases. *Annu. Rev. Med.* 53:319-336, 2002

[101] Poitout V, Robertson RP. Minireview: Secondary beta-cell failure in type 2 diabetes-a convergence of glucotoxicity and lipotoxicity. *Endocrinology*. 143:339-342, 2002

[102] Weir GC, Laybutt DR, Kaneto H, Bonner-Weir S, Sharma A. Beta-cell adaptation and decompensation during the progression of diabetes. *Diabetes*. 50:S154-159, 2001

[103] Prentki M, Joly E, El-Assaad W, Roduit R. Malonyl-CoA signaling, lipid partitioning, and glucolipotoxicity: role in beta-cell adaptation and failure in the etiology of diabetes. *Diabetes*. 51:S405-S413, 2002

peroxides. The nature of the downstream events that lead to β-cell death is not entirely clear; however, increases in oxidant stress and the production of nitric oxide could be involved[100].

Emerging evidence suggests that changes in malonyl-CoA-AMPK signalling are important in the pathogenesis of both β-cell glucolipotoxicity and Type 2 diabetes[52]. Metformin and 5-aminoimidazole-4-carboxamide ribonucleoside (AICAR), agents that activate AMPK and thereby favour fatty acid β-oxidation, prevent glucolipotoxicity-induced apoptosis in INS(832/13) cells[98]; overexpression of SREBP-1c in β-cells leads to activation of FAS gene expression, an accumulation of triglycerides (TG) and a profound inhibition of GSIS[104]; and finally, in the Zucker diabetic fatty (ZDF) rat, a rodent with a mutated, non-functioning leptin receptor (Ob-Rb), overexpression of the Ob-Rb gene in islet tissue *in vitro* allowed leptin, which activates AMPK[105], to reverse the diabetogenic phenotype, reduce TG stores and inhibit FFA-induced apoptosis[100].

In conclusion, when both glucose and FFA levels are high, then the problems arises, and together they may progressively alter the function of various cell types and cause insulin resistance in muscle tissue, impair glucose induced secretion, or promote β-cell apoptosis and the progressive neural diabetes complications. Thus, as Aristotle said: “Everything in moderation”.

9. PPAR

Tight regulation of metabolic pathways involves the rapid modulation of the activity of specific proteins (enzymes, transporters) but also, on a longer-term basis, changes in their quantity. This can be achieved by modulating their transcription rate through the action of specific transcription factors. The discovery of the peroxisome proliferator-activated receptor (PPAR) family of transcription factors has revealed the mechanism of the strong link between lipid/glucose availability and long-term metabolic adaptation. PPARs play a critical physiological role as lipid sensors and regulators of lipid metabolism.

---

[104] Wang H, Maechler P, Antinozzi PA, Herrero L, Hagenfeldt-Johansson KA, Björklund A, Wollheim CB. The Transcription factor SREBP-1c is instrumental in the development of β-cell dysfunction. *J. Biol. Chem*. 278:16622-16629, 2003

[105] Minokoshi Y, Kim YB, Peroni OD, Fryer LG, Muller C, Carling D, Kahn BB. Leptin stimulates fatty-acid oxidation by activating AMP-activated protein kinase. *Nature*. 415:339-343, 2002

PPARs form a subfamily of the nuclear receptor superfamily. Three isoforms, encoded by separate genes, have been identified thus far: PPARα, PPARδ, and PPARγ. The PPARs are ligand-dependent transcription factors that regulate target gene expression by binding to specific peroxisome proliferator response elements (PPREs) in enhancer sites of regulated genes. Each receptor binds to its PPRE as a heterodimer with the 9-*cis*-retinoic acid receptor or retinoid X receptor (RXR)[106]. Upon binding an agonist, the conformation of a PPAR is altered and stabilized such that a binding cleft is created and transcriptional coactivators are recruited. The result is an increase in gene transcription (Fig. 8).

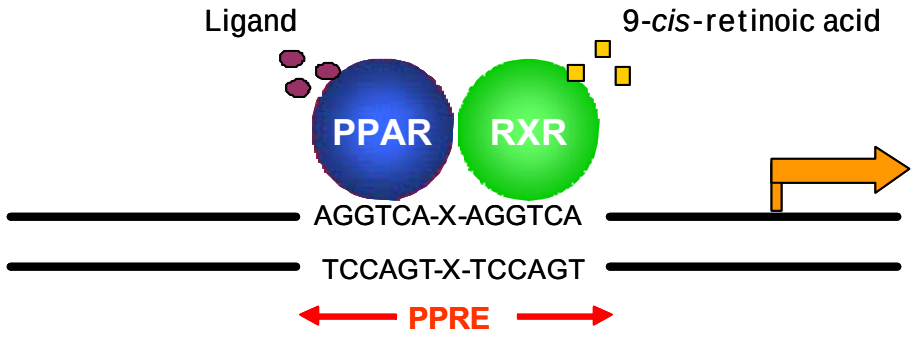

Fig. 8. Mechanism of action of PPARs. Upon ligand binding, PPAR changes its structural conformation, which stimulates its heterodimerization with the 9-*cis*-retinoic acid receptor (RXR), and facilitates the recruitment of cofactors required for the activation of transcription. This heterodimer-cofactor complex controls the expression of genes that contain the peroxisome proliferator response element (PPRE).

PPARδ

PPARδ is expressed in a wide range of tissues and cells, with relatively higher levels of expression in brain, adipose tissue and skin. No PPARδ-specific gene targets have been identified and as PPARα and PPARγ are the most strongly implicated in lipid metabolism and insulin sensitivity they will be further discussed.

[106] Berger J, Moller DE. The mechanisms of action of PPARs. *Annu. Rev. Med.* 53:409-435, 2002

PPARα

PPARα is highly expressed in numerous metabolically active tissues including liver, heart, kidney, skeletal muscle and brown fat. It is also present in monocytic, vascular endothelial, and vascular smooth muscle cells. Its natural ligands are unsaturated fatty acids such as palmitic, oleic, linoleic and arachidonic, and among the synthetic ligands, compounds of the fibrate family (clofibrate, fenofibrate, and bezafibrate) and their derivatives have been widely used to characterize PPARα functions.

In addition to the effects of PPARα on circulating lipoproteins and cholesterol metabolism, it is involved in the regulation of cellular uptake, activation and β-oxidation of fatty acids. PPARα induces expression of fatty acid transport proteins, acetyl-CoA synthetase, pyruvate dehydrogenase kinase 4 (PDK4) and enzymes involved in ketone body synthesis, peroxisomal β-oxidation and mitochondrial β-oxidation such as CPTI, although the latter remains a disputed issue[107].

It has been reported that in PPARα-null mice there is no gross alteration of insulin sensitivity[108] whereas they are protected from high-fat diet-induced insulin resistance[109]. In addition, activation of PPARα in nutritional (high-fat diet), genetic (Zucker obese *fa/fa* rat), or lipoatrophic (A-ZIP/F-1) models of insulin resistance markedly improves insulin sensitivity[108,110,111] and reduces visceral fat in the two former models. So far, no clear explanation has been offered for this discrepancy. In pancreatic β-cells, adenovirus-mediated overexpression of PPARα in INS-1 cells increases fatty

[107] Louet J, Chatelain F, Decaux J, Park E, Kohl C, Pineau T, Girard J, Pegorier J. Long-chain fatty acids regulate liver carnitine palmitoyltransferase I gene (L-CPTI) expression through a peroxisome-proliferator-activated receptor alpha (PPARalpha)-independent pathway. *Biochem. J.* 354:189-197, 2001

[108] Guerre-Millo M, Gervois P, Raspe E, Madsen L, Poulain P, Derudas B, Herber JM, Winegar DA, Willson TM, Fruchart JC, Berge RK, Staels B. Peroxisome proliferator-activated receptor alpha activators improve insulin sensitivity and reduce adiposity. *J. Biol. Chem*. 275:16638-16642, 2000

[109] Guerre-Millo M, Rouault C, Poulain P, Andre J, Poitout V, Peters JM, Gonzalez FJ, Fruchart JC, Reach G, Staels B. PPAR-alpha-null mice are protected from high-fat diet-induced insulin resistance. *Diabetes.* 50:2809-2814, 2001

[110] Ye JM, Doyle PJ, Iglesias MA, Watson DG, Cooney GJ, Kraegen EW. Peroxisome proliferator-activated receptor (PPAR) alpha activation lowers muscle lipids and improves insulin sensitivity in high fat-fed rats: comparison with PPAR gamma activation. *Diabetes*. 50:411-417, 2001

[111] Chou CJ, Haluzik M, Gergory C, Dietz KR, Vinson C, Gavrilova O, Reitman ML. WY14,643, a peroxisome proliferator-activated receptor alpha (PPARalpha) agonist, improves hepatic and muscle steatosis and reverses insulin resitance in lipoatrophic A-ZIP/F-1 mice. *J. Biol. Chem*. 277:24484-24489, 2002

acid oxidation and UCP-2 expression, and decreases GSIS suggesting that PPARα-stimulated fatty acid oxidation can impair β-cell function[112].

In summary, PPARα is an important lipid sensor and regulator of cellular energy-harvesting metabolism. PPARα activation favours fatty acid oxidation, mainly in the liver and heart and to a lesser extent in muscles, and induces glucose sparing, either directly by inducing the expression of PDK4 or indirectly through the synthesis of ketone bodies and the increased fatty acid oxidation capacity. This increased fatty acid oxidation is one of the reasons why fibrates have lipid-lowering effects and why PPARα ligands could in some situations improve insulin sensitivity by reducing lipid accumulation in tissues.

PPARγ

PPARγ is expressed mainly in white and brown adipose tissue, and to a lesser extent in heart, skeletal muscle, colon, small and large intestines, kidney, pancreas, and spleen. PPARγ exists in two protein isoforms (γ1 and γ2) because of the use of alternative promoter and alternative splicing. γ2 has 28 additional amino acids on the N-terminal side in humans. In rodents, the γ2 isoform is the dominant form in adipose tissue, whereas the converse is true in humans. Its natural ligands are polyunsaturated fatty acids such as oleate, linoleate, eicosapentaenoic, and arachidonic acids. It is now clear that members of the thiazolidinedione (TZD) family of antidiabetic compounds are specific PPARγ ligands.

PPARγ is a potent stimulator of fatty acid storage in adipose tissue because it increases both the storage capacity and the fatty acid flux into adipocytes, thus decreasing the circulating free fatty acids. PPARγ is necessary and sufficient to differentiate adipocytes. In adipocytes, PPARγ regulates the expression of numerous genes involved in lipid metabolism by, on one hand, activating those genes involved in fatty acid trapping and storage in adipocytes, such as the genes coding for fatty acid binding proteins, lipoprotein lipase, acyl-CoA synthetase and phosphoenol pyruvate carboxykinase, and, on the other hand, by repressing those genes that induce lipolysis and release of fatty acids, such as the cytokines leptin and the tumor-necrosis factorα

[112] Tordjman K, Standley KN, Bernal-Mizrachi CB, Leone TC, Coleman T, Kelly DP, Semenkovich CF. PPARα suppresses insulin secretion and induces UCP-2 in insulinoma cells. *J. Lipid Research*. 43:936-943, 2002

(TNFα). In addition, PPARγ regulates genes that control cellular energy homeostasis such as the uncoupling proteins (UCPs). PPARγ has also been involved in insulin sensitivity by decreasing the expression of the adipocyte-derived hormones TNFα, leptin and resistin and by increasing the expression of adiponectin and the insulin receptor substrate-2 (IRS-2) [113].

In the pancreatic β-cell evidence is accumulating that PPARγ activation can restore or protect β-cell function from failure and apoptosis during the development of Type 2 diabetes. When circulating glucose and free fatty acids are elevated, energy homeostasis in β-cells is altered, resulting in intracellular accumulation of triglycerides. Treatment with TZD inhibits intracellular triglyceride accumulation in pancreatic β-cells through increases in fatty acid oxidation, thereby delaying β-cell failure[114]. Improvement of cell viability after treatment with troglitazone, a TZD, has also been found in a rodent model of Type 2 diabetes[115], which further suggests that activation of PPARγ prevents β-cell death. In addition, a functional PPRE has been found in the promoter region of GLUT-2[116], the protein responsible for glucose transport in β-cells. PPARγ-mediated stimulation of GLUT-2 expression would increase glucose uptake and trigger the initial steps leading to insulin release. All these observations hence support the hypothesis that PPARγ-mediated restoration or protection of β-cell function is likely to contribute, at least in part, to the mechanisms by which TZD improves and controls glucose homeostasis in diabetic patients.

Some discrepancies have been found concerning with the involvement of PPARγ in insulin sensitivity. When PPARγ (+/-) mice are fed a high-fat diet, they are less insulin resistant[117], but TZD treatment paradoxically decreases their insulin sensitivity.

---

[113] Picard F, Auwerx J. PPARγ and glucose homeostasis. *Annu. Rev. Nutr.* 22:167-197, 2002

[114] Higa M, Zhou YT, Ravazzola M, Baetens D, Orci L, Unger RH. Troglitazone prevents mitochondrial alterations, beta cell destruction, and diabetes in obese prediabetic rats. *Proc. Natl. Acad. Sci. USA*. 96:11513-11518, 1999

[115] Finegood DT, McArthur MD, Kojwang D, Thomas MJ, Topp BG, Leonard T, Buckingham RE. β-cell mass dynamics in Zucker diabetic fatty rats: rosiglitazone prevents the rise in net cell death. *Diabetes*. 50:1021-1029, 2001

[116] Kim HI, Kim JW, Kim SH, Cha JY, Kim Ks, Ahn YH. Identification and functional characterization of the peroxisomal proliferator response element in rat GLUT2 promoter. *Diabetes*. 49:1517-1524, 2000

[117] Kubota N, Terauchi Y, Miki H, Tamemoto H, Yamauchi T, Komeda K, Satoh S, Nakano R, Ishii C, Sugiyama T, Eto K, Tsubamoto Y, Okuno A, Murakami K, Sekihara Ha, Hasegawa G, Naito M, Toyoshima Y, Tanaka S, Shiota K, Kitamura T, Fujita T, Ezaki O, Aizawa S, Nagai R, Tobe K, Kimura S, Kadowaki T. PPAR gamma mediates high-fat diet-induced adipocytes hypertrophy and insulin resistance. *Mol. Cell*. 4:597-609, 1999

These and other studies involving PPARγ mutations[113] with counterintuitive results remain to be explained.

In conclusion, PPARα, by increasing fatty acid oxidation and ketone body production, is a "fasting-lipid oxidation-glucose sparing" regulator, while PPARγ, by increasing triglyceride storage and improving insulin sensitivity, is rather a "well-fed-lipid storing-glucose utilizing" regulator[118]. Clearly, their activation is a means of improving syndromes such as Type 2 diabetes, but their activation in physiological and pathophysiological situations must be further investigated to explain the discrepancies seen in insulin sensitivity.

10. SREBP

The lipogenic transcription factors, sterol regulatory element binding proteins (SREBPs) are transmembrane proteins of the endoplasmic reticulum (ER). In response to low sterol and other unidentified factors, SREBP cleavage-activating protein (SCAP) escorts SREBPs from the ER to the Golgi, where SREBPs are sequentially cleaved by Site-1 protease and Site-2 protease. The processed mature SREBPs enter the nucleus and bind to sterol regulatory elements (SREs) on the promoter regions of target genes involved in the lipid biosynthesis pathway, and activate their transcription[119].

Three SREBP isoforms have been identified: SREBP-1a and -1c (alternatively known as adipocyte determination and differentiation factor-1 (ADD1)), which are derived from the same gene through alternative splicing, and SREBP-2, which is encoded by a distinct gene.

SREBPs play an essential role in the regulation of lipid homeostasis and have been shown to directly activate the expression of more than 30 genes involved in the biosynthesis of cholesterol, fatty acids, triglycerides and phospholipids[120]. SREBP-1a is a potent activator of both the cholesterol and fatty acid biosynthetic pathways. SREBP-1c is relatively specific for fatty acid biosynthesis in the liver and adipocytes, and SREBP-2 preferentially activates genes involved in cholesterol synthesis[119]. In

[118] Ferré P. The biology of peroxisome proliferator-activated receptors. Relationship with lipid metabolism and insulin sensitivity. *Diabetes*. 53:S43-S50, 2004

[119] Brown MS, Goldstein JL. The SREBP pathway: regulation of cholesterol metabolism by proteolysis of a membrane-bound transcription factor. *Cell.* 89:331-340, 1997

[120] Horton JD, Goldstein JL, Brown MS. SREBPs: activators of the complete program of cholesterol and fatty acid synthesis in the liver. *J. Clin. Invest.* 109:1125-1131, 2002

particular, SREBP-1c mediates insulin effects on lipogenic gene expression in both adipocytes and liver[121,122].

The activities of the SREBPs in liver are controlled at two levels: transcriptional and posttranscriptional. Transcription of the SREBP-1c gene is markedly enhanced by insulin and suppressed by glucagon[123]. The insulin-mediated enhancement of SREBP-1c gene transcription provides a mechanism by which insulin increases the synthesis of fatty acids in the liver. SREBP-1c transcription is also activated by liver X receptors (LXRs), whose endogenous ligands include sterol intermediates in the cholesterol biosynthetic pathway[124]. Inhibition of LXR by polyunsaturated fatty acids down-regulates SREBP-1c mRNA levels[125]. Posttranscriptionally, SREBP activity is regulated primarily by sterols, which inhibit the proteolytic processing of the membrane-bound SREBP precursors. This control is mediated by two proteins: SCAP and Insig[126], an intrinsic membrane protein of the ER. Under conditions of sterol excess, the SCAP/SREBP complex binds to Insig which traps it in the ER and prevents the proteolytic process and therefore the maturation of SREBP. As a result, the synthesis of cholesterol and fatty acids declines. Recently it has been reported that the Insig gene is down-regulated by insulin[127] in the liver, thus in conditions of energy excess Insig allows the synthesis of cholesterol and fatty acids by SREBP.

---

[121] Kim JB, Sarraf P, Wright M, Yao KM, Mueller E, Solanes G, Lowell BB, Spiegelman BM. Nutritional and insulin regulation of fatty acid synthetase and leptin gene expression through ADD1/SREBP1. *J. Clin. Invest.* 101:1-9, 1998

[122] Foretz M, Guichard C, Ferre P, Foufelle F. Sterol regulatory element binding protein-1c is a major mediator of insulin action on the hepatic expression of glucokinase and lipogenesis-related genes. *Proc. Natl. Acad. Sci. U. S. A.* 96:12737-12742, 1999

[123] Zhang J, Ou J, Bashmakov Y, Horton JD, Brown MS, Goldstein JL. Insulin inhibits transcription of IRS-2 gene in rat liver through an insulin response element (IRE) that resembles IREs of other insulin-repressed genes. *Proc. Natl. Acad. Sci. USA*. 98:3756-3761, 2001

[124] DeBose-Boyd RA, Ou J, Goldstein Jl, Brown MS. Expression of sterol regulatory element-binding protein 1c (SREBP-1c) mRNA in rat hepatoma cells requires endogenous LXR ligands. *Proc. Natl. Sci. USA*. 98:1477-1482, 2001

[125] Ou J, Tu H, Shan B, Luk A, DeBose-Boyd RA, Bashmakov Y, Goldstein JL, Brown MS. Unsaturated fatty acids inhibit transcription of the sterol regulatory element-binding protein-1c (SREBP-1c) gene by antagonizing ligand-dependent activation of the LXR. *Proc. Natl. Sci. USA*. 98:6027-6032, 2001

[126] Yang T, Espenshade PJ, Wright ME, Yabe D, Gong Y, Aebersold R, Goldstein JL, Brown MS. Crucial step in cholesterol homeostasis: sterols promote binding of SCAP to INSIG-1, a membrane protein that facilitates retention of SREBPs in ER. *Cell*. 110:489-500, 2002

[127] Yabe D, Komuro R, Liang G, Goldstein JL, Brown MS. Liver-specific mRNA for Insig-2 down-regulated by insulin: implications for fatty acid synthesis. *Proc. Natl. Sci. USA*. 100:3155-3160, 2003

Many studies have implicated the up-regulation of SREBP in β-cell dysfunction and Type 2 diabetes. Elevated expression of SREBP-1c has been demonstrated in islets or liver of diabetic animals, such as ZDF rats (*fa/fa*)[128], ob/ob mice[129], IRS-2 deficient mice[130], and a transgenic mouse model of lipodystrophy[131]. On the other hand, preventing SREBP-1c overexpression is a common function of leptin, metformin, and PPARγ agonists, which is well correlated with their antidiabetic effects[128-131]. An important function of leptin in the regulation of fatty acid homeostasis is to restrict the lipid storage in adipocytes and to limit lipid accumulation in non-adipocytes, thereby protecting them from lipotoxicity[100].

Related to insulin secretion, it has been reported that overexpression of SREBP-1c in MIN-6 cells[132], INS-1 cells[104,133] and rat islets[134] results in massive accumulation of cellular TG and impaired GSIS. SREBP-1c induces β-cell dysfunction by targeting multiple genes involved in lipid biosynthesis, carbohydrate metabolism, cell growth, and apoptosis. In INS-1 cells[104] induction of SREBP-1c significantly increased the expression of genes involved in biosynthesis of fatty acids and cholesterol (fatty acid synthase, acetyl-CoA carboxylase, glycerol-phosphate acyltransferase, and 3-hydroxy-3-methyl-glutaryl-CoA), but did not alter the expression of genes involved in β-

[128] Katuma T, Lee Y, Higa M, Wang ZW, Pan W, Shimomura I, Unger RH. Leptin, troglitazone, and the expression of sterol regulatory element binding proteins in liver and pancreatic islets. *Proc. Natl. Sci. USA*. 97:8536-8541, 2000

[129] Lin HZ, Yang SQ, Chuckaree C, Kuhajda F, Ronnet G, Diehl AM. Lin, H. Z., Yang, S. Q., Chuckaree, C., Kuhajda, F., Ronnet, G., and Diehl, A. M. Metformin reverses fatty liver disease in obese, leptin-deficient mice. *Nat. Med.* 6:998-1003, 2000

[130] Tobe K, Suzuki R, Aoyama M, Yamauchi T, Kamon J, Kubota N, Terauchi Y, Matsui J, Akanuma Y, Kimura S, Tanaka J, Abe M, Ohsumi J, Nagai R, Kadowaki T. Increased Expression of the Sterol Regulatory Element-binding Protein-1 Gene in Insulin Receptor Substrate-$2^{-/-}$ Mouse Liver. *J. Biol. Chem.* 276:38337-38340, 2001

[131] Shimomura I, Hammer RE, Ikemoto S, Brown MS, Goldstein JL. Leptin reverses insulin resistance and diabetes mellitus in mice with congenital lipodystrophy. *Nature.* 401:73-76, 1999

[132] Andreolas C, da Silva Xavier G, Diraison F, Zhao C, Varadi A, Lopez-Casillas F, Ferre P, Foufelle F, Rutter GA. Stimulation of acetyl-CoA carboxylase gene expression by glucose requires insulin release and sterol regulatory element binding protein 1c in pancreatic MIN6 β-cells. *Diabetes.* 51:2536-2545, 2002

[133] Yamashita T, Eto K, Okazaki Y, Yamashita S, Yamauchi T, Sekine N, Nagai R, Noda M, Kadowaki T. Role of UCP-2 up-regulation and TG accumulation in impaired glucose-stimulated insulin secretion in a β-cell lipotoxicity model overexpressing SREBP-1c. *Endocrinology*. 145:3566-3577, 2004

[134] Diraison F, Parton L, Ferré P, Foufelle F, Briscoe CP, Leclerc I, Rutter GA. Over-expression of sterol-regulatory-element-binding protein-1c (SREBP1c) in rat pancreatic islets induces lipogenesis and decreases glucose-stimulated insulin release: modulation by 5-aminoimidazole-4-carboxamide ribonucleoside (AICAR). *Biochem. J*. 378:769-778, 2004

oxidation of fatty acids (CPTI and acyl-CoA oxidase) which would explain the increased TG accumulation. SREBP-1c induction also caused marked down-regulation of GK and GLUT-2 but up-regulation of UCP-2. GK is the rate-limiting enzyme for glycolysis and thereby determines β-cell glucose sensing (see section 3.2) and UCP-2 may act as a protonophore and dissipate the mitochondrial membrane potential, thereby uncoupling respiration from ATP synthesis. This would explain the impairment of GSIS. Induction of SREBP-1c also leads to INS-1 cell growth arrest and apoptosis likely due because, as SREBP-1c is a known substrate for caspase 3, it may function as a proapoptotic gene in β-cells. The AMPK agonist AICAR increased fatty acid oxidation and restored TG levels and the impaired GSIS in SREBP-1c-overexpressing β-cells[133], although the effects of AICAR on insulin secretion seem easily influenced by experimental conditions, giving opposite results in other studies[135].

Taken together, these results provide strong evidence that SREBP-1c mediates β-cell dysfunction and may be implicated in the pathogenesis of β-cell glucolipotoxicity and Type 2 diabetes. It is hypothesized that as a result of the persistent hyperglycemia and hyperinsulinemia present in diabetes, SREBP-1c protein is processed and modified to an active form. Activated SREBP-1c alters the expression of various target genes that contribute to β-cell dysfunction and therefore exacerbates the progression of Type 2 diabetes. Development of chemical compounds acting like leptin, PPARγ agonists, and metformin through suppression of SREBP-1c function should have therapeutic potential in the treatment of Type 2 diabetes and its complications.

11. FATTY ACID IMPORT INTO MITOCHONDRIA

11.1 CELL UPTAKE AND ACTIVATION OF LONG-CHAIN FATTY ACIDS

Long-chain fatty acids are the main energy source for many organs, especially muscle and liver. In the liver, oxidation of fatty acids also serves an additional role. It produces ketone bodies which are important fuels for extrahepatic organs. Since most tissues contain only small amounts of storage lipids, energy production depends on a continuous supply of fatty acids, mostly from adipose tissue. Fatty acids are produced by lipolysis, transported bound to albumin in blood and taken up by tissues in a process

[135] da Silva Xavier G, Leclerc I, Varadi A, Tsuboi T, Moule SK, Rutter GA. Role for AMP-activated protein kinase in glucose-stimulated insulin secretion and preproinsulin gene expression. *Biochem. J.* 371:761-774, 2003

mediated by transport proteins present in the plasma membrane[136]. Once within the cell, free fatty acids are bound to fatty acid binding proteins which are present in the cytosol in high amounts[137]. Depending on the tissue and its metabolic demand, fatty acids are either converted to triglycerides or membrane phospholipids or oxidized in the mitochondria for energy production. The β-oxidation of activated fatty acids occurs within the mitochondrial matrix and is catalyzed by the sequential action of four enzyme families (acyl-CoA dehydrogenase, enoyl-CoA hydratase, 3-hydroxyacyl-CoA dehydrogenase and 3-ketoacyl-CoA thiolase), each with different substrate specificity for short-, medium- and long chain-CoAs[138].

Before being directed into storage, membranes or oxidation, fatty acids are first activated to acyl-CoAs. This reaction is catalyzed by long-chain acyl-CoA synthetase (LCAS), which is abundant in microsomes and mitochondria[139]. LCAS is associated with the mitochondrial outer membrane (MOM) and appears to be a transmembrane protein with the active site exposed to the cytosol[140].

This orientation of LCAS gives rise to cytosolic production of LC-CoA, which must cross both mitochondrial boundary membranes for β-oxidation.

Esterification of carboxylic acids to coenzyme A (CoA) through a thioester bond is a common strategy used in metabolic processes to 'activate' the relevant metabolite. This activation has two universal consequences: 1) it renders the acyl-CoA ester impermeant through cellular membranes, and 2) it sequesters CoA from the limited pools that exist in individual subcellular compartments. As a result, the pools of acyl-CoA esters are maintained separate in the different cellular compartments, which is imperative due to the high biological activity displayed by some of them. Consequently, the cell has two requirements: 1) a mechanism for the control of CoA ester concentrations that is rapid and does not involve the energetically expensive hydrolysis and resynthesis of the esters from the free acid, and 2) a system that, after the

[136] Van Nieuwenhoven FA, Van der Vusse GJ, Glatz JFC. Membrane-associated and cytoplasmic fatty acid-binding proteins. *Lipids*. 31:S223-S227, 1996

[137] Bernlohr DA, Simpson MA, Vogel-Hertzel AV, Banaszak LJ. Intracellular lipid-binding proteins and their genes. *Annu. Rev. Nutr*. 17:277-303, 1997

[138] Eaton S, Barlett K, Pourfarzam M. Mammalian mitochondrial β-oxidation. *Biochem. J*. 320:345-357, 1996

[139] Watkins PA. Fatty acid activation. *Prog. Lipid Res*. 36:55-83, 1997

[140] Hesler CB, Olymbios C, Haldar D. Transverse-plane topography of long-chain acyl-CoA synthetase in the mitochondrial outer membrane. *J. Biol. Chem*. 265: 6600-6605, 1990

initial synthesis of the CoA ester, enables the acyl moiety to permeate membranes without the need to re-expend energy.

The cell achieves all these requirements through a single mechanism, the transesterification between acyl-CoA esters and L-carnitine to form the corresponding carnitine ester and regenerate unesterified CoA:

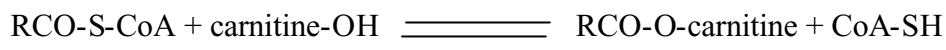

These reactions are catalysed by a family of carnitine acyltransferases[141]. They enable the cell to move the required moieties between intracellular compartments while keeping its pools of CoA esters distinct in their respective compartments. The enzyme involved depends on the length of the fatty acyl moiety to be transported. Carnitine acetyltransferase[142] (CAT) acts with acetyl-CoA as substrate, while carnitine octanoyltransferase (COT) facilitates the transport of medium-chain fatty acids (C8-C10) from peroxisomes to mitochondria through the conversion of shortened fatty acyl-CoA from peroxisomal β-oxidation into fatty acylcarnitine[143]. Peroxisomal β-oxidation does not directly provide energy but is able to shorten very long-chain fatty acids, thus allowing their subsequent mitochondrial β-oxidation. It also has a detoxifying action by oxidizing molecules such as eicosanoids and xenobiotics. Finally, carnitine palmitoyltransferases[144] (CPTs) I and II facilitate the transport of long-chain acyl groups (C16) into the mitochondrial matrix, where they undergo β-oxidation.

One characteristic that differentiates the various carnitine acyltransferases activities is their sensitivity to inhibition by malonyl-CoA. CPTI and COT are sensitive to malonyl-CoA, while CAT and CPTII are not[144].

[141] Zammit VA. Carnitine acyltransferases: functional significance of subcellular distribution and membrane topology. *Progress in lipid research*. 38:199-224, 1999

[142] Bieber LL. Carnitine. *Annu.Rev. Biochem*. 57:261-283, 1988

[143] Ferdinandusse S, Mulders J, Ijlst L, Denis S, Dacremont G, Waterham HR, Wanders RJ. Molecular cloning and expression of human carnitine octanoyltransferase: evidence for its role in the peroxisomal β-oxidation of branched-chain fatty acids. *Biochem. Biophys. Res. Commun*. 263:213-218, 1999

[144] McGarry JD, Brown NF. The mitochondrial carnitine palmitoyltransferase system. From concept to molecular analysis. *Eur. J. Biochem.* 244:1-14, 1997

11.2 CARNITINE PALMITOYLTRANSFERASE SYSTEM

The carnitine-dependent transport of activated fatty acids precedes their β-oxidative chain shortening. This transport system consists of three proteins[145], CPTI, carnitine:acylcarnitine translocase (CACT) and CPTII, each with a different submitochondrial localization. As a first step, LC-CoAs formed by the catalytic action of LCAS in the MOM are converted to acylcarnitines. This transesterification is catalyzed by transmembrane CPTI protein, also localized in the MOM. The reaction products, LC-acylcarnitines, are then translocated into the mitochondrial matrix in an exchange reaction catalyzed by CACT, an integral inner membrane protein. Within the matrix the acylcarnitines are then reconverted to the respective acyl-CoAs by CPTII, an enzyme associated with the inner leaflet of the mitochondrial inner membrane (MIM) (Fig. 9).

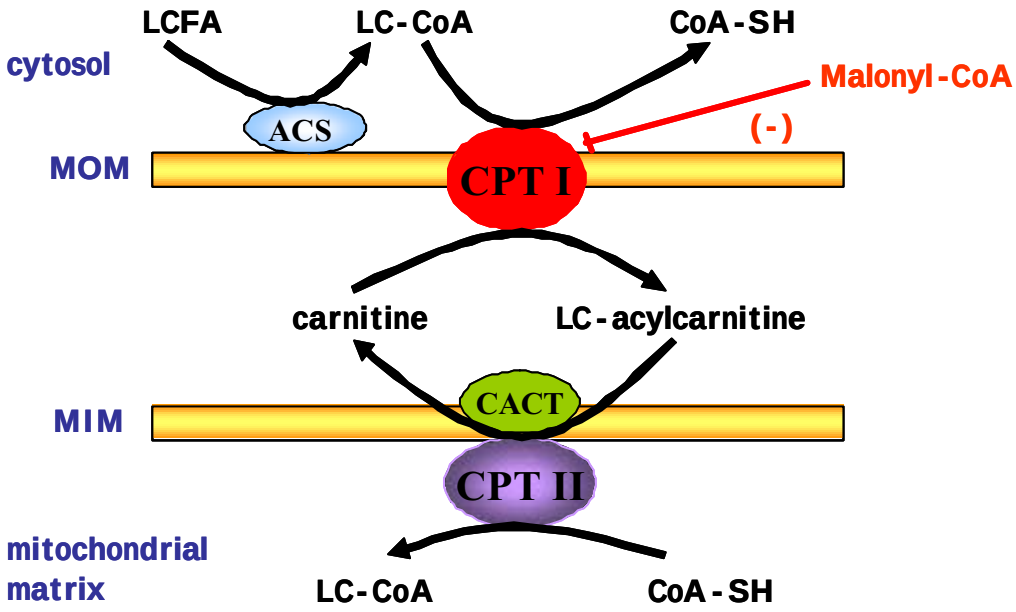

Fig. 9. LC-CoA translocation into the mitochondria by the carnitine palmitoyltransferase system. Long-chain fatty acids (LCFA) are activated to LC-CoA by the action of the acyl-CoA synthetase (ACS). Transport of LC-CoA from the cytosol to the mitochondrial matrix involves the conversion of LC-CoA to acylcarnitines by CPTI, translocation across the mitochondrial inner membrane by the carnitine:acylcarnitine translocase (CACT) and reconversion to LC-CoA by CPTII. MOM: mitochondrial outer membrane; MIM: mitochondrial inner membrane.

[145] Kerner J, Hoppel C. Fatty acid import into mitochondria. Review. *Biochimica et Biophysica Acta*. 1486:1-17, 2000

CPTI is tightly regulated by its physiological inhibitor malonyl-CoA, and thus CPTI is the most physiologically important regulatory step in mitochondrial fatty acid oxidation[146]. This process allows the cell to signal the relative availability of lipid and carbohydrate fuels in liver, heart, skeletal muscle, and pancreatic β-cells[147] and converts CPTI into a potential pharmacological target for the treatment of metabolic disorders such as coronary diseases and diabetes[148].

11.2.1 CPTI isoforms and distribution

Mammals express two isoforms of CPTI, a liver isoform (LCPTI) [149,150] and a heart/skeletal muscle isoform (MCPTI)[151,152], which are the products of two different genes. The human codifying genes are localized at the 11q13 (LCPTI) and 22q13.3 (MCPTI) chromosomes[153]. LCPTI protein contains 773 amino acids (88 kDa) and MCPTI is a protein of 772 amino acids (88 kDa). The identity in amino acids residues is high (62%) but they are differentially regulated by malonyl-CoA. The LCPTI isoform is inhibited by malonyl-CoA to a much lesser extent than the MCPTI isoform (the IC_{50} value for MCPTI is about 2 orders of magnitude lower than for LCPTI)[154]. This

[146] McGarry JD, Foster DW. Regulation of hepatic fatty acid oxidation and ketone body production. *Annu. Rev. Biochem*. 49:395-420, 1980

[147] Zammit VA. The malonyl-CoA-long-chain acyl-CoA axis in the maintenance of mammalian cell function. *Biochem. J.* 343:505-515, 1999

[148] Ruderman NB, Saha AK, Vavvas D, Witters LA. Malonyl-CoA, fuel sensing, and insulin resistance. *Am. J. Physiol*. 276:E1-E18, 1999

[149] Esser V, Britton CH, Weis BC, Foster DW, McGarry JD. Cloning and sequencing and expression of a cDNA encoding rat liver carnitine palmitoyltransferase I. *J. Biol. Chem*. 268:5817-5822, 1993

[150] Britton CH., Schultz RA., Zhang B. Esser V. Foster DW. and McGarry JD. Human liver mitochondrial carnitine palmitoyltransferase I: characterization of its cDNA and chromosomal localization and partial analysis of the gene. *Proc. Natl. Acad. Sci. USA*. 92:1984-1988, 1995

[151] Yamazaki N, Shinohara Y, Shima A, Terada H. High expression of a novel carnitine palmitoyltransferase I like protein in rat brown adipose tissue and heart: isolation and characterization of its cDNA clone. *FEBBS Lett.* 363:41-45, 1995

[152] Yamazaki N, Shinohara Y, Shima A, Yamanaka Y, Terada H. Isolation and characterization of cDNA and genomic clones encoding human muscle type carnitine palmitoyltransferase I. *Biochim. Biophys. Acta.* 1307:157-161, 1996

[153] Britton CH, Mackey DW, Esser V, Foster DW, Burns DK, Yarnall DP, Froguel P, McGarry JD. Fine chromosome mapping of the genes for human liver and muscle carnitine palmitoyltransferase I (CPT1A and CPT1B). *Genomics.* 40:209-211, 1997

[154] Esser V, Brown NF, Cowan AT, Foster DW, McGarry JD. Expression of a cDNA isolated from rat brown adipose tissue and heart identifies the product as muscle isoform of carnitine palmitoyltransferase I (M-CPTI). M-CPTI is the

property is probably involved in the finer regulation of fatty acid oxidation in heart and skeletal muscle in comparison to liver.

Recently a novel CPTI family member (CPTIc) has been described which is mainly expressed in brain and testis[155]. The protein sequence contains all the residues known to be important for both carnitine acyltransferase activity and malonyl-CoA binding in other family members. However, yeast-expressed protein had no detectable catalytic activity with several different acyl-CoA esters that are good substrates for other carnitine acyltransferases, while displaying high-affinity malonyl-CoA binding. It is hypothesized that this novel CPTI related protein may be specialized for the metabolism of a distinct class of fatty acids involved in brain function and/or appetite control.

The distribution and kinetic characteristics of the mitochondrial CPTI enzymes are summarized in the next table:

predominant CPTI isoform expressed in both white (epididymal) and brown adipocytes. *J. Biol. Chem*. 271:6972-6977, 1996

[155] Price NT, van der Leij FR, Jackson VN, Corstorphine CG, Thomson R, Sorensen A, Zammit V. A novel brain-expressed protein related to carnitine palmitoyltransferase I. *Genomics*. 80:433-442, 2002

	LCPTI	MCPTI	CPTII	CPTIc
Mass	88 kDa	88 kDa	70 kDa	88 kDa
Malonyl-CoA IC_{50}	2.5 μM	0.03 μM	–	
Carnitine K_m	30 μM	500 μM	120 μM	
Human chromosome locus	11q13	22q13.3	1p32	19q13.33
Tissue expression				
Liver	++++	–	+	
Skeletal muscle	(+)	++++	+	
Heart	+	+++	+	
Kidney	++++	(+)	+	
Lung	++++	(+)	+	
Spleen	++++	–	+	
Intestine	++++	–	+	(+)
Pancreas (islets and acinar)	++++	–	+	
Brown adipose tissue	(+)	++++	+	
White adipocytes	+	+++	+	
Ovary	++++	(+)	+	(+)
Testis	(+)	++++	+	(+)
Human fibroblasts	++++	–	+	
Brain:				+
Cerebellum	–	++++	+	–
Human deficiency described:	yes	no	yes	no

Table 1. Overview of mitochondrial CPTI enzymes. Relative levels of CPTI isoform expression for each organ are based on northern blot analysis (and in some cases [^{3}H]etomoxir-CoA labelling), but do not indicate precise ratios. (+), trace expression compared with the alternative isoform; –, undetected. Tissue expression data refer to the rat, except in the case of fibroblasts and brain. The K_m for carnitine of CPTII was measured after solubilization of mitochondria in 1% octyl glucoside and therefore should not be compared directly with the values for CPTI. Table obtained from[144] with some modifications.

11.3 CPTI REGULATION

11.3.1 Regulation at transcriptional level

Changes in CPTI mRNA levels are related with changes in the glucagon/insulin ratios and are associated with elevated levels of NEFA and decreased glucose availability[156]. Physiological concentrations of fatty acids induced rapid CPTI gene

[156] Park EA, Mynatt RL, Cook GD, Kashfi K. Insulin regulates enzyme activity, malonyl-CoA sensitivity and mRNA abundance of hepatic carnitine palmitoyltransferase-I. *Biochem. J.* 310:853-858, 1995

expression in pancreatic β-cells. However, fatty acid metabolism beyond LC-CoA formation was not required for the induction[97, 157].

The transcriptional effects of fatty acids may be mediated through PPARα[158] although this is controversial[107]. Functional peroxisome proliferator response elements (PPRE) have been identified in the regulatory region of numerous genes encoding enzymes involved in lipid metabolism[159] including CPTI[160,161].

11.3.2 Malonyl-CoA dependent regulation

CPTI exerts is believed to exert its control as the rate limiting step in fatty acid oxidation *via* changes in concentration of malonyl-CoA (acute or short-term control) and/or through changes in the sensitivity of CPTI to inhibition by malonyl-CoA (long-term control).

If tissue malonyl-CoA concentrations play a key role in the rapid adjustment in fatty acid oxidation rates, then the reactions producing and/or disposing of malonyl-CoA also must be subject to acute regulation. The formation of malonyl-CoA is catalyzed by ACC, which is expressed in two isoforms (ACCα and ACCβ). ACCα predominates in lipogenic tissues while ACCβ is the predominant form in heart and skeletal muscle[162]. There is an interesting correlation between the tissue distribution of the L and M CPTI isoforms and the α and β ACC isoforms[163]. ACCα predominates in those tissues where LCPTI also predominates, while ACCβ is present where MCPTI is mainly expressed. Isoform expression appears to depend on the particular metabolite

---

[157] Chatelain F, Kohl C, Esser V, McGarry JD, Girard J, Pegorier JP. Cyclic AMP and fatty acids increase carnitine palmitoyltransferase I gene transcription in cultured fetal rat hepatocytes. *Eur. J. Biochem*. 235:789-798, 1996

[158] Gulick T, Cresci S, Caira T, Moore DD, Nelly DP. The peroxisome proliferator-activated receptor regulates mitochondrial fatty acid oxidative enzyme gene expression. *Proc. Natl. Acad. Sci.* USA. 91:11012-11016, 1994

[159] Latruffe N, Vamecq J. Peroxisome proliferators and peroxisome proliferator activated (PPARs) as regulators of lipid metabolism. *Biochemie*. 79:81-84, 1997

[160] Brady PS, Marine KA, Brady LJ, Ramsay RR. Co-ordinate induction of hepatic mitochondrial and peroxisomal carnitine acyltransferase synthesis by diet and drugs. *Biochem. J*. 260:93-100, 1989

[161] Marcaro C, Acosta E, Ortiz JA, Marrero PF, Hegardt FG, Haro D. Control of human muscle-type carnitine palmitoyltransferase I gene transcription by peroxisome proliferator-activated receptor. *J. Biol. Chem*. 273:8560-8563, 1998

[162] Brownsey RW, Zhande R, Boone AN. Isoforms of acetyl-CoA carboxylase: structures, regulatory properties and metabolic functions. *Biochem. Soc. Trans*. 25:1232-1238, 1997

[163] Zammit V. The malonyl-CoA-long-chain acyl-CoA axis in the maintenance of mammalian cell function. *Biochem. J*. 343:505-515, 1999

requirement of the different tissues. The activity of ACC isoforms is subject to acute control by rapid covalent modification of the enzyme (inactivation and activation by phosphorylation and dephosphorylation, respectively) and by feed-forward activation by citrate and feed-back inhibition by LC-CoA[164]. When energy supply is scarce, the enzymes responsible for producing malonyl-CoA and synthesizing fatty acids are inhibited while MCD is activated. This enzyme catalyzes the conversion of malonyl-CoA to acetyl-CoA and has a critical role in the regulation of intracellular malonyl-CoA concentration[165].

11.3.2.1 Abolition of malonyl-CoA sensitivity: mutation of methionine 593

Various groups have attempted to establish the basis of the LCPTI/malonyl-CoA interactions. From studies on the pH dependence of the affinity of CPTI for its substrate and from the ability of palmitoyl-CoA to displace [^{14}C]malonyl-CoA bound to skeletal muscle mitochondria, it was hypothesized[166] that the palmitoyl-CoA and malonyl-CoA bind at different sites. A number of studies have shown that in rat liver CPTI there are two malonyl-CoA binding sites: one with greater capacity for binding and regulation of the inhibitor and not susceptible to competition from acyl-CoA, which behaves as an allosteric component[167]; and a second acyl-CoA binding site, which is located near the catalytic site[168].

Either the C-terminus or the N-terminus of LCPTI have been shown to influence the enzyme/inhibitor interaction[169,170]. On the basis of these studies, it was proposed that

[164] Allred JB, Reilly KE. Short-term regulation of acetyl-CoA carboxylase in tissues of higher animals. *Prog. Lipid Res*. 35:371-385, 1997

[165] Dyck JRB, Berthiaume LG, Thomas PD, Kantor PF, Barr AJ, Barr R, Singh D, Hopkins TA, Voilley N, Prentki M, Lopaschuk GD. Characterization of rat liver malonyl-CoA decarboxylase and the study of its role in regulating fatty acid metabolism. *Biochem. J.* 350:599-608, 2000

[166] Mills SE, Foster DW, McGarry JD. Effects of pH on the interaction of substrates and malonyl-CoA with mitochondrial carnitine palmitoyltransferase I. *Biochem. J.* 219:601-608, 1984

[167] Cook GA, Mynatt RL, Kashfi K. Yonetani-Theorell analysis of hepatic carnitine palmitoyltransferase-I inhibition indicates two distinct inhibitory binding sites. *J. Biol. Chem.* 269:8803-8807, 1994

[168] Grantham BD, Zammit VA. Binding of [14C]malonyl-CoA to rat liver mitochondria after blocking of the active site of carnitine palmitoyltransferase I. Displacement of low-affinity binding by palmitoyl-CoA. *Biochem. J.* 233:589-593, 1986

[169] Jackson VN, Zammit VA, Price NT. Identification of positive and negative determinants of malonyl-CoA sensitivity and carnitine affinity within the amino termini of rat liver- and muscle-type carnitine palmitoyltransferase I. *J. Biol. Chem.* 275:38410-38416, 2000

the two malonyl-CoA inhibitable domains might be located at the C-terminus as suggested by several kinetic studies. The development of a CPTI catalytic core model[171] allowed our group to assign the low-affinity binding site to a domain near the catalytic channel in which palmitoyl-CoA is bound, containing the catalytic acyl-CoA binding domain[172].

A recent study by our group[173] used the SequenceSpace algorithm program to identify the amino acid residue methionine 593 (Met^{593}), which contributed to the sensitivity of CPTI to malonyl-CoA. The site-directed mutagenesis study used to identify amino acids responsible for malonyl-CoA inhibition is based on the comparison of the sequences in a range of carnitine and choline acyltransferases, taking the positive or negative sensitivity to malonyl-CoA as a discriminatory criterion (Fig. 10). The proposal was based on the finding that the amino acid Met^{593} is present in malonyl-CoA-inhibitable carnitine acyltransferases (CPTI, isoforms L and M, and COT) from various organisms and absent in non-inhibitable acyltransferases (CPTII, CAT, and choline acetyltransferase (ChAT)).

Mutation of the amino acid Met^{593} to its counterpart in CPTII, serine (Ser) showed that the mutation by itself, M593S, practically abolished malonyl-CoA sensitivity of LCPTI when this mutated LCPTI was expressed in yeast (80% activity at 100 µM malonyl-CoA). It is interesting that this mutant showed higher catalytic efficiency for palmitoyl-CoA as substrate than the wild type. It is proposed that the occurrence of Ser in this position has probably been evolutionary conserved in non-malonyl-CoA-sensitive carnitine acyltransferases because it prevents sensitivity to malonyl-CoA.

---

[170] Shi J, Zhu H, Arvidson DN, Woldegiorgis G. The first 28 N-terminal amino acid residues of human heart muscle carnitine palmitoyltransferase I are essential for malonyl CoA sensitivity and high-affinity binding. *Biochemistry.* 39:712-717, 2000

[171] Morillas M, Gómez-Puertas P, Roca R, Serra D, Asins G, Valencia A, Hegardt FG. Structural model of the catalytic core of carnitine palmitoyltransferase I and carnitine octanoyltransferase (COT): mutation of CPTI histidine 473 and alanine 381 and COT alanine 238 impairs the catalytic activity. *J. Biol. Chem.* 276:45001-45008, 2001

[172] Morillas M, Gómez-Puertas P, Rubí B, Clotet J, Ariño J, Valencia A, Hegardt FG, Serra D, Asins G. Structural model of a malonyl-CoA-binding site of carnitine octanoyltransferase and carnitine palmitoyltransferase I: mutational analysis of a malonyl-CoA affinity domain. *J. Biol. Chem.* 277:11473-11480, 2002

[173] Morillas M, Gomez-Puertas P, Bentebibel A, Selles E, Casals N, Valencia A, Hegardt FG, Asins G, Serra D. Identification of conserved amino acid residues in rat liver carnitine palmitoyltransferase I critical for malonyl-CoA inhibition. Mutation of methionine 593 abolishes malonyl-CoA inhibition. *J. Biol. Chem.* 278:9058-9063, 2003

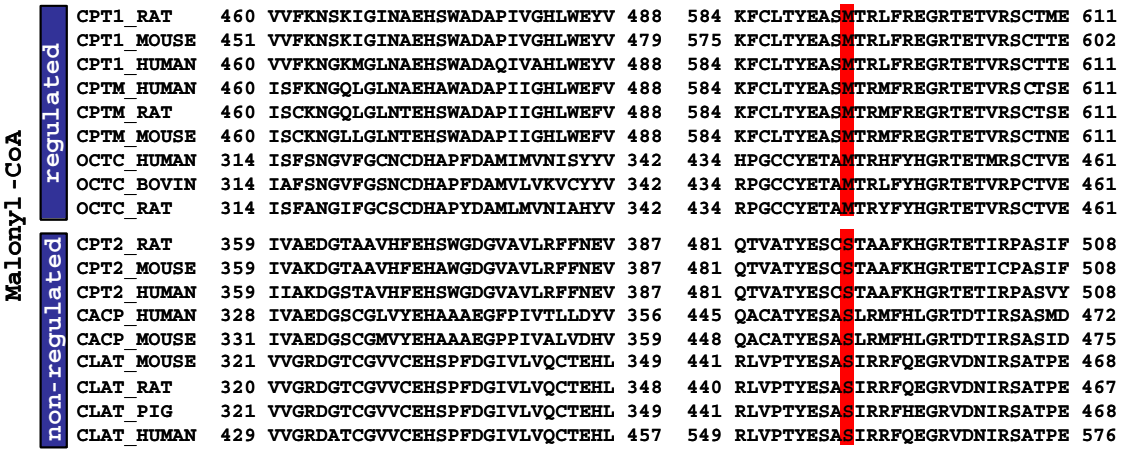

Fig. 10. Alignment of representative sequences of mammalian carnitine-choline acyltransferases. Amino acid sequence of 18 representative members of the malonyl-CoA inhibitable enzymes: LCPTI (CPT1) from rat, mouse, and human; MCPTI (CPTM) from human, rat, and mouse; and COT (*OCTC*) from human, bovine and rat; and the malonyl-CoA-insensitive enzymes: CPTII (CPT2) from rat, mouse, and human; CAT (*CACP*) from human and mouse and ChAT (*CLAT*) from human, pig, rat, and mouse are aligned. The subfamily conserved residue (methionine or serine) according to malonyl-CoA regulation are shaded. Table obtained from[173] with some modifications.

In the present study the malonyl-CoA insensitive form of LCPTI (LCPTI M593S) was overexpressed in pancreatic β-cells to test the hypothesis that the CPTI/malonyl-CoA interaction is involved in GSIS.

11.3.3 Malonyl-CoA independent regulation

In addition to the malonyl-CoA dependent control of mitochondrial fatty acid oxidation, other malonyl-CoA independent mechanisms of CPTI activity regulation have been described.

It has been suggested that CPTI is regulated by direct phosporylation[174,175]. Another mechanism proposed involves direct interaction of cytoskeletal proteins with

[174] Guzman M, Geelen MJH. Activity of carnitine palmitoyltransferase in mitochondrial outer membranes and peroxisomes in digitonin-permeabilized hepatocytes. *Biochem. J.* 287:487-492, 1992

[175] Kerner J, Distler AM, Minkler PE, Parland W, Peterman SM, Hoppel CL. Phosphorylation of rat liver mitochondrial carnitine palmitoyltransferase-I (CPT-I): Effect on the kinetic properties of the enzyme. *J. Biol.Chem*. 279:41104-41113, 2004

CPTI in the mitochondrial outer membrane[176,177]. Other studies provide supportive evidence for stimulation of CPTI by AMPK *via* phosporylation of cytoskeletal components[178,179]. They propose that Ca^{2+}/calmodulin-dependent protein kinase II and possibly AMPK play a central role, not only by activating CPTI but also by phosphorylating (inactivating) ACC, and therefore reinforcing CPTI activation by decreasing tissue malonyl-CoA concentrations. Finally, malonyl-CoA independent regulation of CPTI has been observed, which involves extramitochondrial factors[180], but the mechanism has not been established.

11.3.4 Pharmacological regulation

Inhibition of fatty acid oxidation is clearly an effective strategy for lowering blood glucose levels in diabetic animal models and in NIDDM itself. However, approaches to the direct inhibition of fatty acid oxidation at the level of β-oxidation have so far been unsuccessful due to toxicities and uncontrolled hypoglycemia. Attention has therefore been directed towards an intermediate step, the CPT system. The inhibition of CPTI seems to be a viable target[181] for the treatment of Type 2 diabetes.

Etomoxir is one of the most extensively studied CPTI inhibitors. It acts as an irreversible, active site-directed inhibitor of liver, heart and skeletal muscle CPTI and is functionally active only after metabolic conversion to its CoA-ester, etomoxiryl-CoA[182].

---

[176] Guzmán M, Velasco G, Geelen MJH. Do cytoskeletal components control fatty acid translocation into liver mitochondria? *Trends Endocrinol. Metab.* 11:49-53, 2000

[177] Velasco G, Geelen MJH, Gomez del Pulgar T, Guzman M. Malonyl-CoA-independent acute control of hepatic carnitine palmitoyltransferase I activity. *J. Biol. Chem.* 273:21497-21504, 1998

[178] Velasco G, Geelen MJH, Guzman M. Control of hepatic fatty acid oxidation by 5'-AMP-activated protein kinase involves a malonyl-CoA-dependent and a malonyl-CoA-independent mechanism. *Arch. Biochem. Biophys*. 337:169-175, 1997

[179] Velasco G, Gomez del Pulgar T, Carling M, Guzman M. Evidence that the AMP-activated protein kinase stimulates rat liver carnitine palmitoyltransferase I by phosphorylating cytoskeletal components. *FEBS Lett.* 439:317-320, 1998

[180] Sleboda J, Risan KA, Spydevold O, Bremen J. Short-term regulation of carnitine palmitoyltransferase I in cultured rat hepatocytes: spontaneous inactivation and reactivation by fatty acids. *Biochim. Biophys. Acta*. 1436:541-594, 1999

[181] Anderson RC. Carnitine palmitoyltransferase: A viable target for the treatment of NIDDM? *Curr. Pharmacut. Design* 4:1-15, 1998

[182] Weis BC, Cowan AT, Brown N, Foster DW, McGarry JD. Use of a selective inhibitor of liver carnitine palmitoyltransferase I (CPT I) allows quantification of its contribution to total CPT I activity in rat heart. Evidence

Etomoxir is an orally effective inhibitor of fatty acid oxidation in liver and muscle tissues, thereby giving rise to antiketogenic and hypoglycemic activity in animal models of NIDDM. It has been shown to improve insulin sensitivity in NIDDM patients[183]. However, the drug has not been developed as an antidiabetic agent, probably because mechanism-based myocardial hypertrophy was associated with its use. Therefore, major efforts are required to develop alternative agents targeted at this site.

Finally, a novel compound, the FAS inhibitor C75, has been proposed to pharmacologically regulate CPTI activity (see Section 13.3).

12. TETRACYCLINE-REGULATED INDUCIBLE GENE EXPRESSION SYSTEM

The ability to express gene products in a temporally restricted manner has been an essential experimental strategy in determining gene function in tissue culture and *in vivo*. The best-characterized and most versatile inducible approaches use the tetracycline (tet)-mediated expression systems. The first tet-regulated gene expression system for use in mammalian cells was developed by Gossen and Bujard[184] and it has been widely applied in cultured cells from mammals, plants, amphibians and insects as well as in whole organisms including yeast, *Drosophila*, plants, mice and rats, or implemented in viral vectors. Nowadays these Tet systems are commercially available[185].

The Tet system has two central components: transcriptional transactivators that interact specifically with bacterial *cis* regulatory elements, and antibiotics that modulate the binding of the transactivators at low, non-toxic doses. These rely on the specific, high-affinity binding of the *Escherichia Coli* Tet repressor protein (TetR), or its derivatives, to the tet resistance operator of Tn10 (TetO). When TetR is fused to the herpes simplex virus VP16 activation domain, the hybrid TetR/VP16 protein becomes a powerful tet-responsive transactivator (tTA). In the absence of tet or its analogs as

that the dominant cardiac CPT I isoform is identical to the skeletal muscle enzyme. *J. Biol. Chem.* 269:26443-26448, 1994

[183] Hubinger A, Weikert G, Wolf HP, Gries FA. The effect of etomoxir on insulin sensitivity in type 2 diabetic patients. *Horm. Metab. Res*. 24:115-118, 1992

[184] Gossen M, Bujard H. Tight control of gene expression in mammalian cells by tetracycline-responsive promoters. *Proc. Natl. Acad. Sci. USA*. 89:5547-5551, 1992

[185] Clontech Laboratories, Inc., Palo Alto, California 94303

doxycycline (dox), the tTA protein binds TetO and initiates transcription from artificial promoters containing these sequences as the $P_{hCMV*-1}$ promoter. The $P_{hCMV*-1}$ contains the tet responsive element (TRE), which consists of seven copies of the 42-bp TetO, and the minimal cytomegalovirus promoter (P_{minCMV}), which lacks the enhancer that is part of the complete CMV promoter. In the presence of the antibiotic, the tTA binds the drug, resulting in a conformational change that disrupts DNA binding and inactivates transcription. This is called the Tet-off system.

A second tet-regulated system was developed to address biological problems where prolonged exposure to antibiotics is undesirable (such as during development, in gene therapy or in transgenic animals) or to express potentially toxic target genes during very discrete periods of time. Random mutagenesis of the TetR gene produced a protein that bound to TetO sequences only in the presence of the tet analog doxycycline[186]. Fusion of this mutant to VP16 produced a reverse tTA (rtTA), a protein that required drug interaction to bind TetO sequences and activate transcription. This is called the Tet-on system (Fig. 11).

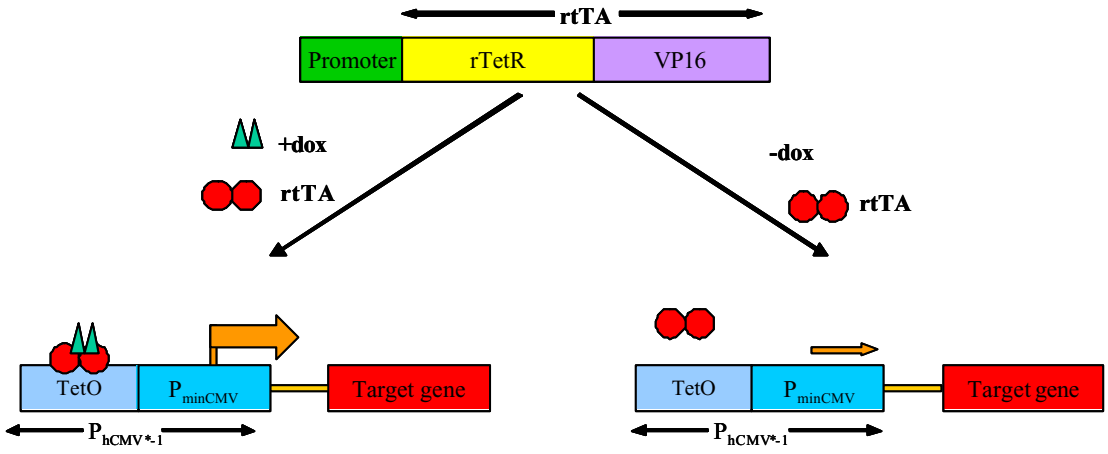

Fig. 11. Schematic representation of the Tet-on system. The reverse tetracycline-controlled transactivator (rtTA) is composed of the reverse tetracycline repressor (rTetR) and the VP16 moiety, driven by an appropriate promoter. In the absence of the effector doxycycline (dox), the transactivator does not recognize its specific DNA target sequence, tetracycline operator (TetO); therefore, transcriptional activation of the target gene will not occur (right). Addition of the effector dox results in binding of rtTA to TetO, which allows the activation of the reporter unit (left). The promoter $P_{hCMV*-1}$ consits of seven copies of TetO located upstream of a minimal sequence of the CMV promoter (P_{minCMV}).

[186] Gossen M, Freundlieb S, Bender G, Muller G, Hillen W, Bujard H. Transcriptional activation by tetracyclines in mammalian cells. *Science*. 268:1766-1769, 1995

When considering properties of the Tet system, such as degree (tightness) of control, expression levels and regulation factors, it is crucial to distinguish between experimental situations in which the systems are stably inserted in the genome of cells in culture or of transgenic organisms, and situations in which the respective regulatory elements are in a nonintegrated state, as in transient expression experiments or when contained in episomes[187]. Therefore, the control of gene activity can be achieved with the Tet systems whenever the experimental strategy permits screening or selection for events in which the expression unit carrying the target gene is integrated into a proper chromosomal site. In transient expression, i.e., when the target gene controlled by the $P_{hCMV*-1}$ is not integrated in the chromosome, an intrinsic basal activity is observed that can reach considerable levels depending on the cell type and experimental conditions[188].

Further analysis of rtTA has revealed that this transactivator has indeed a low residual affinity for TetO in the absence of dox, and that this affinity can cause an elevated basal activity of the $P_{hCMV*-1}$ depending on the intracellular concentration of rtTA[187]. These findings have sparked a reinvestigation of the sequence space of TetR, which yielded a second generation of rtTAs[189,190].

The Tet system has been applied to produce transgenic mice by improving the Cre/lox recombination system in which the genetic changes are irreversible and follow a program that cannot be influenced after its onset[191]. For instance, pancreatic studies show the effectiveness and utility of the Tet-on system in β-cell transplantation[192] and in

[187] Baron U, Bujard H. Tet Repressor-based system for regulated gene expression in eukaryotic cells: principles and advances. *Methods in enzymology*, 327:401-421, 2000

[188] Freundlieb S, Schirra-Müller C, Bujard H. A tetracycline controlled activation/repression system with increased potential for gene transfer into mammalian cells. *J. Gene Med*. 1:4-12, 1999

[189] Urlinger S, Baron U, Thellmann M, Hasan MT, Bujard H, Hillen W. Exploring the sequence space for tetracycline-dependent transcriptional activators: novel mutations yield expanded range and sensitivity. *Proc. Natl. Acad. Sci. USA*. 97:7963-7968, 2000

[190] Stebbins MJ, Urlinger S, Byrne G, Bello B, Hillen W, Yin JCP. Tetracycline-inducible systems for Drosophila. *Proc. Natl. Sci. USA*. 98:10775-10780, 2001

[191] Kistner A, Gossen M, Zimmermann F, Ferecic J, Ullmer C, Lübbert H, Bujard H. Doxycycline-mediated quantitative and tissue-specific control of gene expression in transgenic mice. *Proc. Natl. Sci. USA*. 93:10933-10938, 1996

[192] Milo-Landesman D, Surana M, Berkovich I, Compagni A, Christofori G, Fleischer N, Efrat S. Correction of hyperglycemia in diabetic mice transplanted with reversibly immortalized pancreatic beta cells controlled by the tet-on regulatory system. *Cell Transplant.* 10:645-650, 2001

transgenic mice where the target gene was expressed under the rat or mouse insulin promoter[193,194].

In the present study we decided to utilize the Tet-on system to generate an LCPTI β-cell stable cell line because of the simplicity of the system and the non-toxic effect of doxycycline at the effective concentrations used. The induction of the system in cultured cells is fast as it depends largely on the diffusion constant of the antibiotic.

13. C75, THE FATTY ACID SYNTHASE INHIBITOR

C75 is a chemically stable synthetic inhibitor of fatty acid synthase (FAS) derived from cerulenin, a natural FAS inhibitor obtained from the fungus *Cephalosporium caerulens.* It binds irreversibly to the catalytic site of both type I (mammalian and yeast) and type II (bacterial) FAS, by covalent modification of the β-ketoacyl-acyl carrier protein synthase domain[195,196]. Structurally, C75 is a cell-permeable α-methylene-γ-butyrolactone, designed to be less reactive and potentially safer than cerulenin. It lacks the reactive epoxide present on cerulenin, which enhances chemical stability and specificity allowing its use as a drug (See Fig. 14). Cerulenin, (2R, 3S)-2,3-epoxy-4-oxo-7,10-transdodecadienamide, irreversibly inhibits FAS by forming a covalent adduct with FAS, whereas C75 is probably a slow-binding inhibitor[197].

13.1 C75 AS AN ANTITUMOR DRUG

FAS (EC. 2.3.1.85) is the sole enzyme responsible for the *de novo* synthesis of fatty acids from carbohydrates. It catalyzes the reductive synthesis of long-chain fatty acids from acetyl-CoA and malonyl-CoA. The mechanism by which two carbon units from malonyl-CoA are sequentially added to the growing fatty acid chain is unique

[193] Berkovich I, Efrat S. Inducible and reversible beta-cell autoimmunity and hyperplasia in transgenic mice expressing a conditional oncogene. *Diabetes*. 50:2260-2267, 2001

[194] Lottmann H, Vanselow J, Hessabi B, Walther R. The Tet-On system in transgenic mice: inhibition of the mouse pdx-1 gene activity by antisense RNA expression in pancreatic beta-cells. *J Mol Med*. 79:321-328, 2001

[195] Moche M, Schneider G, Edwards P, Dehesh K, Lindqvist Y. Structure of the Complex between the Antibiotic Cerulenin and Its Target, -Ketoacyl-Acyl Carrier Protein Synthase. *J Biol Chem*., 274:6031-6034, 1999

[196] Price AC, Choi KH, Heath RJ, Li Z, White SW, Rock CO. Inhibition of β-ketoacyl-acyl carrier protein synthases by thiolactomycin and cerulein. *J. Biol. Chem*., 276:6551-6559, 2001

[197] Kuhajda FP, Pizer ES, Li JN, Mani NS, Frehywot GL, Townsend CA. Synthesis and antitumor activity of an inhibitor of fatty acid synthase. *Proc. Natl. Acad. Sci. USA*. 97:3450-3454, 2000

among vertebrates, making FAS an attractive target for the design of therapeutic agents. In fact, elevated expression of FAS and abnormally active endogenous fatty acid synthetic metabolism are frequent phenotypic alterations in many human cancers, including carcinomas of breast, prostate, ovary, colon, lung, stomach, skin, and endometrium[198]. This differential expression of FAS between normal tissues and cancer has led to the notion that FAS is a target for anticancer drug development.

Therefore, C75 was first developed as an antitumor drug to enable FAS inhibition and to be tested for *in vivo* treatment of human cancer xenografts. C75 produced rapid and potent inhibition of DNA replication and S-phase progression in human cancer cells leading to apoptosis[199]. TOFA, 5-(tetradecyloxy)-2-furoic acid, a competitive inhibitor of ACC, the rate-limiting enzyme of fatty acid synthesis, profoundly inhibits fatty acid synthesis, but is essentially non-toxic to cultured human cancer cells[200]. Moreover, treatment of human cancer cells with TOFA before C75 administration reproducibly rescued them from C75 cytotoxicity, and prevented the C75 induced increase in malonyl-CoA[200]. Thus, because C75 blocked FAS, increased malonyl-CoA levels and triggered apoptosis, whereas TOFA blocked the C75 increase in malonyl-CoA, protecting the cells from apoptosis, the authors point to high levels of malonyl-CoA as proapoptotic. Therefore, C75 acts as an antitumor drug and whereas induction of apoptosis in cancer cells appeared related to accumulation of the substrate, malonyl-CoA, after FAS inhibition, the cytostatic effects were independent of malonyl-CoA accumulation and may have resulted from product depletion[201].

---

[198] Kuhajda FP. Fatty-acid synthase and human cancer: new perspectives on its role in tumor biology. *Nutrition.* 16:202-208, 2000

[199] Pizer ES, Chrest FJ, DiGiuseppe JA, HanWF. Pharmacological inhibitors of mammalian fatty acid syntase suppress DNA replication and induce apoptosis in tumor cell lines. *Cancer Res*. 58:4611-4615, 1998

[200] Pizer ES, Thupari J, Han WF, Pinn ML, Chrest FJ, Frehywot GL, Townsend CA, Kuhajda FP. Malonyl-coenzyme-A is a potential mediator of cytotoxicity induced by fatty acid synthase inhibition in human breast cancer cells and xenografts. *Cancer Res*. 60:213-218, 2000

[201] Li JN, Gorospe M, Chrest FJ, Kumaravel TS, Evans MK, Han WF, Pizer ES. Pharmacological inhibition of fatty acid synthase activity produces both cytostatic and cytotoxic effects modulated by p53. *Cancer Research*. 61:1493-1499, 2001

13.2 CENTRAL EFFECT OF C75

However, a source of great interest in C75, related with obesity and the mechanism that control appetite and body weight, was the study by Kuhajda's team[202]. Both systemic and intracerebroventricular (ICV) treatment with C75 led to inhibition of feeding and dramatic weight loss in lean, diet-induced obese (DIO) and genetically obese leptin-deficient (*ob*/*ob*) mice. This action was independent of leptin, since C75 caused profound weight loss in leptin-deficient mice. Lean mice, however, become resistant to C75 over the next few days of treatment and exhibit rebound hyperphagia upon cessation of treatment. In contrast, obese mice showed incipient tolerance to C75, which became evident only after substantial weight loss had occurred.

Recent evidence[203,204] has implicated malonyl-CoA as a possible mediator in the hypothalamic pathway that indicates energy status and mediates the feeding behaviour of mice. Thus C75, by increasing malonyl-CoA levels, was found to alter the metabolism of neurons in the hypothalamus that regulate feeding behaviour. In addition, TOFA largely restored food intake in C75-treated mice, supporting the hypothesis that malonyl-CoA mediates feeding inhibition.

Energy balance is monitored by the hypothalamus, which responds to peripheral status signals by releasing neuropeptides that regulate energy intake and expenditure. Restriction of food intake leads to increased expression of the hypothalamic orexigenic neuropeptides, neuropeptide Y (NPY), and agouti-related protein (AgRP) mRNAs, and decreased expression of the hypothalamic anorexigenic neuropeptides, pro-opiomelanocortin (POMC), and cocaine-amphetamine-regulated transcript (CART). In combination, these changes provoke increased food intake and reduced energy expenditure. When fasted animals are re-fed, the inverse response occurs (Fig. 12).

---

[202] Loftus TM, Jaworsky DE, Freywot GL, Townsend CA, Ronet GV, Lane MD, Kuhajda FP. Reduced food intake and body weight in mice treated with fatty acid synthase inhibitors. *Science* 288:2379-2381, 2000

[203] Gao S, Lane D. Effect of the anorectic fatty acid synthase inhibitor C75 on neuronal activity in the hypothalamus and brainstem. *Proc. Natl. Acad. Sci. USA.* 100:5628-5633, 2003

[204] Hu Z, Cha SH, Chohnan S, Lane MD. Hypothalamic malonyl-CoA as a mediator of feeding behavior, *Proc. Natl. Acad. Sci. USA.* 100:12624-12629, 2003

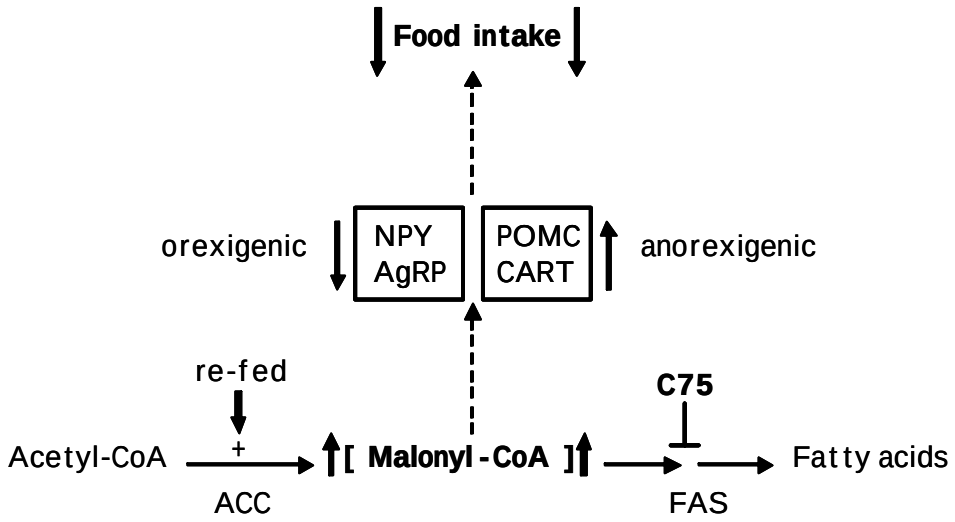

Fig. 12. Model of hypothalamic malonyl-CoA as mediator of expression of orexigenic and anorexigenic neuropeptides and food intake. Figure taken from[204].

ICV administration of C75 increases cellular malonyl-CoA in the hypothalamus, caused by inhibition of FAS, and blocks fasting-induced up-regulation of hypothalamic neuropeptide Y, thus reducing food intake[202]. Furthermore, it appears that C75 exerts its short and long-term effects on food intake by preventing the up-regulation of the orexigenic neuropeptides and down-regulation of the anorexigenic neuropeptides[205206]. In addition, recent data suggest that modulation of FAS activity by C75 in the hypothalamus can alter energy perception by reducing AMPK, which functions as a physiological energy sensor in the hypothalamus[207].

13.3 PERIPHERAL EFFECT OF C75

In addition to its hypothalamic action, it has been reported that C75 reduces in fatty liver and adipose tissue mass[202]. The question was then, how could there be a selective reduction in the fat mass of peripheral tissues in the setting of elevated levels of malonyl-CoA as a result of FAS inhibition? This paradox was investigated under the

[205] Shimokawa T, Kumar MV, Lane MD. Effect of fatty acid synthase inhibitor on food intake and expression of hypothalamic neuropeptides. *Proc. Natl. Acad. Sci. USA*. 99:66-71, 2002

[206] Cha SH, Hu Z, Lane MD. Long-term effects of a fatty acid synthase inhibitor on obese mice: food intake, hypothalamic neuropeptides, and UCP3. *BBRC*. 317:301-308, 2004

[207] Kim EK, Miller I, Aja S, Landree LE, Pinn M, McFadden J, Kuhajda FP, Moran TH, Ronnett GV. C75, a fatty acid synthase inhibitor, reduces food intake via hypothalamic AMP-activated protein kinase. *J. Biol. Chem*. 279:19970-19976, 2004

hypothesis that C75 might have additional effects on fatty acid oxidation and CPTI activity.

C75 was found to increase energy expenditure in DIO mice through an increase in fatty acid oxidation, because the use of etomoxir, the irreversible inhibitor of CPTI, restored this increase in energy production[208]. In addition, C75 treatment of rodent adipocytes and hepatocytes and human breast cancer cells increased fatty acid oxidation and ATP levels by increasing CPTI activity, even in the presence of elevated concentrations of malonyl-CoA. Thus, the authors proposed a second mechanism of action for C75 that is outlined in Fig. 13. In the central nervous system, C75 inhibits FAS, leading to changes in neuropeptide expression that result in a reduced food intake. In peripheral tissues, C75 stimulates CPTI activity, increasing fatty acid oxidation and energy production, thus leading to selective reduction of adipose tissue, liver fat and weight loss. These data describe, for the first time, a pharmacological agonist of CPTI and identify CPTI as a therapeutic target for obesity and Type II diabetes. In addition, it has recently been described that long-term treatment with C75 results in increased expression of UCP-3 mRNA in skeletal muscle of obese mice, suggesting that this up-regulation of UCP-3 may increase thermogenesis and thereby, explain the increase in energy expenditure[206].

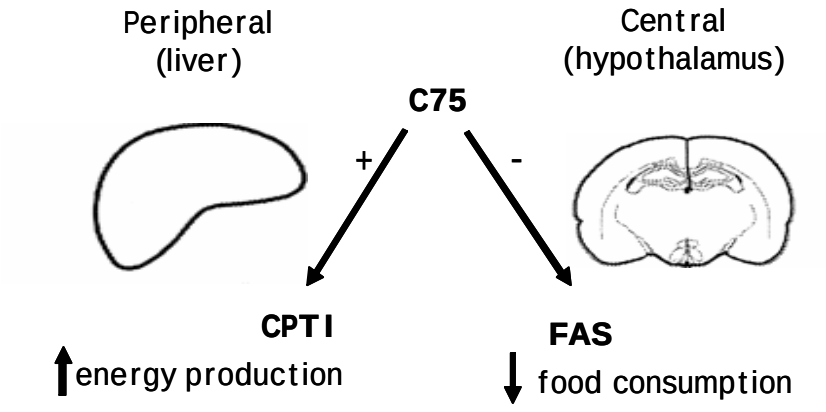

Fig. 13. Model proposed by Thupari *et al*.[208] for central and peripheral C75 mechanisms of action. Centrally, C75 inhibits FAS, leading to changes in neuropeptide expression that result in a net reduction in food consumption. In the peripheral tissues such as liver and adipose tissue, C75 increases CPTI activity, leading to increased fatty acid oxidation and energy production. Both mechanisms contribute to weight loss, but the peripheral mechanism is responsible for the selective reduction in adipose tissue mass and resolution of fatty liver.

[208] Thupari JN, Landree LE, Ronnett GV, Kuhajda FP. C75 increases peripheral energy utilization and fatty acid oxidation in diet-induced obesity. *Proc. Natl. Acad. Sci. USA.* 99:9498-9502, 2002

The amphipathic nature of C75 may account for the stimulation of CPTI activity because palmitoyl-CoA, a CPTI substrate that is similarly amphipathic, also activates the enzyme, and in excess can reverse malonyl-CoA inhibition[209] (Fig. 14). Interestingly, cerulenin, the natural FAS inhibitor, has only a single dicarbonyl group in its cyclized form, it is not amphipathic, and in contrast to C75, it has been described to decrease CPTI activity[210,211]. In the former[210], the decrease in CPTI activity was correlated with a reduction in fatty acid oxidation and an increase in cytotoxicity in human breast cancer cells cultured with cerulenin. In the latter[211], the authors showed that the effect of cerulenin on CPTI activity in mice was biphasic in liver and muscle, with an early suppression followed by a late stimulation after intraperitoneal treatment. They concluded that cerulenin-induced late-phase stimulating effects on CPTI activity were mediated by the activation of the sympathetic nervous system.

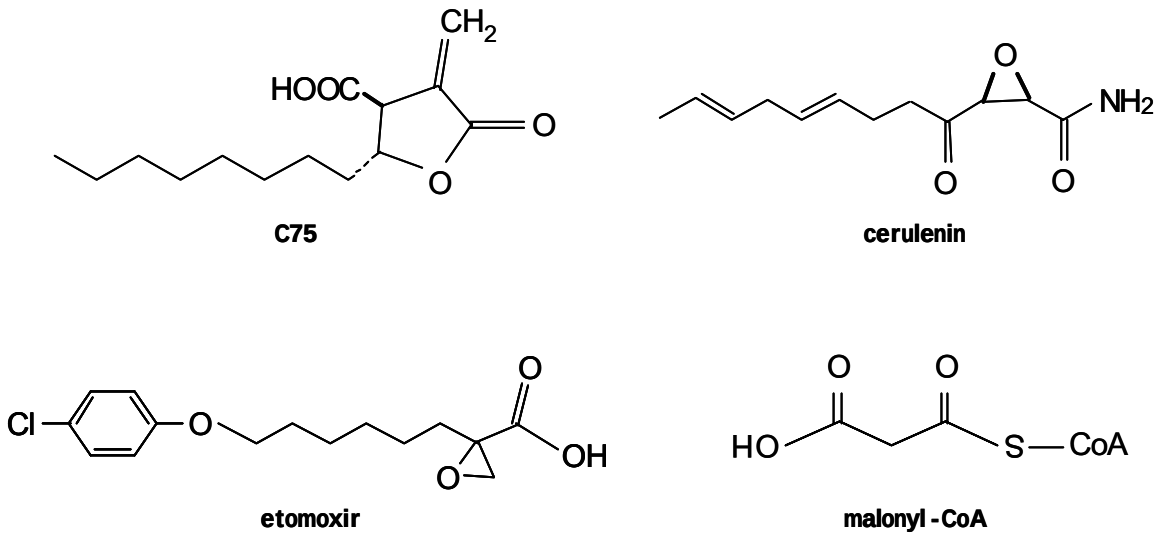

Fig. 14. Structures of C75, cerulenin, etomoxir and malonyl-CoA.

[209] Bremen J, Woldegiorgis G, Schalinske K, Shrago E. Carnitine palmitoyltransferase. Activation by palmitoyl-CoA and inactivation by malonyl-CoA. *Biochim. Biophys. Acta*. 833:9-16, 1985

[210] Thupari JN, Pinn ML, Kuhajda FP. Fatty acid synthase inhibition in human breast cancer cells leads to malonyl-CoA-induced inhibition of fatty acid oxidation and cytotoxicity. *BBRC*. 285:217-223, 2001

[211] Jin YJ, Li SZ, Zhao ZS, An JJ, Kim RY, Kim YM, Baik JH, Lim SK. Carnitine palmitoyltransferase-1 (CPT-1) activity stimulation by cerulenin via sympathetic nervous system activation overrides cerulenin's peripheral effect. *Endocrinology*. 145:3197-3204, 2004

In summary, C75 acts both centrally to reduce food intake and peripherally to stimulate CPTI activity[208,212] and increase fatty acid oxidation, leading to rapid and profound weight loss, loss of adipose mass and resolution of fatty liver. Thus, in peripheral tissues *in vivo*, the inhibitory effect of the high content of malonyl-CoA, due to FAS inhibition, on CPTI seems to be overcome by C75-stimulated CPTI activity.

The present study further examines the C75/CPTI interaction *in vitro* and *in vivo* in the pancreatic β-cell.

[212] Yang N, Kays JS, Skillman TR, Burris L, Seng TW, Hammond C. C75 activates carnitine palmitoyltransferase-1 in isolated mitochondria and intact cells without displacement of bound malonyl-CoA. *J. Pharmacol. Exp. Ther*. PMID: 15356215, 2004

OBJECTIVES

OBJECTIVES

The objectives of the present thesis are:

1. Study of the malonyl-CoA/carnitine palmitoyltransferase I interaction in the pancreatic β cell and its involvement in glucose-induced insulin secretion.

2. Construction of an INS-1 stable cell line overexpressing LCPTI wt and LCPTI M593S.

3. Determine the effect of C75 on the carnitine palmitoyltransferase I activity and palmitate oxidation in pancreatic β-cells.

MATERIALS AND METHODS

MATERIALS AND METHODS

1. DNA AND RNA BASIC TECHNIQUES

1.1 BACTERIAL STRAINS

Three bacterial strains of *Escherichia coli* were used in this study: DH5α, XL1-Blue and DM1.

Strain	Genotype	Resistant to
DH5α	*sup* E44, Δ*lac*U169 (ϕ80 *lac* ZΔM15), *hsd* R17, *rec* A1, *gyr* A96, *thi*-1, *rel* A1	Ampicillin
XL1-Blue	*end* A1, *hsd* R17 (rk-, mk+), *sup* E44, *thi*-1, ?$^{-}$, *rec* A1, *gyr* A96, *rel* A1, *lac*$^{-}$[F', *pro* AB, *lac*/^{q} ZΔM15, *Tn*10(*tet*^{r})]	Tetracycline
DM1	F^{-} *dam*$^{-}$13: *dcm mcr*B *hsd*R^{-}M^{+} *gal*1 *gal*2 *ara lac thr leu ton*^{r} *tsx*^{r} Su^{0} λ^{-}	Ampicillin

The DM1 strain lacks the *dam* and *dcm* methylases which methylate the adenine residues in the sequence GATC and the internal cytosine residues in the sequence CCAGG and CCTGG. This lack of *dam* and *dcm* methylation allows DNA propagating in DM1 to be cleaved by a variety of restriction endonucleases that are sensitive to methylated recognition sequences such as *Bcl*I, *Mbo*I, *Nde*II and *Eco*RI.

1.2 PLASMID AND COSMID VECTORS

The following plasmid and cosmid vectors were used for cloning strategies:

A) pTRE2 plasmid vector

pTRE2 plasmid vector (Clontech, ref. 6241-1) is a response plasmid of 3.8 kbp encoding the tetracycline-response element (TRE) that can be used to express a gene of interest upon activation by either the tTA (tetracycline transactivator) or the rtTA

(reverse tTA) regulatory protein in a tetracycline-regulated expression system[1], Tet-off or Tet-on, respectively.

pTRE2 (Fig. 1) contains the ampicillin-resistance gene and a multiple cloning site (MCS) immediately downstream of the Tet-responsive $P_{hCMV*-1}$ (human cytomegalovirus) promoter. cDNAs or genes inserted into the MCS will be responsive to the tTA and rtTA regulatory proteins in the Tet-off and Tet-on systems, respectively. $P_{hCMV*-1}$ contains the TRE, which consists of seven copies of the 42-bp tet operator sequence (tetO). The TRE is just upstream of the minimal CMV promoter ($P_{min\ CMV}$), which lacks the enhancer that is part of the complete CMV promoter. Consequently, $P_{hCMV*-1}$ is silent in the absence of binding of tTA or rtTA to the tetO sequences. The cloned insert must have an initiating ATG codon.

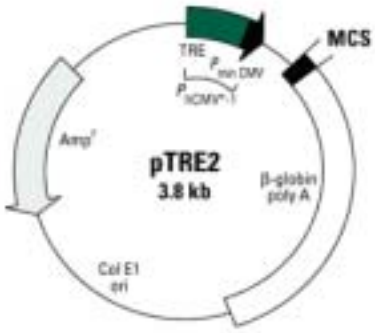

Fig. 1. pTRE2 vector. Response plasmid encoding the tetracycline response element (TRE) for use in the Tet-off or Tet-on systems.

B) pCMV4 plasmid vector

pCMV4 is a high-copy mammalian expression vector of 4.9 kbp. It contains a bacteriophage origin of replication for production of single-stranded DNA, an ampicillin-resistance gene, a promoter-regulatory region of the hCMV and the human growth hormone fragment, which contains transcription termination and poly-adenylation signals.

C) pYES 2.0 plasmid vector

The pYES 2.0 (Stratagene, ref. V825-20) is a high-copy episomal vector of 5.9 kbp which contains the ampicillin-resistance gene. It also contains a yeast gene, URA3, for protein expression in yeast under the galactose promoter GAL1.

[1] Gossen M, Freundlieb S, Bender G, Muller G, Hillen W, Bujard H. Transcriptional activation by tetracyclines in mammalian cells. *Science*. 268(5218):1766-1769, 1995

D) pAxCA wt cosmid vector

pAxCA wt is a cosmid vector (Takara Biomedicals, ref. 6170) of 44.7 kbp which contains the ampicillin-resistance gene and highly efficient CAG promoters (CMV enhancer, chicken β-actin promoter, rabbit β-globin poly A signal) that act in mammals. A foreign DNA of about 5 kbp can be inserted. High gene expression levels can be achieved by inserting the coding regions of the target gene into this cosmid vector.

1.3 BACTERIAL CULTURE

Bacterial strains are cultured in LB medium (Luria-Bertrani Broth) in the presence of the appropriate antibiotic. When cells are grown in a solid medium, 2% of agar is added to the LB medium.

In the case of the bacterial strains and vectors used in this study, the antibiotics ampicillin and tetracycline were used. Ampicillin binds to and inhibits a number of enzymes in the bacterial membrane that are involved in the synthesis of the cell wall. The ampicillin-resistance (*amp*^{r}) gene carried on the plasmid or on the bacterial strain genome codes for an enzyme that is secreted into the periplasmic space of the bacterium, where it catalyzes hydrolysis of the β-lactam ring, with concomitant detoxification of the drug. Therefore, only the cells with the *amp*^{r} gene present on their genome or in the target plasmid will survive in a medium containing this antibiotic. On the other hand, tetracycline binds to a protein of the 30S subunit of the ribosome and inhibits ribosomal translocation. The constitutively expressed tetracycline-resistance (*tet*^{r}) gene carried on the plasmid or on the bacterial strain genome encodes a 399-aminoacid, a membrane-associated protein that prevents the antibiotic from entering the cell.

LB medium: 10 g/L tryptone, 5 g/L yeast extract and 5 g/L NaCl dissolved in distilled water. It is autoclaved immediately and kept at room temperature (r.t.). 100 mg/L ampicillin prepared in water and/or 12.5 mg/L tetracycline prepared in H_2O:ethanol (1:1) is added at the moment of use.

Solid LB medium: LB medium plus 2% (w/v) agar. It is autoclaved immediately. When the temperature is about 50ºC, 100 mg/L ampicillin and/or 12.5 mg/L tetracycline is added and the medium is distributed into 10-cm plates with 30 ml of medium each. Plates are stored at 4ºC.

1.4 PLASMID DNA PREPARATION

Plasmid DNA could be obtained from bacterial cultures that contain the plasmid of interest by growing them in LB medium with the appropriate antibiotic and the later purification of the plasmid DNA from the cell lysate.

Minipreparations of plasmid DNA were obtained using the *Minipreps DNA Purification System* (Promega, A1460) where the yield of high-copy-number plasmids obtained is about 3-5 µg DNA per millilitre of the original bacterial culture. When higher amounts of plasmid DNA were needed or for the obtaining of cosmid DNA, the *QUIAGEN Plasmid Maxi kit* (QUIAGEN, ref. 12163) was used. In this case up to 500 µg DNA could be obtained.

Minipreparations are obtained from 2 ml LB medium with the appropriate antibiotic which has been inoculated with a single colony of *E. coli* cells and grown overnight (o/n) at 37ºC with moderate shaking. For the maxipreparations, 500 ml of LB medium with the appropriate antibiotic is inoculated with the 2 ml preinocul and grown o/n at 37ºC with moderate shaking. In both cases cells are harvested by centrifugation and lysed with NaOH and SDS. The precipitate formed contains the bacterial genomic DNA, proteins, cell debris and SDS. The bacterial RNA is degraded by the action of RNase. Then, the plasmid or cosmid DNA is purified from the supernatant using ion-exchange resin columns. After that, the DNA is washed and eluted, and it is pure enough for enzymatic modifications, PCR, sequencing, etc.

For future preparation of plasmid or cosmid DNA, a stab of each construct is prepared as follows: 1 ml aliquot from the 500 ml maxipreparation inoculum is mixed with 500 µl 50% sterile glycerol and stored at -80ºC.

1.5 DNA ENZYMATIC MODIFICATIONS

1.5.1 DNA digestion with restriction enzymes

Restriction endonucleases are enzymes isolated and purified from bacteria or fungi which bind specifically to and cleave double-stranded DNA (phosphodiester bonds) at specific sites within or adjacent to a particular sequence known as the recognition sequence. The most used restriction enzymes recognize specific sequences that are four, five or six nucleotides in length and display twofold symmetry. The location of cleavage sites within the axis of dyad symmetry differs from enzyme to enzyme: some cleave both strands exactly at the axis of symmetry, generating fragments

of DNA that carry blunt ends; others cleave each strand at similar locations on opposite sides of the axis of symmetry, creating fragments of DNA that carry protruding single-stranded termini (cohesive ends).

Each restriction enzyme requires specific reaction conditions of pH, ionic strength and temperature; therefore in each case the manufacturer's instructions were followed. In general, DNA is digested at a concentration of 0.5 µg/µl using 1-4 units (U) of the enzyme per µg of DNA. Restriction enzymes are stably stored at -20ºC in a buffer containing 50% glycerol. Reaction volumes must be kept to a minimum by reducing the amount of water in the reaction as much as possible. However, the restriction enzyme must contribute less than 0.1 volume of the final reaction mixture; otherwise, the enzyme activity may be inhibited by glycerol. Digestions are carried out for 2-3 h in the specific buffer and the digestion products are analyzed in agarose gels.

When DNA is to be cleaved with two or more restriction enzymes, the digestions can be carried out simultaneously if both enzymes work well at the same temperature and in the same buffer. If the enzymes have different requirements, two alternatives are possible:

1) The DNA should be digested first with the enzyme that works best in the buffer of lower ionic strength. The appropriate amount of salts, BSA, etc. and the second enzyme can then be added and the incubation continued.

2) When the conditions are completely incompatible, after the first digestion the DNA could be recovered using the *QIAquick PCR purification kit* (QUIAGEN, ref. 28106). Up to 10 µg of DNA is selectively adsorbed to a silica-gel membrane and separated from enzymes, salts, etc. Then, the DNA is eluted in the desired volume of water and the second digestion or the next enzymatic modification is performed.

Enzyme digestion	
DNA	0.5 µg/µl
10X Buffer	1X
Enzyme	1-4 U/µg DNA

1.5.2 DNA dephosphorylation

DNAs can be rendered resistant to ligation by enzymatic removal of phosphate residues from their 5' termini with phosphatases. This process is useful to avoid the

ligation of a linearized vector with itself and thus, increase the ligation probability of the vector with the desired insert in the ligation mixture.

The CIP (*Calf Intestinal alkaline Phosphatase*) is the most widely used phosphatase and catalyzes the hydrolysis of the 5'-phosphate residues from linear DNA, RNA and the ribo or deoxyribonucleoside triphosphate. The reaction is performed for 1 h at 37ºC with the manufacturer's buffer. This enzyme requires Zn^{2+}, presents a high specific activity and is easily inactivated by heating to 70ºC for 10 min.

1.5.3 Blunt ends

The filling of 5'-protruding ends or the shortening of 3'-protruding ends allows the cloning by blunt-end ligation of non compatible restriction sites.

The enzyme used for blunt end generation was the *Pfu DNA polymerase* as its has 5' ⟶ 3' polymerase activity and 3' ⟶ 5' exonuclease activity and its efficiency is higher than that obtained with *Klenow* or *T4 DNA polymerase*. In the presence of double-stranded DNA and deoxynucleoside triphosphate (dNTPs) this enzyme fills the gaps left by restriction enzymes that produce 5' protruding ends. In the absence of dNTPs the enzyme eliminates the 3' protruding end nucleosides. The reaction was done following the manufacturer's instructions.

1.6 DNA RESOLUTION AND PURIFICATION

1.6.1 DNA resolution in agarose gels

Electrophoresis through agarose gels is the standard method used to separate, identify and purify DNA fragments. The technique is simple, rapid to perform and capable of resolving fragments of DNA from 50 bp to approximately 25 kbp in length on agarose gels of various concentrations. Higher fragments of DNA will need a lower concentration of agarose gel to be separated. For instance, 1% agarose gels are used to resolve DNA fragments between 0.5-7 kbp.

The location of DNA within the gel can be determined directly by staining the gel with low concentrations of the fluorescent dye ethidium bromide which intercalates between the two strands of the DNA. The presence of the DNA is visualized with low wavelength (310 nm) ultraviolet (UV) light where the DNA fragment appears as a fluorescent orange band. Extra precautions should be taken because ethidium bromide is a powerful mutagen and is moderately toxic and UV radiation is dangerous, particularly to the eyes.

DNA which is negatively charged migrates to the anode of the electrophoresis chamber. This migration of the DNA is inversely proportional to its molecular weight logarithm and therefore, the molecular weight of a desired DNA fragment could be calculated by its interpolation on the regression curve of a molecular marker with known molecular weight DNA fragments or by directly comparison with the molecular marker DNA fragments.

The agarose gel is prepared with low-melting-temperature agarose dissolved in 1X TAE electrophoresis buffer containing 0.5 µg/ml ethidium bromide (AppliChem Biochemica, ref. A1151,0001). Samples are loaded in 1X loading buffer and electrophoresis is run with 1X TAE electrophoresis buffer at 75 V.

1X TAE electrophoresis buffer	
Tris-acetate pH 8.3	40 mM
EDTA	1 mM

5X sample loading buffer	
sucrose	7 g
0.5 M EDTA	1.2 ml
1 M Tris pH 8	300 µl
glycerol	10 ml
bromophenol blue	8 mg
bd. H_2O up to	20 ml

1.6.2 DNA purification

If necessary a DNA fragment can be recovered from the gel to be used for a variety of cloning purposes. To extract and purify a DNA fragment from the agarose gel the *QIAEX II Gel Extraction kit* (QUIAGEN, ref. 20021) was used. Briefly, the agarose gel fragment containing the desired DNA is dissolved in a chaotropic agent and the DNA is selectively adsorbed into a silica resin which has been optimized to enhance recovery of 40 bp to 50 kbp DNA fragments. Impurities such as RNA, proteins, salts and other components of the sample are removed during washing steps. The pure DNA is eluted in water and is suitable for other manipulations.

1.7 DNA AND RNA QUANTIFICATION

1.7.1 DNA and RNA spectrophotometric quantification

RNA and DNA could be quantified in a spectrophotometer measuring the absorbance at 260 and 280 nm in 1 ml quartz cuvettes. The reading at 260 nm allows calculation of the concentration of nucleic acid in the sample. An OD of 1 corresponds to approximately 40 µg/ml for single-stranded DNA and RNA, and 50 µg/ml for double-stranded DNA. The ratio between the readings at 260 and 280 nm (OD_{260}/OD_{280}) provides an estimate of the purity of the nucleic acid. Pure preparations of RNA and DNA have OD_{260}/OD_{280} values higher than 1.65 and 1.8, respectively.

Therefore, the RNA or DNA concentrations in a sample could be given as:

$$\text{RNA } (\mu g/\mu l) = OD \times 40/v$$
$$\text{DNA } (\mu g/\mu l) = OD \times 50/v$$

Where OD is the absorbance at 260 nm and v is the µl of RNA or DNA diluted in 1 ml of water and quantified in the spectrophotometer.

1.7.2 DNA fluorescence quantification

When there is not sufficient DNA (<250 ng/ml) to assay spectrophotometrically (Section 1.7.1), or the DNA is heavily contaminated with other substances that absorb ultraviolet irradiation and therefore impede accurate analysis, DNA could be quantified by fluorescence. The ultraviolet-induced fluorescence emitted by ethidium bromide molecules intercalated into the DNA is used. Because the amount of fluorescence is proportional to the total mass of DNA, the quantity of DNA in the sample can be estimated by comparing the fluorescent yield of the sample with that of a series of standards. As little as 10 ng of DNA can be detected by this method.

1.8 DNA LIGATION

Ligation of a segment of foreign DNA to a linearized plasmid vector involves the formation of new bonds between phosphate residues located at the 5' termini of double-stranded DNA and adjacent 3' hydroxyl moieties. When both strands of the plasmid vector carry 5'-phosphate residues, four new phosphodiester bonds are

generated. However, when the plasmid DNA has been dephosphorylated, only two new phosphodiester bonds can be formed. In this case, the resulting hybrid molecules carry two single-strand nicks that are repaired after the hybrids have been introduced into competent bacteria.

The bacteriophage *T4 DNA ligase* was used for the ligation reactions following the manufacturer's instructions. The reaction is done in the presence of the ligation buffer and ATP for 2-3 h at 16ºC in case of cohesive ends fragments and at 18ºC o/n in case of blunt ends fragments. The ligation reaction should contain between 20-60 µg approx. of vector DNA per ml and an equal or slightly greater concentration of foreign DNA (insert) than of vector DNA. At low concentrations of DNA, recircularization of the plasmid DNA will occur with high efficiency. On the other hand, at high DNA concentrations the initial products of ligation will be dimmers and larger oligomers of the plasmid. Because of this, an adequate plasmid-insert rate is important for the ligation reaction.

When the ligation is done with different protruding termini DNA, the foreign DNA is inserted in only one orientation within the recombinant plasmid and the background of nonrecombinant clones is low. Ligation reactions involving blunt-ended molecules are much less efficient and require higher concentrations both of DNA ligase and plasmid and insert DNAs. Moreover, recombinant plasmids may carry tandem copies of foreign DNA and the background of nonrecombinant clones can be high.

Ligation was checked by PCR or by electrophoresis in an agarose gel before its transformation in competent *E. coli.*

1.9 PREPARATION AND TRANSFORMATION OF COMPETENT *E. coli*

Plasmid DNA can be introduced into competent bacteria by the process of transformation.

1.9.1 Obtaining of competent *E. coli*

Competent cells are those cells which have been treated to increase their capacity to introduce a circular exogenous DNA. They are obtained by concentration through successive washes in water and 10% glycerol.

Competent cells could be purchased from a commercial source or prepared in the laboratory. In both cases, a yield of approx. 10^8-10^{10} transformed colonies/µg of supercoiled plasmid DNA could be achieved.

To obtain competent cells a single colony of *E. coli* cells is inoculated into 5 ml LB medium with the appropriate antibiotic and grown o/n at 37ºC with moderate shaking. The next day, 500 ml of LB plus antibiotic is inoculated with the 5 ml preinocul and grown for approx. 3 h in the shaker at 37ºC to an OD_{600} of 0.5-0.6. Cells are then chilled on ice for 10 min and centrifuged at 4,000 x *g* for 20 min at 2ºC. Cells should be kept at 2ºC for the subsequent steps. After that, the pellet is immediately resuspended in 500 ml of sterile and ice-cold water and centrifuged again. This process is repeated and then the pellet is resuspended by swirling in remaining liquid. 40 ml of sterile, ice-cold 10% glycerol is added and the suspension is centrifuged at 4,000 x *g* for 10 min. Cells are then resuspended in 500 µl of 10% glycerol and 42 µl aliquots are stored at -80ºC.

1.9.2 Transformation of competent *E.coli*

The transformation process consists of introducing the plasmid DNA into the bacterial cells for later amplification and obtaining. Moreover, only the circular DNA will enter the cells, therefore if the DNA which is to be introduced into the cells is the result of a ligation, only the ligated plasmid will be obtained after the transformation. In this way, the non ligated molecules of the ligation reaction will be discarded.

Plasmid DNA could be introduced by heat-shock or by electroporation and cosmid DNA by packaging.

A) Heat-shock transformation

In this process the DNA is introduced into the bacterial cells by a heat-shock.

Briefly, competent cells are thawed on ice at the moment of use and 1-3 µl (1-10 ng) of the DNA ligation reaction or control DNA is added directly to the cells. Cells and DNA are mixed and incubated on ice for 30 min. After that, a heat-shock of 1 min in a 42ºC water bath is applied. Cells are kept on ice for 2 min, 900 µl of LB is added and cells are incubated for 1 h at 37ºC with moderate shaking.

After that, 100 µl of the suspension is plated in LB plates with the appropriate antibiotic near the flame. Plates are incubated at 37ºC o/n.

B) Electrotransformation

In this technique, a high-voltage electric field is applied briefly to cells, apparently producing transient holes in the cell membrane through which plasmid DNA enters. Successful electroporation of *E. coli* requires long, strong pulses. Under these conditions up to 10^9 transformants/µg plasmid DNA can be achieved. In case of large DNA constructs this technique is more effective than the heat-shock transformation.

The procedure was applied following the manufacturer's instructions (BTX Inc. Electro Cell Manipulator^R 600) for DH5α cells.

Electroporation settings: 2 mm gap cuvettes, 129 ohm resistance, 2.45 kV, which gives a 12.25 kV/cm field strength for 5-6 mseconds.

Electroporation procedure: 1 µl (1 ng) of the DNA ligation reaction or control DNA is added to 40 µl of recently thawed competent cells, mixed and kept for 1 min on ice. After that, the cell mixture is placed on a chilled cuvette. The suspension must touch both side walls of cuvette. Immediately after the electroporation, 1 ml of LB is added to the cuvette, mixed thoroughly and incubated at 37ºC for 1 h with moderate shaking. Cells are plated as described before for the heat-shock transformation.

C) Cosmid packaging

For cosmid packaging the *Gigapack^R III XL Packaging Extract kit* (Stratagene, ref. 200208) was used. Packaging extracts are used to package recombinant lambda phage with high efficiency. These extracts are designed for use in cosmid constructions and package large inserts (i.e., 47- to 51-kbp recombinants) with high efficiency.

The cosmid vector was packaged following the manufacturer's instructions. First the cosmid ligation is packaged along with the packaging extract and then this packaging mixture is added to the bacterial cells. Phage adhere to the bacterial cells, infecting them and allowing the cosmid to enter.

The procedure is as follows:

Packaging step: The packaging extract is thawed and mixed by gently pipetting with 1-4 µl (0.1-1.0 µg) of the cosmid ligation reaction. After a 2 h incubation at r.t., 500 µl of SM buffer and 20 µl of chloroform are added. Suspension is briefly centrifuged and the supernatant, diluted to 1:10 and 1:50 in SM buffer, which contains the phage is ready to infect bacterial cells.

Phage infection: A single colony of XL1-Blue cells is inoculated into 2 ml LB medium containing 10 mM $MgSO_4$ and 0.2% (w/v) maltose and grown o/n at 37ºC with moderate shaking. No antibiotic is added since antibiotic will bind to the bacterial cell wall and will inhibit the ability of the phage to infect the cell. The next day, 10 ml of the same medium is inoculated with 1 ml of the preinocul and grown for approx. 2 h in the shaker at 30ºC to a maximal OD_{600} of 1.0. Then, bacteria are centrifuged at 500 x *g* for 10 min, resuspended in half the original volume with sterile 10 mM $MgSO_4$ and diluted to an OD_{600} of 0.5 with 10 mM $MgSO_4$. Immediately, 25 µl of the cosmid packaging extract is mixed with 25 µl of the bacterial cells and incubated at r.t. for 30 min. Then, 200 µl of LB broth is added and the mixture is incubated for 1 h at 37ºC to allow the expression of the antibiotic resistance. After that, cells are plated in ampicillin/tetracycline plates as described before.

SM buffer: 5.8 g of NaCl, 2.0 g of $MgSO_4.7H_2O$, 50 ml of 1 M Tris-HCl pH 7.5 and 5 ml of 2% (w/v) gelatine are dissolved in 1 L of water, autoclaved and kept at r.t.

LB broth: 10 g of NaCl, 10 g of tryptone and 5 g of yeast extract are dissolved in 1 L of water. pH is adjusted to 7.0 with NaOH and the solution is autoclaved and kept at r.t.

1.9.3 Recombinant plasmid selection

The bacteria which have incorporated the desired DNA are selected by plating the cells in LB plates with the appropriate antibiotic. After o/n incubation bacterial colonies are analyzed by PCR (PCR-Preps, Section 1.11.3) or by enzymatic digestion or sequencing after growing them as described before for the DNA minipreparations (Section 1.4).

1.10 DNA SUBCLONING

Subcloning techniques are used for various purposes, such as the obtaining of protein expression constructs, isolation of mutated DNA fragments, adenovirus cosmid construction, etc. The protocol differs in each case although the basic DNA techniques described above were used. Original DNAs were modified enzymatically. The desired DNA fragments were purified and ligated and the resultant DNA construct was transformed, amplified and checked by PCR, sequencing or enzymatic digestion.

1.11 PCR DNA AMPLIFICATION

1.11.1 PCR

The polymerase chain reaction (PCR) is used to amplify a segment of DNA that lies between two regions of known sequence. Two oligonucleotides are used as primers for a series of synthetic reactions that are catalyzed by a DNA polymerase. These oligonucleotides typically have different sequences and are complementary to sequences that (1) lie on opposite strands of the template DNA and (2) flank the segment of DNA that is to be amplified.

The template DNA is first denatured by heating in the presence of a large molar excess of the two oligonucleotides and the four dNTPs. The reaction mixture is then cooled to a temperature that allows the oligonucleotide primers to anneal to their target sequences, after which the annealed primers are extended with DNA polymerase. The cycle of denaturation, annealing and DNA synthesis is then repeated many times. Because the products of one round of amplification serve as templates for the next, each successive cycle essentially doubles the amount of the desired DNA product.

The major product of this exponential reaction is a segment of double-stranded DNA whose termini are defined by the 5' termini of the oligonucleotide primers and whose length is defined by the distance between the primers.

In 1988 Saiki *et al.*[2] introduced a thermo stable DNA polymerase purified from the thermophilic bacterium *Thermus aquaticus* (Taq DNA polymerase). Its optimal temperature for synthesis is 72ºC. This enzyme, which can survive extended incubation at 95ºC, is not inactivated by the heat denaturation step and does not need to be replaced at every round of the amplification cycle. This results in substantial improvements in the specificity and yield of the amplification reaction and in the size of the amplified product. For example, between 0.5 µg and 1 µg of target DNAs up to 2 kb in length can be obtained from 30-35 cycles of amplification with only 10^{-6} µg of starting DNA.

We used a thermal cycler, Minicycler PTC-100^{TM} (M. J. Research), with Peltier refrigeration. The PCR reaction mix and the PCR conditions were the following:

[2] Saiki RK, Gelfand DH, Stoffel S, Scharf SJ, Higuchi R, Horn GT, Mullis KB, Erich HA. Primer-directed enzymatic amplification of DNA with a thermostable DNA polymerase. *Science.* 239: 487-491, 1988

PCR reaction mix	
10X PCR buffer	1X
$MgCl_2$	1.5-2.5 mM
Mixture of four dNTPs	0.25 mM
Primer forward	50 pmol
Primer reverse	50 pmol
Template DNA	1 ng
Taq DNA polymerase	2.5 U
bd. sterile H_2O up to	50 µl

PCR conditions		
First step	94ºC	2-5 min
Denaturation	94ºC	1 min
Annealing	50-65ºC	1 min
Polymerization	72ºC	1 min/kb DNA
25-30 cycles from step 2		
Final extension	72ºC	10 min

At lower annealing temperatures the amplification is more efficient, but the amount of mispriming is significantly increased. At higher temperatures (50-65ºC), the specificity of the amplification reaction is increased, but its overall efficiency is reduced. Usually, the annealing temperature chosen is 2ºC less than the lower melting temperature (Tm) of the two primers used. The Tm of an oligonucleotide could be approximately calculated as [2 x (A + T) + 4 x (C + G) – 9], where A, T, C and G are the number of Adenosine, Thymidine, Cytidine and Guanosine nucleotides present in the primer sequence.

The PCR products are analyzed by electrophoresis in agarose gels.

1.11.2 Primer design

Some previous primer design considerations have to be borne in mind for PCR and sequencing experiments.

The length of the oligonucleotide will be 18 plus one extra base for each 2% decrease related to the 50% of G + C. High A + T percentages prevent the correct annealing of the primer, while high G + C percentages could produce unspecific amplifications due to accidental homology with G +C regions of the template DNA. 40-60% is the ideal range of G + C.

It is recommended to compare the oligonucleotide sequence with the template DNA to detect possible internal or adjacent homologies to the DNA fragment which is to be amplified.

Finally, a G + C equilibrated composition at the 3' terminus of the primer is recommended because this is where the amplification will start.

1.11.3 PCR-Preps

To select the desired recombinant DNA among the bacterial colonies obtained after DNA transformation, a rapid analysis by PCR could be used.

A PCR reaction is performed for each isolated bacterial colony by touching one by one with a sterile tip first the colony, then a new LB plate (for the later identification of the selected colony) and then the PCR mixture placed in a PCR tube. A few cells are enough for the PCR reaction to amplify the desired DNA. The first step of the PCR is 5 min at 94ºC, to break the bacterial membrane by heating and release the internal DNA.

1.12 DNA SEQUENCING

For DNA sequencing we used the *ABI PRISM® BidDye Terminator-Cycle Sequencing Ready reaction Kit* with the *AmpliTaq DNA polymerase* (Applied Biosystems) following the manufacturer's instructions. This kit contains fluorescent nucleosides therefore sequencing products can be detected by fluorescence. The sequence of a single or double-stranded DNA can easily be determined with this kit using an oligonucleotide and performing a PCR reaction. The PCR sequencing mix and the PCR conditions are the following:

PCR sequencing mix		**plasmid**	**cosmid**
Template	single-stranded DNA	50-100 ng	
	double-stranded DNA	200-500 ng	800-1000 ng
	PCR product DNA	1-100 ng	
Primer		3.2 pmol	13 pmol
Ready reaction mix		2 µl	16 µl
bd. sterile H_2O up to		10 µl	40 µl

PCR conditions	**plasmid**		**cosmid**	
First step	96ºC	1 min	95ºC	5 min
Denaturation	96ºC	10 sec	95ºC	30 sec
Annealing	50ºC	5 sec	50-55ºC	10 sec
Polymerization	60ºC	4 min	60ºC	4 min
Cycles from step 2	24		50	

The primer must anneal near the DNA fragment to be sequenced because the PCR reaction extendeds up to 600 bp away from the primer annealing site. After the PCR amplification, samples are precipitated with ethanol for 15 min at r.t., centrifuged at 14,000 rpm for 20 min in a microcentrifuge and washed 3 times in 70% ethanol. Once samples are air-dried (protected from the light) they can be stored at -20ºC.

The polyacrylamide-urea gel electrophoresis and the later analysis of the samples in an *ABI PRISM 3700 DNA Analyzer* (Applied Biosystems) were performed at the Scientific-Technique Services of the University of Barcelona.

1.13 RNA AND DNA ISOLATION FROM CELLS

RNA and DNA were obtained from cells using the TRIzol Reagent (Gibco, ref. 15596-018). This reagent is a mono-phasic solution of phenol and guanidine isothiocyanates, which allows the isolation of total RNA, DNA and protein from cells and tissues. This technique performs well with small quantities of tissue (50-100 mg) and cells (5 x 10^4 cells), and also with large quantities of tissue (= 1 g) and cells (>10^7 cells).

RNA and DNA from cells were extracted according to the manufacturer's instructions. Briefly, cells are grown in 35-mm dishes until confluence and washed in

PBS (see Section 3.3). Cells are lysed by adding 1 ml of TRIzol Reagent directly to the dish, and passing the cell lysate several times through a pipette. The amount of TRIzol Reagent added is based on the area of the culture dish (1 ml per 10 cm^2). An insufficient amount of TRIzol Reagent may result in contamination of the isolated RNA with DNA. During sample homogenization or lysis, TRIzol Reagent maintains the integrity of the RNA, while disrupting cells and dissolving cell components. Addition of chloroform followed by centrifugation, separates the solution into an aqueous phase and an organic phase. RNA remains exclusively in the aqueous phase, DNA in the interphase and proteins in the organic phase. After transfer of the aqueous phase, the RNA is recovered by precipitation with isopropyl alcohol and dissolved in RNase-free water or 0.5% SDS solution. Total RNA isolated by TRIzol Reagent is free of protein and DNA contamination. It can be used for Northern blot analysis or molecular cloning, etc.

DNA and proteins that remain in the organic phase can be recovered by sequential precipitation. Precipitation with ethanol yields DNA from the interphase, and an additional precipitation with isopropyl alcohol yields proteins from the organic phase. Total DNA is dissolved in 8 mM NaOH and pH is adjusted to 8.4 with 0.1 M HEPES. For PCR reaction 0.1-1 mg of the DNA sample could be used.

RNase-free water and 0.5% SDS solution for RNA:

RNase-free water is prepared in RNase-free glass bottles. Diethylpyrocarbonate (DEPC) 0.01% (v/v) is added to the water and solution is left to stand overnight and autoclaved. The 0.5% SDS solution must be prepared using DEPC-treated, autoclaved water.

1.14 NORTHERN BLOT

The Northern blot technique allows identification and comparison a desired RNA within a RNA sample from cells or tissues. RNA obtained from cells or tissues is separated by electrophoresis, transferred to a nylon membrane and hybridized with a radiolabelled cDNA probe which is specific for the desired RNA.

The procedure is as follows:

A) RNA separation by electrophoresis

Electrophoresis is performed in agarose/formaldehyde denaturalizing gels. These gels are used to separate the RNA because they contain formaldehyde which denatures

the possible RNA secondary structures. This fact permits the RNA migration to be inversely proportional to its molecular weight logarithm and therefore, the molecular weight of the RNA transcripts can be calculated. 20 µg of RNA diluted in RNA loading buffer and a RNA molecular marker are incubated at 65ºC for 10 min and loaded into denaturalizing gels. Electrophoresis is performed at 30 V for 5 h or at 10 V o/n. Denaturalizing gels, electrophoresis buffer and RNA loading buffer must be prepared in RNase-free conditions to avoid RNA degradation.

Denaturalizing gels: 1% agarose, 40 mM MOPS/NaOH pH 7, 10 mM sodium acetate, 2.2 M formaldehyde and 1 mM EDTA in DEPC-treated water.
Electrophoresis buffer: 40 mM MOPS/NaOH pH 7, 10 mM sodium acetate, 2.2 M formaldehyde and 1 mM EDTA in DEPC-treated water.
RNA loading buffer: 2.2 M formaldehyde, 50% deionized formamide, 5% glycerol, 0.13 mg/ml ethidium bromide and 5% bromophenol blue in electrophoresis buffer.

B) Transfer

The RNA is transferred from the denaturalizing gel to a nylon membrane (Schleicher and Schuell) by the method of Sambroock[3] with 10X SSC. Then, RNA is fixed to the membrane by UV crosslinking or by a 1 h incubation at 80ºC.

C) Hybridization

The cDNA probe of the desired gene, a cDNA fragment excised from a plasmid, is ^{32}P-labelled using the Random prime labelling system (Rediprime^{TM}II, Amersham Pharmacia Biotech, ref. RPN 1633). The labelled probe is denatured at 100ºC for 5 min and then rapidly placed on ice. Pre-hybridation, hybridation and washing steps are done with the ExpressHyb Hybridization solution (Clontech, ref. 8015-2) following the manufacturer's instructions. Briefly, pre-hybridization is done in ExpressHyb solution at 68ºC for 30 min. Hybridization is performed with ExpressHyb solution plus the labelled cDNA probe at 68ºC for 1 h and washing steps are performed first with 2X SSC and 0.1% SDS and then with a more stringency solution composed of 0.2X SSC and 0.1% SDS.

[3] Sambroock J, Frisch EF, Maniatis T. Molecular cloning: A laboratory Manual, 2nd Edn. Cold Spring Harbour Laboratory, Cold Spring Harbor, N.Y. USA. 1989

20X SSC: 3M NaCl and 0.3 M sodium citrate pH 7.

D) Detection

RNA bands are detected by exposure to X-ray film or by using a Storm 840 Laser scanning system (Molecular dynamics, Amersham Pharmacia Biotech).

To ensure equal RNA loading and even transfer, membranes are stripped and re-hybridized with a "housekeeping gene" probe cyclophilin.

2. ANIMALS

Six-week-old C57BL/6J male mice were purchased from Harlam Co. Wistar rats weighing 200–250 g were used for islet isolation. Animals were maintained under a 12-h dark/light cycle at 23ºC with free access to food and water. After a 1-week acclimatization, experiments with animals were performed. The experimental protocols were approved by the Animal Ethics Committee at the University of Barcelona.

2.1 C75 TREATMENT

For C75 experiments with mice, animals are administered a single intraperitoneal (ip) injection of C75 dissolved in RPMI 1640 medium at 20 mg/kg body weight. Control animals are administered RPMI 1640 medium. Mice are sacrificed at different times post-injection and mitochondrion-enriched fractions from liver and pancreas are obtained for CPTI activity assay.

C75: For the animals 5 mg of C75 is dissolved in 1 ml of RPMI 1640 medium. It is prepared on the day of the experiment and kept at 4ºC.

3. CELL CULTURE

All solutions used for cell culture were sterilized by autoclaving at 121ºC for 30 min (PBS, bd. water, etc.) or by filtering them through a 0.22 µm filter (Millipore) if necessary.

3.1 BETA CELL LINES

Reliable β-cell models are very important for diabetes research. It is generally accepted that the use of primary cells is preferable. However, this requires large amounts of isolated pancreatic islets of Langerhans, which is work-intensive and has the inherent inconvenience of representing a mixed population of β, α, δ and F cells. Because of this, rodent β-cell lines are a usefulness alternative until clonal human β-cells become available.

The main requirements for an insulinoma cell line to faithfully and stably mimic the performance of β-cells within the normal pancreatic islets are the maintenance of tissue-specific differentiation and appropriate proliferation. Numerous rodent β-cell lines have been reported. Among the mouse derived β-cell lines, MIN-6, βTC6-F7 and βHC9 have an insulin content closer to that of normal islets and retain some glucose-stimulated insulin secretion. However, MIN-6 cells exhibit secretory responses to pyruvate, which is not a secretagogue for normal islets, βTC6-F7 cells lose their stable glucose responsiveness after prolonged tissue culture, and βHC9 cells grow very slowly and are thus difficult to study. The hamster-derived β-cell line HIT cells have a lower insulin content and weaker glucose response with increasing passage. Rat-derived β-cell lines, such as RINm5F, BRIN-BD11 and INS-1, have also been studied. RINm5F cells have low insulin content, do not respond to glucose in the physiological concentration range and lose differentiated features after prolonged tissue culture. BRIN-BD11 cells are poorly differentiated, exhibiting low insulin content and weak secretory responses to glucose. INS-1 cells were isolated from a radiation-induced rat insulinoma[4], they are sensitive to physiological glucose concentrations and unresponsive to neurotransmitters, but they exhibit only a 2-to 4-fold increase in insulin secretion in response to glucose, which is far less than the 15-fold responses achievable with freshly isolated primary islets. Moreover, due to their nonclonal nature, INS-1 cells are heterogeneous and are not stable over extended culture periods. Consequently, two clonal INS-1 derived cell lines have been generated: INS-1E and INS(832/13). Clonal INS-1E[5] cells were isolated

[4] Asfari M, Janjic D, Meda P, Li G, Halban PA, Wollheim CB. Establishment of 2-mercaptoethanol-dependent differentiated insulin-secreting cell lines. *Endocrinology*. 130:167-178, 1992

[5] Merglen A, Theander S, Rubi B, Chaffard G, Wollheim CB, Maechler P. Glucose sensitivity and metabolism-secretion coupling studied during two-year continuous culture in INS-1E insulinoma cells. *Endocrinology*. 145(2):667-678, 2004

from parental INS-1 based on both their insulin content and their secretory responses to glucose (6.2-fold). INS(832/13)[6] cells were stably transfected with a plasmid containing the human proinsulin gene and have a potent response to glucose (average of 10-fold).

Therefore, we chose INS(832/13) cells for our studies due to their higher secretory response to glucose, their K_{ATP} channel-independent pathway of glucose sensing and their adequate proliferation in culture.

3.1.1 INS(832/13) cells

The INS(832/13) clone was kindly given by Dr. M. Prentki (Montreal, Canada). INS(832/13) cells (passages 48-60) are cultured in a humidified atmosphere containing 5% CO_2 in complete medium composed of RPMI 1640 (Gibco, ref. 21875-034) containing 11 mM glucose and supplemented with 10% (v/v) heat-inactivated fetal bovine serum (FBS) (Wisent Inc, USA, ref. 80150, Lot. 102703), 10 mM HEPES (pH 7.4), 2 mM glutamine, 1 mM sodium pyruvate, 50 µM 2-β-mercaptoethanol, 100 U/ml penicillin and 100 µg/ml streptomycin.

500 ml of complete medium contains the following:

INS(832/13) medium	
RPMI 1640	430 ml
FBS	50 ml
100X HEPES	5 ml
100X Glutamine	5 ml
100X Na Pyruvate-2-β-mercaptoethanol	5 ml
Penicillin-Streptomycin (10^4 U/ml-10^4 mg/ml)	5 ml

INS cells grow correctly in plastic culture from Falcon. Medium is changed every 2-3 days: cells are first washed in PBS preheated to 37ºC and medium (also at 37ºC) is added as follows: 4 ml for 25 cm^2 flasks, 15 ml for 75 cm^2 flasks, 10 ml for 10-cm dishes, 15 ml for 15-cm dishes or 2 ml/well for 12-well plates.

[6] Hohmeier HE, Mulder H, Chen G, Henkel-Rieger R, Prentki M, Newgard CB. Isolation of INS-1-derived cell lines with robust ATP-sensitive K^+ channel-dependent and -independent glucose-stimulated insulin secretion. *Diabetes.* 49(3):424-430, 2000

The maintenance culture is passaged once a week by gentle trypsinization. To trypsinise the cells they are first washed in PBS preheated to 37ºC and then 1.5 ml of the proteolytic enzyme and chelating agent mix Trypsin-EDTA 1X (Gibco, ref. 25300-062) is added. The trypsin solution has to be enough to cover the cells. After 2 min when the cells have come detached, the medium is added, and the cells are gently resuspended by pipetting to avoid the aggregates and they are spread as desired.

3.1.2 INS-r9 cells

The rat insulinoma INS-1 cell-derived clone, which stably expresses the reverse tetracycline-dependent activator[7], was kindly given by Dr. CB Wollheim (Geneva, Switzerland). INS-r9 cells are cultured in a humidified atmosphere containing 5% CO_2 in complete medium composed of RPMI 1640 containing 11 mM glucose and supplemented with 10% (v/v) heat-inactivated tetracycline-free FBS (Clontech, ref. 8630-1), 10 mM HEPES (pH 7.4), 2 mM glutamine, 1 mM sodium pyruvate, 50 µM 2-β-mercaptoethanol, 0.1 mg/ml G418 (Calbiochem, ref. 345812), 100 U/ml penicillin and 100 µg/ml streptomycin.

500 ml of complete medium contains the following:

INS-r9 medium	
RPMI 1640	429 ml
FBS	50 ml
100X HEPES	5 ml
100X Glutamine	5 ml
100X Na Pyruvate-2-β-mercaptoethanol	5 ml
G418 (50 mg/ml)	1 ml
Penicillin-Streptomycin (10^4 U/ml-10^4 mg/ml)	5 ml

Cells are cultured and trypsinised as described above for INS(832/13) cells.

[7] Wang H, Iynedjian PB. Modulation of glucose responsiveness of insulinoma β-cells by graded overexpression of glucokinase. *Proc. Natl. Acad. Sci.* USA. 94:4372-4377, 1997

3.1.3 naSREBP-1c STABLE CELL LINE

The rat insulinoma INS-1 cell-derived clone which stably expresses naSREBP-1c was obtained from INS-r9 cells stably transfected with the naSREBP-1c gene[8], a nuclear localized N-terminal form of SREBP-1c with intact transcriptional activity. naSREBP-1c stable cells are cultured in a humidified atmosphere containing 5% CO_2 in complete medium composed of RPMI 1640 containing 11 mM glucose and supplemented with 10% (v/v) heat-inactivated tetracycline-free FBS (Chemie Brunschwig AG, ref. BRA 15-043, Lot. A01122-007), 10 mM HEPES (pH 7.4), 2 mM glutamine, 1 mM sodium pyruvate, 50 µM 2-β-mercaptoethanol, 0.1 mg/ml G418 (Calbiochem, ref. 345812), 0.1 mg/ml hygromycin (Calbiochem, ref. 400051), 100 U/ml penicillin and 100 µg/ml streptomycin.

500 ml of complete medium contains the following:

naSREBP-1c medium	
RPMI 1640	428 ml
FBS	50 ml
100X HEPES	5 ml
100X Glutamine	5 ml
100X Na Pyruvate-2-β-mercaptoethanol	5 ml
G418 (50 mg/ml)	1 ml
Hygromycin (50 mg/ml)	1 ml
Penicillin-Streptomycin (10^4 U/ml-10^4 mg/ml)	5 ml

Cells are cultured and trypsinised as described above for INS(832/13) cells.

3.2 HEK 293 CELLS

Human embryo kidney (HEK) 293 cells obtained from ECACC (European Collection of Cell Cultures) are cultured in a humidified atmosphere containing 5% CO_2 in complete medium composed of Dulbecco's Modified Eagle Medium (DMEM,

[8] Wang H, Maechler P, Antinozzi PA, Herrero L, Hagenfeldt-Johansson KA, Björklund A, Wollheim CB. The transcription factor SREBP-1c is instrumental in the development of β-cell dysfunction. *J. Biol. Chem.* 278(19):16622-16629, 2003

Gibco, ref. 41965-039) containing 4,500 mg/L glucose and supplemented with 10% (v/v) heat-inactivated FCS (Biological Industries, ref. 04-001-1A, Lot. 816983), 100 U/ml penicillin and 100 µg/ml streptomycin.

500 ml of complete medium contains the following:

HEK 293 medium	
DMEM	445 ml
FCS	50 ml
Penicillin-Streptomycin (10^4 U/ml-10^4 mg/ml)	5 ml

The maintenance culture is passaged twice a week and the medium is changed every 2-3 days. To passage HEK 293 cells it is not necessary to trypsinise them. Cells are first washed in PBS preheated to 37ºC and then detached by simply up and down pippetting with medium preheated to 37ºC and spread as desired. For experiments cells are grown until confluence.

3.3 SOLUTIONS AND BASIC PROCEDURES IN CELL CULTURE

FBS inactivation

The main role of serum in cell cultures is to provide complexes of hormones and growth factors. The serum complement system has to be inactivated before use in culture. The complement is a heat-labile cascade system in the sera of all vertebrates and composed of at least 20 glycoproteins. Activated complement has high proteolytic activity, which may affect the function of membrane proteins of the cultured cells and thus cell viability.

Serum bottles are stored at -20ºC. To inactivate the FBS, serum is thawed in a water bath at 37ºC and mixed well by inverting the bottle. FBS is inactivated by 30 min incubation at 56ºC. Then it is kept at 4ºC or stored at -20ºC.

100X HEPES (1 M)

11.91 g of HEPES is dissolved in 50 ml of RPMI 1640, pH is adjusted to 7.3 with NaOH and the solution is filtered through a 0.22 µm filter and stored at 4ºC for about 2 months. HEPES gives the pH range that supports optimal cellular growth in culture cells.

100X Glutamine (205 mM)

3 g of L-Glutamine is dissolved in 100 ml of RPMI 1640 preheated to 37ºC. When glutamine is dissolved, it is filtered through a 0.22 µm filter and aliquots of 5 ml are stored at -20ºC. The half life of the glutamine in solution at 4ºC is 15 days.

100X Na pyruvate plus 2-β-mercaptoethanol (14.33 M)

1.1 g of Na pyruvate and 34.9 µl of 2-β-mercaptoethanol are dissolved in 100 ml of RPMI 1640 and filtered through a 0.22 µm filter. 5 ml aliquots are stored at -20ºC. Many types of culture cells as INS require pyruvate or other small alpha-oxo-acids. The requirement is relatively non-specific and may reflect the need of a substrate that can be used to oxidize NADH, rather than the requirement for a specific metabolic intermediate. The main proposed role of 2-β-mercaptoethanol in INS cells and other cell lines is the activation of cystine uptake and the increase of glutathione levels. It also promotes cell proliferation.

Hygromycin (50 mg/ml)

To prepare a 50 mg/ml hygromycin stock, 2 ml of hygromycin (Calbiochem, ref. 400051) is diluted in 14 ml of PBS, filtered through a 0.22 µm filter and stored at 4ºC.

PBS

To obtain 1 L of Phosphate-Buffered Saline (PBS) 8 g of NaCl, 1.44 g of $Na_2HPO_4.2H_2O$, 0.2 g of KCl and 0.2 g of KH_2PO_4 are dissolved in 1 L of bd. water. Then, pH is adjusted to 7.4 and solution is autoclaved and stored at 4ºC. PBS is useful to remove floating and dead cells and for washing because it provides the cells with water and inorganic ions, while maintaining physiological pH and osmotic pressure.

Counting the cells

Cells are counted in a Neubauer chamber. One drop of cells resuspended in medium is placed between the coverslip and the chamber. Cells from one large square (which contains 16 small squares) are counted and multiplied by 10,000 to calculate the number of cells per ml.

Freezing the cells

The number of cells recommended for freezing is approximately 20 million for INS and 10 million for HEK 293. First cells are detached with medium (HEK 293) or with Trypsin-EDTA (INS) as described above. Then, they are resuspended in 10 ml of medium, centrifuged at 1,200 rpm for 5 min and resuspended in 1.5 ml of medium plus 150 µl of DMSO in a 1.5 ml cryogenic tube. DMSO is a cryoprotector agent that physically protects the cells from the forming ice crystals, changes in osmotic pressure or fast freezing. However the 10% DMSO used to freeze the cells is toxic at 37ºC, so cells must be frozen immediately at -80ºC in a recipient with isopropanol and stored in liquid N_2 the following day.

Thawing the cells

Cells stored in the cryogenic tube are thawed in a 37ºC water bath. Then, they are diluted in 10 ml of medium and centrifuged at 1,200 rpm for 5 min to eliminate medium with DMSO. After that, cells are resuspended in the desired volume of medium and seeded. Medium is changed the next day.

3.4 MYCOPLASMA DETECTION AND TREATMENT

Mycoplasma species are the smallest known free-living organisms. They constitute a common and pervasive tissue culture contaminant. The small size and the lack of a cell wall make *mycoplasmas* extraordinarily difficult to detect by conventional methods. The effects of *mycoplasma* infection are significant, including changes in cell morphology, growth rates, viability and metabolic states[9,10]. These changes can profoundly affect the results obtained in any cell culture-based bioassay system.

The more frequent contaminants are the *mycoplasma* species *M. orale* and *M. hominis* (human origin), *M. arginini* (bovine) and *M. hyorhinis* (porcine). Sources of *mycoplasma* contamination are water, medium, serum and the cells. Cell culture can be contaminated by breath from the pharynx (*M. orale*), by using contaminated serum or, more frequently, by the parallel use of other contaminated cell cultures. Commercial serum and media are both tested for *mycoplasma* contaminations.

[9] Barile MF, Razin S. The mycoplasmas, vol. I. *Cell Biology*. Academic Press, Inc., New York, 1979

[10] Masover GK, Buck DW. Detecting mycoplasmas in cell cultures. *Med. Device & Diagn. Ind*. 5(11):43-48, 1983

Mycoplasmas usually grow slowly in the cell culture without destroying the host cells and without producing gross turbidity. They are resistant to many antibiotics, they pass easily through 0.22 µm filters and they are relatively difficult to detect by microscopy, so the cells must be checked periodically. The most common methods for *mycoplasma* detection are based on fluorescence, PCR or immuno-detection. PCR detection, which is rapid, simple and sensitive, was applied as follows.

Mycoplasma PCR detection in tissue culture

Mycoplasma PCR detection uses a pair of primers that detect all the most frequent *Mycoplasma* species without cross-reacting with other common tissue culture contaminants such as bacteria or yeasts.

Cell culture must be kept for 3 days in the same medium without antibiotics to allow maximum *mycoplasma* expression. One dish containing medium alone must also be kept to check for medium contamination. After 3 days 1 ml of the supernatant of the culture dish and the dish with medium alone is taken and the PCR is done as follows:

***Mycoplasma* PCR mix**	
10X PCR buffer	5 µl
$MgCl_2$ (50 mM)	1.5 µl
dNTPs (2 mM)	5 µl
primer Myc.for (50 µM)	1 µl
primer Myc.rev (50 µM)	1 µl
Taq polymerase (5U/µl)	0.25 µl
Sample	2 µl
bd. A.C. H_2O	34.25 µl
(Total volume = 50 µl)	

Samples consists of: 2 µl of the supernatant of the cell culture, 2 µl of only the medium, 2 µl of sterile water as a negative control, 2 µl of a positive control and 2 µl of a 1/100 dilution in water of the supernatant cell culture sample, because the degree of infection is unknown for each sample and a high degree of infection will inhibit the PCR.

The amplification product is a band of 500 bp and the PCR program is:

***Mycoplasma* PCR**	
95ºC	5 min
94ºC	1 min
60ºC	1 min
72ºC	2 min
30 cycles from step 2	
72ºC	10 min
4ºC	30 min

It is also possible to use a *Mycoplasma* PCR detection kit from Takara Biomedicals (ref. 20-700-20).

***Mycoplasma* treatment**

If the cell culture is contaminated it is advisable to start again with a non-contaminated new stock of cells. Extra precautions should be taken to avoid contamination, by cleaning incubators and hoods with an appropriate detergent for *mycoplasma* (70% ethanol does not kill *mycoplasma*) or by autoclaving PBS, water, etc. (not media or trypsin...).

When it is impossible to start again with a new stock treatment with BAYCIP (Bayer, ref. 982421) could be applied. For 3 weeks the cell culture must be grown and cultured normally in the medium plus 0.01 mg/ml of BAYCIP. The treatment must be repeated until *mycoplasma* PCR detection is negative.

3.5 CELL CULTURE TREATMENTS

3.5.1 Basal treatment

This basal treatment is applied before experiments such as CPTI activity assay, palmitate oxidation, insulin secretion or viability, where the presence of etomoxir is examined or when there is a need to complex free fatty acids to BSA.

Cells are washed in KRBH 0.1% (w/v) defatted BSA, preincubated at 37ºC for 30 min in KRBH plus 1% BSA in the absence or the presence of 200 µM etomoxir and washed again with KRBH 0.1% BSA. After this, the desired experiment is performed.

Since this treatment was done for insulin secretion experiments, it was chosen as the basal conditions for the rest of the experiments. Consequently, the cells started at the same point at the beginning of all experiments, and the results were therefore comparable.

KRBH buffer: 135 mM NaCl, 3.6 mM KCl, 0.5 mM NaH_2PO_4, 0.5 mM $MgSO_4$, 1.5 mM $CaCl_2$, 2 mM $NaHCO_3$ and 10 mM HEPES, pH 7.4. KRBH is prepared on the day of the experiment as follows:

KRBH buffer (100 ml)	
5X KRB	20 ml
100 mM $NaHCO_3$	2 ml
1M HEPES pH 7.4	1 ml
bd. H_2O	77 ml

5X KRB: It contains $CaCl_2$, which must be dissolved separately because it precipitates. 5X KRB is stored at 4ºC.

5X KRB (500 ml)	
NaCl	19.72 g
KCl	0.67 g
NaH_2PO_4	0.17 g
$MgSO_4$	0.25 g
$CaCl_2$	0.55 g
bd. H_2O up to	500 ml

BSA: To prepare a 10% (w/v) stock of defatted BSA, 3 g of BSA (Sigma-Aldrich, ref. A-6003) is dissolved in 30 ml of KRBH. Solution is divided into 1 ml aliquots and stored at -20ºC.

3.5.2 C75 treatment

For C75 experiments with culture cells, INS(832/13) and HEK 293 cells are grown in 12-well plates or 15-cm dishes until confluence. Cells are incubated for 1 h at 37ºC in complete culture medium with either C75 (Alexis Biochemicals, ref. 270-286-

M005, 5 mg) at 10 or 30 µg/ml or etomoxir at 30 µg/ml. C75 and etomoxir are added from a 100 mM stock solution in DMSO. Control cells are incubated with the same volume of DMSO. After this time, cells are washed in PBS and the experiment is performed.

C75: The stock solution is prepared at 100 mM in DMSO and it is stored at -20ºC.

Etomoxir: The stock solution is prepared at 100 mM in DMSO. It is stored at -20ºC.

3.5.3 Doxycycline induction

For tet-on systems, doxycycline induction is performed by incubating the cells with complete medium containing 500 ng/ml of doxycycline (Sigma-Aldrich, ref. D-9891, 25 g) for 24 h or with 75 ng/ml of doxycycline for 48 h. Doxycycline is distributed in 1.5 ml tubes, stored at 4ºC and used fresh by dissolving it in bd. A.C. water at the moment of utilization.

3.6 VIABILITY

The cytotoxic effect of C75 or naSREBP-1c expression on cell growth and viability was measured in culture cells. Quantification of cell proliferation or viability was performed with an assay based on the reduction of a tetrazolium salt to formazan by cellular mitochondrial dehydrogenases[11]. Expansion in the number of viable cells results in an increase in the overall activity of the mitochondrial dehydrogenases and subsequently an augmentation in the amount of formazan dye formed. The formazan dye produced by viable cells is quantified with a spectrophotometer by measuring the absorbance at 570 nm.

The procedure is as follows:

Cells grown in 12-well plates are treated with C75 or etomoxir in case of INS(832/13) and HEK 293 or with doxycycline in case of naSREBP-1c stable cells, as described in CELL CULTURE TREATMENTS (Section 3.5). Cells are cultured for 2 h with 1 ml of fresh medium plus 200 µl of MTT solution (3-(4,5-dimethylthiazol-2-yl)-2,5-

[11] Mosmann T. Rapid colorimetric assay for cellular growth and survival: application to proliferation and cytotoxicity assays. *J. Immunol. Methods.* 65:55-63, 1983

diphenyltetrazolium bromide solution). MTT is reduced by cellular mitochondrial dehydrogenases giving blue crystals of formazan. After that, cells are gently collected in a 1.5 ml tube and washed twice in PBS. The pellet of cells is resuspended in 1 ml of MTT lysis solution and therefore, cells are lysated and the blue crystals are released and dissolved. The formazan dye produced is quantified with a spectrophotometer at 570 nm with the MTT lysis solution as the blank. Results are expressed as the percentage of absorbance related to control cells.

MTT solution (0.25%): 25 mg of MTT (Sigma-Aldrich, ref. M-2128, 1 g) is dissolved in 10 ml of PBS, filtered through a 0.22 µm filter and stored at 4ºC, light protected.

MTT lysis solution: 10% SDS and 1 mM acetic acid in DMSO. For 30 ml, 171.6 µl of acetic acid and 3 g of SDS are dissolved in 30 ml of DMSO. It is prepared on the day of the experiment.

It is also possible to use the Quick Cell Proliferation Assay Kit (LabForce, MBL, Nunningen, Switzerland) which is based on the same method described above.

3.7 APOPTOSIS

DNA fragmentation and mitochondrial cytochrome *c* release are characteristic hallmarks of cells undergoing apoptosis. Both experiments were done with naSREBP-1c cells cultured with 500 ng/ml doxycycline for 4 days or with 75 ng/ml doxycycline for a week.

Experiments for DNA fragmentation were performed using a Quick Apoptosis DNA Ladder Detection Kit (LabForce, MBL) following the manufacturer's protocol.

To detect the mitochondrial cytochrome *c* release into cytosol, cells are grown in 15-cm dishes, resuspended in buffer A and homogenized by a Dounce homogenizer. Cell debris and nuclei are removed by centrifugation at 1,000 x *g* for 10 min at 4ºC. The supernatant is further centrifuged at 10,000 x *g* for 20 min and the cytosolic proteins (supernatant fractions) are separated by 15% SDS-PAGE and analyzed by Western blotting with a specific antibody against cytochrome c (LabForce, MBL).

Buffer A	
HEPES-KOH, pH 7.5	20 mM
KCl	10 mM
$MgCl_2$	1.5 mM
EDTA	1 mM
EGTA	1 mM
DTT	1 mM
Sucrose	250 mM
PMSF	1 mM

4. CELL TRANSFECTION BY CALCIUM PHOSPHATE

The calcium phosphate method was chosen for transient transfection, for adenovirus production and also to generate stable clones because it is the best choice for stable transfection of INS-1 cells.

In calcium phosphate mediated transfection, the calcium ions bind to the negatively charged phosphate groups of DNA. When phosphate ions are added to the mixture, they bind ionically to the calcium ions resulting in the formation of a crystalline complex which precipitates. Although the exact mechanism is not understood, it is believed that the precipitate attaches to the cell surface and uptake into the cell occurs *via* endocytosis.

Calcium-phosphate-DNA coprecipitation

Five million of cells are seeded in 10-cm dishes. The next day, cells which are approximately 50% confluent, are fed with 5 ml of fresh and complete medium 2 h before transfection. It is important to use cells in exponential growth because the efficiency of transfection is poor in slow-growing cells. Plasmid DNA is prepared, as clean as possible, at a concentration of 1-10 µg/µl in sterilized bd. water.

The solution A (DNA-Ca mix) is prepared under sterile conditions in a 1.5 ml tube as follows:

DNA-Ca mix	
DNA	30 µg
2 M $CaCl_2$/Tris (pH 7.6)	62.5 µl
bd. H_2O up to	500 µl

500 µl of 2X HEBS (pH 7.1), solution B, is placed in a 15 ml sterile tube. Solution A is added dropwise to solution B while gently vortexing. The precipitate is incubated at r.t. for 40 min. It should be visible, i.e., the solution should appear opaque. The precipitate is mixed by vortexing and poured onto the cells that have 5 ml of medium. Precipitates are left on cells for 24 h. By observing the culture under the microscope, a fine precipitate should appear and settle.

The day after it could be optionally done a glycerol shock. The transfection medium is aspirated, washed twice in medium and 3 ml of 15% glycerol (v/v in medium and filtered through a 0.22 µm filter) is added for 4 min. Cells are rinsed twice with medium and cultured in complete medium for 24-48 h.

After this, cells are either removed for transient transfection or split into two 10-cm dishes for clones generation.

20X HEBS: 2.8 M NaCl, 15 mM Na_2HPO_4 and 0.5 M HEPES. For 50 ml:

20X HEBS	
NaCl	8.18 g
HEPES	5.95 g
Na_2HPO_4	0.1065 g
bd. H_2O	40 ml to dissolve
pH	7.1
bd. H_2O up to	50 ml

The solution is passed through a 0.22 µm filter and stored in a 5 ml sterile tube at -20ºC.

2X HEBS: 280 mM NaCl, 1.5 mM Na_2HPO_4 and 50 mM HEPES. For 40 ml:

2X HEBS	
20X HEBS	4 ml
bd. H_2O	30 ml
pH to	7.1
bd. H_2O up to	40 ml

The solution must be filtered through a 0.22 µm filter and used fresh or stored in 5 ml sterile tube at -20ºC for less than 6 months. An exact pH is extremely important in order to get a fine precipitate. The pH must never be below 7.0 or above 7.1.

2M $CaCl_2$/Tris. For 30 ml:

2M $CaCl_2$/Tris	
$CaCl_2$. $2H_2O$ (Merck)	8.82 g
1 M Tris-HCl (pH 7.5)	3 ml
bd. H_2O	20 ml to dissolve
1 M Tris-Base pH to	7.6
bd. H_2O up to	30 ml

The solution must be filtered through a 0.22 µm filter and stored in 1.5 ml sterile tubes at -20ºC.

For adenovirus generation the cosmid was transfected onto HEK 293 cells by calcium phosphate using the *CellPhect Transfection kit* from Amersham Pharmacia Biotech (ref. 27-9268-01).

5. STABLE CELLS CONSTRUCTION

Stable cells are constructed by integrating a gene of interest into a cell line. DNA is stably transfected by calcium-phosphate-DNA coprecipitation along with a selection plasmid in much less amount than the target DNA. After 5 days, selection with the selection plasmid antibiotic is initiated, therefore cells which have not been transfected

with this selection plasmid die. Usually, a few clones appear 3 weeks later. As the DNA of interest was added in much larger amounts than the selection plasmid, these clones are also assumed to have integrated the target DNA. Its presence is checked by Western blot, enzyme activity, Northern blot, etc. The clone with the highest expression of the gene is chosen and it is continuously grown with the selection antibiotic in the medium.

The procedure is as follows:

A) DNA transfection

Cells are grown in four 10-cm dishes until approx. 50% confluence (5 x 10^6 million of cells per 10-cm dish seeded the day before). Calcium phosphate transfection is done as described above with 25 µg of the DNA of interest and 5 µg of hygromycin selection plasmid (pTK-Hyg). 48 h after the glycerol shock, cells are washed first with PBS and then with 5 ml of trypsin because cells are difficult to detach. Then, they are trypsinised in 3 ml of trypsin plus 7 ml of medium by up and down pipetting. One dish of 10-cm is split into 2 dishes of 10-cm with 5 ml of medium.

B) Clones selection

Three days later, medium with 0.1 mg/ml hygromycin is added to the cells and thus clone selection is started. Medium is changed every 3-4 days and three weeks later clones are clearly visible by simply eye observation. Medium with hygromycin is used from this point on. The concentration 0.1 mg/ml of hygromycin in the medium is chosen because it is the enough amount of hygromycin to kill all normal cells after a 3-day incubation.

C) Clones trypsinization

To trypsinise the clones it is used small glass cloning cylinders (Bellco Glass, Inc. Size: 6 x 8 mm, ref. 2090-00608), a glass petri dish and silicone grease (Bayer Baysilone, ref. 85402, 35 g). Cloning cylinders are kept in a bottle with detergent. The day before, cylinders are washed inside the bottle several times with water and then, they are sterilized in a beaker covered with aluminium foil at 180ºC o/n. Silicone grease is put onto the base of the glass petri dish and it is also sterilized at 180ºC o/n wrapped with aluminium foil.

Next, the process is done under the hood. Cells are first washed in PBS. Not all the PBS is aspirated to keep the cells moist. Some cloning cylinders are placed with one

base in contact with the grease of the petri dish. With a forceps one cylinder is located onto one clone. The cylinder is adhered to the 10-cm dish with silicone and the clone is thus in the middle of the cylinder and isolated from the rest of the dish. After that, 30 µl of trypsine is added to each clone. Five min later, 50 µl of medium is added to each clone and by up and down pipetting clones are detached and placed into one well of a 24-well plate. Clones are grown for 2 weeks and medium is changed every 3-4 days.

D) Clones growth and analysis

When clones have grown until 80% confluence, each clone is detached and split into one well of two 12-well plates. Clones grown in one 12-well plate will be analyzed by Western blot and the other 12-well plate will be used to keep on growing the clones to do more experiments. The clone with a higher expression of the target gene is chosen.

6. ADENOVIRUS CONSTRUCTION AND UTILIZATION

The ability to transfer DNA rapidly and efficiently in mammalian cells has been improved by the development of a number of gene transfer vectors and techniques based on the properties of DNA viruses such as adenovirus, retrovirus and adeno-associated virus. Among them, we have used the adenoviruses for gene delivery because of their growth and infectivity characteristics. Adenovirus rapid and efficiently deliver DNA into a wide range of mammalian cell types, including primary cell types with low replicative activity such as cells of the islets of Langerhans with a transfer efficiency of 70-80%, and to insulinoma cell line models with an efficiency approaching 100%. Moreover, they express relatively large DNA inserts (up to 5-7 kbp) and propagate stable high-titer viral stocks. Adenovirus integrates into genomic DNA with very low efficiency and exists predominantly in an episomal mode, therefore the expression of the transgene is transient[12].

[12] Becker TC, Noel RJ, Coats WS, Gómez-Foix AM, Alam T, Gerard RD, Newgard CB. Use of Recombinant adenovirus for metabolic engineering of mammalian cells. *Methods in cell biology*. 43:161-189, 1994

6.1 ADENOVIRUS BIOLOGY

Adenoviruses (Ad) are a large family of nonenveloped, double-stranded DNA viruses. The virus was originally isolated from human adenoidal tissue in 1953[13]. Human adenovirus serotypes 2 (Ad2) and 5 (Ad5) are the most extensively studied. For our study we chose the Ad5.

The adenoviral particle consists of an icosahedral protein capsid approximately 75 nm in diameter encasing a double-stranded DNA molecule of approx. 36 kb (see fig. 2). The most abundant viral protein is hexon, which makes up most of the outer shell of the virus. At each vertex there is a complex composed of the penton base and fiber proteins, both of which interact with cellular receptors during the process of virus infection. Ad DNA is packaged in a complex with several viral proteins and each end of the chromosome is covalently attached to a single molecule of terminal protein (TP). TP acts as a primer for DNA synthesis and also anchors the viral chromosome to the nuclear matrix.

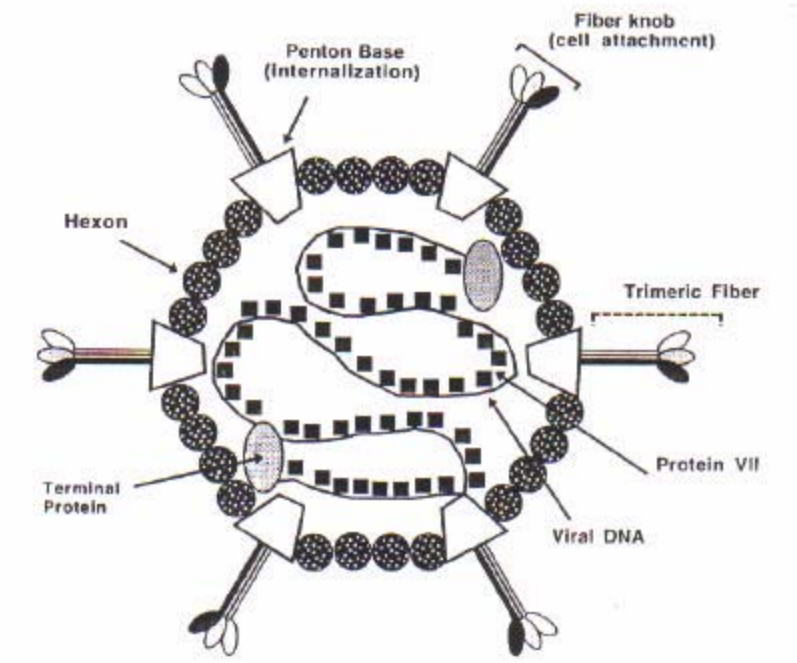

Fig. 2. Cross section of the adenovirus particle. Hexon protein makes up most of the capsid by mass. A complex of penton base and fiber proteins is located at each vertex. The 36-kb double-stranded DNA chromosome is packaged as a complex with protein VII, and one molecule of terminal protein is attached covalently at each end.

[13] Rowe WP, Huebner RJ, Gilmore LK, Parrott RH, Ward TG. Isolation of a cytopathogenic agent from human adenoids undergoing spontaneous degeneration in tissue culture. *Proc. Soc. Exp. Biol. Med*. 84:570-573, 1953

The lytic life cycle of the wild-type virions can be divided into early and late phases, which are defined as occurring before and after the onset of viral DNA replication, respectively. Therefore the adenoviral genome could be classified into early (E1, E2, E3 and E4) genes and late genes. Strategies for adenovirus vector design are focused on deleting portions of the genome to allow packaging of relatively large DNA inserts. Wild-type adenovirus can only accommodate 2 kbp of foreign DNA, but deletion of E1 and E3 genes can allow recombinants with inserts up to 7 kbp. Deletion of the E1 gene blocks most viral gene expression as well as DNA synthesis and therefore renders Ad replication defective. E3 proteins are involved in evading the host antiviral immune response. By using a replication-defective Ad vector, cells can be infected without grossly perturbing normal functions, thus allowing analysis of the functional properties of the recombinant protein.

In the case of deletion of the essential E1 gene, viral propagation is conditional because the function of the E1 gene must be provided in *trans*. This is achieved by growing E1-deleted recombinant virus in the HEK 293 cell line, which was originally transformed with Ad5 and contains the left 14% of the adenovirus genome integrated into cellular DNA, including the E1 region[14].

Although the recombinant virus cannot propagate in cells other than HEK 293 cells, if it attaches to the skin or the airway, it efficiently enters cells and expresses the target gene. Therefore, the use of security measures such as a safety hood to prevent inhalation or adhesion of the virus is strongly recommended.

6.2 PRINCIPLES OF GENERATION OF RECOMBINANT ADENOVIRUSES

The recombinant adenovirus cosmid was obtained using the *Adenovirus Expression Vector kit* (Takara, ref. 6170). It is based on the DNA-TPC (terminal protein complex) method[15]. Cosmid DNA is transfected into HEK 293 cells along with an adenovirus DNA-TPC complex that has been digested by a restriction enzyme that cuts the viral backbone many times. Fragmentation of the viral backbone reduces background due to the carryover of donor virus or to religation of its fragments.

[14] Graham FL, Smiley J, Russeell WC, Nairn R. Characteristics of a human cell line transformed by DNA from human adenovirus type 5. *J. Gen. Virol*. 36:59-72, 1977

[15] Miyake S, Makimura M, Kanegae Y, Harada S, Sato Y, Takamori K, Tokuda D, Saito I. Efficient generation of recombinant adenoviruses using adenovirus DNA-terminal protein complex and a cosmid bearing the full-length virus genome. *Proc. Natl. Acad. Sci. U.S.A*. 93:1320-1324, 1996

Homologous recombination between the cosmid and the terminal fragments of the donor viral DNA regenerates a full-length chromosome that has a molecule of TP covalently attached at each end. Therefore, the desired recombinant adenovirus can be obtained with high viral particles production efficiency.

To generate a recombinant adenovirus the subsequent steps are followed: cosmid construction, cotransfection in HEK 293 cells, recombinant viruses analysis, purification and titration. See fig. 3.

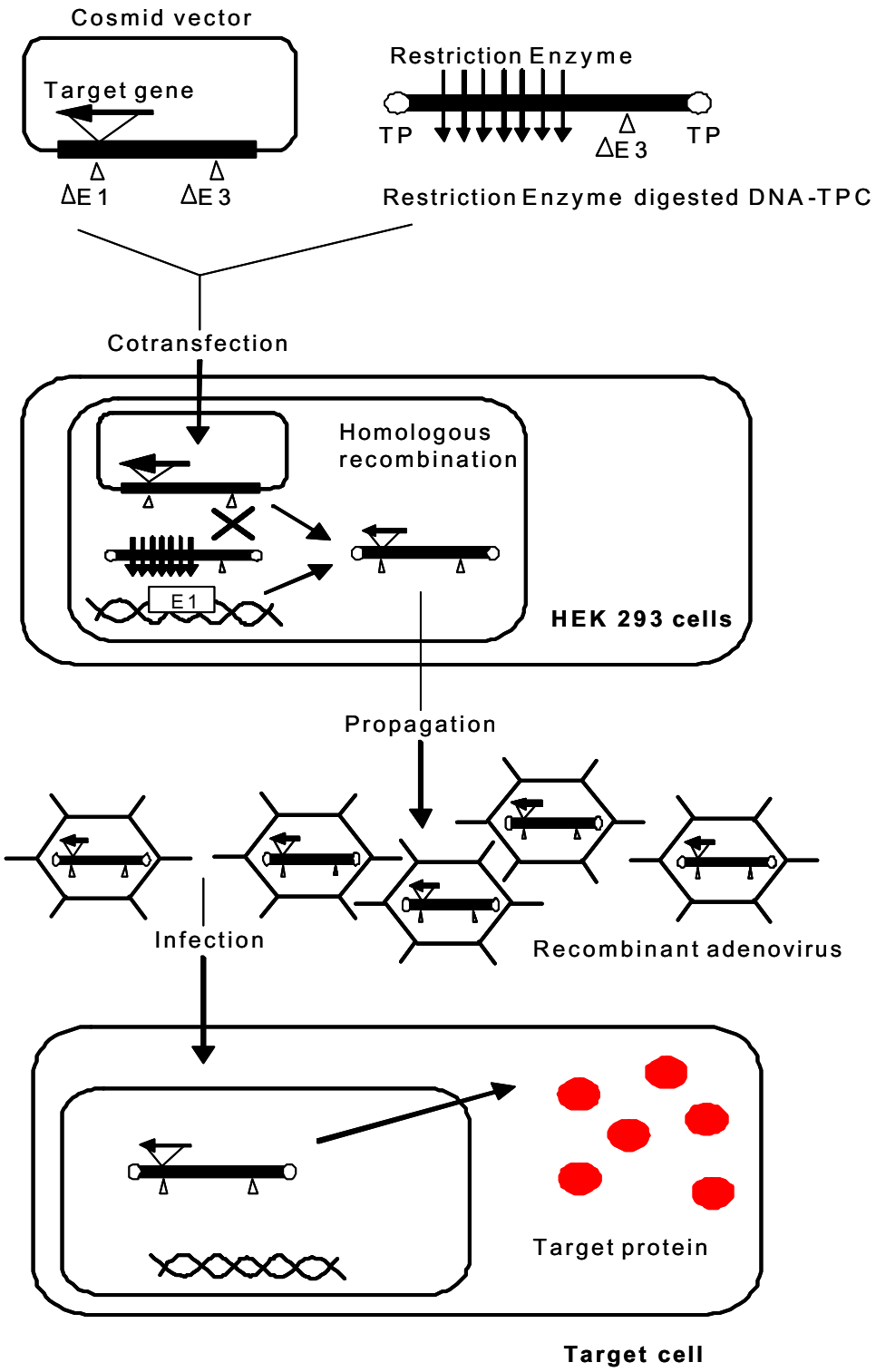

Fig. 3. Principles of generation and use of recombinant adenoviruses. In the first step the desired target DNA is inserted into the cosmid vector. Then, the recombinant cosmid and the DNA-TPC, which has been digested with a restriction endonuclease, are cotransfected into HEK 293 cells. Homologous recombination occurs in the cells, and recombinant adenoviruses are generated. Since HEK 293 cells express E1 gene, non-proliferative type recombinant adenoviruses can proliferate. Adenoviruses are used to infect target cells where the desired protein is expressed without adenovirus replication.

6.3 COSMID CONSTRUCTION

A) Cosmid digestion

The cosmid pAxCA wt (1.5 µg) is digested with *Swa*I at 25ºC for 3 h. The digestion is checked by resolving 1 µl of the digestion mixture in a 0.4% agarose gel. Then, the cosmid is dephosphorylated with CIP for 1 h at 37ºC. After CIP inactivation the cosmid is purified by phenol/chloroform extraction and precipitated with ethanol. The cosmid concentration is quantified by fluorescence in an agarose gel.

B) Plasmid digestion

The insert DNA fragment is prepared by digesting 10–20 µg of plasmid with the appropriate enzymes. The DNA is resolved in an agarose gel and the desired DNA fragment is purified. If the terminals are not blunt, they are made blunt-end using the *Pfu DNA polymerase* and the DNA fragment is purified by phenol/chloroform extraction and precipitated with ethanol. The concentration is quantified by fluorescence in an agarose gel.

C) Ligation

0.2 µg of insert DNA is added to the digested and dephosphorylated cosmid, they are co-precipitated with ethanol and ligated at 25ºC for 30 min. The ligation is checked by PCR.

D) Recombinant cosmid packaging and transformation

4 µl of the cosmid ligation mixture is packaged, transformed in XL1-Blue cells and plated in ampicillin/tetracycline plates as described in Section 1.9.2.

E) Recombinant cosmid analysis

The bacterial colonies obtained are analyzed by PCR-Preps and the positive colony containing the desired recombinant cosmid is amplified performing a maxipreparation. The presence and right orientation of the insert are checked by restriction enzyme digestions using *Cla*I and *Bgl*II and the presence of a mutation by sequencing.

6.4 COTRANSFECTION IN HEK 293 CELLS

The recombinant cosmid (8 µg) is cotransfected along with 1 µg of DNA-TPC by calcium phosphate (CellPhect, Amersham Pharmacia Biotech) in HEK 293 cells grown in a 25-cm^2 flask until 80% confluence. Cells are incubated o/n without removing the precipitate and on the morning of the next day the medium is changed. In the afternoon, cells are resuspended in 10 ml of 5% FCS-medium and undiluted cells or 1/10 and 1/100 dilutions are distributed in three 96-well plates with 100 µl per well. The desired recombinant adenovirus is generated by overlapping recombination.

After 5-6 days, as cells continue growing 50 µl of 10% FCS-medium is added to each well to avoid cells dying of starvation. Approximately 8-15 days after transfection it is possible to see that in some wells cells start to be more rounded, inflated and detached indicating that they contain the viruses. The content of these wells (viral clones) is placed in 1.5 ml tubes and is frozen in liquid N_2 and thawed in a water bath at 37ºC three times to liberate the adenoviruses which remain in the cells. Then, tubes are centrifuged at 5,000 rpm for 5 min and the supernatant is stored at -80ºC as the first seed.

6.5 RECOMBINANT ADENOVIRUS ANALYSIS

Co-transfection of the cosmid and the DNA-TPC could give recombinant adenoviruses carrying or not the desired DNA. Clones obtained after HEK 293 transfection are analyzed by Western blot performed in the target cells, i.e. INS(832/13) cells.

INS(832/13) cells are grown in 24-well plates until 90% confluence. Cells of one well are infected with 1-10 µl of each viral clone suspension (first seed) in 0.1 ml of medium. After 1 h viral suspension is removed, fresh medium is added and cells are further cultured for approx. 48h.

All the cells from one well are resuspended in 80 µl of 1X loading buffer and directly analyzed by Western blot probed with LCPTI-specific antibody. The viral clone that gives the highest protein expression is selected.

6.6 ADENOVIRUS PURIFICATION

Once the desired viral clone is selected it is amplified and purified. This purified adenovirus does not contain proteins or cellular membranes that are present in the HEK 293 cell-lysate and is therefore preferred for infection of INS(832/13) cells or rat islets.

A) Amplification

HEK 293 cells grown in a 24-well plate until 90% confluence are infected with 10 µl of the viral suspension of the first seed in 0.1 ml of 5% FCS-medium per well. After 1 h, 0.4 ml of 5% FCS-medium is added. When cells start to detach, approximately 3 days after infection, the culture medium containing the cells is collected and is frozen/thawed 3 times in liquid N_2 and a water bath at 37ºC. Cell debris are removed by centrifugation at 3,000 rpm for 10 min at 4ºC and the supernatant obtained will be the second seed.

To obtain the third seed, 15 µl of the second seed along with 0.5 ml of 5% FCS-medium is used to infect HEK 293 cells grown in a 25-cm^2 flask until 70% confluence. After 1 h, 4.5 ml of 5% FCS-medium are added and 3-4 days later, when cells have died, the medium containing the cells is collected. After 3 freeze-thaw cycles cell debris are removed as described above and the third seed obtained is stored at -80ºC in 1 ml aliquots.

To obtain the fourth seed, 50 µl of the third seed along with 2 ml of 5% FCS-medium is used to infect HEK 293 cells grown in a 75-cm^2 flask until 70% confluence. After 1 h, 13 ml of 5% FCS-medium are added and 3-4 days later, when cytopathic effects are complete, the medium containing the cells is collected. After 3 freeze-thaw cycles cell debris are removed and the fourth seed is stored at -80ºC in 1 ml aliquots. This suspension has a high titer of about 10^9 pfu/ml (plaque forming units of adenovirus per ml).

To obtain the final amplification, 400 µl of the fourth seed along with 9 ml of 5% FCS-medium per dish is used to infect HEK 293 cells grown in eight 150-cm dishes until 60% confluence. After 1 h, 6 ml of 5% FCS-medium is added to each dish and 3-4 days later, when cells just start to detach but are not completely died, the medium containing the cells is collected in 50 ml tubes. Cells are pelleted by centrifugation at 1,000 rpm for 10 min at r.t. After that, cells are resuspended in 6 ml of 10 mM Tris-HCl pH 8. To liberate the adenoviruses which are inside the cells, the suspension is

subjected to 3 freeze-thaw cycles and centrifuged at 3,000 rpm for 10 min at 4ºC. The supernatant containing the adenovirus is stored at -80ºC.

B) Purification

The adenovirus was purified by the CsCl method[16] which is extremely effective and gives a final adenovirus titer of about 10^9-10^{10} pfu/ml. Adenovirus can also be purified chromatographically with the *Adeno-X™ Virus Purification Kit* (Clontech, ref. K1654-1).

The CsCl purification is as follows:

The supernatant containing the adenovirus from the final amplification is poured onto 5 ml of a CsCl (density 1.43) solution in an ultraclear tube (Beckman, ref. 344059). Without mixing, the solution is ultracentrifuged at 25,000 rpm for 1 h at 4ºC in a Sw41Ti rotor using the mode 7 for acceleration and brake. After centrifugation a white adenovirus ring appears approximately in the middle of the tube. The virus layer (about 2.5 ml) is collected carefully using a syringe and mixed with 8 ml of CsCl (density 1.34) solution. The counterweight is also prepared with CsCl (density 1.34) solution. Tubes are ultracentrifuged at 30,000 rpm for 19-21 h (o/n) at 4ºC in a Sw41Ti rotor using the mode 7 for acceleration and brake. The white adenovirus ring of about 1-2 ml is collected using a syringe.

CsCl (density 1.43) solution: 8.3 g of CsCl powder (Applichem, ref. A1126) are dissolved in 12 ml of bd. autoclaved water. The solution is sterilized by filtering.

CsCl (density 1.34) solution: 7.6 g of CsCl powder are dissolved in 14.5 ml of bd. autoclaved water. The solution is sterilized by filtering.

C) Adenovirus concentration

The virus solution is loaded onto a Sephadex column (Pharmacia PD-10, ref. 17-0851-01) which has been previously equilibrated with 25 ml of adenovirus elution buffer. When the virus solution has completely entered the column, 3.5 ml of the adenovirus elution buffer is added on top of the column and the eluted solution is

[16] Graham FL, Prevec L. Manipulation of adenovirus vectors. In Methods in Molecular Biology, vol. 7: Gene transfer and expression protocols. Ed. Murray, EJ. (Human Press Inc., Clifton, NJ). 109-128, 1991

collected in 1.5 ml tubes in 8 drops fractions. The adenovirus peak is determined by measuring the absorbance at 260 nm using 1/50 dilutions of the fractions in water. During this time the adenovirus fractions are kept on ice. Those fractions in which absorbance at 260 nm is higher than 0.05-0.07 are combined. The adenovirus is stored in 0.1% BSA plus 10% glycerol at -80ºC in 10 µl one-use aliquots.

Adenovirus elution buffer: 137 mM NaCl, 5 mM KCl, 1 mM $MgCl_2$ and 10 mM Tris-HCl pH 7.4

6.7 ADENOVIRUS TITRATION

Quantification of adenoviral stocks, i.e. the determination of the viral plaque forming units (pfu) per ml, is important to ensure consistency between samples and to achieve the right level of transient expression. Careful titration was done using the *Adeno-X™ Rapid Titer kit* (Clontech, ref. K1653-1). This method takes advantage of production of viral hexon proteins for the quantification of viral stocks. Dilutions of the viral stock are used to infect HEK 293 cells. Just 48 h later, these cells are fixed and stained with the antibody specific to the adenovirus hexon protein. Signal is detected after a secondary antibody conjugated with horseradish peroxidase (HRP) amplifies the signal of the antihexon antibody. Subsequent exposure to metal-enhanced 3,3'-diaminobenzidine (DAB) peroxidase substrate turns only the infected cells dark brown. Then the titer of the stock can be determined by counting the number of brown cells in a given area. Each stained cell corresponds to a single infectious unit.

The titration procedure is as follows:

One milliliter of HEK 293 cells (5×10^5 cells/ml) is seeded in each well of a 12-well plate. Using medium as diluent, 10-fold serial dilutions from 10^{-2} to 10^{-7} of the viral stock are prepared and 100 µl of each one is added to each well. After 48 h of incubation, medium is aspirated and cells are allowed to dry in the hood for 5 min. Then, cells are fixed by adding very gently without dislodging the cell monolayer, 1 ml of ice-cold 100% methanol to each well. After keeping them at -20ºC for 10 min they are gently rinsed three times with 1 ml PBS + 1% BSA (Sigma, Fraction V, ref. A-3803). Cells are then incubated for 1 h at 37ºC with 0.5 ml/well of Anti-Hexon Antibody diluted 1/3,000 in PBS + 1% BSA. Next, cells are gently rinsed three times with 1 ml PBS + 1% BSA and incubated for 1 h at 37ºC with 0.5 ml/well of Rat Anti-

Mouse Antibody (HRP conjugate) diluted 1/500 in PBS + 1% BSA. The rinsing steps are repeated as before and then cells are finally incubated at r.t. for 10 min with 500 µl/well of the DAB substrate.

To calculate the titer of the viral stock the DAB substrate is aspirated, 1 ml PBS is added to each well and at least three fields of brown/black positive cells are counted on a microscope with a 20X objective. The pfu/ml is calculated from the resulting average number of positive cells/unit dilution as follows:

Adenovirus titer (pfu/ml) = [(infected cells/field) x 573] : [0.1 x dilution factor]

Where 573 is the number of fields/well in a 20X objective and 0.1 is the volume of viral dilution used in ml.

6.8 ADENOVIRUS INFECTION

70-80% confluent cells are infected with adenovirus over a 90 min incubation with medium plus adenovirus. Then, medium is aspirated and cells are cultured in fresh medium for 24 h to allow the transgenes to be expressed before initiating metabolic studies or measurements of insulin secretion. At these incubation times no toxicity effect of the adenoviruses was seen.

For INS(832/13) cells the protocol of infection is as follows:

INS(832/13) cells are homogeneously seeded in 12-well plates (0.5 x 10^6 cells/well), 25-cm^2 flasks (2 x 10^6 cells), 10-cm dishes (7 x 10^6 cells) or 15-cm dishes (10 x 10^6 cells) depending on the experiment and further cultured for 48 h before infection. On the day of the infection, cells of one well or one dish are detached and counted to calculate the required amount of virus. Cells are infected with 4.1 pfu/cell of Ad-LacZ (which expresses bacterial β-galactosidase), 1.7 pfu/cell of Ad-LCPTI wt or 4.1 pfu/cell of Ad-LCPTI M953S. The required amount of each adenovirus is mixed with complete medium in 15 ml tubes. Infection is done in approx. ¼ volume of the total volume of the well or dish, i.e. in 500 µl of medium for 12-well plates or in 5 ml of medium for 15-cm dishes. Therefore, proximity of the virus to the cells is enhanced. Cells are incubated with the different adenoviruses at 37ºC for 90 min. After this time,

medium is aspirated and cells are cultured in fresh medium for further 24 h before the experiment.

7. PROTEIN ANALYSIS

7.1 BRADFORD PROTEIN QUANTIFICATION

The protein determination method introduced by Bradford[17] is based on the fact that some colorants, when adsorbing onto protein molecules, change their absorption spectrum. The Bradford reagent contains copper in an acid medium of orthophosphoric acid and methanol. When the protein binds to copper its absorption maximum shifts in an acidic solution from 465 to 595 nm. This method, which has little interference, has large sensitivity and linearity.

Protein is measured according to the manufacturer's instructions (BioRad protein assay), using BSA as a protein standard in the range of 2-20 µg/ml. Bradford reagent is diluted 1/5 in water and stored at 4ºC for about 2 months. BSA standard stock is prepared in water at 1 µg/µl and the absorbance of the blank, standard curve or the samples is measured at 595 nm in a spectrophotometer with plastic cuvettes in a total volume of 1 ml.

Sample	Volume	Bradford reagent
blank	-	1000 µl
BSA 2 µg	2 µl	998 µl
BSA 5 µg	5 µl	995 µl
BSA 10 µg	10 µl	990 µl
BSA 15 µg	15 µl	985 µl
BSA 20 µg	20 µl	980 µl
Problem	2-10 µl	up to 1000 µl

7.2 WESTERN BLOT

The Western Blot technique detects, with a specific antibody, a protein between a sample of proteins that have been separated by electrophoresis and transferred to a

[17] Bradford MM. A rapid and sensitive method for the quantification of microgram quantities of protein utilizing the principle of protein-dye binding. *Anal. Biochem*. 72:248-254, 1976

nitrocellulose membrane. Western blot was applied for the analysis of LCPTI, SREBP-1 and PKC proteins. The procedure has the following steps: electrophoresis, transference, antibody incubation (Western Blot) and detection.

A) Electrophoresis

Electrophoresis in polyacrylamide-SDS gels (SDS-PAGE) is the most widely used technique for resolving proteins denatured with SDS. Proteins and protein subunits are separated by its molecular weight when they are migrating through the gel towards the anode.

Sample preparation: For LCPTI or naSREBP-1c proteins, cells are directly detached from one well of a 12-well plate, which contains approx. 50 µg of protein, by resuspending them in 80-100 µl of 1X loading buffer. This loading buffer contains the denaturalizing agent SDS and β-mercaptoethanol that reduces disulfide bonds. For PKC protein, cytosol or membrane fractions were diluted in 4X loading buffer. Samples are sonicated and dissolved by heating to 95ºC for 5 min. Then, they are briefly centrifuged and placed on ice before loading on-to the gel. Samples could be stored in loading buffer at -20ºC for 4-6 months. However, after 10 or more freeze-thaw cycles the proteins will begin to degrade and fail to give sharp bands.

Gel preparation: For LCPTI and PKC proteins, an 8% separating gel is prepared (9% for naSREBP-1c protein). Separating gel is prepared by adding the polymerizing agent TEMED at the end and it is immediately cast between the two ethanol cleaned glasses of the electrophoresis apparatus. Some drops of isopropanol are added on the top to achieve a straight edge of the gel. Once the gel is polymerized isopropanol is removed. Then, stacking gel is prepared and cast and a 1.5 mm comb is adjusted between the two glasses. Both the separating and stacking gel take approximately 30 min to polymerize. Bubbles must be avoided during all the process.

Electrophoresis performance: To run the electrophoresis, the 1.5 mm comb is removed and electrophoresis buffer is added on to the electrophoresis chamber and on to the sample loading wells. Samples and protein marker (Invitrogen, ref. LC5925) are loaded on to the gel and electrophoresis is performed at a constant current of 25 mA for 1 h approximately. Electrophoresis is stopped when bromophenol blue is just off the bottom of the gel.

1X Loading Buffer: 62.5 mM Tris-HCl pH 6.8, 4% SDS, 5% β-mercaptoethanol, 10% glycerol and 10% bromophenol blue. It is stored at -20ºC in 1 ml aliquots for 4-6 months. For 25 ml:

1X Loading Buffer	
1.25 M Tris-HCl pH 6.8	1.25 ml
SDS	0.5 g
β-mercaptoethanol	1.25 ml
glycerol (87%)	2.9 ml
bromophenol blue	2.5 mg
H_2O up to	25 ml

SDS-PAGE recipes for one 1.5 mm gel:

Separating gel	**8%**	**9%**
bd.H_2O	4.4 ml	4.2 ml
40% Acrylamide	1.5 ml	1.7 ml
1.875 M Tris-HCl pH 8.8	1.5 ml	1.5 ml
10% SDS	75 µl	75 µl
10% ammonium persulphate	25 µl	25 µl
TEMED	3.75 µl	3.75 µl
Total volume for one 1.5 mm gel =	7.5 ml	7.5 ml

Stacking gel	
bd.H_2O	1.8 ml
40% Acrylamide	0.4 ml
1.25 M Tris-HCl pH 6.8	250 µl
10% SDS	25 µl
10% ammonium persulphate	8.5 µl
TEMED	2.5 µl
Total volume for one 1.5 mm gel =	2.5 ml

Acrylamide is a potent cumulative neurotoxin. Contact with the skin and inhalation must be avoided. 10% Ammonium persulphate is prepared by dissolving 0.5 g of ammonium persulfate in 5 ml of bd. H_2O and it is stored at -20ºC.

Electrophoresis buffer: 25 mM Tris, 192 mM glycine and 0.1% SDS. It is stored at r.t. For 1 L:

Electrophoresis buffer	
Tris	3.03 g
Glycine	14.42 g
SDS	1 g
H_2O up to	1 L

B) Transference

Once electrophoresis is finished, stacking gel is removed and proteins in the separating gel are transferred to a nitrocellulose membrane for its later antibody incubation. The transference sandwich contains, in the following order from the negative to the positive pole: a sponge, 3 Whatman papers, the gel, the nitrocellulose membrane, 3 Whatman papers and another sponge. All must be submersed in transfer buffer avoiding bubbles. Whatman papers and the nitrocellulose membrane must have the same size as the gel. The side of the membrane in contact with the gel is marked to identify the side where proteins are, for later antibody incubation and detection. The transference is performed at 4ºC for 1 h at 250 mA or for 2 h at 125 mA. Once it is finished, membrane is washed in water and effectiveness of the transference is checked by Ponceau S solution (Sigma-Aldrich, ref. P-7170) staining of the protein bands. To remove the red staining, membrane is washed in PBS-Tween for a few minutes.

Transfer buffer: 20 mM Tris, 20% methanol and 150 mM glycine. It is stored at 4ºC.

Transfer buffer	
Tris	2.42 g
Glycine	12 g
Methanol	200 ml
H_2O up to	1 L

PBS-Tween: Tween 0.1% in 1X PBS. 1 ml of Tween-20 is diluted in 1000 ml of PBS. It is stored at r.t.

C) Antibody incubation

For the immunoblotting, we used the Enhanced ChemiFluorescence (ECF) Western Blotting kit (Amersham Biosciences, ref. RPN 5781-anti-mouse and RPN 5783-anti-rabbit), which allows the use of a Storm 840 Laser scanning system (Molecular dynamics, Amersham Pharmacia Biotech) to quantify by fluorescence the intensity of the bands. This immunodetection permits the use of either anti-mouse (for PKC) or anti-rabbit (for LCPTI) alkaline phosphatase-linked immunoglobulin, followed by addition of ECF substrate. The alkaline phosphatase catalyses the conversion of ECF substrate to a highly fluorescent product which fluoresces strongly at 540-560 nm.

According to the manufacturer's instructions the protocol is as follows:

Blocking the membrane: Non-specific binding sites are blocked by immersing the membrane in blocking solution for 1 h on an orbital shaker at r.t. After this time, membrane is rinsed and washed once for 15 min and twice for 5 min in PBS-Tween on an orbital shaker.

First antibody incubation: First antibodies used were the rabbit LCPTI-specific polyclonal antibody against amino acids 317-430 of the rat liver CPTI[18], the mouse anti-PKC monoclonal antibody specific for the conventional PKC isoforms present in the pancreatic β-cell: α, β and γ (MC5, Santa Cruz Biotechnology, Santa Cruz, CA) and the antibody against the N terminus of SREBP-1 (Santa Cruz Biotechnology). First antibody is diluted (1/6,000 for LCPTI Ab., 1/100 for PKC Ab. or 1/1,000 for SREBP

[18] Prip-Buus C, Cohen I, Kohl C, Esser V, McGarry JD, Girard J. Topological and functional analysis of the rat liver carnitine palmitoyltransferase 1 expressed in Saccharomyces cerevisiae. *FEBS Lett.* 429(2):173-178, 1998

Ab.) in blocking solution. Incubation is done over 1 h at r.t. or o/n at 4ºC on an orbital shaker. After this time, membrane is rinsed and washed once for 15 min and twice for 5 min in PBS-Tween on an orbital shaker. The first antibody could be reused by storing it at -20ºC.

Second antibody incubation: The second antibody (anti-rabbit for LCPTI or anti-mouse for PKC) is diluted 1/10,000 in PBS-Tween. Incubation is done over 1 h at r.t. on an orbital shaker. After this time, membrane is rinsed and washed once for 15 min and twice for 5 min in PBS-Tween on an orbital shaker.

Blocking solution: 5% (w/v) skimmed milk in PBS-Tween.

Blocking solution	
skimmed milk	2.5 g
PBS-Tween	50 ml
pH is adjusted to 7.4 with KOH	

D) Detection

The membrane is incubated for 20 min with the ECF substrate. The volume of ECF should be enough to cover the membrane surface. After this time, the membrane is drained and placed directly on to the sample holder of the fluorescence scanning instrument and intensity of the bands is quantified.

7.3. IMMUNOFLUORESCENCE

The immunofluorescence technique permits the localization of a protein inside the cell using a confocal fluorescent microscope. Cells have to be fixed, permeabilized and incubated with a specific antibody. Immunofluorescence staining was performed for the subcellular detection of naSREBP-1c protein in naSREBP-1c stable cells.

The protocol for the immunofluorescence technique is as follows:

A) Preparing the cells

On the hood, one flamed glass coverslip is located in each well of a 6-well plate. 1 ml of polyornithine solution is added to the wells to facilitate the later attachment of the cells onto the coverslip. After 30 min, polyornithine solution is removed and

coverslips are washed twice with PBS. 0.2 x 10^6 cells are seeded in each well and grown in 2 ml of medium for 48 h. If desired, cells are treated during this period.

B) Fixing the cells

A piece of parafilm is placed onto the base of a 15-cm dish and the coverslips with the cells are located onto the parafilm. Cells must never become dry. Cells are washed in 500 µl of PBS and 100 µl of 4% (w/v) paraformaldehyde in PBS is added to each coverslip to fix the cells for 10 min at r.t. Then, cells are washed twice with PBS.

C) Permeabilizing the cells

Cells are permeabilized for 10 min with 100 µl of 0.1% (v/v) Triton X-100 in PBS containing 1% BSA. Then, cells are washed in PBS.

D) Blocking and first antibody incubation

Cells are blocked for 1 h with 100 µl of 1% BSA-PBS, washed in PBS and incubated o/n with 100 µl of the first antibody diluted in 1% BSA-PBS (1/100 dilution in the case of SREBP-1 antibody).

E) Second antibody incubation

Cells are washed five times with PBS, incubated for 1 h with 100 µl of the second fluorescent antibody diluted in 1% BSA-PBS and washed again 4 times with PBS. Coverslips are maintained isolated from the light to avoid loss of fluorescence.

F) Immunofluorescence detection

One drop of mounting medium for fluorescence (Vectashield, ref. H-100, Vector) is placed onto a glass microscope slide. Coverslips are drained with a Whatman paper, without touching the cells, and located onto the microscope slide with the cells facing the drop of mounting medium. Cells are dried at r.t. and stored at 4ºC until visualizing them on the confocal fluorescent microscope.

Polyornithine solution: Polyornithine (Sigma-Aldrich, ref. P-3655) is used to increase the attachment of the cells to the surface. Polyornithine has positive charge, therefore cells that have negative charge attach to it. To prepare the polyornithine solution, 1 g of

polyornithine is dissolved in 100 ml of bd. A.C. water. Then it is filtered through a 0.22 µm filter, aliquoted and stored at 4ºC.

8. CPTI ACTIVITY ASSAY

CPTI activity assays were performed with mitochondrion-enriched fractions from cell culture or mitochondria extracted from mice tissues. Fresh mitochondria are used for the CPTI activity assay or stored at -80ºC.

8.1 ISOLATION OF MITOCHONDRIA

8.1.1 Mitochondria from cell culture

To obtain the mitochondrion-enriched fractions, cells are washed in PBS and resuspended in 2 ml of the same solution. All the process is performed at 4ºC. Cells are centrifuged for 5 min at 1,200 x *g* and after resuspension in 1 ml of homogenization buffer A, they are broken with a glass homogenizer fitted with a loose and a tight pestle. 20 cycles are done with each one. Further centrifugation is performed for 3 min at 2,000 x *g* to remove cell nucleus and membranes. Supernatant is centrifuged at 16,000 x *g* for 30 min and mitochondria are resuspended in 25 µl of homogenization buffer A. The concentration of the mitochondria obtained, quantified by the Bradford assay, is approx. 3-5 µg/µl and 8-10 µg is used for the CPTI activity assay.

8.1.2 Mitochondria from mouse liver and pancreas

The tissue of interest is homogenized in an isotonic cold sucrose solution and mitochondria are separated from the other cellular components by centrifugation. All the process is performed at 4ºC.

To obtain mitochondrion-enriched fractions from liver[19], mice liver weighing approx. 1 g is mechanically homogenized in 1/10 (w/v) buffer B, using a Potter-Elvehjem homogenizer (600 rpm; 6 strokes). Liver suspension is centrifuged for 15 min at 560 x *g* and the supernatant is centrifuged again for 20 min at 12,000 x *g*. Pellet is resuspended in 2 ml of homogenization buffer B, centrifuged for 10 min at 7,000 x *g*, washed and finally resuspended in 1 ml of homogenization buffer B. The concentration

[19] Saggerson ED, Carpenter CA. Carnitine palmitoyltransferase in liver and five extrahepatic tissues in the rat. Inhibition by DL-2-bromopalmitoyl-CoA and effect of hypothyroidism. *Biochem. J.* 236:137-141, 1986

of the mitochondria obtained, quantified by the Bradford assay, is approx. 4-10 µg/µl and 20 µg is used for the CPTI activity assay.

To obtain mitochondrion-enriched fractions from pancreas[20], mice pancreas is mechanically homogenized (1,000 rpm; 10 strokes) in 1 ml of homogenization buffer C. Solution is centrifuged at 900 x *g* for 10 min to remove cell nucleus, membranes and unbroken cells. Supernatant is centrifuged at 5,500 x *g* for 10 min and pellet is resuspended with a Dounce homogenizer. The homogenate is centrifuged at 2,000 x *g* for 2 min and the supernatant is further centrifuged at 4,000 x *g* for 8 min. Pellet is resuspended in 250 µl of homogenization buffer A and 20 µg of mitochondria is used for the CPTI activity assay.

Homogenization buffer A: It is stored at r.t.

KCl	150 mM
Tris-HCl pH 7.2	5 mM

Homogenization buffer B: It is stored at 4ºC.

Sucrose	250 mM
EDTA	1 mM
Tris-HCl pH 7.4	10 mM

Homogenization buffer C: It is stored at 4ºC and proteases inhibitors are added on the day of the experiment.

Tris-HCl pH 7.4	20 mM
EDTA	0.5 mM
EGTA	0.5 mM
Sucrose	250 mM
DTT	1 mM
Leupeptin	10 µg/ml
Aprotinin	4 µg/ml
Pepsatin	2 µg/ml
PMSF	100 µM

[20] Li G, Kowluru A, Metz A. Characterization of phenylcysteine methyltransferase in insulin-secreting cells. *Biochem. J.* 316:345-351, 1996

8.2 CPTI ACTIVITY ASSAY

CPTI activity is determined by the radiometric method as previously described[21] with minor modifications. CPTI was assayed with the mitochondrion-enriched fractions obtained as described above where the mitochondria remain largely intact. When mitochondria are frozen, membranes could be broken, allowing CPTII to contribute to the measured activity. To avoid CPTII interferences freshly obtained mitochondria were used for each experiment.

The substrates for the CPTI activity assay are L-[*methyl*-^{3}H]carnitine hydrochloride (Amersham Biosciences, ref. TRK762) and palmitoyl-CoA and the reaction is done in the following direction:

$$^3\text{H-carnitine} + \text{palmitoyl-CoA} \longrightarrow \text{palmitoyl-}^3\text{H-carnitine} + \text{CoA-SH}$$

The procedure takes advantage of the fact that the product of the reaction, palmitoyl-^{3}H-carnitine, is soluble in an organic medium. Therefore, it could be separated by extraction from the radioactive substrate, ^{3}H-carnitine, that has not been reacted and which will remain in the aqueous phase.

The final concentration of the components in the reaction are:

CPTI reaction mix	
Tris-HCl pH 7.2	105 mM
KCN	2 mM
KCl	15 mM
$MgCl_2$	4 mM
ATP	4 mM
GSH	250 µM
Palmitoyl-CoA	50 µM
L-[*methyl*-^{3}H]carnitine (0.3 µCi)	400 µM
defatted BSA	0.1 %

[21] Morillas M, Clotet J, Rubi B, Serra D, Asins G, Ariño J, Hegardt FG. Identification of the two histidine residues responsible for the inhibition by malonyl-CoA in peroxisomal carnitine octanoyltransferase from rat liver. *FEBS Lett*. 466(1):183-186, 2000

Deacylases convert the substrate acyl-CoA in acyl plus CoA-SH, generating ATP. This process will reduce the availability of the substrate palmitoyl-CoA in the reaction. Therefore, ATP is added to the reaction mix to minimize this process, by inverting the equilibrium of the deacylase reaction and by stimulating the reaction of the acyl-CoA synthetases and thus regenerating the substrate palmitoyl-CoA. KCN is added to avoid mitochondrial oxidation. Glutathione (GSH, reduced form) is used as a reduction agent instead of dithiothreitol (DTT) or dithioeritrol (DTE) because DTT and DTE have been shown to reduce malonyl-CoA sensitivity[22]. Defatted BSA is added to protect mitochondria from the detergent effect of fatty acids. However, BSA concentration must not be higher than 0.1% because this could give a sigmoidal effect in the enzyme *v.s.* acyl-CoA kinetic[18]. Finally, KCl is added because it increases enzyme activity[23].

Since activity and sensitivity to malonyl-CoA depend on pH[24,25], we chose pH 7.2, the optimum for both conditions. The temperature for the assay is 30ºC to compensate a good enzymatic activity, which increases with the temperature, with a convenient inhibition, which decreases with the temperature[26].

The procedure for the CPTI activity assay is as follows:

The reaction mix is prepared in a 15 ml tube kept on ice. GSH is prepared by dissolving it in water on the day of the experiment. Samples are done in duplicate. The following amounts are per point:

[22] Saggerson ED, Carpenter CA. Malonyl-CoA inhibition of carnitine acyltransferase activities: effects of thiol-group reagents. *FEBS Lett.* 137:124-128, 1982

[23] Saggerson ED. Carnitine acyltransferase activities in rat liver and heart measured with palmitoyl-CoA and octanoyl-CoA. Latency, effects of K^+, bivalent metal ions and malonyl-CoA. *Biochem. J.* 202:397-405, 1982

[24] Mills SE, Foster DW, McGarry JD. Effects of pH on the interaction of substrates and malonyl-CoA with mitochondrial carnitine palmitoyltransferase I. *Biochem. J.* 219:601-608, 1984

[25] Bieber LL, Wagner M. Effect of pH and acyl-CoA chain length on the conversion of heart mitochondrial CPTI/CPTIo to a high affinity, malonyl-CoA-inhibited state. *Biochim. Biophys. Acta* 1290:261-266, 1996

[26] Kashfi K, Cook GA. Temperature effects on malonyl-CoA inhibition of carnitine palmitoyltransferase I. *Biochim. Biophys. Acta* 1257:133-139, 1995

CPTI reaction mix/point	
bd. water	92.33 µl
4X CPTI buffer	40 µl
1 mM palmitoyl-CoA	10 µl
80 mM ATP	10 µl
30% BSA	0.67 µl
25 mM GSH	2 µl
16 mM ^{3}H-carnitine	5 µl
Total volume	160 µl

Protein samples are prepared on ice in 1.5 ml tubes by diluting the protein in 4X CPTI buffer and by adjusting the volume with bd. water up to 40 µl. The blank will contain bd. water instead of protein.

Protein samples	
Protein	8-20 µg
4X CPTI buffer	10 µl
bd. water up to	40 µl

One by one, 160 µl of the reaction mix is added to each protein sample. Samples are vortex-mixed and placed on a water bath at 30ºC for exactly 5 min. Reaction is stopped with the addition of 200 µl of 1.2 M HCl. Samples are vortex-mixed and placed on ice. Extractions of the product of the reaction, palmitoyl-^{3}H-carnitine, are done by adding 600 µl of water-saturated butanol. Samples are vortex-mixed and centrifuged for 2 min at 13,000 rpm in a microcentrifuge. 400 µl of the upper phase is added to another 1.5 ml tube with 200 µl of bd. water. Samples are vortex-mixed and centrifuged for 2 min at 13,000 rpm. 250 µl of the upper phase is counted in plastic scintillation vials with 5 ml of scintillation liquid (Ecolite, ICN). ^{3}H radioactivity is counted in a RackBeta apparatus.

Specific activity of the enzyme is calculated as follows:

S.A.(nmol.mg^{-1} prot.min^{-1})= (cpm x 600 µl) / (S.R. x mg prot. x min x 250 µl)

Where cpm are the counts per minute and S.R. is the ^{3}H-carnitine specific radioactivity (approx. 3000 cpm/nmol).

4X CPTI buffer: Stored at 4ºC.

Tris-HCl pH 7.2	420 mM
KCN	8 mM
KCl	60 mM
MgCl	16 mM

16 mM ^{3}H-carnitine: 6.6 mg of cold carnitine is dissolved in 982.3 µl of 95% ethanol plus 982.3 µl of bd. water and 125 µl of L-[*methyl*-^{3}H]carnitine hydrochloride (80 Ci/mmol) is added. Aliquots of 125 µl are stored at -80ºC.

8.3 MALONYL-CoA INHIBITION ASSAY

For malonyl-CoA inhibition assays, the different amounts of malonyl-CoA are added to the protein samples adjusting the final volume up to 40 µl. The stock of 2 mM malonyl-CoA used is prepared in 1 mM sodium acetate pH 5.9 and stored at -20ºC. Samples are vortex-mixed and preincubated for 1 min at 30ºC prior to the addition of the reaction mix. It has been described[27] that this preincubation increases the inhibition level. CPTI activity assay is performed as described above.

8.4 ETOMOXIRYL-CoA INHIBITION ASSAY

Etomoxir (R-(+)-sodium 2-[6-(4-chlorophenoxy)hexyl]oxirane-2-carboxylate) is an irreversible inhibitor of CPTI which is only active when it is activated to the etomoxiryl-CoA form. Etomoxir was kindly provided by Dr. H. P. O. Wolf (Allensbach, Germany).

[27] Zammit VA. Time-dependence of inhibition of carnitine palmitoyltransferase I by malonyl-CoA in mitochondria isolated from livers of fed or starved rats. Evidence for transition of the enzyme between states of low and high affinity for malonyl-CoA. *Biochem. J.* 218:379-386, 1984

The effect of etomoxir on CPTI activity was seen in culture cells and in mitochondrion-enriched cell fractions. For culture cells, etomoxir is directly added to the medium for a 30 min or a 1 h preincubation as described above. In this case the cellular machinery converts etomoxir in its CoA derivative. After this, mitochondrion-enriched cell fractions are obtained and CPTI activity assay is performed as described above. For etomoxir *in vitro* assays, mitochondrion-enriched cell fractions are preincubated for 1 min at 30ºC with etomoxiryl-CoA as described for malonyl-CoA inhibition assay. In this case the inhibitor has to be added to the protein sample already activated to etomoxiryl-CoA. Then, protein samples are vortex-mixed and CPTI activity assay is performed as described above.

Activation of etomoxir to etomoxiryl-CoA by *Pseudomonas* sp. Acyl-CoA synthetase.

The activation of etomoxir is done by a simple enzymatic method[28] which uses the *Pseudomonas* sp. Acyl-CoA synthetase (EC 6.2.1.3).

The reaction is performed with 1 µmol of etomoxir in a total volume of 1 ml of an activation buffer containing:

Activation buffer	
Triton X-100	0.1% (w/v)
CoA-SH	5 mM
ATP	10 mM
DTT	1 mM
$MgCl_2$	10 mM
MOPS-NaOH pH 7.5	100 mM

The mix is sonicated for 5 min to permit etomoxir emulsion and 0.25 U of the acyl-CoA synthetase is added. The reaction is carried out at 35ºC for 2 h and stock aliquots are stored at –80ºC. It is assumed that all the etomoxir has been converted to etomoxiryl-CoA and thus its final concentration in the solution is 1 mM.

[28] Taylor DC, Weber N, Hogge LR, Underhill EW. A simple enzymatic method for the preparation of radiolabelled erucoyl-CoA and other long-chain fatty acyl-CoAs and their characterization by mass spectrometry. *Anal. Biochem*. 184:311-316, 1990

8.5 CPTI ACTIVITY ASSAY IN THE PRESENCE OF C75

The effect of C75 on CPTI activity was seen in mitochondrion-enriched fractions from cells and mouse tissues.

It has been described[29] that C75 has to be previously activated to C75-CoA to interact with CPTI activity. Thus, as in the case of etomoxir, when CPTI activity is studied with mitochondrion-enriched cell fractions, C75-CoA is added to the protein sample and preincubated for 1 min at 30ºC prior to CPTI activity assay. Activation to C75-CoA by the acyl-CoA synthetase is done as described above for etomoxiryl-CoA.

For cells in culture, which are previously incubated with C75, and mice, which are previously ip injected with C75, mitochondrion-enriched fractions are obtained and CPTI activity assay is performed as described above.

9. PKC TRANSLOCATION ASSAY

Protein kinase C (PKC) is a family of enzymes, the conventional isoforms α, β and γ of which are expressed in the pancreatic β-cell. These PKC isoforms require phosphatidylserine (PS), diacylglycerol (DAG) and Ca^{2+} for optimal activity. When PKC is activated by glucose, DAG or fatty acids, the protein is translocated from the cytosol to the cell membrane. Thus, to measure PKC translocation, cytosol and membrane fractions from INS(832/13) cells were obtained and analyzed by Western blot with a specific PKC antibody.

To measure the PKC translocation we followed the protocol described by Alcázar *et al*.[30] with minor modifications. INS(832/13) cells are grown in 10-cm dishes and infected with the different adenoviruses as described above. After a basal preincubation as described in BASAL TREATMENTS (Section 3.5.1), cells are incubated for 30 min at 37ºC with KRBH 0.1% BSA plus 2.5 or 15 mM glucose. After that, cells are washed in cold PBS, scraped into 1 ml of PBS and centrifuged at 2,000 rpm for 5 min at 4ºC in a microcentrifuge. Then, cells are sonicated in 100 µl of PKC buffer and the homogenate is centrifuged at 100,000 x *g* at 4ºC for 1 h. The supernatant (cytosolic

[29] Bentebibel A, Sebastián D, Herrero L, Serra D, Asins G, Hegardt FG. C75-CoA inhibits Carnitine Palmitoyltransferase I activity thus decreasing palmitate oxidation. Submitted.

[30] Alcázar O, Qiu-yue Z, Giné E, Tamarit-Rodriguez J. Stimulation of islet protein kinase C translocation by palmitate requires metabolism of the fatty acid. *Diabetes* 46(7):1153-1158, 1997

fraction) is separated, and the precipitate (membrane fraction) is resuspended with mild sonication in 100 µl of the same PKC buffer but supplemented with 0.1% (v/v) Triton X-100. Both fractions are incubated on ice for 45 min and Western blot is performed using a specific antibody against the PKC isoforms expressed in pancreatic β-cells (α, β and γ) as described in Section 7.2.

PKC buffer: 20 mM Tris-HCl pH 7.5, 250 mM sucrose, 2 mM EDTA, 5 mM EGTA, 10 mM β-mercaptoethanol, 1 mM PMSF and 10 µg/ml leupeptin. β-mercaptoethanol, PMSF and leupeptin are added on the day of the experiment. PKC buffer is stored at 4ºC. For 50 ml of PKC buffer it is needed:

PKC buffer	
1 M Tris-HCl pH 7.5	1 ml
1 M sucrose	12.5 ml
0.5 M EDTA	200 µl
EGTA	95.1 mg
β-mercaptoethanol	35 µl
100 mM PMSF	500 µl
leupeptin	50 µl
bd. water up to	50 ml

10. CELLULAR METABOLISM DETERMINATION

10.1 PALMITATE OXIDATION

Palmitate oxidation assay is done with attached cells and allows studying the capacity of the cells to oxidize palmitate. Cells are incubated with [1-^{14}C]palmitate and the $^{14}CO_2$ released and the acid-soluble products (ASP; essentially ketone bodies[31]) are measured. Total palmitate oxidation will be the sum of both. Palmitate oxidation has been done by two different methods: 12-well plates or 25 cm^2 flasks. Both are explained here.

[31] Fulgencio JP, Kohl C, Girard J, Pegorier JP. Troglitazone inhibits fatty acid oxidation and esterification, and gluconeogenesis in isolated hepatocytes from starved rats. *Diabetes*. 45:1556-1562, 1996

A) Palmitate oxidation assay in 12-well plates

This method was originally described by Collins *et al.*[32] and enables the use of cells in adherent culture and easy analysis of multiple samples. It is an improvement over previous methods that used detached cells and where oxidation was found to be reduced by 30-82%.

The procedure is as follows:

Cells seeded in 12-well plates are infected with the different adenoviruses or treated with C75 or etomoxir as described above. The day of the palmitate oxidation assay cells must be approx. 90% confluents. Before starting the experiment, cells are washed in KRBH 0.1% (w/v) defatted BSA, preincubated at 37ºC for 30 min with 500 µl of KRBH 1% BSA with or without 200 µM etomoxir and washed again with KRBH 0.1% BSA as described in BASAL TREATMENTS (Section 3.5.1). Then, 500 µl of the palmitate oxidation mix, prepared on the day of the experiment, is added to each well. Palmitate oxidation mix contains fresh KRBH with 2.5, 7.5 or 15 mM glucose in the presence of 0.8 mM carnitine plus 0.25 mM palmitate and 1 µCi/ml [1-^{14}C]palmitate bound to 1% (w/v) BSA. Blanks are wells without cells.

Palmitate oxidation mix (500 µl)	
KRBH	400 µl
2.5 mM [1-^{14}C]palmitate	50 µl
25, 75 or 150 mM glucose + 8 mM carnitine	50 µl

The system is closed as described in fig. 4. One rubber sheet the size of the 12-well plate, with a 6-mm hole centered over the site of each well, is placed over the culture plate. Then, a Whatman paper of the same size and soaked in 0.1 N KOH is placed over the rubber sheet. Finally, another rubber sheet without holes is placed on

[32] Collins CL, Bode BP, Souba WW, Abcouwer SF. Multiwell $^{14}CO_2$-capture assay for evaluation of substrate oxidation rates of cells in culture. *BioTechniques* 24:803-808, 1998

the top and the system is closed with the cover of the culture plate and wrapped in parafilm.

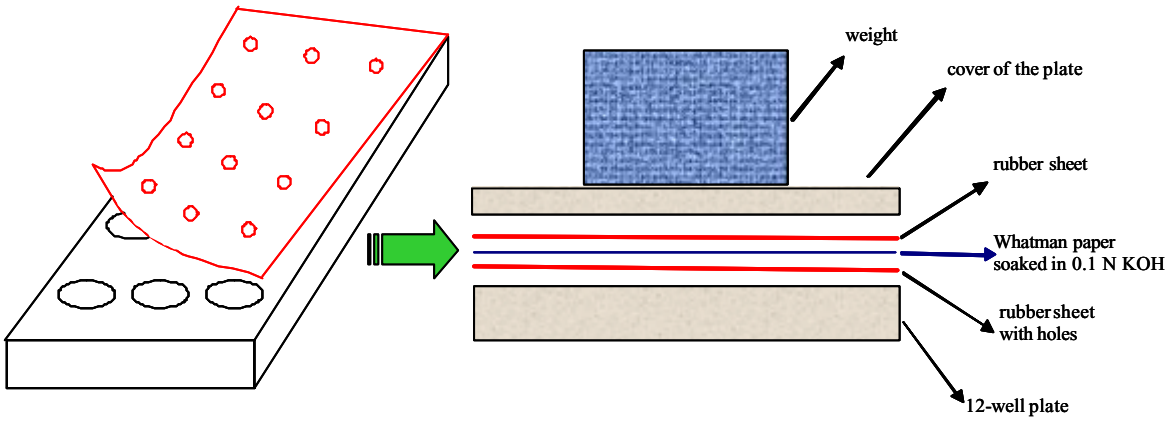

Fig. 4. Palmitate oxidation system in 12-well plates. Palmitate oxidation mix is added to the wells that contain cells still attached. The system is closed by placing in this order: a rubber sheet with holes centered over each well, a Whatman paper soaked in 0.1 N KOH, another rubber sheet without holes and the cover of the plate, all wrapped in parafilm. The assembly is incubated at 37ºC for 2 h with a weight on the top to ensure no $^{14}CO_2$ is escaped.

The assembly is incubated at 37ºC in a CO_2-free incubator for 2 h with a weight on the top to ensure that no $^{14}CO_2$ escapes. During this time the acid gas $^{14}CO_2$ will pass through the rubber sheet holes and react with the base KOH being therefore caught in the Whatman paper. $^{14}CO_2$ contamination from adjacent wells has been found not to be significant and the captured radioactivity has a linear rate of accumulation between 2-6 h after apparatus assembly.

After the incubation time, the piece of Whatman paper corresponding to each well is cut and placed inside scintillation vials with 5 ml of scintillation fluid and counted. Radioactive medium is removed and cells are scrapped in 250 µl of KRBH for the Bradford protein assay.

Results are expressed as:

nmol of palmitate.mg^{-1} prot.h^{-1} = (cpm-blank cpm) x 125 / (total cpm x mg prot x h)

Where 125 is the total nmol of palmitate per well, total cpm are the counts resulting from directly counting on the scintillation fluid 50 µl of the 2.5 mM [1-^{14}C]palmitate used per well and h is the time of incubation.

B) Palmitate oxidation assay in 25-cm^2 flasks

This method has been described by Roduit *et al.*[33] and utilizes 25-cm^2 flasks in which the $^{14}CO_2$ released is also trapped in a KOH soaked Whatman paper. The reaction is stopped by the addition to the cells of perchloric acid. The system, still closed, is left o/n and therefore all the $^{14}CO_2$ in the atmosphere of the flask is captured by the Whatman paper. Palmitate oxidation in 12-well plates is faster and needs fewer cells, virus, solutions and reagents. On the other hand, palmitate oxidation in 25-cm^2 flasks allows time for the $^{14}CO_2$ to be taken up into the Whatman paper in a closed system giving slightly higher oxidation rates.

The procedure is as follows:

Cells are seeded in 25-cm^2 flasks, infected, treated and preincubated as described above for the palmitate oxidation assay in 12-well plates. Then, 2 ml of the palmitate oxidation mix is added to each flask. Blanks are flasks without cells.

The 25-cm^2 flasks are sealed at the beginning of the incubation with a rubber stopper (size 14.5, Fisher, ref. 14-126BB) supporting a 3 cm length of PVC tubing (I.D. 4.7 mm, Fisher, ref. 14-169-7B) containing a piece of Whatman paper soaked in 0.1 N KOH (fig. 5). One end of the PVC tubing is wrapped in parafilm without covering the lumen, so that tubing will fit firmly into the under-side of the stopper. The Whatman paper inside the tubing must be well clear to the opening. Flasks are then incubated at 37ºC in a CO_2-free incubator for 2 h.

[33] Roduit R, Nolan C, Alarcon C, Moore P, Barbeau A, Delghingaro-Augusto V, Przybykowski E, Morin J, Masse F, Massie B, Ruderman N, Rhodes C, Poitout V, Prentki M. A Role for the Malonyl-CoA/Long-Chain Acyl-CoA Pathway of Lipid Signaling in the Regulation of Insulin Secretion in Response to Both Fuel and Nonfuel Stimuli. *Diabetes* 53(4):1007-1019, 2004

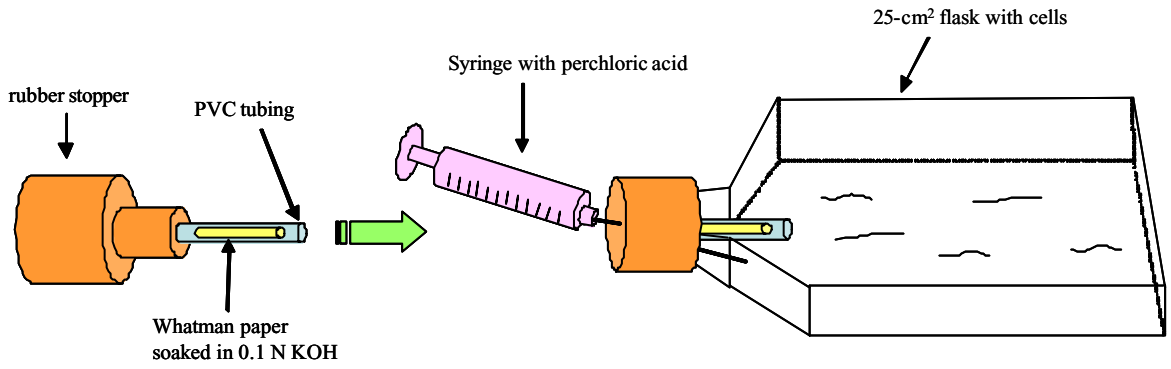

Fig. 5. Palmitate oxidation system in 25-cm² flasks. Palmitate oxidation mix is added to the flask with cells still attached. Flasks are sealed with a rubber stopper supporting a 3 cm length of PVC tubing containing a piece of Whatman paper soaked in 0.1 N KOH. Flasks are incubated at 37ºC in a CO_2-free incubator for 2 h.

At the end of the incubation period, 0.2 ml of 40% (v/v) perchloric acid is injected into each flask *via* a needle through the rubber stopper to acidify the medium, liberate $^{14}CO_2$ and stop palmitate oxidation. Perchloric acid must be well mixed. After o/n isotopic equilibration at r.t., Whatman papers are removed and the trapped $^{14}CO_2$ is measured by liquid scintillation counting after o/n equilibration in 5 ml of the scintillation fluid. It is left o/n because it takes more than 12 h to $^{14}CO_2$ to leach out of Whatman paper into scintillation fluid. The addition of perchloric acid generates a precipitate, therefore for the Bradford protein assay cells from parallel flasks, without perchloric acid, are removed with 1 ml of KRBH.

Results are expressed as:

nmol of palmitate.mg^{-1} prot.h^{-1} = (cpm-blank cpm) x 500 / (total cpm x mg prot x h)

Where 500 is the total nmol of palmitate per flask, total cpm are the counts resulting from directly counting on the scintillation liquid the amount of 2.5 mM [1-^{14}C]palmitate used per flask and h is the time of incubation.

C) Palmitate oxidation to ASP

Fatty acid oxidation into acid-soluble products (ASP) is measured from the perchloric acid treated medium. The perchloric acid injected into the media precipitates the fatty acid tracer bound to proteins leaving the ASPs in solution. In case of the palmitate oxidation assay performed in 25-cm^2 flasks, 1 ml of the incubation media already treated with perchloric acid is taken and centrifuged at 14,000 rpm for 10 min in a microcentrifuge. 800 µl of the supernatant is counted on a scintillation vial with 5 ml of scintillation fluid.

Results are expressed as:

nmol of palmitate.mg^{-1} prot.h^{-1} = (cpm-blank cpm) x 500 x (2,200/800) / (total cpm x mg prot x h)

Where 500 is the total nmol of palmitate per flask, total cpm are the counts resulting from directly counting on the scintillation liquid the amount of 2.5 mM [1-^{14}C]palmitate used per flask, 2,000/800 is the dilution factor and h is the time of incubation.

<u>2.5 mM [1-^{14}C]palmitate bound to BSA</u>

To prepare the labelled palmitate bound to BSA, 500 µl of [1-^{14}C]palmitic acid (Amersham Pharmacia Biotech, ref. CFA23, 250 µCi) is placed on a glass vial under the hood to evaporate the toluene solution. It is stirred and heated if necessary. 6.97 mg of cold palmitate and 1 ml of 0.1 N NaOH is added to the vial and heated at 80-100ºC until the solution is clear. On a beaker, 1 g of defatted BSA (Sigma-Aldrich, ref. A-6003) is dissolved in 8 ml of 0.9% NaCl by stirring and heating it in a water bath to 50ºC maximum. Heating to more than 55ºC will turn the BSA solution into a gel. Palmitate solution is added rapidly drop by drop onto the BSA solution. The resulting solution is filtered through a 0.45 µm filter and 1 ml aliquots are stored at -20ºC.

25, 75 or 150 mM glucose plus 8 mM carnitine

To prepare 25, 75 or 150 mM glucose plus 8 mM carnitine 250 µl, 750 µl or 1.5 ml of 1 M glucose, respectively are mixed with 16 mg of carnitine and dissolved in KRBH up to a total volume of 10 ml. 1 ml aliquots are stored at -20ºC.

10.2 GLUCOSE OXIDATION

Glucose oxidation assay is done with attached cells and examines the capacity of the cells to oxidize glucose. Cells are incubated with [U-^{14}C]glucose and the $^{14}CO_2$ released is measured. Experimental procedure is similar to the one explained before for the palmitate oxidation assay, except that the incubation mix contains fresh KRBH 1% BSA plus 2.5 or 15 mM glucose in the presence of 0.5 µCi/ml [U-^{14}C]glucose.

Glucose oxidation mix (500 µl)	
KRBH	400 µl
25 or 150 mM [U-^{14}C]glucose	50 µl
10% BSA	50 µl

Cells are incubated at 37ºC in a CO_2-free incubator for 2 h. Then, Whatman papers are removed and the trapped $^{14}CO_2$ is measured by liquid scintillation counting.

In case of glucose oxidation in a 12-well plate system, results are expressed as:

For 2.5 mM glucose:

nmol of glucose.mg^{-1} prot.h^{-1} = (cpm-blank cpm) x 1250 / (total cpm x mg prot x h)

For 15 mM glucose:

nmol of glucose.mg^{-1} prot.h^{-1} = (cpm-blank cpm) x 7500 / (total cpm x mg prot x h)

Where 1250 or 7500 is the total nmol of glucose in 50 µl of the 25 or 150 mM [U-^{14}C]glucose respectively, used per well, total cpm are the counts resulting from directly counting on the scintillation liquid 50 µl of 25 or 150 mM [U-^{14}C]glucose respectively, used per well and h is the time of incubation.

25 or 150 mM [U-^{14}C]glucose

A 150 mM glucose solution in KRBH is passed through a 0.22 µm filter. Sufficient quantity of D-[U-^{14}C]glucose (Amersham Pharmacia Biotech, CFB96, 250 µCi) to have 500,000 cpm per point is added. Some of this solution is diluted in KRBH to obtain the 25 mM [U-^{14}C]glucose. 1 ml aliquots are stored at -20ºC.

10.3 LIPID ESTERIFICATION PROCESSES

In esterification experiments cells are incubated with [1-^{14}C]palmitate and we measure the glucose-induced incorporation of this fatty acid into the different lipid complexes such as phospholipids (PL), diacylglycerols (DAG), triacylglycerols (TG), cholesterol esters (CE) as well as the non-esterified labelled palmitate (NE palm). The esterification products are separated by thin layer chromatography (TLC) and quantified with a Storm 840 Laser scanning system.

The procedure is as follows:

A) [1-^{14}C]palmitate incubation

The [1-^{14}C]palmitate incubation is the same as the one described above for the palmitate oxidation assay in 12-well plates. INS(832/13) cells are seeded in 12-well plates, infected with the different adenoviruses, preincubated with KRBH 1% BSA and incubated for 2 h at 37ºC with fresh KRBH containing 2.5 or 15 mM glucose in the presence of 0.8 mM carnitine plus 0.25 mM palmitate and 1 µCi/ml [1-^{14}C]palmitate bound to 1% (w/v) BSA.

B) Lipids extraction

After the incubation period cells are washed in cold PBS and 1 ml of methanol:PBS (2:3, v/v) is added to each well. Cells are gently collected in a pipette, centrifuged at 700 x *g* for 5 min at 4ºC and washed in PBS; 20 µl of the samples is taken at this point for the Bradford protein assay. After that, 200 µl of 0.2 M NaCl is added to the pellet and the mixture is immediately frozen in liquid N_2. To separate aqueous and lipid phases, 750 µl of Folch reagent[34] (chloroform:methanol, 2:1) and 50 µl of 0.1 M KOH are added and, after vigorous vortex-mixing, the phases are separated

[34] Folch J, Lees M, Sloane Stanley GH. A simple method for the isolation and purification of total lipids from animal tissues. *J. Biol. Chem.* 226(1):497-509, 1957

by a 15 min centrifugation at 2000 x *g* at 4ºC. The top aqueous phase is removed and the lipid phase is washed with 200 µl of methanol/water/chloroform (48:47:3). After vortex-mixing and centrifugation at 700 x *g* for 5 min at 4ºC the lower phase is taken and dried with a speed vac.

C) TLC separation

Total lipids are dissolved in 30 µl of chloroform and separated by thin layer chromatography in TLC plates (Merck). Plates are eluted with hexane:diethylether:acetic acid (70:30:1, v/v/v)[35] and quantified with a Storm 840 Laser scanning system (Molecular dynamics, Amersham Pharmacia Biotech). A known amount of labelled palmitate is eluted in the same plate. This allows us to quantify the nmols present in each dot. Intensities of the spots are expressed as $nmol.mg^{-1}$ $prot.h^{-1}$ and results are given as the differences (ΔG) between high (15 mM) and low (2.5 mM) glucose.

The labelled control palmitate is also assessed following TLC separation as a migration reference for NE palm. Migration references from Sigma-Aldrich prepared at 2 mg/ml in chloroform:ethanol (2:1): phosphatidyl-serine (ref. P-5660), dipalmitoyl-glycerol (ref. D-9135), glyceryl tripalmitate (ref. T-5888) and cholesteryl palmitate (ref. C-6072) are developed in TLC plates with iodine. Complex lipids are easily oxidized, therefore migration references must be recently prepared and stored at -20ºC under N_2 atmosphere.

To elute the TLC plates it is used an apolar solvent (hexane:diethylether:acetic acid, 70:30:1, v/v/v), therefore apolar lipids will migrate with the solvent while the more polar ones will stay near the application point in the polar silica gel. CE are the most apolar lipids, so they will migrate further than the others. TGs have a glycerol molecule, so they will migrate less than CE. Then, we will find NE palm and DAG because they have only one fatty acid moiety or one molecule of glycerol, respectively. PLs are the most polar complex lipids so they will remain near the base. For the conditions used, the Rf (rate factors) of these complex lipids are: PL (0.09), DAG (0.12), NE palm (0.27), TG (0.66) and CE (0.92).

[35] Montell E, Turini M, Marotta M, Roberts M, Noé V, Ciudad CJ, Macé K, Gómez-Foix AM. DAG accumulation from saturated fatty acids desensitizes insulin stimulation of glucose uptake in muscle cells. *Am. J. Physiol. Endocrinol. Metab*. 280:E229-E237, 2001

10.4 MITOCHONDRIAL MEMBRANE POTENTIAL $\Delta\Psi_m$

Mitochondrial membrane potential $\Delta\Psi_m$ reflects the electron transport chain activity in the cell. Glucose metabolism in the Krebs cycle gives a hyperpolarization of the mitochondrial membrane. This electron transport chain activity or the hyperpolarization in the mitochondrial membrane could be measured in attached cells by monitoring rhodamine-123[36], a fluorescent compound which dyes cells mitochondria in a mitochondrial potential-dependent manner[37].

Rhodamine-123 is a cationic cyanide which is accumulated in negative compartments as mitochondria. The large surface of the membrane in the mitochondrial matrix could contribute to the dyeing, accumulating large amounts of rhodamine. Rhodamine has a maximal absorption peak at approximately 485 nm (blue) and a maximal emission peak at 530 nm. Uncoupling agents or inhibitors decrease the mitochondrial fluorescence.

To measure the mitochondrial membrane potential $\Delta\Psi_m$, naSREBP-1c stable cells are seeded in 24-well plates and cultured with or without 500 ng/ml of doxycycline for 1, 2 or 4 days. Cells are maintained for 2 h in 2.5 mM glucose medium at 37ºC before loading with 10 µg/ml rhodamine-123 for 20 min at 37ºC in KRBH. The $\Delta\Psi_m$ is monitored in a plate-reader fluorimeter (Fluostar Optima, BMG Labtechnologies, Offenburg, Germany) with excitation and emission filters set at 485 and 520 nm, respectively, at 37ºC with automated injectors for glucose (addition of 13 mM on top of basal 2.5 mM) and carbonyl cyanide 4-trifluoromethoxyphenyl-hydrazone (FCCP) which is a protonophore that depolarizes the $\Delta\Psi_m$.

Rhodamine: It is soluble in DMSO or DMF. It is stored at 4ºC protected against the light.

[36] Maechler P, Kennedy E, Pozzan T, Wollheim CB. Mitochondrial activation directly triggers the exocytosis of insulin in permeabilized pancreatic β-cells. *EMBO J* 16:3833-3841, 1997

[37] Johnson LV, Walsh ML, Chen LB. Localization of mitochondria in living cells with rhodamine 123. *Proc. Natl. Acad. Sci. USA* 77:990-994, 1980

11. METABOLITES DETERMINATION

11.1 TRIGLYCERIDE CONTENT

Triglyceride content measurement in culture cells is based on the lipid extraction of the cells followed by the hydrolysis of the triglycerides to glycerol and free fatty acids and the quantification of the glycerol released. The Triglyceride (GPO-Trinder) kit (Sigma-Aldrich, ref. A-337), which allows the quantitative enzymatic determination of triglycerides by measuring the absorbance at 540 nm, is used.

The procedure is as follows:

A) Lipid extraction

Cells are grown in 12-well plates until approx. 80% confluence. Then, they are treated or infected and preincubated with KRBH 1% BSA as described above. Cells are washed in cold PBS and 1 ml of methanol:PBS (2:3, v/v) is added to each well. Then, cells are gently collected in a pipette, centrifuged at 700 x *g* for 5 min at 4ºC and washed with 1ml of PBS. 20 µl of the samples is taken at this point for the Bradford protein assay. After another centrifugation at 700 x *g* for 5 min at 4ºC, 200 µl of 0.2 M NaCl is added to the pellet and the mixture is immediately frozen in liquid N_2. Lipids are extracted with Folch reagent as described in LIPID ESTERIFICATION PROCESSES (Section 10.3).

Total lipids obtained are dissolved in 50 µl of chloroform. 20 µl of the lipid samples, 20 µl of chloroform (blank) or 20 µl of a triolein standard curve are placed on 1.5 ml tubes and air dried. Then, 10 µl of Thesit (Fluka, ref. 17228) 20% (v/v) in chloroform is added, samples are vortex-mixed, air dried o/n and dissolved in 50 µl of water. Thesit allows lipids to dissolve in water for the following enzymatic assay.

Triolein standard curve:

µg triolein	µl stock solutions	µl chloroform:methanol (2:1)
0	0	20
1	2 (0.5 mg/ml)	18
2.5	5 (0.5 mg/ml)	15
5	10 (0.5 mg/ml)	10
10	2 (5 mg/ml)	18
25	5 (5 mg/ml)	15
50	10 (5 mg/ml)	10
Total volume	20 µl	

Triolein stock solutions (5 mg/ml and 0.5 mg/ml): To prepare the 5 mg/ml stock solution, 5.5 µl of triolein (Sigma-Aldrich, ref. T-7140) is diluted in 1 ml of chloroform:methanol (2:1). To prepare the stock at 0.5 mg/ml a 1/10 dilution in chloroform:methanol (2:1) is done. Triolein solutions are stored at -20ºC under N_2 atmosphere.

B) Triglyceride quantification

Triglycerides are measured enzymatically with the Triglyceride (GPO-Trinder) kit following the manufacturer's instructions. Briefly, triglycerides are hydrolyzed by lipoprotein lipase to glycerol and free fatty acids. The glycerol produced is then measured by coupled enzyme reactions catalyzed by glycerol kinase, glycerol phosphate oxidase and peroxidase. This kit differentiates between endogenous glycerol and glycerol derived by hydrolytic action of lipase allowing measuring true triglycerides. The product of the last enzymatic reaction shows absorbance at 540 nm and the increase in absorbance is directly proportional to triglycerides concentration of the sample.

Triglycerides could be qualitatively observed by Oil O Red (Sigma-Aldrich, ref. O-0625) cells staining and the lipid droplets formed visualized using phase-contrast microscopy.

11.2 MALONYL-CoA MEASUREMENT

To quantify the malonyl-CoA content in culture cells, malonyl-CoA is extracted from the cells and assayed with a radioenzymatic method using [1-^{14}C]acetyl-CoA (ICN, ref. 13070, 48 mCi/mmol). The assay requires the enzyme fatty acid synthase (FAS) which is isolated from rat liver.

A) FAS isolation

Fatty acid synthase (FAS) catalyses the *de novo* synthesis of long-chain fatty acids from acetyl-CoA and malonyl-CoA. FAS was purified from rat liver using polyethylene glycol (PEG) as described by Linn[38]. This procedure results in high yields of the enzyme which is essentially free of endogenous proteolytic nicking and from proteases contamination.

Buffers used:

Buffer 1	**Buffer 2**	**Buffer 3**
0.1 M KH_2PO_4 pH 7.5	0.1 M KH_2PO_4 pH 7.2	0.1 M KH_2PO_4 pH 7.5
	1 mM $MgCl_2$	1 mM $MgCl_2$
	0.1 mM EDTA	0.1 mM EDTA
	10% glycerol	10% glycerol
	1 mM DTT	1 mM DTT
	2% rabbit serum	2% rabbit serum
		2 mg/ml defatted BSA

Buffer 4	**Buffer 5**	**Buffer 6**
0.05 M KH_2PO_4 pH 7.2	0.05 M KH_2PO_4 pH 7.5	0.15 M KH_2PO_4 pH 7.5
1 mM $MgCl_2$	1 mM $MgCl_2$	1 mM $MgCl_2$
0.1 mM EDTA	0.1 mM EDTA	0.1 mM EDTA
10% glycerol	10% glycerol	10% glycerol
1 mM DTT	2 mM DTT	5 mM DTT
2 mg/ml defatted BSA		

[38] Linn TC. Purification and crystallization of rat liver fatty acid synthetase. *Arch. Biochem. Biophysics* 209:613-619, 1981

DTT is added immediately before use and it prevents the formation of protein disulfide bonds. In order to minimize the proteolysis of the enzyme during isolation, rabbit serum is added to the crude fractions and the pH of all fractions is maintained at 7.0 or above. It is assumed that the active components in the rabbit serum are the α_2-macroglobulins which adsorb proteases. Glycerol is added to give the adequate density to the fractions.

The enzyme is purified with PEG (M_r 6000, Merck, ref. 807491) and ammonium sulphate, which absorb the water molecules and thus precipitates the protein. PEG is a neutral polymer and therefore is adequate for the later use of a DEAE Sepharose column.

10 male, Sprague-Dawley rats weighing 200-250 g are fasted 2 days and then fed *ad libitum*, a fat-free high-carbohydrate diet for 3 days. With this treatment FAS expression is maximized.

The procedure is as follows:

To isolate the protein all the steps are carried out at 4ºC (fig. 6). After successive precipitations with PEG and ammonium sulphate FAS is purified by loading the last fraction through a column of DEAE Sepharose Fast Flow (Amersham Pharmacia Biotech, ref. 17-0709-01). The gradient is arranged with buffer 5 and 6 and the FAS obtained this way has a specific activity approx. between 0.5-0.9 U/ml. It is split into 1 ml aliquots and stored at -80ºC.

A sample of the pellet (ppt.) or the supernatant (sup.) is taken at each step to check FAS activity before discarding the fraction. The activity is measured by a spectrophometric assay which is faster but not as sensitive as the radioenzymatic method described below. Therefore, the efficiency of the purification could be followed.

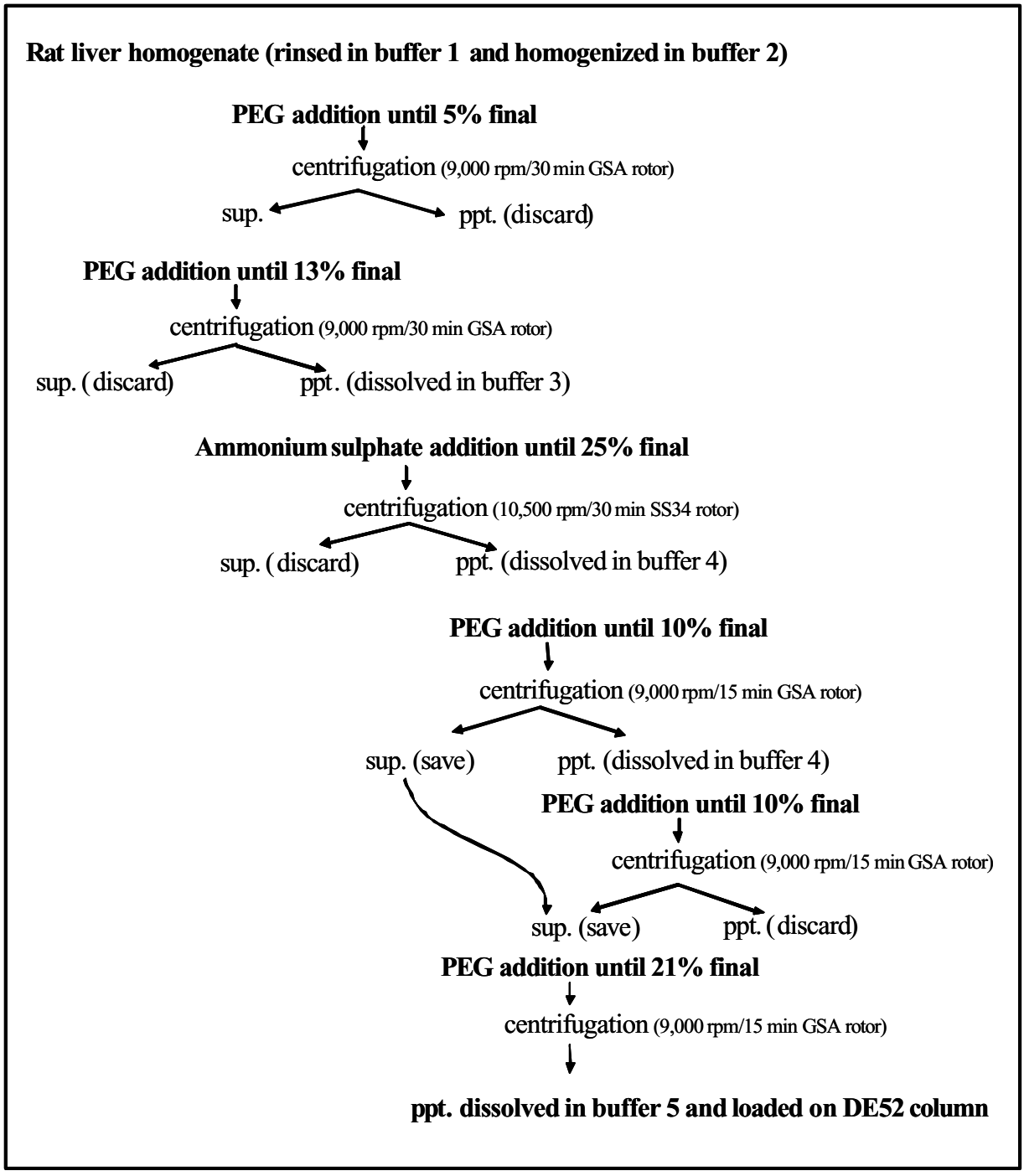

Fig. 6. Scheme for FAS purification. FAS is isolated from rat liver with successive precipitations with PEG and ammonium sulphate. Finally FAS is purified with a DEAE Sepharose column.

Measurements are carried out in 1 cm cuvettes using a recording spectrophotometer at 25ºC. The reaction measures the disappearance of NADPH which has a maximal absorbance at 340 nm.

$$\text{Acetyl-CoA + Malonyl-CoA + NADPH} \xrightarrow{\text{FAS}} \text{palmitic acid}$$

The reaction is started by the addition of the sample to the following components:

FAS assay/point	
FAS buffer	0.9 ml
25 mM NADPH	10 µl
20 mM acetyl-CoA	10 µl
20 mM malonyl-CoA	10 µl
H_2O	20 µl
Sample	50 µl

FAS buffer: 0.1 M KH_2PO_4 pH 7.2, 0.2 mM EDTA, 4 mM DTT and 0.2% defatted BSA.

The initial velocity (ΔOD) at 340 nm is recorded for each sample prior and after malonyl-CoA addition. The rate of NADPH oxidation prior to malonyl-CoA addition serves as a blank value which is subtracted from the overall rate.

One unit of FAS activity is defined as the amount of enzyme which catalyzes the oxidation of 1 µmol of NADPH in 1 min at 25ºC.

B) Malonyl-CoA extraction from cells

INS(832/13) cells are grown in 10-cm dishes until 80% confluence. 24 h after the infection with the different adenoviruses, cells are preincubated with KRBH 1% BSA as described in BASAL TREATMENTS (Section 3.5.1) and incubated for 30 min at 37ºC with fresh KRBH 0.1% BSA containing 2.5 or 15 mM glucose. Cells are then collected into 2 ml tubes by adding 1.5 ml of ice-cold 3.5% (v/v) perchloric acid to each dish and centrifugation of the collected extract at 12,000 rpm for 5 min at 4ºC in a

microcentrifuge. Pellets of cells from parallel dishes without perchloric acid are kept for Bradford protein assay. The supernatant containing acid-soluble metabolites is neutralized to pH 2-3 with 5 N KOH and to pH 6 with 2.5 M $KHCO_3$. After centrifugation at 2,000 rpm for 5 min, the supernatant volume is measured and kept for the malonyl-CoA assay.

C) Malonyl-CoA assay

Malonyl-CoA is quantified by a radioenzymatic method[39] based on the malonyl-CoA-dependent incorporation of labelled acetyl-CoA into palmitic acid catalyzed by FAS in the presence of NADPH.

Malonyl-CoA + [1-^{14}C]acetyl-CoA + NADPH $\xrightarrow{\text{FAS}}$ [^{14}C]palmitic acid

The [^{14}C]palmitic acid formed could be separated by successive extractions in an organic solvent. The advantage of this radioenzymatic method over the spectrophotometric method is that it is extremely sensitive and allows the determination of pmol quantities of malonyl-CoA.

For the assay, each sample is divided into two 200 µl aliquots and 100 pmol of malonyl-CoA is added to one of the two samples. The reaction mixture contains, in a total volume of 1.025 ml/point:

Malonyl-CoA reaction mix/point	
KH_2PO_4 pH 7	0.2 M
DTT	2.5 mM
EDTA	2 mM
NADPH	0.2 mM
defatted BSA	1 mg
[1-^{14}C]acetyl-CoA	2 nmol
Total volume	1.025 ml

[39] McGarry JD, Stark MJ, Foster DW. Hepatic malonyl-CoA levels of fed, fasted and diabetic rats as measured using a simple radioisotopic assay. *J. Biol. Chem*. 253:8291-8293, 1978

200 µl of the samples with or without 100 pmol of malonyl-CoA is added to the reaction mix. Then, the reaction is initiated by the addition of 25 mU FAS to each tube. After a 45 min incubation at 37ºC, the reaction is terminated by the addition of 25 µl of 70% (v/v) perchloric acid. Then, 1 ml of ethanol and 5 ml of petroleum ether are added to each tube and they are vortex-mixed for 30 sec. After centrifugation, 4 ml of the petroleum ether phase (superior) is transferred to another tube containing 2 ml of water. The tubes are then shaken and, after a brief centrifugation, 2 ml of the petroleum ether phase is counted in scintillation vials with 5 ml of scintillation fluid.

Tissue and cell extracts also contain malonyl-CoA and probably variable quantities of acetyl-CoA or other acyl-CoA species that might act as primers for condensation with malonyl-CoA in the FAS reaction. The presence of such compounds would effectively reduce to an unknown degree the specific activity of the labelled acetyl-CoA present in the assay mixture and thereby result in low artifact values for the malonyl-CoA content. This problem is solved by running the assay for each sample extract in the absence and presence of a standard quantity of malonyl-CoA. Thus, the malonyl-CoA content of the sample can be calculated as follows:

$$\text{pmol malonyl-CoA.mg prot}^{-1} = (a \times b) \times (V_t/200)/(c-b)$$

Where: a is the pmol of malonyl-CoA added to one sample (100 pmol)

b are the cpm of the sample without malonyl-CoA

V_t is the total µl of the neutralized extract collected in perchloric acid

c are the cpm of the sample plus malonyl-CoA

12. INSULIN SECRETION

To measure insulin secretion, cells are incubated with different secretagogues and the secreted medium is analyzed by radioimmunoassay (RIA) using ^{125}I-insulin[40].

A) Insulin secretion

INS-1 cells are seeded in 12-well plates at 0.5 x 10^6 cells/well. After 48 h cells are treated or infected as described above and further cultured before starting insulin secretion experiments.

The day of the experiment cells are first washed in fresh KRBH 0.1% (w/v) defatted BSA (RIA grade, Sigma-Aldrich, ref. A-7888), preincubated at 37ºC for 30 min in 500 µl of KRBH plus 1% BSA in the absence or the presence of 200 µM etomoxir and finally washed again with KRBH 0.1% BSA.

Then, cells are incubated for 1 h at 37ºC with 1 ml of KRBH 0.1% BSA in the presence of either 2.5 mM glucose, 15 mM glucose, 15 mM glucose plus 0.25 mM palmitate bound to 1% (w/v) BSA or 2.5 mM glucose plus 30 mM KCl. For studies of K_{ATP} channel-independent insulin secretion, cells are incubated for 1 h at 37ºC with 1 ml of KRBH 0.1% BSA plus 35 mM KCl and 250 µM diazoxide at 2.5 mM glucose or 15 mM glucose. These assays are performed at 35 mM KCl (depolarizing K^+); consequently, the Na^+ concentration in the KRBH was reduced from 135 to 89.9 mM to maintain osmolarity.

After the incubation the solution is collected in 1.5 ml tubes and centrifuged at 10,000 rpm for 1 min in a microcentrifuge to remove cell debris. To measure the total insulin content, the liquid remaining in the wells is completely aspirated and cells are extracted with 1 ml of 75% ethanol/0.2 M HCl per well. Solutions for insulin secretion measurement or insulin content measurement can be stored at -20ºC for a few days.

250 mM diazoxide: To prepare a 250 mM stock of diazoxide, 57.7 mg of diazoxide is dissolved in 1 ml of DMSO and aliquots are stored at -20ºC.

[40] Rubi B, Ishihara H, Hegardt FG, Wollheim CB, Maechler P. GAD65-mediated glutamate decarboxylation reduces glucose-stimulated insulin secretion in pancreatic beta cells. *J. Biol. Chem*. 276: 36391-36396, 2001

Glucose and KCl stock solutions are prepared in KRBH, filtered through a 0.22 µm filter and stored at 4ºC. Palmitate bound to 1% (w/v) BSA is prepared as described before for PALMITATE OXIDATION (Section 10.1).

B) Radioimmunoassay

The insulin content was determined by radioimmunoassay using the Coated Tube Insulin RIA kit (Insulin-CT, Schering, ref. INK-0206). The principle of the assay is based on the competition between the labelled insulin contained in standards or samples for a fixed and limited number of antibody binding sites bound on the solid phase (coated tubes). After the incubation, the unbound tracer is removed by washing. The amount of labelled insulin bound to the antibody is inversely proportional to the amount of unlabelled insulin in the sample.

The coated tubes contain guinea pig anti-porcine insulin serum coated to the bottom of the tube. This antibody also binds to human and rat insulin that are present in INS(832/13) cells. The labelled insulin used is ^{125}I-porcine insulin dissolved in phosphate buffer in the presence of bovine albumin and sodium azide.

For the RIA, samples are thawed and diluted 1/10 (insulin secretion samples) or 1/100 (insulin content samples) in KRBH. 100 µl of KRBH (blank), standards (5.5, 15, 35, 70, 175 and 310 µIU/ml) or diluted samples is placed into the coated tubes plus 1 ml of ^{125}I-insulin. After vortex-mixing, samples are incubated 18-20 h at r.t. and, washed in water, and the remaining radioactivity bound to the tubes is measured with a gamma scintillation counter calibrated for 125 iodine. Results for insulin secretion are represented as % of insulin content.

13. PANCREATIC RAT ISLETS

13.1 RAT ISLET ISOLATION

Rat islets were isolated for adenovirus infection and Western blot or insulin secretion measurements. Pancreatic rat islets were isolated with collagenase as previously described[41]. The following protocol is described for islet isolation from one rat.

[41] Gotoh M, Maki T, Satomi S, Porter J, Bonner-Weir S, O'Hara Cj, Monaco AP. Reproducible high yield of rat islets by stationary *in vitro* digestion following pancreatic ductal or portal venous collagenase injection. *Transplantation* 43:725-730, 1987

Material preparation

First 25% Ficoll solution is prepared by dissolving in a beaker 5 g of Ficoll DL-400 (Sigma-Aldrich, ref. F-9378, 100 g) in 15 ml of HBSS/HEPES 20 mM (Hanks Balanced Salt Solution/HEPES buffer) and mixing it with a magnet. When it is dissolved, total volume is adjusted up to 20 ml with HBSS/HEPES buffer and filtered through a 0.45 µm filter.

Collagenase is prepared by dissolving 20 mg of collagenase type 4 (Worthington biochemical corporation, ref. S9J3119, 5 mg, 180 U/mg) kept at 4ºC in 10 ml of HBSS/HEPES buffer and filtering it through a 0.22 µm filter. DNase at 1/3000 is added just at the moment of collagenase utilization. DNase stock is prepared at 10 mg /ml, so for 10 ml of collagenase 3.33 µl of DNase will be added. The collagenase and a flask or a 50 ml tube for the pancreas location are kept on ice.

Surgery

One Wistar rat weighing approx. 200 g is sacrificed by dislocation and dissected. All the organs are placed on the left side when the head of the animal is at the bottom. In this position the pancreatic canal is visible. The clamp has to be done at the point where the pancreatic canal joins the duodenum intestine. This point could be identified by a whiter area in the intestine with a red dot. The clamp must be placed at the left, in the same direction on the canal. The clamp prevents the collagenase from escaping from the pancreas through the intestine.

The pancreatic canal area where the collagenase is to be injected i.e., the bottom part of the canal, near the liver, is cleaned and cleared of fat with the help of a forceps and a needle. 10 ml of collagenase is injected slowly with a needle connected to a syringe through this point. The syringe must not contain bubbles. It is possible to see how the pancreas is being inflated during this process. See fig. 7.

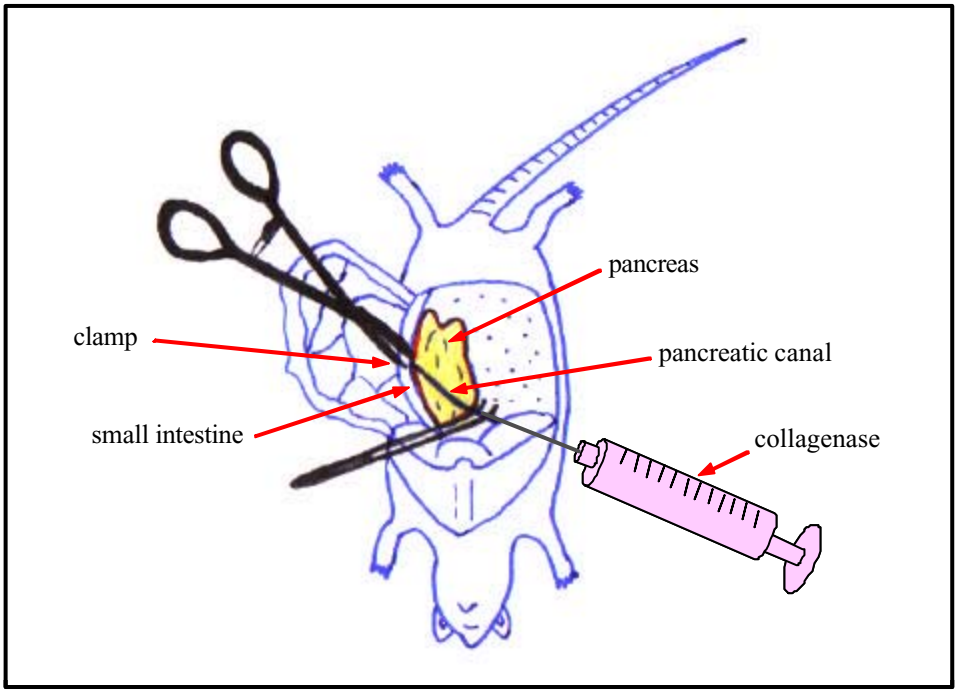

Fig. 7. Scheme of collagenase injection into the pancreas of the rat. The pancreatic canal is clamped at the point where it joins the duodenum intestine. Then, 10 ml of collagenase is injected through the pancreatic canal.

Once the clamp is released, all the organs are placed on the right side of the rat to see if the collagenase reached the spleen. The pancreas is separated carefully, without cutting it to prevent the collagenase from escaping. First the spleen is taken out, then the pancreas is separated from the large intestine and after that the mesentery and the small intestine are cut. The intestine must not be cut, to avoid contamination. Finally the pancreas is detached from the stomach and the liver.

Collagenase digestion

The pancreas is placed inside the flask or the 50 ml tube maintained on ice. If more pancreas samples are needed they will be added to the same flask. Collagenase digestion is done for 25 min at 37ºC shaking the flask once or twice to homogenize the digestion.

Ficoll gradient

For one rat two gradient steps are necessary. Each gradient is performed with 23, 20.5 and 11% of Ficoll. The 23% Ficoll is prepared in a 15 ml tube by mixing 4.6 ml of

25% Ficoll plus 0.4 ml of HBSS/HEPES buffer, 20.5% Ficoll with 4.1 ml of 25% Ficoll plus 0.9 ml of HBSS/HEPES buffer and 11% Ficoll with 2.2 ml of 25% Ficoll plus 2.8 ml of HBSS/HEPES buffer (see table below of Ficoll gradients).

Collagenase digestion is stopped by the addition of 50 ml of cold HBSS/HEPES buffer, with vigorous shaking. The pancreas solution is centrifuged at 1,400 rpm for 1 min at r.t. Supernatant is removed and more HBSS/HEPES buffer is added and mixed vigorously. This process is repeated until supernatant is almost transparent (not red).

To eliminate the floating fat, the solution is filtered with a gauze and the original tube is washed twice with HBSS/HEPES buffer and also filtered through the gauze. The solution is centrifuged at 1,400 rpm for 1 min at r.t.

Islets are then distributed into 15 ml tubes with 10 ml HBSS/HEPES buffer/rat/tube. The solution is centrifuged at 1,400 rpm for 1 min at r.t. All the supernatant must be well aspirated because the remaining liquid will change the gradient. 4 ml of 25% Ficoll is added to each 15 ml tube by vortexing to yield a good homogenate. 25% Ficoll is viscous and does not damage the cells. With a 5 ml pipette, 2 ml of 23% Ficoll, then 2 ml of 20.5% Ficoll and finally 2 ml of 11% Ficoll are added to the tube very slowly, leaving the liquid to slide down the wall of the tube and turning it at the same time. Solution is centrifuged at 1,700 rpm for 7 min at 24ºC without brake. With this gradient, islets will be separated from the rest of the cells and will remain in a ring between 11-20.5% and 20.5-23% Ficoll.

Islets are removed with a Pasteur pipette and placed in a 15 ml tube with HBSS/HEPES buffer. The Pasteur pipette must be prewashed in HBSS/HEPES buffer to avoid losing islets, which attach to glass. Islets are centrifuged at 1,400 rpm for 1 min at r.t. with brake. Some islets are still floating because the gradient is still high. Half of the supernatant is aspirated and more HBSS/HEPES buffer is added to reduce the gradient and wash the islets out. This process is repeated until hardly any islets are floating. If more than one rat has been used, islets are placed together in one 15 ml tube and pelleted.

Once the supernatant is completely aspirated the gradient is repeated as described above. 4 ml of 25%, 2 ml of 23%, 2 ml of 20.5% and 2 ml of 11% Ficoll are added and the solution is centrifuged at 1,700 rpm for 7 min at 24ºC without brake. Islets are removed with a Pasteur pipette and washed as described above.

Preparing islets for culture

Under the hood 10 ml of PBS is added to the pellet of islets to resuspend them. Islets are centrifuged at 1,400 rpm for 1 min at r.t., washed twice with PBS and then twice with medium preheated at 37ºC.

Islets from one rat (approx. 400 islets) are resuspended in medium and seeded at 200 islets/10-cm dish using a microscope to count them (20 islets/ml). Islets are cultured o/n at 37ºC.

HBSS/HEPES 20 mM

HBSS/HEPES buffer is prepared by mixing 50 ml of HBSS 10X (Gibco, ref. 14065-056) with 10 ml of 1 M HEPES and adjusting the volume with bd. A.C. H_2O up to 500 ml. The solution is filtered through a 0.22 µm filter and stored at 4ºC. HBSS contains basically water, salts, glucose, penicillin, streptomycin and BSA at pH 7.2.

Ficoll gradients

The next table shows how to prepare the different Ficoll gradients according to the number of rats used.

Num. Rats	**Num. Gradients**	**25%** (g Ficoll/ml HBSS/HEPES buffer)	**23%** (ml 25% Ficoll/ml HBSS/HEPES buffer)	**20.5%** (ml 25% Ficoll/ml HBSS/HEPES buffer)	**11%** (ml 25% Ficoll/ml HBSS/HEPES buffer)
1	2	5 g/20 ml	4.6/0.4 ml	4.1/0.9 ml	2.2/2.8 ml
2	3	7.5 g/30 ml	6.9/0.6 ml	6.15/1.35 ml	3.3/4.2 ml
3	4	10 g/40 ml	9.2/0.8 ml	8.2/1.8 ml	4.4/5.6 ml
4	5	12.5 g/50 ml	11.5/1 ml	10.25/2.25 ml	5.5/7 ml
5	6	15 g/60 ml	13.8/1.2 ml	12.3/2.7 ml	6.6/8.4 ml
6	7	17.5 g/70 ml	16.1/1.4 ml	14.35/3.15 ml	7.7/9.8 ml
7	8	20 g/80 ml	18.4/1.6 ml	16.4/3.6 ml	8.8/11.2 ml

13.2 RAT ISLET CULTURE

After the isolation step islets are maintained in culture at 20 islets/ml in regular RPMI 1640 medium containing 11 mM glucose supplemented with 10% (v/v) FBS, 100 U/ml penicillin and 100 µg/ml streptomycin at 37ºC in a humidified atmosphere containing 5% CO_2.

13.3 RAT ISLET INFECTION

One day after the isolation, 200 islets are taken, centrifuged at 1,400 rpm for 1 min and resuspended in 1 ml of medium. Islets are transferred to one 35-mm dish

containing 1 ml of medium plus the different purified adenoviruses at 10-150 x 10^4 pfu/islet. Islets are incubated with the adenoviruses for 1 h at 37ºC. After that, as much medium as possible is removed. This is possible because islets are grouped together. Then they are resuspended in 4 ml of medium and transferred to a 60-mm dish. Islets are cultured for 24 h before experiments are done.

13.4 INSULIN SECRETION

Islets were infected with the different adenoviruses one day after isolation and further cultured for 24 h before the insulin secretion experiments were done.

For the insulin secretion measurements, islets are first preincubated for 30 min in KRBH plus 2.8 mM glucose. Then, 10 islets/tube are incubated with 1 ml of KRBH 0.1% BSA plus 2.8 or 16.7 mM glucose for another 30 min. After this incubation time the supernatant is collected. To measure the total insulin content, islets are dissolved in 1 ml of 75% ethanol/0.2 M HCl. Insulin is detected by RIA as described in Section 12.

14. MASS SPECTROSCOPY

The MALDI-TOF mass spectra of C75, C75-CoA, etomoxir and etomoxiryl-CoA were obtained on a Voyager DE-RP (Applied Biosystems) mass spectrometer equipped with a nitrogen laser (337 nm, 3 ns pulse). The acceleration voltage is set to 20 kV. Data are acquired in the reflector mode with delay times of 320 ns for both the positive and negative polarities. Spectra are calibrated externally using a calibration mixture (Calibration Mixture 1, Applied Biosystems): CHCA, des-Arg^1-Bradykinin, Angiotensin I, Glu^1-Fibrinopeptide B, Neurotensin m/z 300-1700.

Samples are prepared by diluting 1 µl of the activation buffer of each drug to 100 µl with H_2O, and mixing 1 µl of this diluted solution with 1µl of matrix solution (10 mg/ml of 2,5-dihydroxybenzoic acid (2,5-DHB, Aldrich) in methanol:water 1:1). One microliter of the sample:matrix mixture is spotted onto the stainless steel sample plate, allowed to evaporate to dryness in air and introduced into the mass spectrometer. Spectra are acquired in the positive and negative ion mode.

MALDI-TOF spectra were performed by the Mass Spectrometry Service (SCT, University of Barcelona).

15. STATISTICAL ANALYSIS

Data are expressed as means ± SE for at least four independent experiments performed in triplicate. Different experimental groups were compared either with the Student's *t* test or with the one-way ANOVA followed by Bonferroni's test for comparisons post hoc. A probability level of $p<0.05$ was considered to be statistically significant.

RESULTS

RESULTS

1. ALTERATION OF THE MALONYL-CoA/CPTI INTERACTION IN THE PANCREATIC β-CELL

To directly test the hypothesis that the CPTI/malonyl-CoA interaction is involved in glucose-stimulated insulin secretion (GSIS) we overexpressed LCPTI M593S, a mutant LCPTI enzyme that is insensitive to malonyl-CoA[1], in pancreatic β-cells. In this way we would establish whether the availability of long-chain fatty acyl-CoA (LC-CoA) affects the regulation of insulin secretion and whether malonyl-CoA may acts as a metabolic coupling factor in the β-cell.

1.1 CONSTRUCTION OF THE RECOMBINANT ADENOVIRUS Ad-LCPTI M593S

A) Ad-LCPTI M593S

We used the following adenoviruses: Ad-LCPTI wt, Ad-LacZ and Ad-LCPTI M593S. Ad-LCPTI wt encoding LCPTI wt was constructed as previously described[2]. Ad-LacZ, which expresses bacterial β-galactosidase, was used as a control adenovirus. Ad-LCPTI M593S, encoding the malonyl-CoA-insensitive LCPTI M593S cDNA under the chicken β-actin (CA) promoter, was constructed as described in Fig. 1.

[1] Morillas M, Gomez-Puertas P, Bentebibel A, Selles E, Casals N, Valencia A, Hegardt FG, Asins G, Serra D. Identification of conserved amino acid residues in rat liver carnitine palmitoyltransferase I critical for malonyl-CoA inhibition. Mutation of methionine 593 abolishes malonyl-CoA inhibition. *J. Biol. Chem.* 278:9058-9063, 2003

[2] Rubi B, Antinozzi PA, Herrero L, Ishihara H, Asins G, Serra D, Wollheim CB, Maechler P, Hegardt FG. Adenovirus-mediated overexpression of liver carnitine palmitoyltransferase I in INS1E cells: effects on cell metabolism and insulin secretion. *Biochem. J.* 364:219-226, 2002

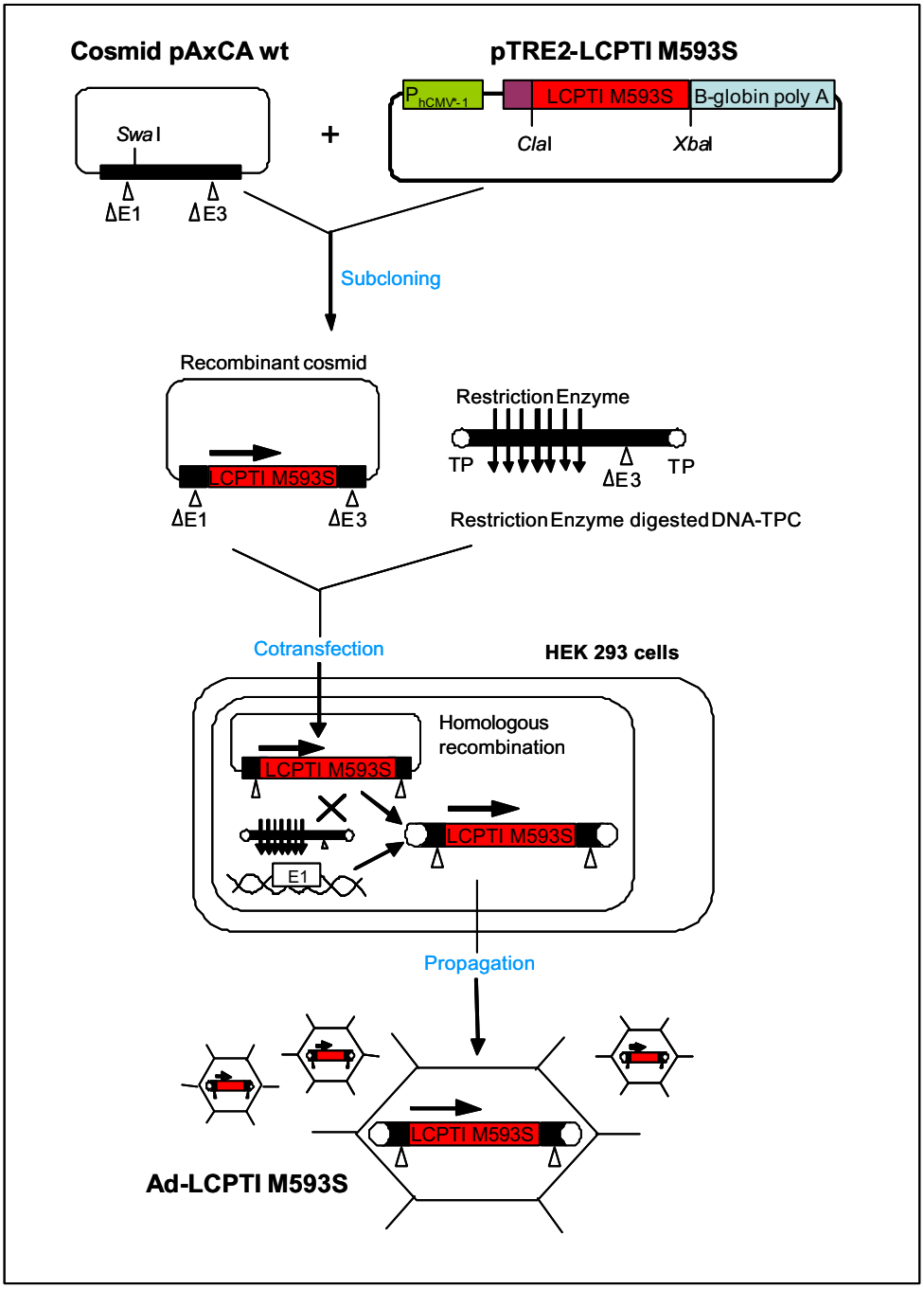

Fig. 1. Generation of the recombinant adenovirus Ad-LCPTI M593S. Blunt-ended LCPTI M593S cDNA was subcloned into the cosmid pAxCA wt previously cut with *Swa*I and dephosphorylated. This cosmid contains the CMV enhancer, the chicken β-actin promoter, the rabbit β-globin poly A signal and the adenovirus genome which lacks the E1 gene and thus renders adenovirus replication defective. The recombinant cosmid was cotransfected with DNA-TPC (adenovirus DNA of terminal protein complex) in HEK 293 cells. The recombinant adenovirus was generated by homologous recombination and propagated in HEK 293 cells, which express the adenoviral E1 gene.

Briefly, the LCPTI M593S cDNA was obtained from pTRE2-LCPTI M593S (Section 2.1) by digestion with *Cla*I and *Xba*I. The terminals were blunt-ended and the cDNA was subcloned into the cosmid pAxCA wt which had been previously digested with *Swa*I and dephosphorylated. This cosmid contains the adenovirus genome which lacks the E1 gene and thus renders adenovirus replication defective. It also contains the CMV enhancer, the chicken β-actin promoter and the rabbit β-globin poly A signal. The presence and right orientation of the insert were checked by restriction enzyme digestions using *Cla*I and *Bgl*II and the presence of the mutation was confirmed by sequencing. The resultant pAxCA-LCPTI M593S cosmid was cotransfected with DNA-TPC (adenovirus DNA of terminal protein complex) in HEK 293 cells. The recombinant adenovirus was generated by homologous recombination and was propagated in HEK 293 cells, which express the adenoviral E1 gene.

B) Recombinant adenovirus analysis

To select the viral clone with highest LCPTI expression, INS(832/13) cells infected with the different clones were analyzed by Western blot.

INS(832/13) cells were infected with 2, 5 or 10 µl of the viral suspension of three viral clones obtained or with Ad-LacZ as a control. Cell lysate was collected and analyzed by Western blot with an anti-LCPTI specific antibody (Fig. 2).

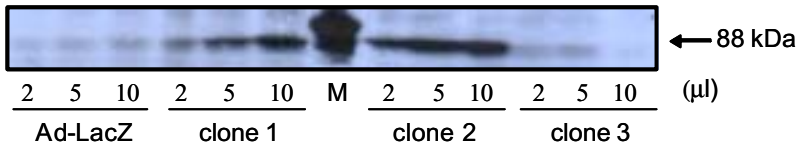

Fig. 2. Western blot analysis of three Ad-LCPTI M593S clones. INS(832/13) cells were infected with 2, 5 or 10 µl of a suspension of three different viral clones or with Ad-LacZ as a control. Cell lysate was analyzed by Western blot with an anti-LCPTI specific antibody, giving a single band of 88 kDa. The protein marker is shown as (M).

Ad-LCPTI M593S clone 2 was selected since it showed the highest LCPTI expression by Western blot and no toxicity in INS(832/13) cells. The adenovirus was amplified in HEK 293 cells, purified by CsCl and carefully titrated as detailed in

MATERIALS AND METHODS (Section 6.7). The titer obtained was 8.1 x 10^9 pfu/ml. The titers of Ad-LacZ and Ad-LCPTI wt were 2.3 x 10^9 and 1.9 x 10^8 pfu/ml, respectively.

1.2 CPTI ACTIVITY IN INS(832/13) CELLS INFECTED WITH Ad-LCPTI wt AND Ad-LCPTI M593S

1.2.1 CPTI inhibition by malonyl-CoA

The capacity of the LCPTI mutant to show enzyme activity despite the presence of malonyl-CoA was evaluated in pancreatic β-cells.

INS(832/13) cells were infected with Ad-LCPTI wt and Ad-LCPTI M593S as described in MATERIALS AND METHODS (Section 6.8). Mitochondrion-enriched cell fractions were incubated with different amounts of malonyl-CoA and CPTI activity assay was performed.

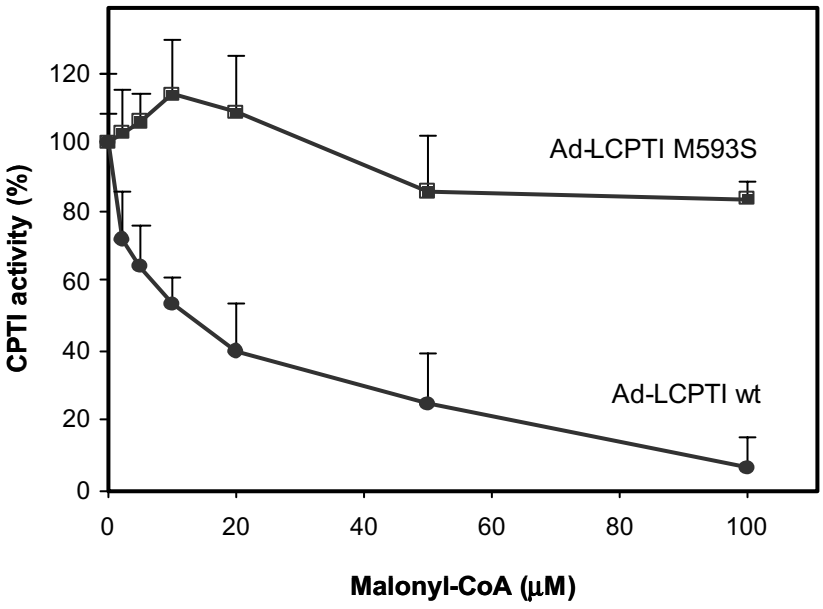

Fig. 3. Malonyl-CoA inhibition of CPTI in INS(832/13) cells infected with Ad-LCPTI wt and Ad-LCPTI M593S. INS(832/13) cells were infected with Ad-LCPTI wt or Ad-LCPTI M593S and 24 h later CPTI activity assay was performed with 8 μg of mitochondrion-enriched cell fractions incubated with different amounts of malonyl-CoA. Data are expressed relative to control values in the absence of malonyl-CoA (100%) as the mean ± SE of 6 independent experiments performed in duplicate.

As shown in Fig. 3 in the presence of 100 μM malonyl-CoA mitochondrion-enriched fractions of cells infected with Ad-LCPTI M593S retained 84% of their

activity while that of the LCPTI wt was almost completely inhibited. LCPTI M593S showed enzyme activity despite the presence of malonyl-CoA, therefore this LCPTI mutant is indeed insensitive to malonyl-CoA in pancreatic β-cells.

1.2.2 CPTI inhibition by etomoxiryl-CoA

We also studied the behaviour of LCPTI M593S with the irreversible CPTI inhibitor etomoxir. The active inhibitory form of etomoxir is its CoA-derivative, etomoxiryl-CoA[3], therefore mitochondrion-enriched fractions of INS(832/13) cells infected with Ad-LCPTI wt and Ad-LCPTI M593S were incubated with different amounts of etomoxiryl-CoA and CPTI activity was assayed.

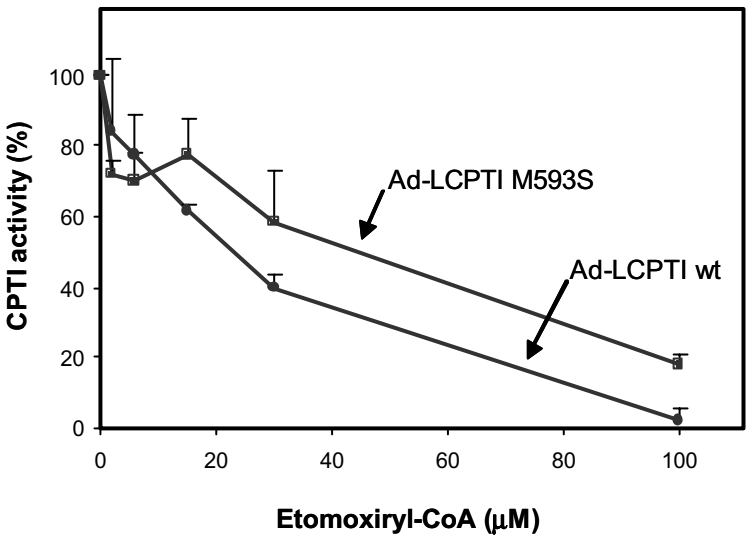

Fig. 4. Etomoxiryl-CoA inhibition of CPTI in INS(832/13) cells infected with Ad-LCPTI wt and Ad-LCPTI M593S. INS(832/13) cells were infected with Ad-LCPTI wt or Ad-LCPTI M593S and 24 h later CPTI activity assay was performed with 8 μg of mitochondrion-enriched cell fractions incubated with different amounts of etomoxiryl-CoA. Data are expressed relative to control values in the absence of etomoxiryl-CoA (100%) as the mean ± SE of 6 independent experiments performed in duplicate.

[3] Weis BC, Cowan AT, Brown N, Foster DW, McGarry JD. Use of a selective inhibitor of liver carnitine palmitoyltransferase I (CPT I) allows quantification of its contribution to total CPT I activity in rat heart. Evidence that the dominant cardiac CPT I isoform is identical to the skeletal muscle enzyme. *J. Biol. Chem.* 269:26443-26448, 1994

In the presence of 100 µM etomoxiryl-CoA mitochondrion-enriched fractions of cells infected with Ad-LCPTI M593S retained 18% of their activity while that of the LCPTI wt was almost completely inhibited (Fig. 4). Therefore, in INS(832/13) cells LCPTI M593S was partially inhibited by etomoxiryl-CoA although this LCPTI mutant form was still less sensitive to etomoxiryl-CoA than LCPTI wt. The differences between Fig. 3 and Fig. 4 could be explained because etomoxir binds covalently and irreversibly to the protein LCPTI.

1.2.3 CPTI activity in INS(832/13) cells infected with different amounts of Ad-LCPTI wt and Ad-LCPTI M593S

To study the variation of CPTI activity *vs* the amount of virus used and to find equal conditions of CPTI activity for both Ad-LCPTI wt and Ad-LCPTI M593S, CPTI activity was analysed in detail.

INS(832/13) cells were infected with different amounts of Ad-LCPTI wt (Fig. 5A) and Ad-LCPTI M593S (Fig. 5B) and CPTI activity assay was performed with 8 µg of mitochondrion-enriched cell fractions. In both cases CPTI activity increased to a plateau of 9-10 fold compared with the endogenous LCPTI, calculated from Ad-LacZ infected cells (5.0 ± 1.8 nmol.mg^{-1} prot.min^{-1}). For subsequent experiments we decided to use the amount of adenovirus LCPTI wt (1.7 pfu/cell) and LCPTI M593S (4.1 pfu/cell) that increased CPTI activity 6-fold (30 nmol. mg^{-1}prot. min^{-1}) with respect to the control Ad-LacZ.

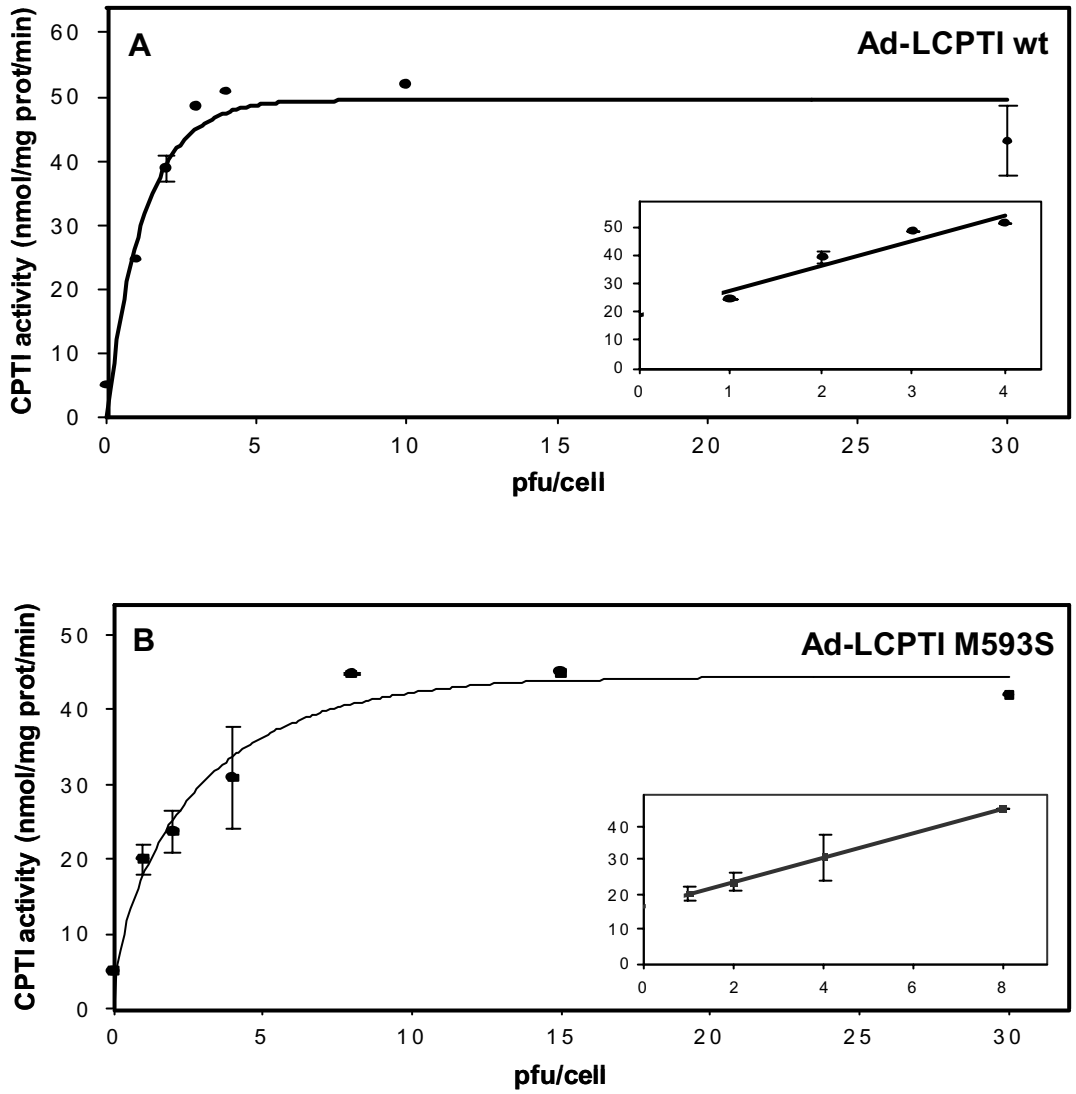

Fig. 5. CPTI activity of INS(832/13) cells infected with different amounts of Ad-LCPTI wt and Ad-LCPTI M593S. INS(832/13) cells were infected with different pfu/cell of Ad-LCPTI wt (**A**) or Ad-LCPTI M593S (**B**). 24 h later mitochondrion-enriched cell fractions were obtained and 8 µg of protein were used for the CPTI activity assay. The amount of both viruses that increased CPTI activity 6-fold, compared with Ad-LacZ (0 pfu/cell), were chosen for further experiments (1.7 pfu/cell for Ad-LCPTI wt and 4.1 pfu/cell for Ad-LCPTI M593S). Insert: expanded dose-response curve. Data are the mean ± SE of 4 independent experiments performed in duplicate.

In an additional experiment cells were also incubated for 30 min with or without 200 µM of etomoxir and CPTI activity assay was performed with 8 µg of mitochondrion-enriched cell fractions. The 200 µM concentration of etomoxir was chosen as is the amount of etomoxir enough to completely inhibit LCPTI wt (Fig. 4).

This irreversible CPTI inhibitor blocked CPTI activity in Ad-LacZ- and Ad-LCPTI wt-infected cells, leaving the malonyl-CoA/etomoxiryl-CoA insensitive CPTII activity, probably present due to some broken mitochondria. However, etomoxir left 65% CPTI activity in Ad-LCPTI M593S-infected cells (Fig. 6).

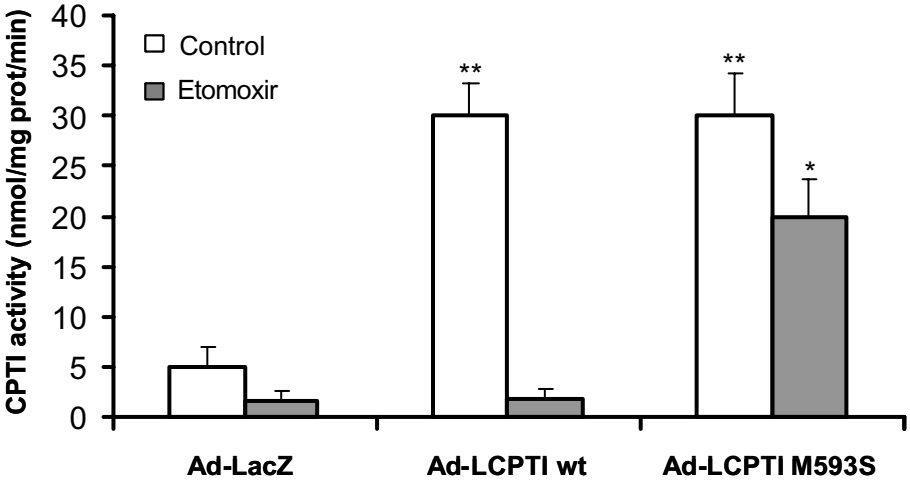

Fig. 6. CPTI activity in INS(832/13) cells infected with Ad-LCPTI wt and Ad-LCPTI M593S. INS(832/13) cells were infected with Ad-LacZ, Ad-LCPTI wt or Ad-LCPTI M593S. CPTI activity assay was performed with mitochondrion-enriched fractions of cells incubated for 30 min in KRBH 1% BSA with or without etomoxir (200 μM). Data are the mean ± SE of 4 independent experiments performed in duplicate. *P<0.05 *vs* Ad-LCPTI M593S without etomoxir; **P<0.001 *vs* Ad-LacZ.

Thus, expression of LCPTI wt and LCPTI M593S in the β-cell was successful in markedly increasing enzymatic activity of CPTI. Moreover, in pancreatic β-cells LCPTI M593S showed enzyme activity despite the presence of malonyl-CoA and was even less sensitive to etomoxiryl-CoA than LCPTI wt.

1.3 CPTI PROTEIN IN INS(832/13) CELLS AND RAT ISLETS INFECTED WITH Ad-LCPTI wt AND Ad-LCPTI M593S

To examine whether the increase in CPTI activity seen with Ad-LCPTI wt and Ad-LCPTI M593S-infected cells was correlated with an increase in LCPTI protein expression, Western blot analysis was performed.

INS(832/13) cells were infected with different amounts of Ad-LCPTI wt and Ad-LCPTI M593S and 24 h after the infection, total protein analyzed by Western blot

with the anti-LCPTI specific antibody revealed the expected 88 kDa band corresponding to LCPTI protein. As shown in Fig. 7, in both adenoviruses the signal increased consistent with the increased pfu/cell used.

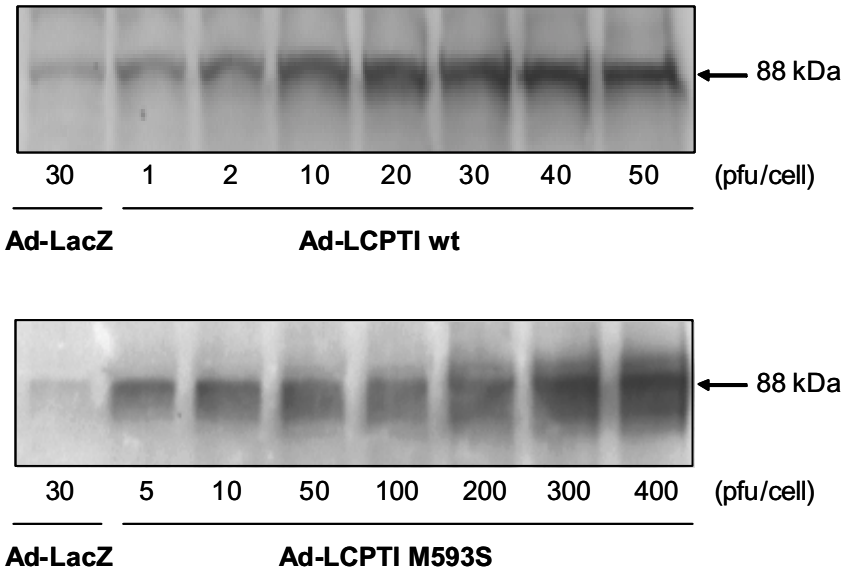

Fig. 7. Western blot of INS(832/13) cells infected with different amounts of Ad-LCPTI wt and Ad-LCPTI M593S. INS(832/13) cells were infected with different amounts of Ad-LCPTI wt and Ad-LCPTI M593S and with 30 pfu/cell of Ad-LacZ as a control. Cell lysate was analyzed by Western blot with the anti-LCPTI specific antibody giving a unique band of 88 kDa.

As explained above, we used the amount of adenovirus LCPTI wt and LCPTI M593S that increased CPTI activity 6-fold respect to the control Ad-LacZ. Therefore, a Western blot analysis was performed with INS(832/13) cells infected with 1.7 pfu/cell of Ad-LCPTI wt and 4.1 pfu/cell of Ad-LCPTI M593S (Fig. 8A) and, consistent with the activity assays, it showed similar amounts of protein in Ad-LCPTI wt and Ad-LCPTI M593S-infected cells.

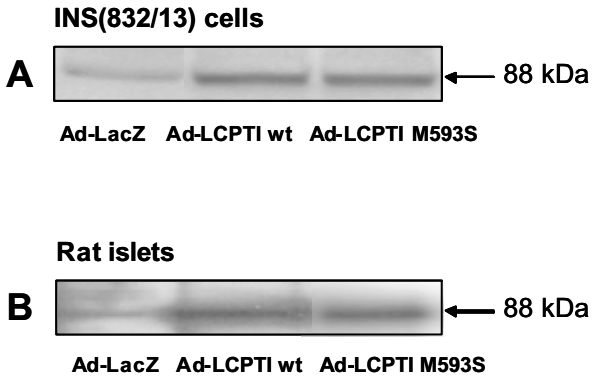

Fig. 8. Immunoblot analysis of LCPTI expressed in infected INS(832/13) cells and rat islets. (**A**) INS(832/13) cells infected with Ad-LacZ (4.1 pfu/cell), Ad-LCPTI wt (1.7 pfu/cell) and Ad-LCPTI M593S (4.1 pfu/cell) were collected and protein extracts were separated by SDS/PAGE (8% gels) and subjected to immunoblotting by using a specific antibody for CPTI from liver. A unique band corresponding to a protein of approx. 88 kDa was seen in control, Ad-LCPTI wt and Ad-LCPTI M593S infected cells. (**B**) Rat islets (batches of 100-200) were infected with the different adenoviruses as described in MATERIALS AND METHODS (Section 13.3) and 24 h later LCPTI protein expression was determined by Western blot.

When rat islets were infected with Ad-LacZ, Ad-LCPTI wt and Ad-LCPTI M593S as detailed in MATERIALS AND METHODS (Section 13.3), again as with INS(832/13) cells, Western blot analysis showed similar LCPTI protein levels with both LCPTI wt and LCPTI M593S constructs (Fig. 8B). Thus, expression of LCPTI wt and LCPTI M593S in the β-cell was successful in markedly increasing LCPTI protein.

1.4 EFFECT OF LCPTI M593S EXPRESSION ON PALMITATE OXIDATION

To test the metabolic relevance of a malonyl-CoA-insensitive LCPTI, we assessed fatty acid oxidation in pancreatic β-cells. [1-^{14}C]palmitate oxidation to CO_2 and to acid soluble products (ASP), which is an important component of total fatty acid oxidation in β-cells[4] composed essentially by ketone bodies[5], was measured in adenovirus-treated INS(832/13) cells. These cells were infected with Ad-LacZ, Ad-LCPTI wt or Ad-LCPTI M593S. 24 h after viral treatment cells were preincubated for 30 min in KRBH medium containing 1% BSA and then incubated for 2 h at 2.5, 7.5 or 15 mM glucose in the presence of [1-^{14}C]palmitate. Fatty acid oxidation to CO_2 and to ASP was measured as detailed in MATERIALS AND METHODS (Section 10.1).

Elevated glucose suppressed palmitate oxidation in both control and LCPTI-overexpressing cells (LCPTI wt and LCPTI M593S) (Fig. 9). This finding indicates that the overexpressing cells respond normally to glucose with respect to palmitate oxidation. However, the degree of suppression observed in response to elevated glucose in LCPTI wt and LCPTI M593S overexpressing cells was insufficient to normalize palmitate oxidation to the levels obtained in control Ad-LacZ-infected cells.

Interestingly, fatty acid oxidation was highest in cells infected with Ad-LCPTI M593S at all the glucose concentrations tested. At high glucose (15 mM) fatty acid oxidation to CO_2, ASP, and their sum were increased by 8.3, 3.4 and 4.4 fold respectively, compared with Ad-LacZ-infected cells. These oxidation rates were higher than those obtained when overexpression was performed with Ad-LCPTI wt (3.3, 1.5 and 1.8 fold, respectively).

These findings confirm that even at high malonyl-CoA concentrations (high glucose), fatty acid oxidation in LCPTI M593S overexpressing cells is much higher than in the control Ad-LacZ-infected cells and still higher than in cells infected with Ad-LCPTI wt. Since LCPTI M593 is resistant to malonyl-CoA, β-oxidation to CO_2 and ketone bodies (acid soluble compounds) is accelerated in cells overexpressing the mutated enzyme.

---

[4] Roduit R, Nolan C, Alarcon C, Moore P, Barbeau A, Delghingaro-Augusto V, Przybykowski E, Morin J, Masse F, Massie B, Ruderman N, Rhodes C, Poitout V, Prentki M. A Role for the Malonyl-CoA/Long-Chain Acyl-CoA Pathway of Lipid Signaling in the Regulation of Insulin Secretion in Response to Both Fuel and Nonfuel Stimuli. *Diabetes* 53:1007-1019, 2004

[5] Fulgencio JP, Kohl C, Girard J, Pegorier JP. Troglitazone inhibits fatty acid oxidation and esterification, and gluconeogenesis in isolated hepatocytes from starved rats. *Diabetes* 45:1556-1562, 1996

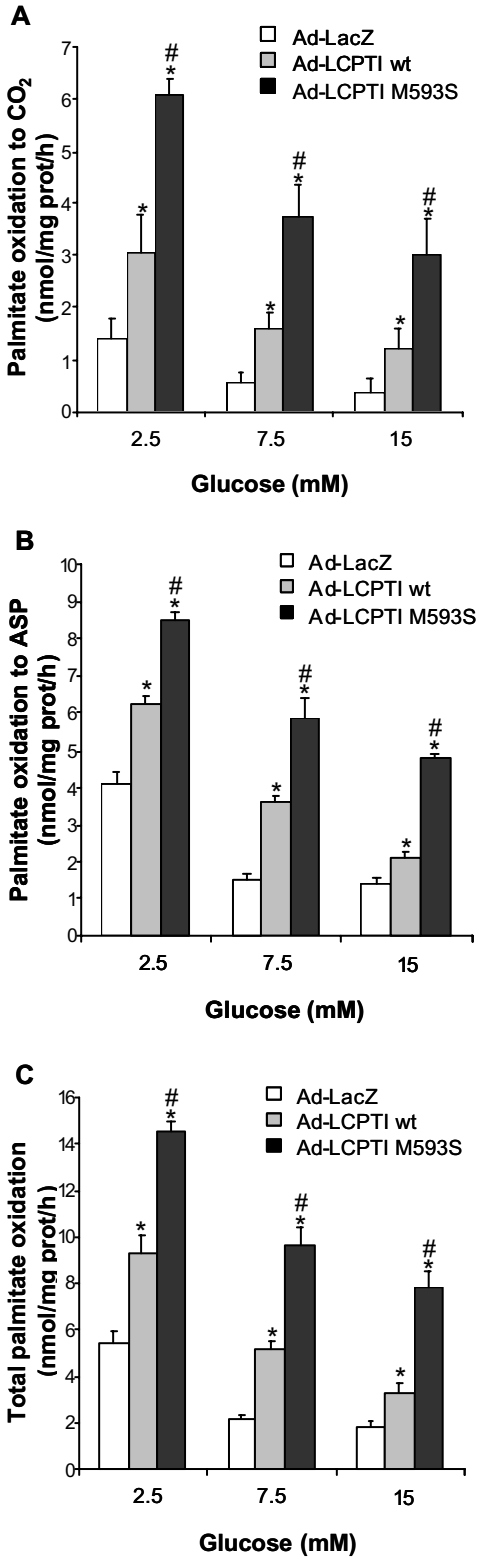

Fig. 9. Fatty acid oxidation in INS(832/13) cells infected with Ad-LCPTI wt and Ad-LCPTI M593S. Cells were infected with Ad-LacZ, Ad-LCPTI wt or Ad-LCPTI M593S. 24 h after viral treatment cells were preincubated for 30 min at 37ºC in KRBH medium containing 1% BSA and then incubated for 2 h at 2.5, 7.5 or 15 mM glucose in the presence of 0.8 mM carnitine, 1 µCi/ml [1-^{14}C]palmitate and 0.25 mM unlabeled palmitate bound to 1% (w/v) BSA. Palmitate oxidation to CO_2 (**A**), ASP (**B**), and total palmitate oxidation (CO_2 + ASP) (**C**), was measured as described in MATERIALS AND METHODS (Section 10.1). Data are the mean ± SE of 5 independent experiments performed in triplicate. *P<0.05 *vs* Ad-LacZ; #P<0.05 *vs* Ad-LCPTI wt.

In an additional experiment cells were also incubated for 30 min with or without 200 μM of etomoxir and palmitate oxidation to $^{14}CO_2$ was measured at low (2.5 mM) and high (15 mM) glucose (Fig. 10).

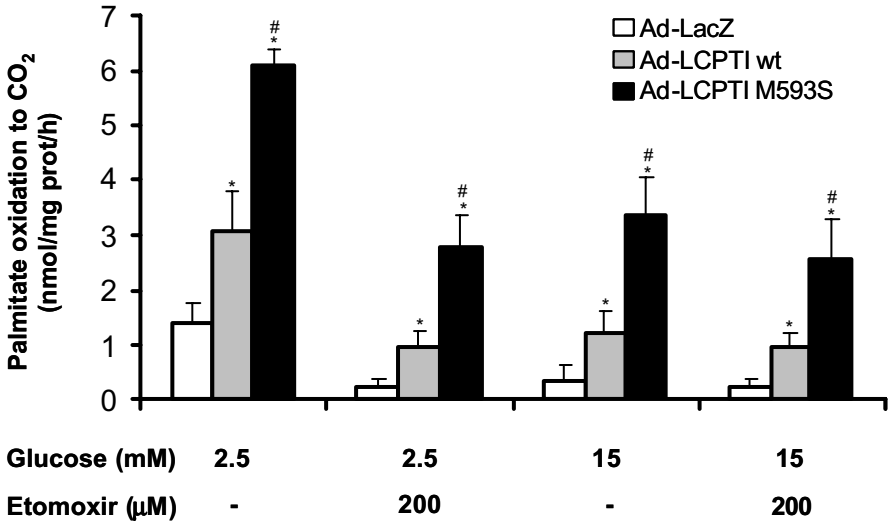

Fig. 10. Fatty acid oxidation in INS(832/13) cells infected with Ad-LCPTI wt and Ad-LCPTI M593S and incubated with or without etomoxir. INS(832/13) cells were infected with Ad-LacZ, Ad-LCPTI wt or Ad-LCPTI M593S. 24 h after viral treatment cells were preincubated for 30 min at 37ºC in KRBH medium containing 1% BSA with or without 200 μM etomoxir, washed with KRBH 0.1% BSA to completely eliminate etomoxir and then incubated for 2 h at 2.5 or 15 mM glucose in the presence of 0.8 mM carnitine, 1 μCi/ml [1-^{14}C]palmitate and 0.25 mM unlabeled palmitate bound to 1% (w/v) BSA. Palmitate oxidation to CO_2 was measured as described in MATERIALS AND METHODS (Section 10.1). Data are the mean ± SE of 3 independent experiments performed in triplicate. *P<0.05 *vs* Ad-LacZ; #P<0.05 *vs* Ad-LCPTI wt.

This irreversible CPTI inhibitor decreased palmitate oxidation at low glucose and to a lesser extent at high glucose in both Ad-LCPTI wt- and Ad-LCPTI M593S-infected cells. However, the LCPTI M593S construct continued to produce a higher palmitate oxidation rate than those obtained when overexpression was performed with Ad-LCPTI wt, either at low or at high glucose. In the presence of etomoxir, fatty acid oxidation to CO_2 was increased by 11.8 and 11.0 fold at 2.5 and 15 mM glucose respectively, compared with Ad-LacZ-infected cells, while LCPTI wt produced an increase of 4.2 and 4.1 at 2.5 and 15 mM glucose respectively.

It is important to notice that, in all cases, LCPTI M593S construct caused higher palmitate oxidation than LCPTI wt despite the fact that INS(832/13) cells were infected with the appropriate amount of each virus to yield the same LCPTI activity, a 6-fold increase respect to control Ad-LacZ-infected cells. Thus, the increase in palmitate oxidation of LCPTI M593S compared to LCPTI wt was due to its insensitiveness to malonyl-CoA, which is effective either at low or at high glucose, i.e. either at low or at high malonyl-CoA levels.

1.5 MALONYL-CoA LEVELS

To examine the effect of the expression of LCPTI wt and LCPTI M593S on malonyl-CoA levels in the β-cell, the malonyl-CoA content was measured at the same infection and preincubation conditions as those used in palmitate oxidation assays. INS(832/13) cells were infected with Ad-LacZ, Ad-LCPTI wt or Ad-LCPTI M593S and 24 h later cells were incubated for 30 min at 2.5 or 15 mM glucose. Then, malonyl-CoA was extracted from the cells and measured with a radioactive method using purified fatty acid synthase.

Malonyl-CoA levels were not modified by LCPTI wt or LCPTI M593S overexpression, compared with LacZ control cells, either at 2.5 mM glucose or at 15 mM glucose (Fig. 11).

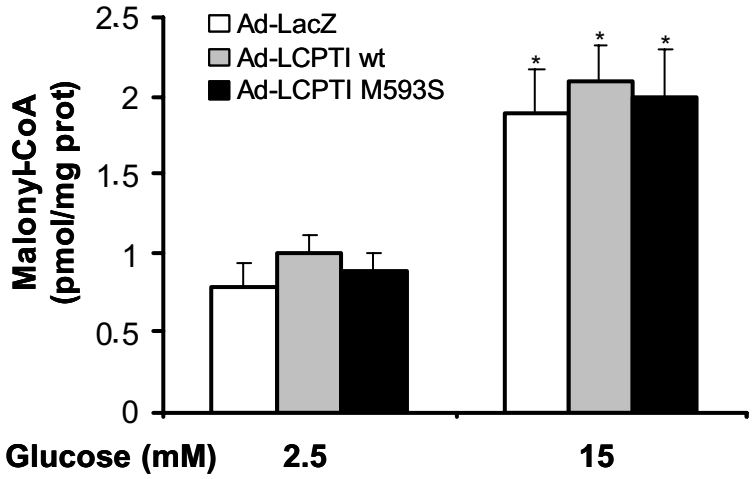

Fig. 11. Malonyl-CoA content in INS(832/13) cells overexpressing LCPTI wt and LCPTI M593S. INS(832/13) cells were infected with Ad-LacZ, Ad-LCPTI wt or Ad-LCPTI M593S and 24 h later, cells were incubated for 30 min with KRBH 0.1% BSA containing 2.5 or 15 mM glucose. Malonyl-CoA was extracted and assayed with a radioactive method using purified fatty acid synthase as detailed in MATERIALS AND METHODS (Section 11.2). Data are the mean ± SE of 4 independent experiments performed in duplicate. *P<0.05 *vs* 2.5 mM glucose.

Therefore, the differences seen in palmitate oxidation between LCPTI M593S and LCPTI wt were not due to changes in malonyl-CoA levels in the β-cell.

1.6 GLUCOSE OXIDATION

No toxicity was seen in INS(832/13) cells or rat islets infected with any of the adenoviruses used, but the adenovirus expression of an enzyme could alter the cellular metabolism. Thus, as a control, [U-^{14}C]glucose utilization was measured in INS(832/13) cells infected with the different adenoviruses at the same infection and incubation conditions used in palmitate oxidation assays.

INS(832/13) cells were infected with Ad-LacZ, Ad-LCPTI wt or Ad-LCPTI M593S and 24 h later, [U-^{14}C]glucose oxidation to $^{14}CO_2$ was measured after a 2 h incubation of the cells at 2.5 or 15 mM glucose.

Glucose oxidation at low (2.5 mM) and high (15 mM) glucose remained unaltered in cells overexpressing both the wt and mutated LCPTI constructs (Fig. 12). This is in accordance with the view that a Randle cycle is inoperative in the β-cell[6] and that adenovirus expression did not affect glucose metabolism.

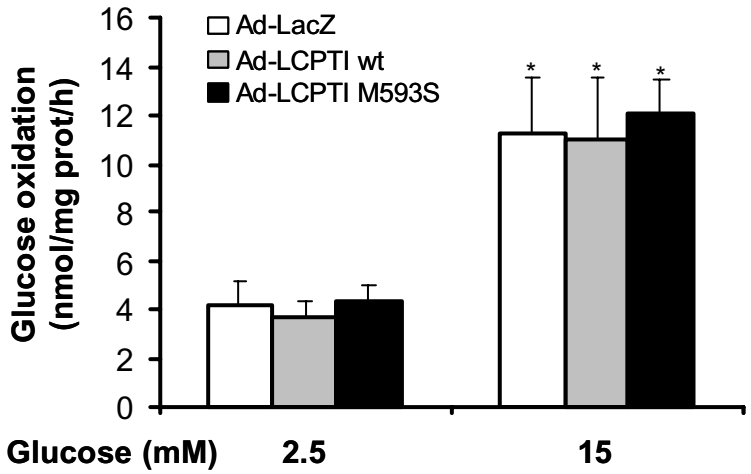

Fig. 12. G**lucose oxidation in INS(832/13) cells expressing LCPTI M593S.** INS(832/13) cells were infected with Ad-LacZ, Ad-LCPTI wt or Ad-LCPTI M593S and 24 h later, they were preincubated for 30 min at 37ºC in KRBH medium containing 1% BSA. Glucose oxidation to $^{14}CO_2$ was measured after a 2 h incubation of the cells at 2.5 or 15 mM glucose in the presence of 0.5 μCi/ml [U-^{14}C]glucose as described in MATERIALS AND METHODS (Section 10.2). Data are the mean ± SE of 4 independent experiments performed in triplicate. *P<0.05 *vs* 2.5 mM glucose.

[6] Segall L, Lameloise N, Assimacopoulos-Jeannet F, Roche E, Corkey P, Thumelin S, Corkey BE, Prentki M. Lipid rather than glucose metabolism is implicated in altered insulin secretion caused by oleate in INS-1 cells. *Am. J. Physiol*. 277:E521-528, 1999

1.7 GLUCOSE-STIMULATED INSULIN SECRETION IN Ad-LCPTI M593S-INFECTED INS(832/13) CELLS AND RAT ISLETS

1.7.1 GSIS in INS(832/13) cells expressing LCPTI M593S

At the same CPTI activity and protein levels, LCPTI M593S produced higher rates of palmitate oxidation than LCPTI wt, although control experiments of malonyl-CoA content and glucose utilization indicated that adenovirus infection or LCPTI expression did not affect these parameters. We then examined if β-cells transduced with LCPTI M593S had more impaired GSIS than cells transduced with LCPTI wt.

We used the same culture, infection and preincubation conditions as in the previous experiments. INS(832/13) cells were infected with Ad-LacZ, Ad-LCPTI wt or Ad-LCPTI M593S and 24 h later, cells were incubated for 1 h in KRBH 0.1% BSA containing the different secretagogues.

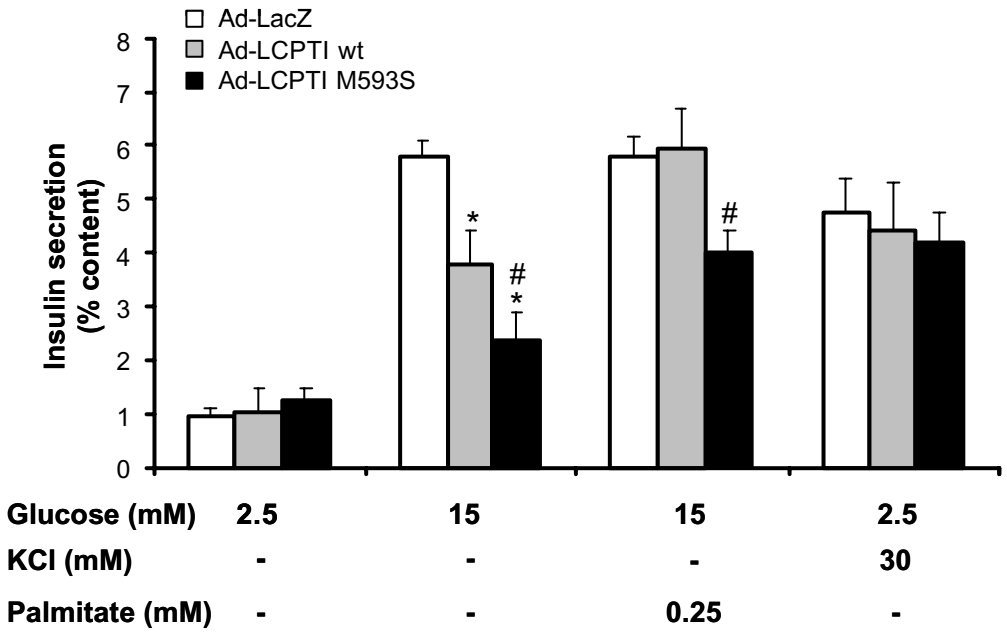

Fig. 13. Effect of LCPTI M593S expression on GSIS in INS(832/13) cells. INS(832/13) cells were infected with Ad-LacZ, Ad-LCPTI wt or Ad-LCPTI M593S. 24 h later, cells were preincubated for 30 min in KRBH 1% BSA and incubated for 1 h in KRBH 0.1% BSA containing either 2.5, 15 mM glucose, 15 mM glucose plus 0.25 mM palmitate bound to 1% (w/v) BSA or 2.5 mM glucose plus 30 mM KCl as described in MATERIALS AND METHODS (Section 12). Insulin release was determined by RIA. Data are the mean ± SE of 4 independent experiments performed in triplicate. *P<0.05 *vs* Ad-LacZ and $^{\#}$P<0.05 *vs* Ad-LCPTI wt.

As shown in Fig. 13, GSIS was reduced by 60% in INS(832/13) cells infected with Ad-LCPTI M593S and by 40% in Ad-LCPTI wt-infected cells, both with respect to control Ad-LacZ. The higher decrease in GSIS caused by LCPTI M593S expression indicates the deep metabolic influence of a malonyl-CoA non-regulated fatty acid oxidation system.

GSIS was recovered completely in the presence of 0.25 mM palmitate only in the case of LCPTI wt, suggesting that at high glucose the provision of exogenous FFA was not matched by a rise in intracellular FFA (non-esterified palmitate) in cells overexpressing the mutated enzyme due to the dramatically enhanced fatty acid oxidation. The results in Fig. 18D described below are in total accordance with this view.

As a control of the insulin secretion mechanism, cells were incubated at low glucose in the presence of 30 mM KCl and insulin release was found to be similar in the three cases of adenovirus-infected cells, indicating that the exocytotic machinery is preserved in cells transduced with the various constructs.

Insulin secretion was also measured in the presence of etomoxir. Infected cells were preincubated for 30 min with or without 200 µM etomoxir. After that, cells were washed to remove etomoxir and then incubated for 1 h at 2.5 or 15 mM glucose. The irreversible CPTI inhibitor restored the impairment in GSIS caused either by LCPTI wt or by LCPTI M593S overexpression (Fig. 14).

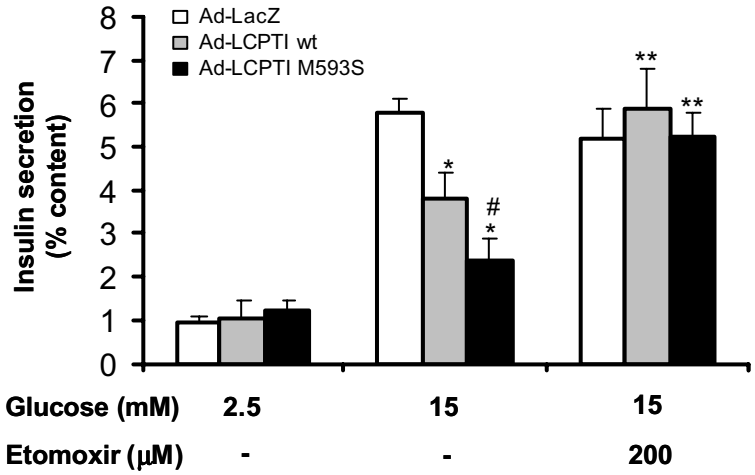

Fig. 14. Effect of LCPTI M593S expression on GSIS in the presence of etomoxir. INS(832/13) cells were infected with Ad-LacZ, Ad-LCPTI wt or Ad-LCPTI M593S. 24 h after viral treatment cells were preincubated for 30 min at 37ºC in KRBH medium containing 1% BSA with or without 200 µM etomoxir, washed with KRBH 0.1% BSA to completely eliminate etomoxir and then incubated for 1 h in KRBH 0.1% BSA containing either 2.5 or 15 mM glucose. Insulin release was determined by RIA. Data are the mean ± SE of 3 independent experiments performed in triplicate. *P<0.05 *vs* Ad-LacZ, #P<0.05 *vs* Ad-LCPTI wt and **P<0.05 *vs* without etomoxir.

Insulin secretion was also studied in the presence of 35 mM K^+ plus 250 µM diazoxide, a condition revealing the K_{ATP} channel-independent pathway of glucose sensing[7]. The expression of LCPTI wt and LCPTI M593S led to a decrease in insulin release (the difference between 15 and 2.5 mM glucose) of 55 ± 12% and 85 ± 17% (n=3) respectively, compared with Ad-LacZ-infected cells. This is consistent with the view that K_{ATP}-independent signalling (also referred as the amplification pathway) was affected in cells overexpressing LCPTI construct (Fig. 15).

[7] Henquin JC. Triggering and amplifying pathways of regulation of insulin secretion by glucose. *Diabetes* 49:1751-1769, 2000

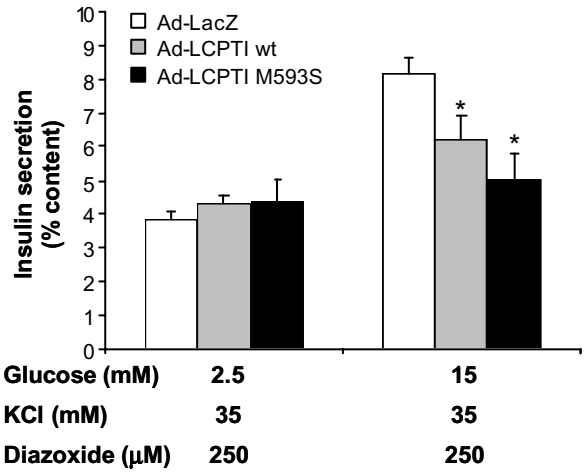

Fig. 15. Effect of LCPTI M593S expression on the K_{ATP} channel-independent GSIS in INS(832/13) cells. INS(832/13) cells were infected with Ad-LacZ, Ad-LCPTI wt or Ad-LCPTI M593S. 24 h later, cells were preincubated for 30 min in KRBH 1% BSA and incubated for 1 h with KRBH 0.1% BSA in the presence of depolarizing K^+ (35 mM) and 250 μM diazoxide at 2.5 mM glucose or 15 mM glucose, to measure K_{ATP} channel-independent glucose sensing as described in MATERIALS AND METHODS (Section 12). Insulin release was determined by RIA. Data are the mean ± SE of 4 independent experiments performed in triplicate. $^*P<0.05$ *vs* Ad-LacZ.

1.7.2 GSIS in rat islets expressing LCPTI M593S

The insulin secretion experiments described above were performed in a rat insulinoma cell line that do not function in the same manner as normal islets and therefore may not entirely reflect the situation in native β-cells. For this reason we performed insulin secretion experiments with isolated rat islets overexpressing LCPTI wt and LCPTI M593S.

Isolated rat islets were infected with Ad-LacZ, Ad-LCPTI wt or Ad-LCPTI M593S as described in MATERIALS AND METHODS (Section 13.3) and 24 h after infection batches of 10 islets each were incubated for 30 min at 2.8 and 16.7 mM glucose.

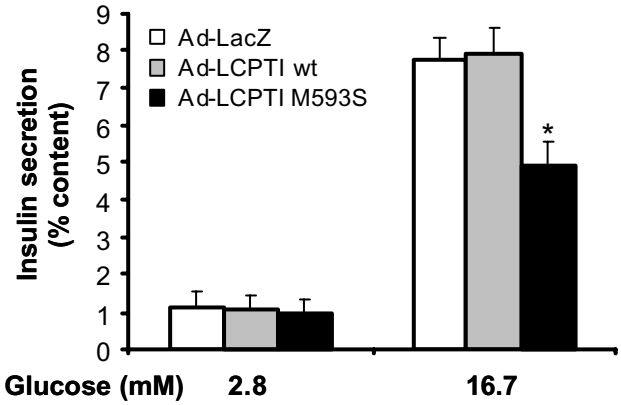

Fig. 16. Effect of LCPTI M593S expression on GSIS in rat islets. Isolated rat islets were infected with Ad-LacZ, Ad-LCPTI wt or Ad-LCPTI M593S as detailed in MATERIALS AND METHODS (Section 13.3). Batches of 10 islets each were washed and incubated for 30 min in KRBH 0.1% BSA containing 2.8 or 16.7 mM glucose and insulin release was determined by RIA. Data are the mean ± SE of 3 independent experiments performed in triplicate. *P<0.05 *vs* Ad-LacZ.

In control islets, raising glucose from 2.8 mM to 16.7 mM induced insulin secretion 6.8-fold (Fig. 16). In islets overexpressing LCPTI M593S, GSIS was decreased by 40% compared to the Ad-LacZ control, while no difference was seen with Ad-LCPTI wt-infected islets. To explain the difference in the results between INS(832/13) cells and islets we hypothesize that normal β-cells are more protected than INS cells against lipid depletion due to enhanced fat oxidation such that only the more efficient LCPTI M593S construct is active in rat islets.

1.8 ESTERIFICATION PROCESSES

To examine whether the increase in fatty acid oxidation could reduce the availability of LC-CoA for lipid signalling we measured esterification processes in INS(832/13) cells transduced with LCPTI wt and LCPTI M593S.

INS(832/13) cells infected with Ad-LacZ, Ad-LCPTI wt or Ad-LCPTI M593S were preincubated for 30 min in KRBH medium containing 1% BSA and then incubated for 2 h at 2.5 or 15 mM glucose in the presence [1-^{14}C]palmitate. The levels of [1-^{14}C]palmitate incorporated to phospholipids (PL), diacylglycerol (DAG), triacylglycerides (TG), cholesterol esters (CE) as well as the levels of non-esterified palmitate (NE Palm) were measured as described in MATERIALS AND METHODS (Section 10.3) (Fig. 17).

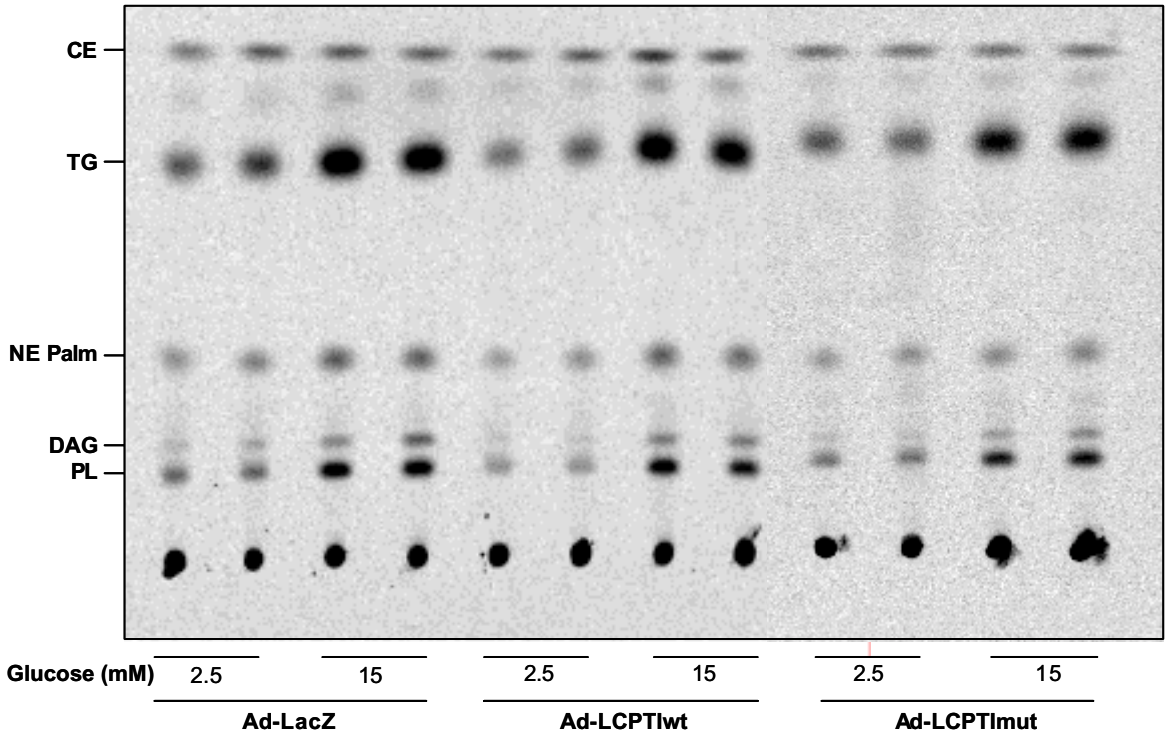

Fig. 17. Representative experiment of TLC in esterification processes measurements. INS(832/13) infected with Ad-LacZ, Ad-LCPTI wt or Ad-LCPTI M593S were preincubated for 30 min at 37ºC in KRBH medium containing 1% BSA and then incubated for 2 h at 2.5 or 15 mM glucose in the presence of 0.8 mM carnitine, 1 µCi/ml [1-^{14}C]palmitate and 0.25 mM unlabeled palmitate bound to 1% (w/v) BSA. Total lipids were extracted and fatty acid esterification into phospholipids (**PL**), diacylglycerol (**DAG**), triglyceride (**TG**), non-esterified palmitate (**NE Palm**) and cholesterol esters (**CE**) were separated by thin layer chromatography (TLC) and identified using migration references. Plates are eluted with hexan:diethylether:acetic acid (70:30:1, v/v/v) and quantified with a Storm 840 Laser scanning system. The lowest and darkest spots are other cellular lipids that did not migrate with the solvent and were retained at the application point. Data are a representative experiment out of 4 performed in duplicate.

We also measured the total triglyceride content in Ad-LacZ, Ad-LCPTI wt and Ad-LCPTI M593S-infected cells. TG content was extracted by the Folch method and measured with a spectrophotometric assay.

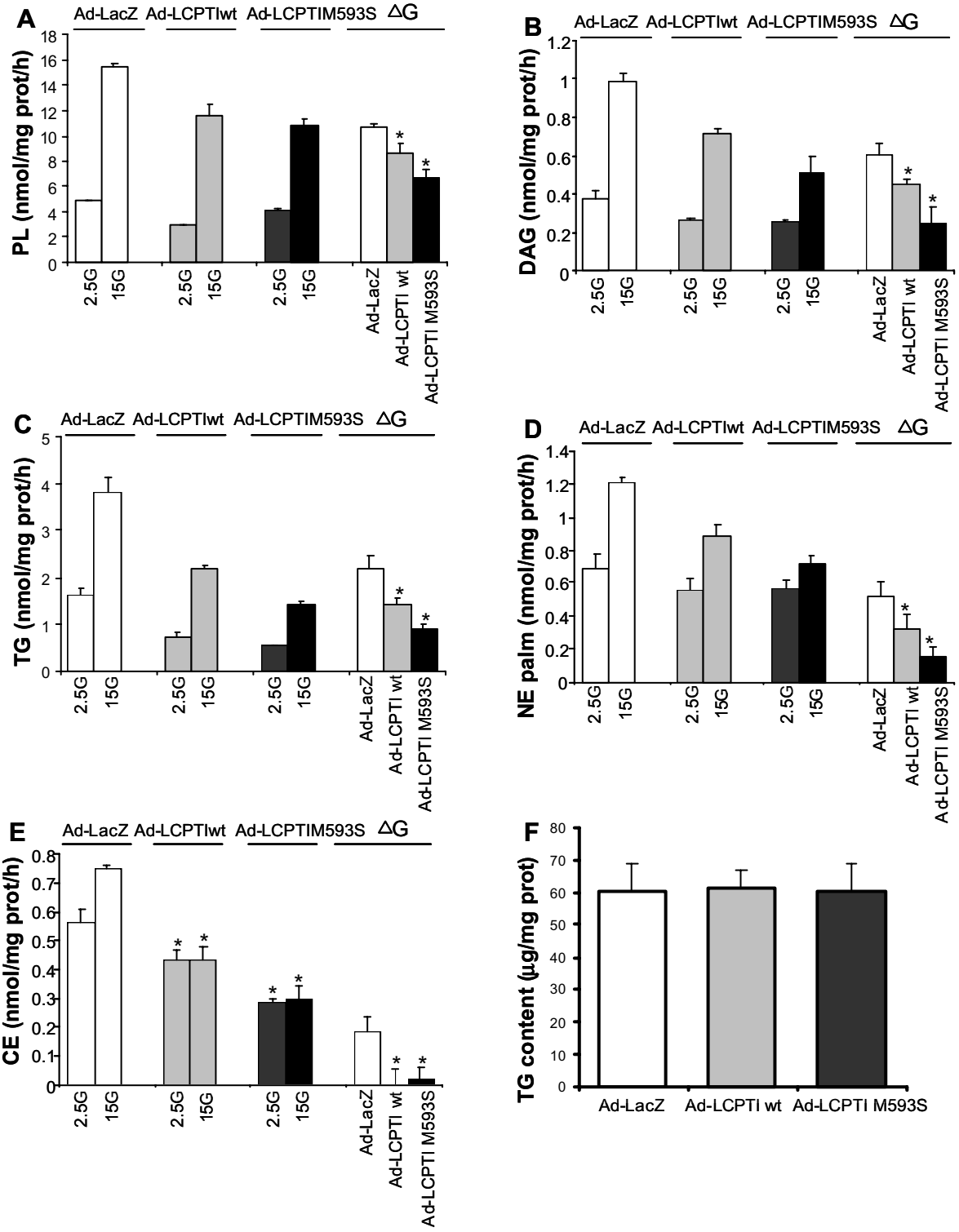

Fig. 18. Glucose-induced fatty acid esterification processes in INS(832/13) cells expressing LCPTI. INS(832/13) infected with Ad-LacZ, Ad-LCPTI wt or Ad-LCPTI M593S were preincubated for 30 min at 37ºC in KRBH medium containing 1% BSA and then incubated for 2 h at 2.5 or 15 mM glucose in the presence of 0.8 mM carnitine, 1 µCi/ml [1-^{14}C]palmitate and 0.25 mM unlabeled palmitate bound to 1% (w/v) BSA. Fatty acid esterification into phospholipids (**A**), diacylglycerol (**B**), triglyceride (**C**), non-esterified palmitate (**D**) and cholesterol esters (**E**) were assessed using thin layer chromatography after lipid extraction. ΔG is the difference between the incorporation of palmitate in the particular lipid class at 15 mM glucose *vs* 2.5 mM glucose. Total triglyceride content (**F**) was extracted by Folch method and measured with a spectrophotometric assay. Data are the mean ± SE of 4 independent experiments performed in duplicate. *P<0.05 *vs* Ad-LacZ.

Glucose-induced palmitate esterification into the different complex lipid species was expressed as the differences (ΔG) between high (15 mM) and low (2.5 mM) glucose (Fig. 18). The glucose-induced rise in PL, DAG, TG and NE Palm was decreased by 20%, 25%, 35% and 38% respectively for Ad-LCPTI wt-infected cells and by 37%, 58%, 59% and 71% respectively, for Ad-LCPTI M593S-infected cells (Fig. 18 A, B, C, D), both compared to Ad-LacZ-infected cells. Palmitate esterification to CE was reduced by 23% and 50% for Ad-LCPTI wt and Ad-LCPTI M593S respectively at low glucose and by 42% and 60% for Ad-LCPTI wt and Ad-LCPTI M593S respectively at high glucose, both compared to the Ad-LacZ control (Fig. 18E). The cellular TG content was not changed by the overexpression of LCPTI wt nor LCPTI M593S (Fig. 18F), supporting the results on Fig. 18 showing that increased fatty acid oxidation in the β-cell affects lipid esterification processes mostly upon a glucose challenge. However, at low glucose, palmitate incorporation into TG was decreased in LCPTI transduced cells (Fig. 18C), indicating that LCPTI overexpression could affect TG incorporation while the general pool of TG content remains constant. This is probably due to the fact that differences in the incorporation of LC-CoA into TG are not reflected in the large and stable total TG pool. Fig. 18D also shows that the glucose-induced rise in NE Palm, an indirect measurement of cytosolic fatty acyl-CoA[4], was markedly curtailed in cells overexpressing the LCPTI construct and that the CPTI mutant was most effective in this respect.

1.9 PKC ACTIVITY

DAG and FA-CoA activate many PKC enzymes[8,9]. To assess whether the decrease of the glucose-induced rise in DAG and NE Palm seen in Ad-LCPTI wt and Ad-LCPTI M593S-infected cells was associated with alteration in PKC activity in the β-cell, we measured PKC activation as estimated by its translocation from cytosol to membranes.

INS(832/13) cells were infected with Ad-LacZ, Ad-LCPTI wt and Ad-LCPTI M593S. 24 h after viral treatment, cells were incubated for 30 min at 2.5 mM or 15 mM glucose and cytosolic and membrane fractions were obtained as described in

[8] Yaney GC, Korchak HM, Corkey BE. Long-chain acyl-CoA regulation of protein kinase C and fatty acid potentiation of glucose-stimulated insulin secretion. *Endocrinology* 141:1989-1998, 2000

[9] Alcázar O, Qiu-yue Z, Giné E, Tamarit-Rodriguez J. Stimulation of islet protein kinase C translocation by palmitate requires metabolism of the fatty acid. *Diabetes* 46:1153-1158, 1997

MATERIALS AND METHODS (Section 9). Western blot of membrane and cytosolic fractions was performed using a specific antibody against the PKC isoforms expressed in pancreatic β-cells (α, β and γ) giving a unique PKC band of 80 kDa. Band intensity was quantified with a Storm 840 Laser scanning system (Fig. 19).

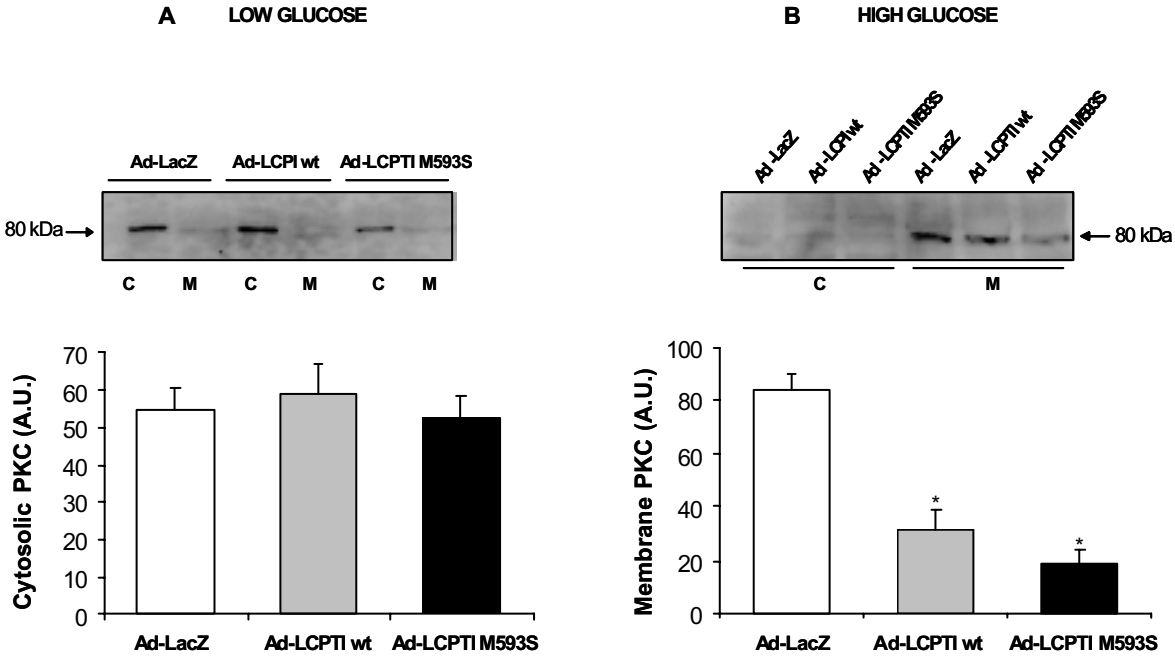

Fig. 19. PKC activation in Ad-LCPTI wt and Ad-LCPTI M593S-INS(832/13)-infected cells. INS(832/13) cells were infected with Ad-LacZ, Ad-LCPTI wt and Ad-LCPTI M593S. 24 h after infection cells were incubated for 30 min at low (2.5 mM) (**A**) or high (15 mM) (**B**) glucose. Western blot of membrane (M) and cytosolic (C) fractions was performed using a specific antibody against the PKC isoforms expressed in pancreatic β-cells (α, β and γ) giving a unique band of 80 kDa. Intensity of the PKC bands were quantified with a Storm 840 Laser scanning system. The lower panels in A and B show mean results ± SE of 3 experiments. (A.U.; arbitrary optical units). *P<0.05 *vs* Ad-LacZ.

Western blot carried out on membrane and cytosol proteins of INS(832/13) cells incubated at high (15 mM) glucose showed that PKC translocation of Ad-LCPTI wt and Ad-LCPTI M593S-infected cells was decreased by 63% and 78%, respectively, compared with Ad-LacZ-infected cells. No change in PKC translocation between Ad-

LacZ, Ad-LCPTI wt and Ad-LCPTI M593S-infected cells was seen at low glucose (2.5 mM). Since both DAG and FA-CoA activate a number of PKC enzymes, the lower values of DAG and NE Palm (an indirect determination of FA-CoA levels) observed in the LCPTI M593S-overexpressing cells suggest that enhanced β-oxidation by the LCPTI M593S mutant reduces GSIS as a result of a decrease in PKC activation.

2. STABLE EXPRESSION OF LCPTI wt AND LCPTI M593S

2.1 CLONING OF pTRE2-LCPTI wt AND pTRE2-LCPTI M593S

To stably express LCPTI wt and LCPTI M593S in INS cells we utilized the tet-on system, where the protein could be induced by doxycycline incubation.

A) Cloning of pTRE2-LCPTI wt

The cDNA of LCPTI wt had been previously cloned in our group[10] from the screening of a rat liver cDNA library. This cDNA includes the complete LCPTI codifying domain and the TAA stop codon giving a sequence of 2,700 bp. The LCPTI wt cDNA subcloned into the pCMV4 vector was used to obtain the pTRE2-LCPTI wt plasmid as follows.

The LCPTI cDNA was obtained from pCMV4-LCPTI by digestion with *Cla*I and *Xba*I. This insert was ligated with the pTRE2 vector also digested with *Cla*I and *Xba*I and the plasmid obtained was checked by sequencing and by enzymatic digestions (Fig. 20A).

B) Cloning of pTRE2-LCPTI M593S

The LCPTI M593S cDNA had been previously constructed in our group[1] using the QuickChange polymerase chain reaction-based mutagenesis procedure (Stratagene) with the pYES-LCPTI wt plasmid as template.

To obtain pTRE2-LCPTI M593S, the mutated region of LCPTI was acquired from the pYES-LCPTI M593S plasmid by digestion with *Bcl*I and *Xba*I. The pTRE2-LCPTI wt plasmid, described above, was also digested with *Bcl*I and *Xba*I and ligated

[10] Rubi B. El glutamato y los ácidos grasos participan en la transducción de la señal para la liberación de insulina estimulada por glucosa en la célula β del páncreas. Thesis, 2001

with the mutated region of LCPTI. The resultant pTRE2-LCPTI M593S plasmid was checked by sequencing to confirm the presence of the mutation (Fig. 20B).

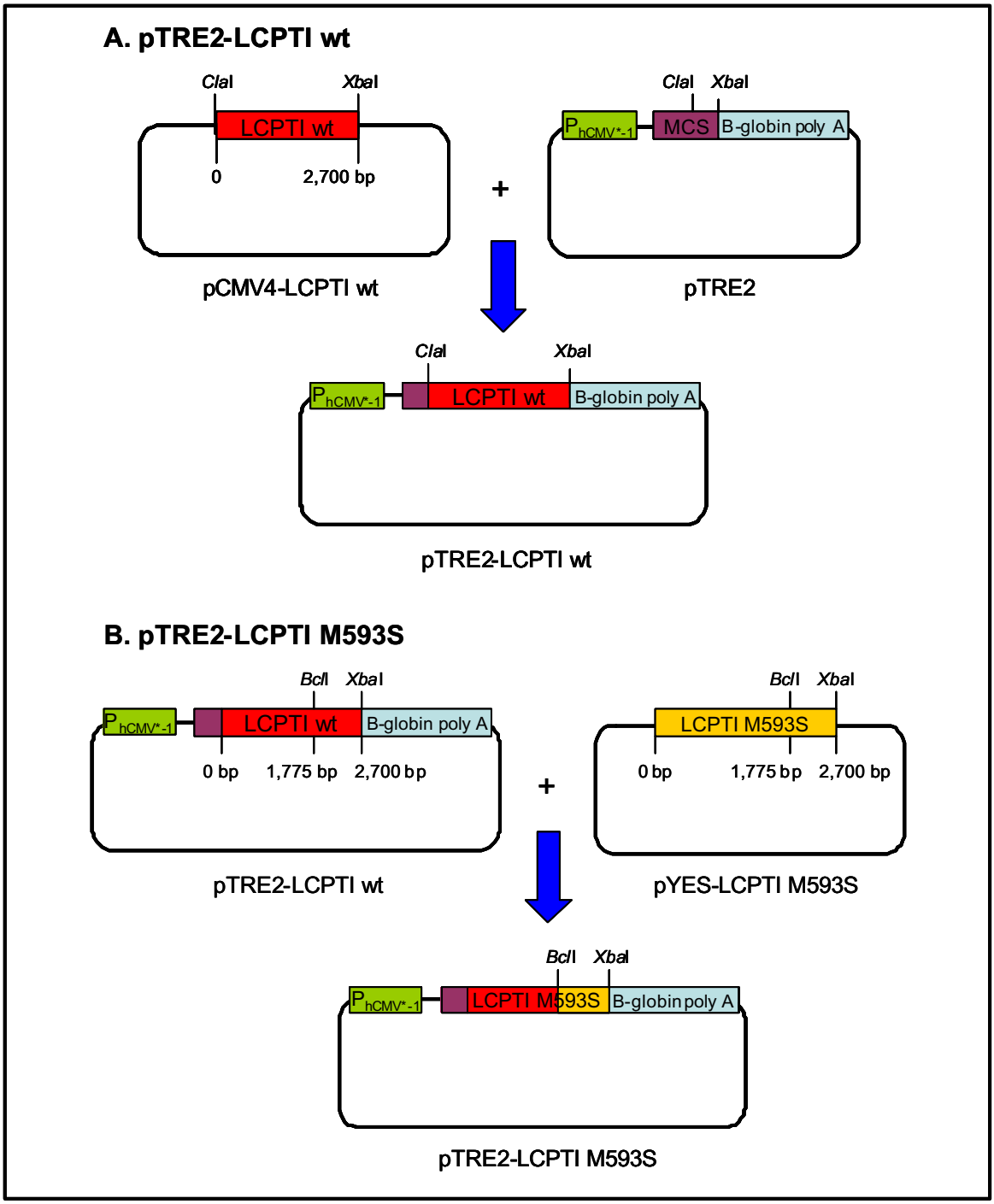

Fig. 20. pTRE2-LCPTI wt and pTRE2-LCPTI M593S construction. (**A**) pCMV4-LCPTI wt was digested with *Cla*I and *Xba*I. The fragment of 2,700 bp corresponding to the LCPTI wt was subcloned into the pTRE2 vector also digested with *Cla*I and *Xba*I to obtain pTRE2-LCPTI wt. (**B**) pYES-LCPTI M593S was digested with *Bcl*I and *Xba*I. The fragment containing the LCPTI mutation was ligated with pTRE2-LCPTI wt previously digested with *Bcl*I and *Xba*I to obtain the pTRE2-LCPTI M593S plasmid.

2.2 TRANSIENT EXPRESSION OF pTRE2-LCPTI wt

The functionality of the pTRE2-LCPTI wt construct and the correct LCPTI protein expression were checked by transient expression of pTRE2-LCPTI wt into HEK 293 rtTA cells which stably express the transactivator rtTA. HEK 293 rtTA cells were transfected by calcium phosphate with 25 µg of pTRE2-LCPTI wt as described in MATERIALS AND METHODS (Section 4) and incubated for 48 h with 1µg/ml doxycycline immediately after transfection. The cell lysate was then analyzed by Western blot using an anti-LCPTI specific antibody.

Figure 21 shows the immunoblot of HEK 293 rtTA cells transfected or not with pTRE2-LCPTI wt and incubated with or without doxycycline.

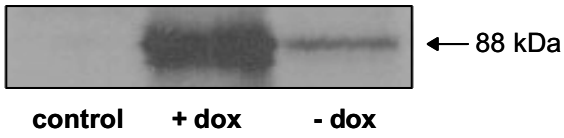

Fig. 21. Western blot of HEK 293 rtTA cells transfected with pTRE2-LCPTI wt. Untransfected HEK 293 rtTA cells (control), HEK 293 rtTA cells transfected with pTRE2-LCPTI wt and incubated with 1µg/ml doxycycline (+ dox) or without doxycycline (- dox) were analyzed by Western blot using an anti-LCPTI specific antibody. A unique band of 88 kDa corresponding to LCPTI was seen in pTRE2-LCPTI wt-transfected cells incubated with doxycycline. A small band of basal expression was observed in pTRE2-LCPTI wt-transfected cells incubated without doxycycline.

A unique band of 88 kDa corresponding to LCPTI was seen in HEK 293 rtTA cells transfected with pTRE2-LCPTI wt and incubated with doxycycline, while the endogenous LCPTI band corresponding to untransfected cells was almost undetected. A faint band was seen in pTRE2-LCPTI wt-transfected cells without doxycycline probably due to basal expression of the plasmid even in the absence of doxycycline incubation. Therefore, pTRE2-LCPTI wt was efficient in transient expression of LCPTI wt under the tet-on system.

2.3 STABLE CELLS CONSTRUCTION

Once the functionality of the pTRE2 vector and the expression of the LCPTI protein had been checked, INS cells which stably express LCPTI wt and LCPTI M593S under the tet-on system were constructed as follows.

INS-r9 cells, that stably express rtTA, were transfected with 25 µg of pTRE2-LCPTI wt or pTRE2-LCPTI M593S along with 5 µg of hygromicin selection plasmid (pTK-Hyg) as described in MATERIALS AND METHODS (Section 5). Three weeks after starting the selection with 0.1 mg/ml hygromycin, approximately 45 clones of pTRE2-LCPTI wt and 65 clones of pTRE2-LCPTI M593S appeared. They were incubated with 500 ng/ml doxycycline for 24 h and cell lysates were analyzed by Western blot with the anti-LCPTI specific antibody. Immunoblot of some of these clones is shown in Fig. 22.

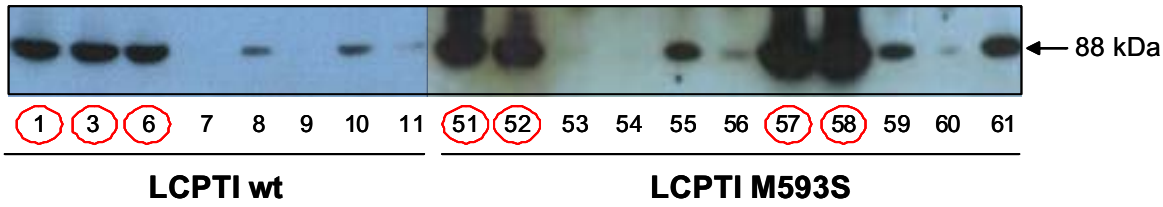

Fig. 22. Western blot of INS-r9 cells transfected with pTRE2-LCPTI wt and pTRE2-LCPTI M593S. Clones of INS-r9 cells transfected with pTRE2-LCPTI wt and pTRE2-LCPTI M593S resulting from the selection with 0.1 mg/ml hygromycin were induced for 24 h with 500 ng/ml doxycycline and analyzed by Western blot using an anti-LCPTI antibody. Clones with higher LCPTI expression (red circles) were selected for further analysis.

Western blot was performed after incubation of the clones with 500 ng/ml doxycycline to see the maximum LCPTI expression. Incubation without doxycycline was not necessary since clones which do not express pTRE2-LCPTI wt or pTRE2-LCPTI M593S serve as negative controls of the Western blot.

Clones with a higher LCPTI protein expression were chosen (red circles). After performing the Western blot of all the LCPTI wt and LCPTI M593S clones, we obtained four stable clones of LCPTI wt (numbers 1, 3, 6 and 37) and nine stable clones of LCPTI M593S (numbers 3, 25, 26, 27, 28, 51, 52, 57 and 58). These clones were selected and further cultured for additional analysis.

2.4 WESTERN BLOT ANALYSIS OF THE STABLE CLONES

To choose within the selected clones the one with the highest LCPTI expression, clones were incubated for 24 h with or without 500 ng/ml doxycycline. After that, the cell lysate was collected and a Western blot was performed with the anti-LCPTI antibody (Fig. 23).

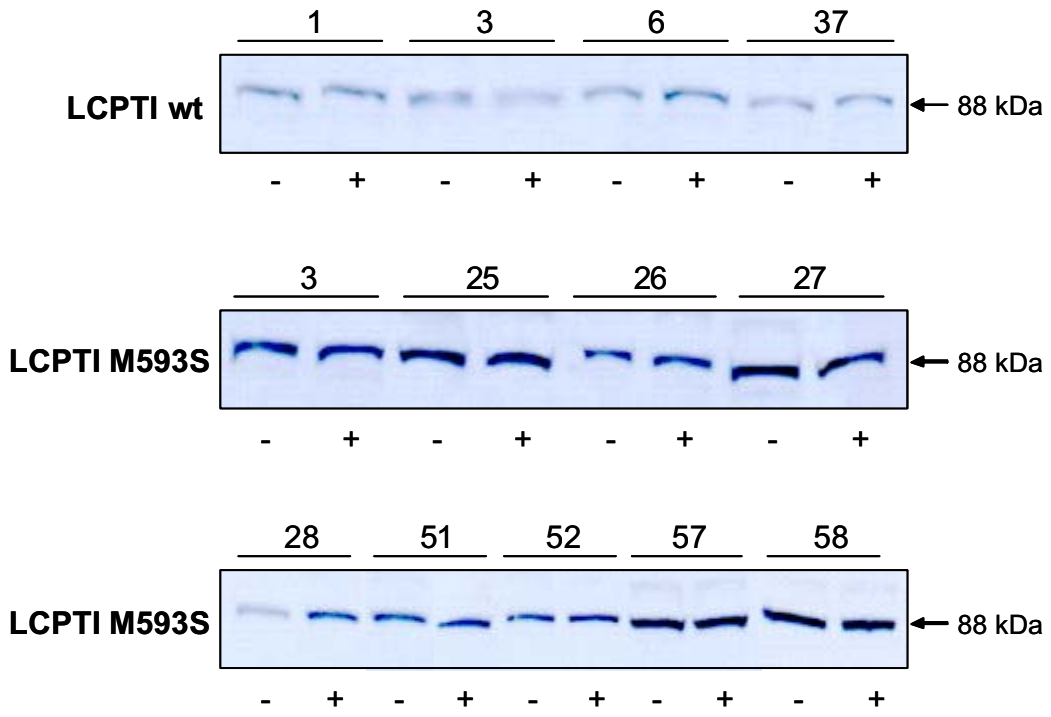

Fig. 23. Western blot of the selected LCPTI wt and LCPTI M593S clones. LCPTI wt clones (1, 3, 6 and 37) and LCPTI M593S clones (3, 25, 26, 27, 28, 51, 52, 57 and 58) were incubated with (+) or without (-) 500 ng/ml doxycycline for 24 h and cell lysates were analyzed by Western blot with the anti-LCPTI antibody. Data are a representative experiment out of 5.

Western blot showed no differences in LCPTI expression in any of the clones when they were incubated with or without doxycycline. The band seen in all of them was probably the endogenous LCPTI protein present in INS-r9 cells.

2.5 PCR ANALYSIS

To check whether the lack of differences in LCPTI expression in the selected clones incubated with or without doxycycline was due to the loss of the pTRE2-LCPTI wt or pTRE2-LCPTI M593S plasmids, a PCR analysis was performed. Total genomic DNA was obtained from each clone and a specific amplification for the transfected plasmids was done with the pTRE2.for and CPTI*Nco*I.rev primers, which give a band of 1028 bp. As a control of the quality of the genomic DNA obtained as well as an internal control of the PCR, we amplified a band of 300 bp of the COT gene using the COTH131A.for and COT*Xba*I.rev primers (Fig. 24A).

To rule out the possibility that the clones do not respond to doxycycline because of the loss of the rtTA transactivator stably expressed in the INS-r9 cells, the presence of the rtTA construct was also checked by specific PCR amplification of a 216 bp band with the rtTA.for and rtTA.rev primers (Fig. 24B).

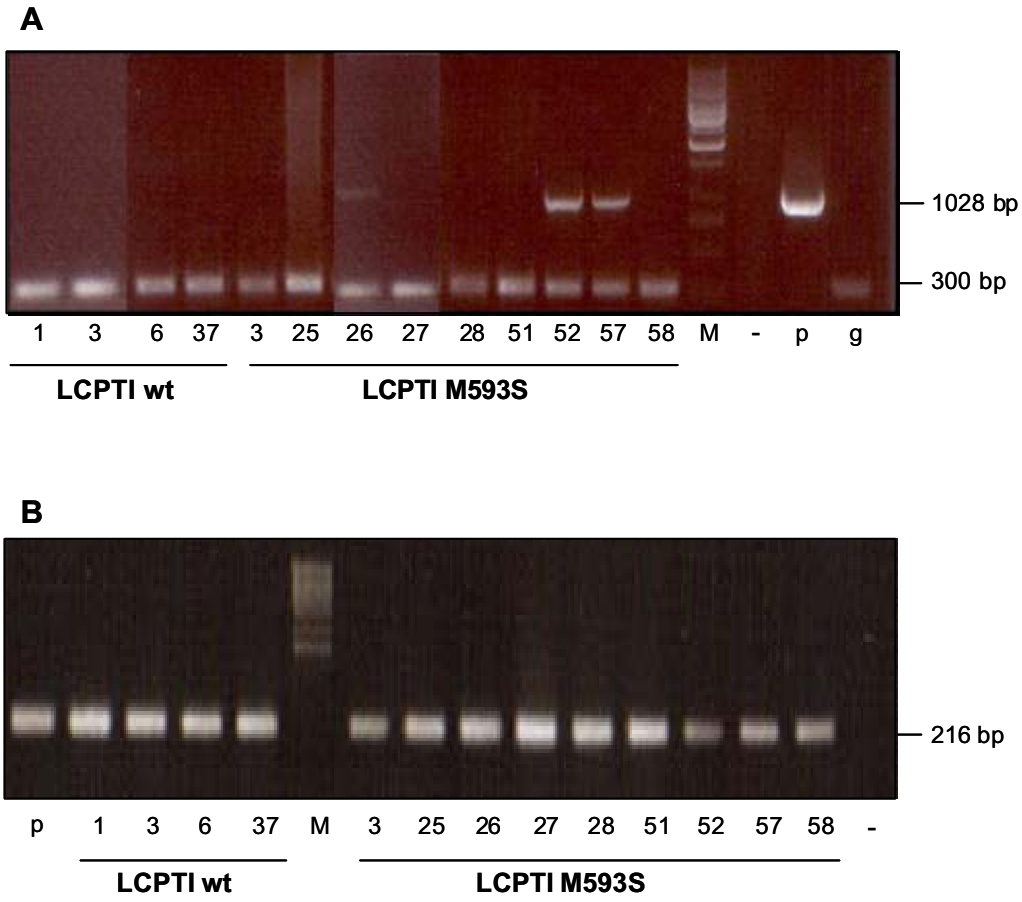

Fig. 24. PCR analysis of the genomic DNA of the clones. The genomic DNA was obtained from the LCPTI wt clones (1, 3, 6 and 37) and LCPTI M593S clones (3, 25, 26, 27, 28, 51, 52, 57 and 58). (**A**) The presence of the pTRE2-LCPTI wt and pTRE2-LCPTI M593S plasmids was analyzed by a specific PCR amplification of a 1028 bp band with the pTRE2.for and CPTI*Nco*I.rev primers. The amplification of 300 bp with COTH131A.for and COT*Xba*I.rev primers was an internal PCR control as well as a quality control of the genomic DNA obtained. The plasmid pTRE2-LCPTI wt (p) and a genomic DNA (g) previously obtained were used as positive controls of the PCR. (**B**) The presence of the rtTA construct was checked by a specific PCR amplification of a 216 bp band with the rtTA.for and rtTA.rev primers. The plasmid pRIP-rtTA was used as a positive control (p) of the PCR. The DNA marker is represented as (M) and the negative PCR control as (-).

Although the presence of the 300 bp band demonstrated the quality of the genomic DNA obtained, Fig. 24A shows that little of the pTRE2-LCPTI wt construct

was present in clone 26, and the pTRE2-LCPTI M593S construct was only present in clones 52 and 57, as is shown by the presence of the 1028 bp band. The rest of the clones had lost the transfected plasmids while the rtTA construct was present in all of them, as shown by the presence of the 216 bp band (Fig. 24B). This indicates that only those clones that did not overexpress LCPTI survived during growth.

The medium for the stable clones contained G418, the selection antibiotic for INS-r9 cells which stably express rtTA, and hygromycin, the selection antibiotic for stable clones transfected with pTK-Hyg along with the pTRE2-LCPTI wt and pTRE2-LCPTI M593S plasmids. We hypothesize that a slight basal overexpression of LCPTI, even in the absence of doxycycline, which continued during cell growth, could be toxic for the cells and so only those cells which do not contain the LCPTI plasmids survived throughout cell passages.

2.6 CPTI ACTIVITY

Among the clones selected, only one clone of LCPTI wt, number 26, and two clones of LCPTI M593S, numbers 52 and 57, retained the transfected construct. Although no differences in LCPTI protein expression were revealed by Western blot when clones were incubated with or without doxycycline, to check if the presence of the LCPTI construct seen by PCR could produce changes in CPTI activity, we performed a CPTI activity assay of the three clones.

Clones 26, 52 and 57 were incubated with or without 500 ng/ml doxycycline for 24 h. After that, mitochondrion-enriched cell fractions were obtained and CPTI activity assay was performed with 8 µg of protein from each clone.

Figure 25 shows no differences in CPTI activity between the incubation with or without doxycycline for any clone.

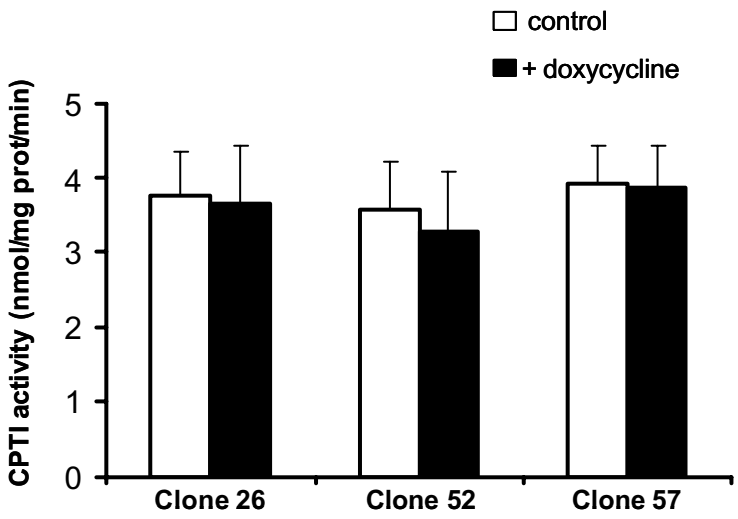

Fig. 25. CPTI activity of the clones 26, 52 and 57. Clones 26, 52 and 57 were incubated with or without 500 ng/ml doxycycline for 24 h and CPTI activity assay was performed with 8 µg of mitochondrion-enriched cell fractions of each clone. Data are the mean ± SE of 3 independent experiments.

In conclusion, when these clones were incubated with doxycycline the lack of increase in LCPTI protein expression compared to endogenous LCPTI seen by Western blot was correlated with the lack of increase in CPTI activity. Therefore, slight basal overexpression of LCPTI even in the absence of doxycycline could probably be toxic for the cells, as a result of which only those cells that do not contain the LCPTI plasmids survived throughout cell passages. The presence of the LCPTI construct in the genome of the clones 26, 52 and 57 suggests that the construct is not well integrated into the genome causing no LCPTI overexpression.

3. STUDY OF THE INTERACTION BETWEEN C75 AND LCPTI IN THE PANCREATIC β-CELL

C75 is a chemically stable synthetic inhibitor of fatty acid synthase (FAS) which has been described to act both centrally to reduce food intake and peripherally to stimulate CPTI activity[11,12] and increase fatty acid oxidation, leading to rapid and profound weight loss by reducing the fat mass. When FAS is inhibited by C75, the high content of malonyl-CoA should inhibit CPTI activity, but paradoxically, in peripheral tissues, this effect seems to be overcome by C75-stimulated CPTI activity. On the other hand, cerulenin, the natural FAS inhibitor, has been described to decrease CPTI activity[13,14] *in vivo* and *in vitro* accompanied with a reduction in fatty acid oxidation.

We wanted to further investigate the effect of C75 on CPTI activity *in vitro* and *in vivo* in the pancreatic β-cell, where the FAS expression is very low, thus allowing us to study the C75/CPTI interaction more directly.

3.1 MALDI-TOF ANALYSIS OF C75-COA

Studies performed in our group[15] demonstrated that C75 itself neither inhibited nor activated mitochondrial LCPTI or MCPTI enzymes overexpressed in yeast. The same occurred with the incubation with etomoxir itself. As it has been described[3] that the active inhibitory form of etomoxir is its CoA-derivative, etomoxiryl-CoA, C75 was also converted to C75-CoA and effectively, only when C75 or etomoxir were transformed to their CoA derivatives did they alter CPTI activity in yeast overexpressing L or MCPTI.

---

[11] Thupari JN, Landree LE, Ronnett GV, Kuhajda FP. C75 increases peripheral energy utilization and fatty acid oxidation in diet-induced obesity. *Proc. Natl. Acad. Sci. USA.* 99**:**9498-9502, 2002

[12] Yang N, Kays JS, Skillman TR, Burris L, Seng TW, Hammond C. C75 activates carnitine palmitoyltransferase-1 in isolated mitochondria and intact cells without displacement of bound malonyl-CoA. *J. Pharmacol. Exp. Ther*. PMID: 15356215, 2004

[13] Thupari JN, Pinn ML, Kuhajda FP. Fatty acid synthase inhibition in human breast cancer cells leads to malonyl-CoA-induced inhibition of fatty acid oxidation and cytotoxicity. *BBRC*. 285:217-223, 2001

[14] Jin YJ, Li SZ, Zhao ZS, An JJ, Kim RY, Kim YM, Baik JH, Lim SK. Carnitine palmitoyltransferase-1 (CPT-1) activity stimulation by cerulenin via sympathetic nervous system activation overrides cerulenin's peripheral effect. *Endocrinology*. 145:3197-3204, 2004

[15] Bentebibel A, Sebastián D, Herrero L, Serra D, Asins G, Hegardt FG. C75-CoA inhibits Carnitine Palmitoyltransferase I activity thus decreasing palmitate oxidation. Submitted.

To confirm that either C75 or etomoxir had reacted with CoA to produce a stable derivative, a MALDI-TOF analysis was carried out. Both drugs were converted into their CoA-derivatives in the presence of CoA and by the action of acyl-CoA synthase as described in MATERIALS AND METHODS (Section 8.4), and a sample of the activation reaction was directly analyzed by MALDI-TOF. Figure 26A shows the peak of 1020.4 Da corresponding to the molecular mass of the product formed by reaction of the two compounds, C75 and CoA. A similar analysis for etomoxiryl-CoA (Fig. 26B) corroborates its formation, in the peak of 1064.0 Da. Other peaks present in the spectra correspond to the matrix used in the analysis, the compound CoA in excess or products of its fragmentation.

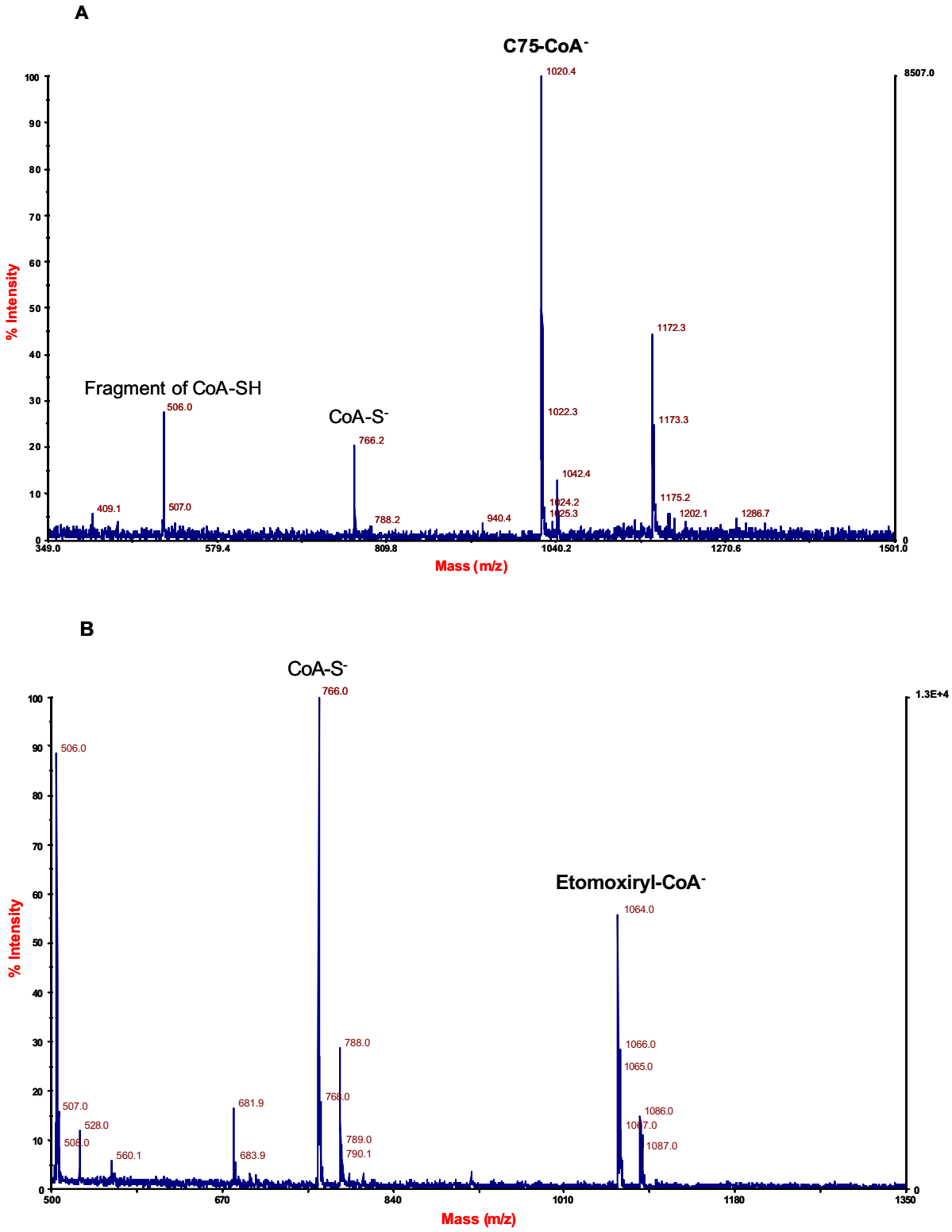

Fig. 26. MALDI-TOF spectra of C75-CoA and etomoxiryl-CoA. Spectra were directly obtained from the activation reaction product of C75-CoA and etomoxiryl-CoA using a Voyager-DE-RP from Applied Biosystems with DHB (10 mg/ml in water: methanol, 1:1) as described in MATERIALS AND METHODS (Section 14). The detection was done with a reflector and in the negative mode. The product C75-CoA (**A**) is confirmed by the peak at 1020.4 Da and etomoxiryl-CoA (**B**) by the peak at 1064.0 Da.

3.2 EFFECT OF C75 ON CPTI ACTIVITY IN INS(832/13) CELLS AND MITOCHONDRION-ENRICHED CELL FRACTIONS

To test the effect of C75 on CPTI activity in the β-cell, INS(832/13) cells were incubated with C75 and CPTI activity was measured.

INS(832/13) cells grown in 15-cm dishes were incubated for 1 h with complete medium containing either 0, 10 and 30 µg/ml C75 or 30 µg/ml etomoxir as a control. It was not necessary in this case to transform the drugs to their CoA derivatives, since this conversion occurs inside the cells *via* the mitochondrial long-chain acyl-CoA synthase. After that, mitochondrion-enriched cell fractions were obtained and CPTI activity assay was performed with 10 µg of protein.

Figure 27 shows that CPTI activity decreased at increasing C75 concentrations. CPTI activity was reduced by 34% and 49% at 10 and 30 µg/ml C75, respectively and by 80% at 30 µg/ml etomoxir. Thus, C75 in pancreatic β-cells behaves as a CPTI inhibitor.

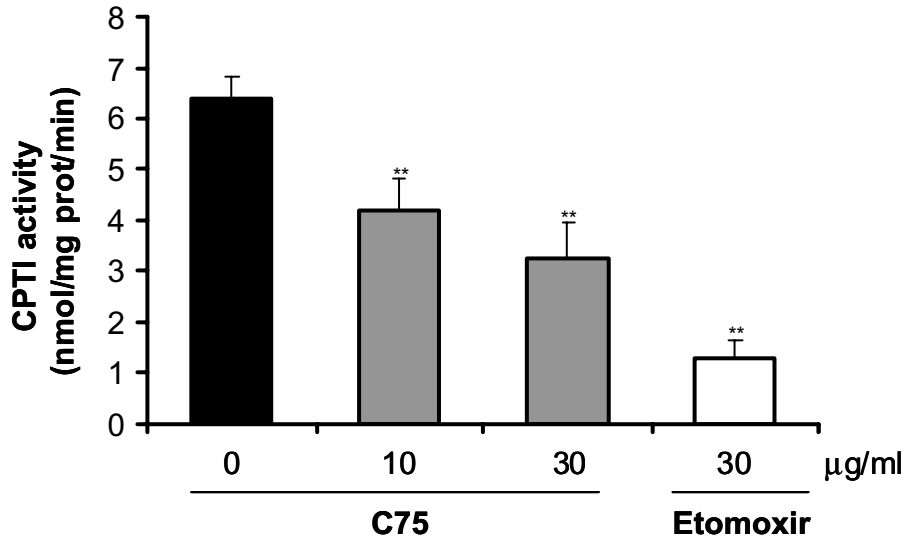

Fig. 27. CPTI activity in INS(832/13) cells incubated with C75. INS(832/13) cells were incubated for 1 h with complete medium containing either 0, 10, and 30 µg/ml C75 or 30 µg/ml o etomoxir. Mitochondrion-enriched cell fractions were obtained and 10 µg of protein were used for the CPTI activity assay. Data are presented as the mean ± SE of 3 independent experiments performed in duplicate. **P<0.01 *vs* control without C75.

To study the effect of C75 directly on the CPTI protein, purified mitochondria from INS(832/13) cells were preincubated for 1 min with increasing concentrations of C75-CoA or etomoxiryl-CoA and CPTI activity assay was performed with 10 µg of protein. As shown in Fig. 28, C75-CoA inhibited CPTI activity with similar kinetics to etomoxiryl-CoA. At 50 µM of each drug CPTI activity was almost completely inhibited. Therefore, *in vitro* C75 behaves as a potent inhibitor of CPTI activity in pancreatic β-cells.

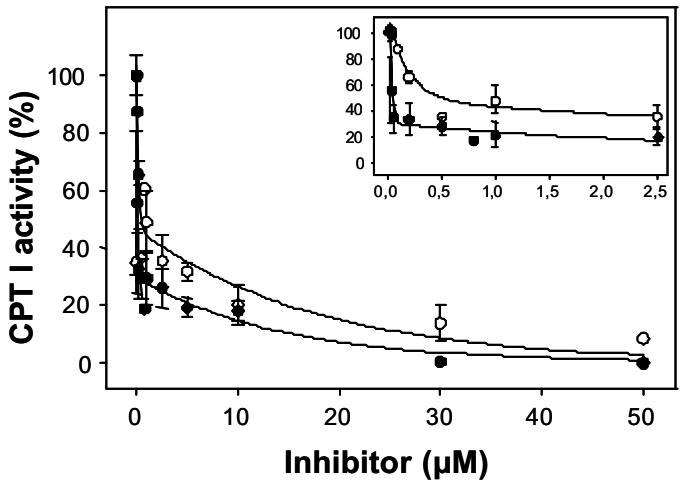

Fig. 28. Effect of C75-CoA and etomoxiryl-CoA on CPTI activity. Mitochondrion-enriched fractions of INS(823/13) cells were preincubated for 1 min with increasing concentrations of C75-CoA (black circles) or etomoxiryl-CoA (open circles) and CPTI activity was assayed as described in MATERIALS AND METHODS (Section 8.2). Data are the mean ± SE of 3 independent experiments and are expressed relative to control values in the absence of inhibitor (100%). Insert: expanded dose-response curve for the two inhibitors.

3.3 CPTI PROTEIN IN INS(832/13) CELLS INCUBATED WITH C75

A Western blot analysis of INS(832/13) cells treated with C75 and etomoxir was performed. INS(832/13) cells were incubated for 1 h with complete medium containing either 0, 10 and 30 µg/ml C75 or 30 µg/ml etomoxir as a control. Cell lysate was analyzed by Western blot with the anti-LCPTI antibody (Fig. 29).

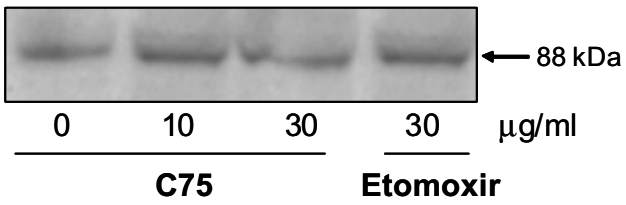

Fig. 29. Western blot of C75-treated INS(832/13) cells. INS(832/13) cells were incubated for 1 h with complete medium containing either 0, 10 and 30 µg/ml C75 or 30 µg/ml etomoxir as a control. Protein extracts were separated by SDS/PAGE (8% gels) and subjected to immunoblotting by using a specific antibody for CPTI from liver. A unique band of approx. 88 kDa corresponding to LCPTI was observed.

No differences were seen in the LCPTI protein expression between the cells incubated either with or without C75 nor etomoxir, indicating that the drugs did not affect the protein expression.

3.4 EFFECT OF C75 ON PALMITATE OXIDATION IN INS(832/13) CELLS

To assess whether CPTI inhibition by C75 in pancreatic β-cells is followed by a similar decrease in fatty acid oxidation, INS(812/13) cells were incubated with or without C75 and etomoxir as a control, and palmitate oxidation assay was performed.

INS(832/13) cells were incubated for 1 h with complete medium containing either 0, 10 and 30 µg/ml C75 or 30 µg/ml etomoxir as a control. After that, cells were preincubated for 30 min in KRBH medium containing 1% BSA and then incubated for 2 h at 2.5 mM glucose in the presence of [1-^{14}C]palmitate. Palmitate oxidation to $^{14}CO_2$ was measured as detailed in MATERIALS AND METHODS (Section 10.1).

Figure 30 shows that palmitate oxidation was reduced by 62% and by 71% at 30 µg/ml C75 and etomoxir respectively. Thus, C75 inhibits β-oxidation in INS(832/13) cells in acute accordance with CPTI activity inhibition.

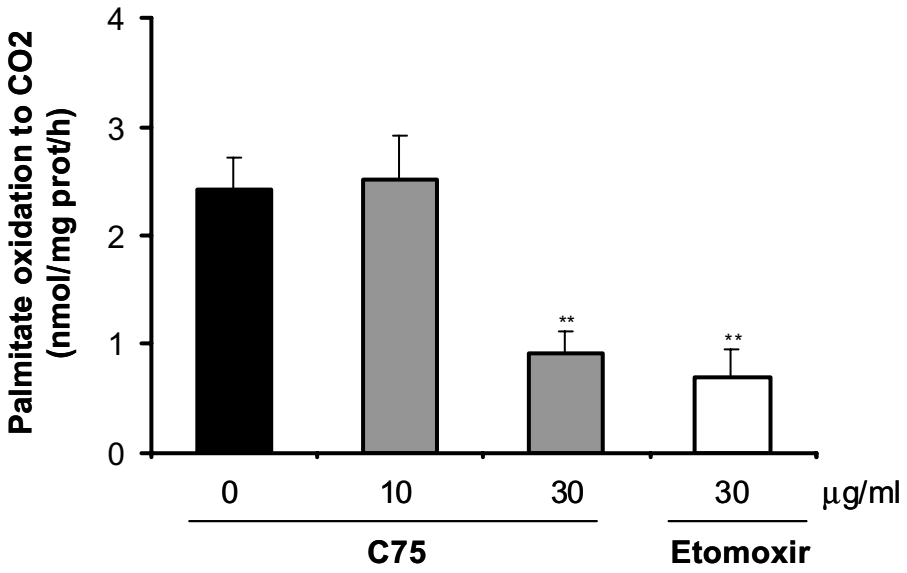

Fig. 30. Palmitate oxidation in INS(832/13) cells incubated with C75. INS(832/13) cells were incubated for 1 h with complete medium containing either 0, 10 and 30 µg/ml C75 or 30 µg/ml etomoxir. Cells were then preincubated for 30 min at 37 ºC with KRBH 1% BSA and then incubated for 2 h at 2.5 mM glucose in the presence of 0.8 mM carnitine, 0.25 mM palmitate and 1 µCi/ml [1-^{14}C]palmitate. Palmitate oxidation to CO_2 was measured as described in MATERIALS AND METHODS (Section 10.1). Data are the mean ± SE of 3 independent experiments performed in triplicate. **P<0.01 *vs* control without C75.

3.5 CELL VIABILITY

To rule out the possibility that the inhibition of palmitate oxidation was not due to an increase in cell death caused by C75, we performed viability experiments using the MTT assay.

INS(832/13) cells were incubated for 1 h with complete medium containing either 0, 10 and 30 µg/ml C75 or 30 µg/ml etomoxir as a control. After that, cells were cultured for 2 h with the MTT solution as detailed in MATERIALS AND METHODS (Section 3.6). Results are expressed as the percentage of absorbance related to control cells.

Figure 31 shows that in all cases cell viability was higher than 98% of control, so the decrease seen in the palmitate oxidation assay was due to the inhibitory effect of C75 on CPTI activity rather than a C75 toxicity effect.

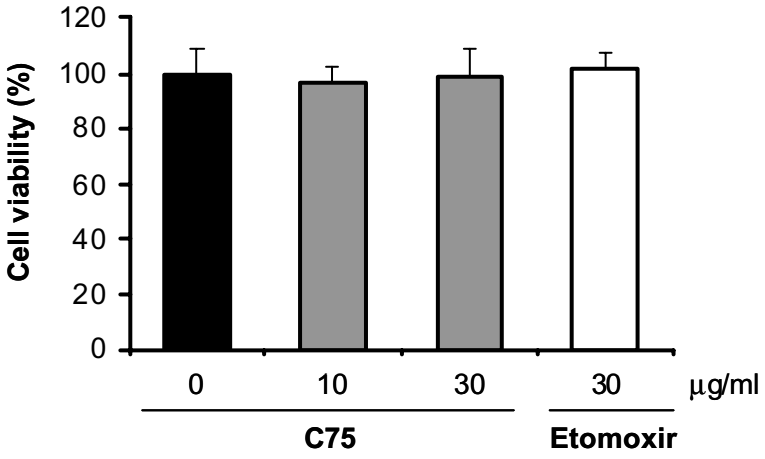

Fig. 31. Cell viability assay in INS(832/13) cells incubated with C75. INS(832/13) cells were incubated for 1 h with complete medium containing either 0, 10 and 30 µg/ml C75 or 30 µg/ml etomoxir as a control. After that, cells were cultured for 2 h with the MTT solution as detailed in MATERIALS AND METHODS (Section 3.6) and the formazan dye produced was quantified with a spectrophotometer at 570 nm with the MTT lysis solution as the blank. Results are expressed as the percentage of absorbance related to control cells. Data are the mean ± SE of 3 independent experiments.

3.6 EFFECT OF C75 TREATMENT ON MICE LIVER AND PANCREAS

We examined the effect of C75 on CPTI activity *in vivo*. Mice were injected ip with a single dose of C75 (20 mg/kg body weight) or only RPMI medium as a control and sacrificed at 0, 0.5, 3 and 5 h after injection. Liver and pancreas tissue samples were taken and mitochondria were isolated as described in MATERIALS AND METHODS (Section 8.1.2) and used for the CPTI activity assay.

Fig. 32 shows that CPTI activity was decreased at short times, but then recovered, the kinetics depending on the tissue. Inhibition of liver CPTI decreased by 59% at 1 h and by 70% after 3 h of treatment and at 5 h CPTI values were similar to control. In pancreas CPTI activity was decreased by 35% of control after 30 min of C75 treatment. In no case did CPTI activation exceed control; therefore the *in vivo* experiments were also consistent with the *in vitro* assays on CPTI activity and palmitate oxidation. C75 produced a short-term inhibition of CPTI in liver and pancreas in mice, with the maximum CPTI-inhibitory properties shown in the liver. The differential extent of inhibition of CPTI could be explained by differences in the rate of C75-CoA

endogenous activation, tissue pharmacokinetics or time scale turn over of the CPTI protein in each tissue.

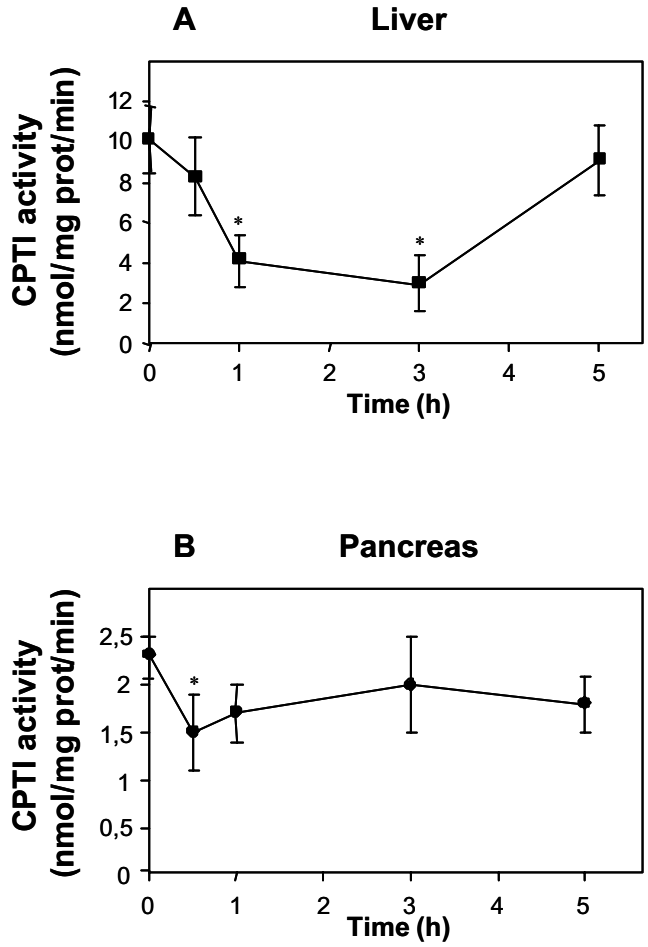

Fig. 32. C75 effect on CPTI activity in mice liver and pancreas. C75 was injected ip in mice at 20 mg/kg body weight and animals were sacrificed at 0, 0.5, 1, 3, and 5 h after injection. Mitochondrion-enriched fractions from liver and pancreas were obtained and CPTI activity was assayed. Results are the mean ± SE of data obtained from 6 mice. *P<0.05 *vs* control (0 h).

DISCUSSION

DISCUSSION

1. ALTERATION OF THE MALONYL-CoA/CPTI INTERACTION IN THE PANCREATIC β-CELL

Lipid metabolism in the ß-cell is critical for the regulation of insulin secretion[1]. Depletion of lipid stores together with deprivation of free fatty acids (FFA) alters glucose-stimulated insulin secretion (GSIS) in rats and humans[2,3]. FFAs, presumably *via* long-chain fatty acyl-CoA (LC-CoA), generate signals for insulin secretion[4].

Stimulation of insulin secretion by glucose alters levels of CoA derivatives in clonal pancreatic β-cells, in particular malonyl-CoA and LC-CoAs. The malonyl-CoA/LC-CoA model of GSIS holds that in addition to the K_{ATP} channel-dependent pathway, a parallel anaplerotic/lipid signaling pathway exists wherein malonyl-CoA acts as a coupling factor[4]. Both malonyl-CoA and LC-CoA are thought to participate in the signal transduction for insulin secretion: the former as a regulator and the latter as an effector[5]. Systems that regulate both malonyl-CoA and LC-CoA appear to be involved in insulin secretion. Accordingly, ACC, which controls the synthesis of malonyl-CoA, MCD, which catalyzes malonyl-CoA degradation, and CPTI which is regulated by malonyl-CoA, are components of a metabolic signalling network that senses the level of fuel stimuli. Moreover, since the level of fatty acid synthase in normal β-cells is very low[6], the physiological role of malonyl-CoA in the endocrine pancreas, unlike many

[1] Yaney GC, Corkey BE. Fatty acid metabolism and insulin secretion in pancreatic beta cells. *Diabetologia.* 46:1297-1312, 2003

[2] Stein DT, Esser V, Stevenson BE, Lane KE, Whiteside JH, Daniels MB, Chen S, McGarry JD. Essentiality of circulating fatty acids for glucose-stimulated insulin secretion in the fasted rat. *J. Clin. Invest.* 97:2728-2735, 1996

[3] Dobbins RL, Chester MW, Daniels MB, McGarry JD, Stein DT. Circulating fatty acids are essential for efficient glucose-stimulated insulin secretion after prolonged fasting in humans. *Diabetes.* 47:1613-1618, 1998

[4] Prentki M, Vischer S, Glennon MC, Regazzi R, Deeney JT, Corkey BE. Malonyl-CoA and long chain acyl-CoA esters as metabolic coupling factors in nutrient-induced insulin secretion. *J. Biol. Chem.* 267:5802-5810, 1992

[5] Corkey BE, Deeney JT, Yaney GC, Torheim, Prentki M. The role of long-chain fatty acyl-CoA esters in β-cell signal transduction. *J. Nutr.* 130:299S-304S, 2000

[6] Brun T, Roche E, Assimacopoulos-Jeannet F, Corkey BE, Kim KH, Prentki M. Evidence for anaplerotic/malonyl-CoA pathway in pancreatic β-cell nutrient signalling. *Diabetes*. 45:190-198, 1996

other tissues, is not *de novo* synthesis of fatty acids but rather the regulation of CPTI activity. Therefore, the metabolism of several nutrients that converge to form malonyl-CoA and increase LC-CoA esters might play a key role in fuel regulated-insulin secretion in the β-cell.

In an earlier study our group evaluated the capacity of LCPTI wt overexpression to alter the insulin response to glucose in ß-cells[7]. The results showed that adenovirus-mediated overexpression of a cDNA encoding LCPTI not only increased β-oxidation in INS-1E cells but also decreased GSIS by 40%. However, using this approach, glucose-derived malonyl-CoA is still able to inhibit LCPTI in cells overexpressing the enzyme and consequently fat oxidation was moderately altered.

In view of the interest in the malonyl-CoA/LC-CoA model of GSIS, which is still under discussion[8,9], we decided to overexpress LCPTI M593S, a mutant enzyme that is insensitive to malonyl-CoA[10], in pancreatic β-cells. This would test the hypothesis that the CPTI/malonyl-CoA interaction is involved in GSIS. Since liver CPTI is the only isoform present in the β-cell, we used the rat liver isoform of CPTI to construct the adenovirus. Therefore, the LCPTI mutant and the native LCPTI were overexpressed in INS(832/13) cells and rat islets using recombinant adenoviruses.

1.1 CPTI ACTIVITY IS NOT INHIBITED BY MALONYL-CoA IN INS(832/13) CELLS EXPRESSING LCPTI M593S

The capacity of the LCPTI mutant to show enzyme activity despite the presence of malonyl-CoA was evaluated in pancreatic β-cells. In the presence of 100 μM malonyl-CoA mitochondrion-enriched fractions of cells infected with Ad-LCPTI

[7] Rubi B, Antinozzi PA, Herrero L, Ishihara H, Asins G, Serra D, Wollheim CB, Maechler P, Hegardt FG. Adenovirus-mediated overexpression of liver carnitine palmitoyltransferase I in INS1E cells: effects on cell metabolism and insulin secretion. *Biochem. J.* 364:219-226, 2002

[8] Mulder H, Lu D, Finley IV J, An J, Cohen J, Antinozzi PA, McGarry JD, Newgard CB. Overexpression of a modified human malonyl-CoA decarboxylase blocks the glucose-induced increase in malonyl-CoA level but has no impact on insulin secretion in INS-1-derived (832/13) β-cells. *J. Biol. Chem.* 276: 6479-6484, 2001

[9] Boucher A, Lu D, Burgess SC, Telemaque-Potts S, Jensen MV, Mulder H, Wang MY, Unger RH, Sherry AD, Newgard CB. Biochemical mechanism of lipid-induced impairment of glucose-stimulated insulin secretion and reversal with a malate analogue. *J. Biol. Chem.* 279:27263-27271, 2004

[10] Morillas M, Gomez-Puertas P, Bentebibel A, Selles E, Casals N, Valencia A, Hegardt FG, Asins G, Serra D. Identification of conserved amino acid residues in rat liver carnitine palmitoyltransferase I critical for malonyl-CoA inhibition. Mutation of methionine 593 abolishes malonyl-CoA inhibition. *J. Biol. Chem.* 278:9058-9063, 2003

M593S retained 84% of their activity while that of the LCPTI wt was almost completely inhibited. This lack of sensitivity to malonyl-CoA was described in yeast overexpressing LCPTI M593S[10], but the results in the present thesis provide the first evidence that LCPTI M593S is insensitive to malonyl-CoA in pancreatic β-cells.

We attempted to study the effect of the irreversible CPTI inhibitor etomoxir on CPTI activity in INS(832/13) cells transduced with LCPTI wt or LCPTI M593S. Etomoxir blocked CPTI activity in Ad-LacZ and Ad-LCPTI wt-infected cells, but left 65% of CPTI activity in Ad-LCPTI M593S-infected cells. However, when mitochondrion-enriched cell fractions were incubated with 100 μM etomoxiryl-CoA, the LCPTI M593S form retained certain sensitivity to etomoxiryl-CoA (18% remaining activity). Etomoxiryl-CoA binds covalently and irreversibly to the protein LCPTI in the mitochondrion-enriched cell fractions, while when cells are incubated for 30 min with etomoxir, the inhibitor has to be converted to its CoA derivative and reach the protein. This could explain the different extent of inhibition seen in etomoxir-incubated cells or mitochondrion-enriched cell fractions.

Nevertheless, the LCPTI mutant was designed to be insensitive to the physiological inhibitor malonyl-CoA and the effects of etomoxir were only tested as a control. A thorough study of the amino acid in CPTI which covalently bound to etomoxir, and the location of this drug on the CPTI model remains to be performed.

1.2 EXPRESSION OF LCPTI M593S INCREASES CPTI ACTIVITY AND PROTEIN LEVELS

Having shown that the LCPTI mutant acted as a malonyl-CoA insensitive LCPTI in pancreatic β-cells, we established the conditions for subsequent experiments. Comparison of the effects of Ad-LCPTI M593S with the control Ad-LCPTI wt requires equal CPTI activity conditions. Therefore, the variations of CPTI activity *vs* the amount of virus used were studied in each case. In both cases CPTI activity increased to a plateau of 9-10 fold compared with the endogenous LCPTI. This plateau may be attributable to a saturation effect in the mitochondrial membrane, which may have altered the conformation of CPTI, leading to an increase in the protein level without more than a 9-10 fold increase in CPTI activity.

For subsequent experiments we decided to use the amount of adenovirus LCPTI wt and LCPTI M593S that increased CPTI activity 6-fold with respect to the control

Ad-LacZ (CPTI endogenous). In these conditions, consistent with the activity assays, Ad-LCPTI wt and Ad-LCPTI M593S-infected INS(832/13) cells and rat islets showed similar LCPTI protein levels.

1.3 LCPTI M593S EXPRESSION INCREASES PALMITATE OXIDATION WITHOUT CHANGING MALONYL-CoA LEVELS OR GLUCOSE OXIDATION

Overexpression of the malonyl-CoA-insensitive form of LCPTI increased fatty-acid oxidation rates in INS(832/13) cells at all the glucose concentrations tested. Fat oxidation rates were much higher than in control Ad-LacZ-infected cells and still higher than in cells infected with Ad-LCPTI wt, even at high malonyl-CoA concentrations (high glucose). Moreover, palmitate oxidation increased whereas malonyl-CoA content and glucose oxidation remained unaltered, indicating that LCPTI expression did not modify the malonyl-CoA levels or the glucose metabolism in the β-cell. The unaltered glucose oxidation is consistent with the view that a Randle cycle is inoperative in the β-cell[11].

In a previous study[7], LCPTI wt-overexpression induced a slight increase in ATP generation due to the over-activity of CPTI and the consequent increase in fatty acid oxidation. However, the percentage increase in ATP between LCPTI wt-overexpressing cells and control cells was identical when glucose was increased from low to high concentrations, indicating that LCPTI wt overexpression had no effect on the electron transport chain.

1.4 GLUCOSE-STIMULATED INSULIN SECRETION IS REDUCED IN INS(832/13) CELLS AND RAT ISLETS EXPRESSING LCPTI M593S

INS(832/13) cells overexpressing LCPTI M593S secreted less insulin in response to high glucose concentration (60% reduction) but not in response to a depolarizing concentration of KCl. Thus, exocytosis *per se* was preserved in cells overexpressing the mutated LCPTI, since the effect of the Ca^{2+} raising agent (30 mM KCl) was unaltered. The control Ad-LCPTI wt-infected cells showed 40% decrease in GSIS, as previously reported by our group[7]. The higher decrease in GSIS caused by

[11] Segall L, Lameloise N, Assimacopoulos-Jeannet F, Roche E, Corkey P, Thumelin S, Corkey BE, Prentki M. Lipid rather than glucose metabolism is implicated in altered insulin secretion caused by oleate in INS-1 cells. *Am. J. Physiol*. 277:E521-528, 1999

LCPTI M593S expression indicates the strong metabolic influence of a malonyl-CoA non-regulated fatty acid oxidation system.

The utilization of elevated K^+ and diazoxide to discern between the K_{ATP} channel-dependent and -independent pathways of glucose sensing showed that LCPTI wt and LCPTI M593S overexpression affected the K_{ATP}-independent pathway of GSIS, thus supporting the view that the malonyl-CoA/CPTI interaction is involved in the amplification arm of secretion.

Insulin secretion experiments in the presence of etomoxir showed that the irreversible CPTI inhibitor restored the impairment in GSIS caused by either LCPTI wt or LCPTI M593S overexpression. However, CPTI activity was not completely inhibited by etomoxir in Ad-LCPTI M593S-infected cells. The slight inhibition of CPTI activity by etomoxir, although covalent and irreversible, may have been enough to inhibit palmitate oxidation (as was shown in the results) and to restore impaired GSIS in LCPTI M593S-transduced cells. This indicates that insulin secretion is sensitive to slight changes in palmitate oxidation, and therefore to slight variations in the LC-CoA cytosolic pool. To prevent any non-specific effect on the secretory machinery, etomoxir was eliminated after the preincubation and the cells were washed prior to the experiments. Thus, we consider that the only effect of etomoxir was the inhibition of CPTI through direct and irreversible covalent binding of CPTI and that it did not act as a fatty acid analogue. Under these conditions control cells did not show any enhancement of GSIS, in contrast with what has been shown previously[12]. In the work of Chen *et al.*[12] 200 μM etomoxir, added with the glucose in rat perfusion experiments stimulated GSIS. This discrepancy could be explained by the presence of etomoxir throughout all the secretion experiments.

Similar results were obtained in isolated rat islets, *i.e.,* reduced secretory responses to high glucose upon LCPTI M593S expression (40% reduction). Interestingly, overexpression of LCPTI wt did not affect GSIS in islets, suggesting preserved lipid signalling above a critical threshold of cytosolic LC-CoA. To explain the difference in the results between INS(832/13) cells and islets we hypothesize that normal β-cells are more protected than INS cells against lipid depletion due to enhanced fat oxidation, such that only the more efficient LCPTI M593S construct is active in rat

[12] Chen S, Ogawa A, Ohneda M, Unger RH, Foster D, McGarry JD. More direct evidence for a malonyl-CoA-carnitine palmitoyltransferase I interaction as a key event in pancreatic beta-cell signalling. *Diabetes*. 43:878-883, 1994

islets. In addition, DNA transfer efficiency in insulinoma cell line models approaches 100% while in islets it is about 70-80%, which could also explain the different effectiveness of the LCPTI constructs in clonal β-cells and islets.

Incubation of LCPTI M593S transduced cells with 0.25 mM palmitate did not completely restore GSIS, while LCPTI wt did. This shows the strong metabolic influence of LCPTI M593S on fatty acid oxidation and insulin secretion in the pancreatic β-cell. This result points to a possible mechanism by which increased metabolic flux through LCPTI diminishes insulin secretion *via* the depletion of a critical lipid synthesized at or near the mitochondrial outer membrane that would act as a signal molecule.

It is interesting to compare the present results with those of Roduit *et al.*[13], who overexpressed MCD in the cytosol (MCDc) by infecting INS(832/13) cells and rat islets with an adenovirus containing the cDNA for MCD devoid of its mitochondrial and peroxisomal targeting sequences. The authors found that MCDc overexpression in the absence of exogenous FFA had no effect on GSIS and that MCDc overexpression suppressed the additional secretion in response to glucose provided by the presence of exogenous FFA (0.1-0.25 mM palmitate complexed to 0.5% BSA). This is in concordance with the malonyl-CoA/LC-CoA model, which predicts that the effectiveness of malonyl-CoA to couple nutrient sensing to insulin secretion depends on the availability of FFAs to the β-cell.

Potentiation of insulin secretion by palmitate has been described in HIT cells[4] and islets[14]. In HIT cells examination of the dose dependence of the effect of palmitate at a fixed concentration of albumin (1%) indicated that the threshold concentration of the fatty acid was 0.2-0.5 mM and that a marked potentiating action on secretion occurred at 1 mM[4]. They also showed that the free (unbound) palmitate is the important factor causing secretion. In the present study, however, exogenous fatty acids had no effect on GSIS at 15 mM glucose, perhaps because we used a relatively low

[13] Roduit R, Nolan C, Alarcon C, Moore P, Barbeau A, Delghingaro-Augusto V, Przybykowski E, Morin J, Masse F, Massie B, Ruderman N, Rhodes C, Poitout V, Prentki M. A Role for the Malonyl-CoA/Long-Chain Acyl-CoA Pathway of Lipid Signaling in the Regulation of Insulin Secretion in Response to Both Fuel and Nonfuel Stimuli. *Diabetes.* 53:1007-1019, 2004

[14] Malaisse WJ, Malaisse-Lagae F. Stimulation of insulin secretion by noncarbohydrate metabolites. *J. Lab. Clin. Med*. 72:438-448, 1968

concentration of fatty acids (0.25 mM bound to 1% BSA) or possibly because lipolysis was higher in the current study.

Nonetheless, it is interesting to note that altering β-cell lipid partitioning with the malonyl-CoA-insensitive mutant of LCPTI had more profound consequences for both GSIS and lipid partitioning than doing so with the overexpression of cytosolic MCD[13]. Fat oxidation was more enhanced and esterification processes were more reduced at both low and elevated glucose. The enhanced fat oxidation caused by LCPTI M593S was also higher than that obtained with the stable expression of an ACC-antisense construct in INS-1 cells[15]. It is important to highlight that both MCD and ACC modulate CPTI activity through changes in malonyl-CoA levels, whereas CPTI directly controls the LC-CoA flux into the mitochondria for their oxidation.

In other studies[8,9], however, the lack of correlation between malonyl-CoA levels and β-oxidation has been remarked on. In the former[8] the authors showed unimpaired secretion of insulin in β-cells overexpressing MCD in the cytoplasm in the absence of exogenous FFAs. They also performed experiments in the presence of 1 mM oleate/palmitate, but this high concentration of FFAs might have overridden the consequences of reducing malonyl-CoA and LC-CoA in the cytoplasm. These authors proposed that glucose might regulate cytosolic LC-CoA in a manner not entirely dependent on malonyl-CoA, suggesting that in the β-cell, ATP-different factors derived from glucose metabolism could regulate CPTI activity. Interestingly, malonyl-CoA-independent regulation of CPTI has been demonstrated in several studies[16,17,18,19]. Another explanation could be the presence of different pools of malonyl-CoA in the

---

[15] Zhang S, Kim K H. Essential role of acetyl-CoA carboxylase in the glucose-induced insulin secretion in a β-cell line. *Cell Signal.* 10:35-42, 1998

[16] Kerner J, Distler AM, Minkler PE, Parland W, Peterman SM, Hoppel CL. Phosphorylation of rat liver mitochondrial carnitine palmitoyltransferase-I (CPT-I): Effect on the kinetic properties of the enzyme. *J. Biol.Chem*. 279:41104-41113, 2004

[17] Velasco G, Geelen MJH, Gomez del Pulgar T, Guzman M. Malonyl-CoA-independent acute control of hepatic carnitine palmitoyltransferase I activity. *J. Biol. Chem.* 273:21497-21504, 1998

[18] Velasco G, Gomez del Pulgar T, Carling M, Guzman M. Evidence that the AMP-activated protein kinase stimulates rat liver carnitine palmitoyltransferase I by phosphorylating cytoskeletal components. *FEBS Lett.* 439:317-320, 1998

[19] Sleboda J, Risan KA, Spydevold O, Bremen J. Short-term regulation of carnitine palmitoyltransferase I in cultured rat hepatocytes: spontaneous inactivation and reactivation by fatty acids. *Biochim. Biophys. Acta*. 1436:541-594, 1999

cell. There are two ACCs, one in the cytosol the other in the mitochondrion, the latter directly modulating the malonyl-CoA levels accessible to CPTI[20].

Whatever the explanation for the differences in alterations in GSIS in the absence or presence of exogenous FFA when MCDc[13], ACC-antisense[15] or CPTI (present thesis) are expressed, these studies show clearly a reduction of GSIS when the malonyl-CoA/CPTI interaction is perturbed.

1.5 EXPRESSION OF LCPTI M593S REDUCES LIPID PARTITIONING

The results of the present study with cells overexpressing a malonyl-CoA insensitive CPTI together with previous results[7,13] provide evidence that malonyl-CoA acts as a glucose-driven coupling factor that regulates the partitioning of fatty acids into effector molecules in the insulin secretory pathway. The nature of these molecules (NE palm, LC-CoA, PL and/or DAG) and their mechanisms of action on insulin secretion are poorly understood.

In the present study, overexpression of LCPTI M593S altered lipid partitioning of exogenous palmitate from oxidation into esterification products. The incorporation of palmitate into PL, DAG, TG, NE Palm and CE was reduced compared to controls. Thus, the increase in fatty acid oxidation reduced the availability of LC-CoA for lipid signalling in INS(832/13) cells. Moreover, the glucose-induced rise in NE Palm, an indirect measurement of cytosolic LC-CoA[13], was markedly curtailed in cells expressing the LCPTI construct and, interestingly, the CPTI mutant was more effective in this respect. However, the TG content was not changed by the expression of the LCPTI constructs. This is probably due to the fact that little differences in the incorporation of LC-CoA into TG are not reflected in the large and stable total TG pool. This is consistent with previous studies[7,13].

1.6 PKC ACTIVITY IS IMPAIRED IN INS(832/13) CELLS EXPRESSING LCPTI M593S

Possible candidates for the effector molecules involved in the insulin secretory pathway are NE Palm, LC-CoA, phospholipids and/or DAG. PKC isoforms are also reasonable candidates to either initiate secretion or augment GSIS, as they respond to

[20] Ha J, Lee JK, Kim KS, Witters LA, Kim KH. Cloning of human acetyl-CoA carboxylase-β and its unique features. *Proc. Natl. Acad. Sci. USA*. 93:11466-11470, 1996

both lipid signals and Ca^{2+}. Insulin exocytosis is a likely process for regulation by fatty acid moieties, acting directly on signal transducing effectors of secretion or indirectly *via* activation of some kinases, in particular the PKC enzymes. In addition, three recent reports suggested that exogenous FFAs could also act directly on β-cells as ligand for the orphan G-protein receptor GPR40[21,22,23]. Possibilities of more direct distal effects include: 1) DAG modulation of exocytotic machinery proteins such as the synaptic vesicle priming protein Munc-13[24] and 2) LC-CoA acylation of proteins, such as the exocytotic proteins synaptosomal-associated protein-25[25] and synaptogamin[26], which can enhance their association with target membranes, and PKC, which has been suggested as a possible target for acylation, because its translocation to membrane bilayers was facilitated upon palmitoylation[27].

As both DAG and LC-CoA activate a number of PKC enzymes[28,29] and the glucose-induced rise in DAG and NE Palm (an indirect determination of LC-CoA levels) were decreased in INS(832/13) cells overexpressing the LCPTI constructs, we assessed whether these events could PKC activity. Determination of PKC translocation

---

[21] Itoh Y, Kawamata Y, Harada M, Kobayashi M, Fujii R, Fukusumi S, Ogi K, Hosoya M, Tanaka Y, Uejima H, Tanaka H, Maruyama M, Satoh R, Okubo S, Kizawa H, Komatsu H, Matsumura F, Noguchi Y, Shinohara T, Hinuma S, Fujisawa Y, Fujino M. Free fatty acids regulate insulin secretion from pancreatic beta cells through GPR40. *Nature*. 422:173-176, 2003

[22] Kotarsky K, Nilsson NE, Flodgren E, Owman C, Olde B. A human cell surface receptor activated by free fatty acids and thiazolidinedione drugs. *Biochem Biophys Res Commun*. 301:406-410, 2003

[23] Briscoe CP, Tadayyon M, Andrews JL, Benson WG, Chambers JK, Eilert MM, Ellis C, Elshourbagy NA, Goetz AS, Minnick DT, Murdock PR, Sauls HR Jr, Shabon U, Spinage LD, Strum JC, Szekeres PG, Tan KB, Way JM, Ignar DM, Wilson S, Muir AI. The orphan G protein-coupled receptor GPR40 is activated by medium and long chain fatty acids. *J. Biol. Chem*. 278:11303-11311, 2003

[24] Rhee JS, Betz A, Pyott S, Reim K, Varoqueaux F, Augustin I, Hesse D, Sudhof TC, Takahashi M, Rosenmund C, Brose N. Beta phorbol ester- and diacylglycerol-induced augmentation of transmitter release is mediated by Munc13s and not by PKCs. *Cell*. 108:121-133, 2002

[25] Gonzalo S, Linder ME. SNAP-25 palmitoylation and plasma membrane targeting require a functional secretory pathway. *Mol. Biol. Cell*. 9:585-597, 1998

[26] Chapman ER, Blasi J, An S, Brose N, Johnston PA, Sudhof TC, Jahn R. Fatty acylation of synaptotagmin in PC12 cells and synaptosomes. *Biochem. Biophys. Res. Commun*. 225:326-332, 1996

[27] Ford DA, Horner CC, Gross RW. Protein kinase C acylation by palmitoyl coenzyme A facilitates its translocation to membranes. *Biochemistry*. 37:11953-11961, 1998

[28] Yaney GC, Korchak HM, Corkey BE. Long-chain acyl-CoA regulation of protein kinase C and fatty acid potentiation of glucose-stimulated insulin secretion. *Endocrinology*. 141:1989-1998, 2000

[29] Alcázar O, Qiu-yue Z, Giné E, Tamarit-Rodriguez J. Stimulation of islet protein kinase C translocation by palmitate requires metabolism of the fatty acid. *Diabetes*. 46:1153-1158, 1997

from cytosol to membrane showed that PKC activation was decreased in Ad-LCPTI wt-infected cells and was even more reduced in Ad-LCPTI M593S-infected cells, both compared with control LacZ. This suggests that enhanced beta oxidation of fatty acids by the LCPTI M593S mutant and LCPTI wt reduces GSIS as a result of a decrease in PKC activation.

1.7 GLUCOSE-STIMULATED INSULIN SECRETION IN THE β-CELL

The results presented in this thesis are in accordance with the malonyl-CoA/LC-CoA model. However, this model does not oppose, but rather complements, other candidate mechanisms of the metabolic signal transduction, such as the cataplerotic output of glutamate or the exchange of pyruvate with TCA cycle intermediates (pyruvate cycling). Figure 1 provides a general view obtained from the literature of the potential mechanisms involved in the glucose-stimulated insulin secretion of the pancreatic β-cell.

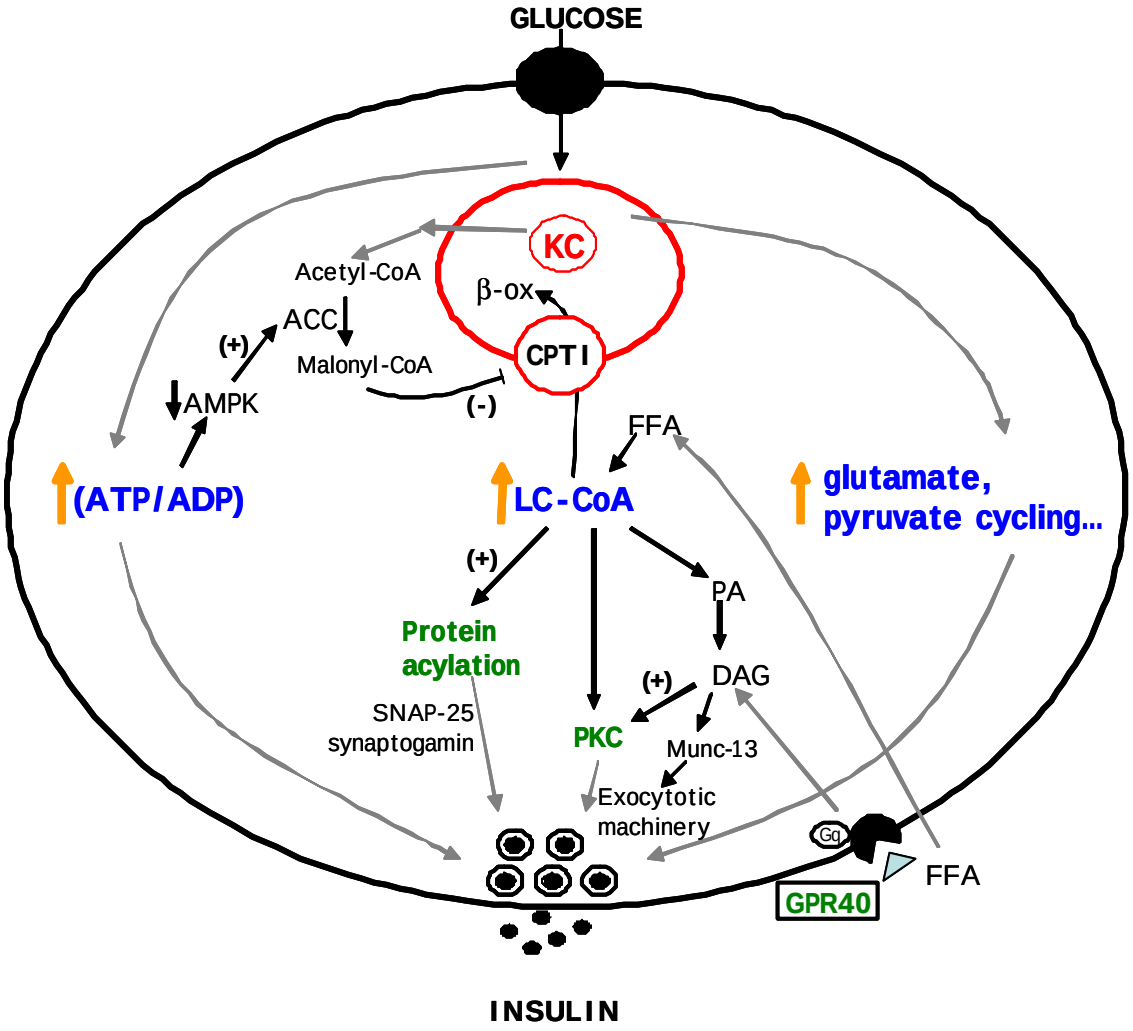

Fig. 1. Metabolic signal transduction mechanisms involved in GSIS. Glucose metabolism raises the ATP/ADP ratio, which results in calcium influx and leads to the release of insulin through the K_{ATP} channel-dependent pathway. The increase in ATP (decrease in AMP) inhibits AMPK, which in turn activates ACC, resulting in an increase of the CPTI inhibitor malonyl-CoA. Malonyl-CoA, also derived from the anaplerosis pathway, modulates partitioning of exogenous FFAs *via* LC-CoA from fatty acid β-oxidation (β-ox) to lipid signalling involved in insulin vesicle exocytosis. LC-CoAs may provide substrate for acylation of proteins such as the exocytotic proteins synaptosomal-associated protein-25 (SNAP-25) and synaptogamin or, through the production of phosphatidic acid (PA) and DAG, LC-CoA may promote DAG modulation of exocytotic machinery proteins such as the synaptic vesicle priming protein Munc-13, or modulate PKC enzyme activity resulting in insulin release. FFAs can either enter the cell and be activated into LC-CoAs, or bind to and activate the G-protein coupled receptor (GPR40). This binding activates a heterotrimeric G-protein containing the α-subunit Gq, which leads to the activation of PKC and the release of insulin. The cataplerotic output of glutamate could act on the secretory vesicle, enhancing its fusion with the plasma membrane and stimulating insulin secretion. Finally, other mechanisms such as the glucose-mediated increment in pyruvate cycling, *i.e.*, the exchange of pyruvate with the Krebs cycle (KC) intermediates, could participate in the release of insulin.

Pancreatic β-cells detect the energy excess through the glucose metabolism, which gives metabolic signals that lead to the release of insulin. Mitochondrial metabolism plays a pivotal role by generating signals that couple glucose sensing to insulin secretion. These metabolic coupling signals are proposed to be: ATP, LC-CoA, glutamate and pyruvate cycling.

1) Mitochondrial metabolism is crucial in generating ATP, leading to a rise in $[Ca^{2+}]$, which is the main and necessary signal triggering insulin exocytosis.

2) An early metabolic event caused by glucose is a shift from fatty acids to glucose as an oxidative fuel. This occurs through glucose conversion to the "switch compound" malonyl-CoA, which, by inhibiting CPTI, blocks LC-CoA transport into the mitochondrion where they are oxidized. Therefore, the increase in malonyl-CoA may be responsible for the accumulation of LC-CoA in the cytosol[30]. The identification of LC-CoA or complex lipids rather than malonyl-CoA as candidate coupling factors during β-cell activation stems from the fact that LC-CoA and complex lipids such as DAG, lysophosphatidic acid (LPA) and PA are known to directly influence many biological processes[31,32,33,34]. On the other hand, malonyl-CoA, by modulating CPTI and the level of cytosolic LC-CoA, regulates fuel partitioning (the relative rates of glucose and FFA oxidation) and the fate of LC-CoA (oxidation, esterification and acylation). Thus, malonyl-CoA may be considered a *regulatory signaling* molecule in insulin secretion, whereas LC-CoA or complex lipids act as *effector signals.* This malonyl-CoA/LC-CoA model holds that the malonyl-CoA "signal of plenty" plays a pivotal role through inhibition of CPTI and thus leads to the accumulation of LC-CoA in the cytoplasm which stimulates insulin release, either directly on exocytosis or indirectly *via* complex lipid formation, PKC activation or protein acylation.

---

[30] Liang Y, Matschinsky FM. Content of CoA-esters in perifused rat islets stimulated by glucose and other fuels. *Diabetes.* 40:327-333, 1991

[31] Goetzl EJ, An S. Diversity of cellular receptors and functions for the lysophospholipid growth factors lysophosphatidic acid and sphingosine 1-phosphate. *Faseb J.* 12:1589-1598, 1998

[32] Hodgkin MN, Pettitt TR, Martin A, Michell RH, Pemberton AJ, Wakelam MJ. Diacylglycerols and phosphatidates: which molecular species are intracellular messengers? *Trends Biochem Sci.* 23:200-204, 1998

[33] Nietgen GW, Durieux ME. Intercellular signaling by lysophosphatidate. *Cell Adhes. Commun.* 5:221-235, 1998

[34] Brindley DN, Waggoner DW. Phosphatidate phosphohydrolase and signal transduction. *Chem. Phys. Lipids* 80:45-57, 1996

3) Other glucose-derived factors participating in insulin secretion are proposed to be glutamate and pyruvate cycling. Glutamate, which can be produced from the Krebs cycle intermediate α-ketoglutarate by glutamate dehydrogenase, is proposed to act on the secretory vesicle, by undefined mechanisms which may involve granule priming or modification of vesicles pH, enhancing the competence of the vesicle for fusion with the plasma membrane[35,36]. Thus, glutamate would act as a potentiator of insulin release, sensitizing exocytosis to the effect of calcium. Glutamate and fatty acid metabolism would be related, as glutamate activates ACC increasing malonyl-CoA and thus, LC-CoA levels in the cytosol[37]. On the other hand, pyruvate cycling has been correlated with glucose-stimulated insulin secretion and with the degree of glucose responsiveness in INS-1-derived cell lines[9,38]. The term pyruvate cycling refers to the exchange of pyruvate with TCA cycle intermediates or the flux through either the pyruvate-malate or pyruvate-citrate cycles. It has been described that long-term exposure of pancreatic β-cells to FFA inhibits GSIS *via* the decreased NADPH content due to the inhibition of pyruvate carboxylase and malate pyruvate shuttle flux[39]. Therefore, NADPH could be a candidate coupling factor which may link mitochondrial reducing equivalents and GSIS, indicting a direct relationship between changes in NADPH levels, mitochondrial activation and insulin secretion.

Overall, the results presented in this thesis show, for the first time, that when the malonyl-CoA/CPTI interaction is altered, glucose-induced insulin release is impaired. The results also indicate the importance of a tight control in lipid homeostasis and the implication of LC-CoA as effector signals in GSIS.

---

[35] Maechler P, Wollheim CB. Mitochondrial glutamate acts as a messenger in glucose-induced insulin exocytosis. *Nature*. 402:685-689, 1999

[36] Rubi B, Ishihara H, Hegardt FG, Wollheim CB, Maechler P. GAD65-mediated glutamate decarboxylation reduces glucosa-stimulated insulin secretion in pancreatic beta cells. *J. Biol. Chem*. 276:36391-36396, 2001

[37] Kowluru A, Chen HQ, Mordirck L, Stefanelli C. Activation of acetyl-CoA carboxylase by a glutamate and magnesium sensitive protein phosphatase in the islet β-cell. *Diabetes*. 50:1580-1587, 2001

[38] Lu D, Mulder H, Zhao P, Burgess SC, Jensen MV, Kamzolova S, Newgard CB, Sherry AD. ^{13}C isotopomer analysis reveals a connection between pyruvate cycling and glucose-stimulated insulin secretion (GSIS). *Proc. Natl. Acad. Sci. USA.* 99:2708-2713, 2002

[39] Iizuka K, Nakajima H, Namba M, Miyagawa J, Miyazaki J, Hanafusa T, Matsuzawa Y. Metabolic consequence of long-term exposure of pancreatic beta cells to free fatty acid with special reference to glucose insensitivity. *Biochim. Biophys. Acta*. 1586:23-31, 2002

1.8 FUTURE: ALTERATION OF MALONYL-CoA/CPTI INTERACTION IN THE STUDY OF DIABETES AND OBESITY

Many studies implicate FFAs in Type 2 diabetes[40,41]. Long-term exposure of β-cells to FFAs *in vitro* has several effects: 1) it increases basal insulin release and decreases secretion in response to glucose[42]; 2) it alters the coupling of glucose metabolism to insulin secretion by acting on the expression of specific genes, such as UCP-2[43,44]; 3) it increases the expression of CPTI, which is considered the rate-limiting step in fatty acid oxidation[45]. Low levels of lipid oxidation are associated with, and predictive for, obesity in both humans and rodents[46,47], and decreased CPTI activity has been demonstrated in obese patient populations[48,49].

Taking into account the results presented in this study of the LCPTI M593S mutant, fatty acid oxidation would be markedly increased in a system where the malonyl-CoA/CPTI interaction was altered and the CPTI was insensitive to its inhibitor malonyl-CoA. This would lead to dysregulation of β-oxidation even at high malonyl-CoA levels (high glucose like in a diabetic state), and probably to the impairment of GSIS due to the huge presence of FFAs (like in an obese state) will be restored. Related to this hypothesis, a recent and very interesting study showed that in rats fed a high-fat-

---

[40] Unger RH. Lipotoxicity in the pathogenesis of obesity-dependent NIDDM. Genetic and clinical implications. *Diabetes.* 44:863-870, 1995

[41] McGarry JD. Dysregulation of fatty acid metabolism in the etiology of type 2 diabetes. *Diabetes.* 51:7-18, 2002

[42] Zhou YP, Grill V. Long-term exposure of rat pancreatic islets to fatty acids inhibits glucose-induced insulin secretion and biosynthesis through a glucose fatty acid cycle. *J. Clin. Invest.* 93:870-876, 1994

[43] Lameloise N, Muzzin P, Prentki M, Assimacopoulos-Jeannet F. Uncoupling protein 2: a possible link between fatty acid excess and impaired glucose-induced insulin secretion? *Diabetes*. 50:803-809, 2001

[44] Zhang CY, Baffy G, Perret P, Krauss S, Peroni O, Grujic D, Hagen T, Vidal-Puig AJ, Boss O, Kim YB, Zheng XX, Wheeler MB, Shulman GI, Chan CB, Lowell BB. Uncoupling protein-2 negatively regulates insulin secretion and is a major link between obesity, beta cell dysfunction and type 2 diabetes. *Cell.* 105:745-755, 2001

[45] Assimacopoulos-Jeannet F, Thumelin S, Roche E, Esser V, McGarry JD, Prentki M. Fatty acids rapidly induce the carnitine palmitoyltransferase I gene in the pancreatic β-cell line INS-1. *J. Biol. Chem*. 272:1659-1664, 1997

[46] Zurlo F, Lillioja S, Esposito-Del Puente A, Nyomba BL, Raz I, Saad MF, Swinburn BA, Knowler WC, Bogardus C, Ravussin E. Low ratio of fat to carbohydrate oxidation as predictor of weight gain: study of 24-h RQ. *Am. J. Physiol*. 259:E650-E657, 1990

[47] Pagliassotti MJ, Gayles EC, Hill JO. Fat and energy balance. *Ann. N Y Acad. Sci*. 827:431-448. Review, 1997

[48] Simoneau JA, Veerkamp JH, Turcotte LP, Kelley DE. Markers of capacity to utilize fatty acids in human skeletal muscle: relation to insulin resistance and obesity and effects of weight loss. *FASEB J.* 13:2051-2060, 1999

[49] Kim JY, Hickner RC, Cortright RL, Dohm GL, Houmard JA. Lipid oxidation is reduced in obese human skeletal muscle. *Am. J. Physiol. Endocrinol. Metab*. 279:E1039-E1044, 2000

diet, whole-animal, muscle and liver insulin resistance was ameliorated following hepatic overexpression of MCD by tail vein injection of an adenovirus encoding MCD[50]. In addition, insulin action was enhanced within the liver and at a remote site (muscle). These changes were associated with a fall in circulating FFA, a rise or no significant change in muscle triglycerides and LC-CoA levels, and a marked decrease in intramuscular β-OH-butyrate levels. The authors propose that hepatic expression of MCD lowered circulating FFA levels, which led to lowering of muscle β-OH-butyrate levels and improvement of insulin sensitivity. In addition, ACC mutant mice ($ACC\beta^{-/-}$) had been reported to be protected against obesity and diabetes induced by high-fat/high-carbohydrate diets[51]. $ACC\beta^{-/-}$ mice have a normal lifespan, a higher fatty acid oxidation rate and lower amounts of fat[52]. When these mutant mice were fed with a high-fat/high-carbohydrate diets they weighed less than their wt cohorts, accumulated less fat, and maintained normal levels of insulin and glucose, whereas the wt mice became Type 2 diabetic with hyperglycemic and hyperinsulinemic status. The broader implication of these findings is that enzymes involved in lipid partitioning such as MCD, ACC and CPTI could be potential targets in therapy against obesity and related diseases such as diabetes. Therefore, a parallel study on the LCPTI M593S mutant might be expected to lead to similar or even more enhanced results because it is insensitive to malonyl-CoA and because, unlike MCD and ACC, CPTI directly controls the flux of LC-CoAs into the mitochondria for their oxidation.

Moreover, in pancreatic β-cells chronically exposed to high glucose and/or high fatty acids, overexpression of the LCPTI M593S mutant may prevent the impairment of GSIS and β-cell apoptosis. This hypothesis, however, is challenged by a recent study of the MCD overexpression in chronic culture of INS(832/13) cells with high concentrations of FFAs and lipid-laden islets from Zucker diabetic fatty rats[9]. Adenovirus-mediated MCD overexpression resulted in reduced TG stores, but no

[50] An J, Muoio DM, Shiota M, Fujimoto Y, Cline GW, Shulman GI, Koves TR, Stevens R, Millington D, Newgard CB. Hepatic expression of malonyl-CoA decarboxylase reverses muscle, liver and whole-animal insulin resistance. *Nat. Med*. 10:268-274, 2004

[51] Abu-Elheiga L, Oh W, Kordari P, Wakil SJ. Acetyl-CoA carboxylase 2 mutant mice are protected against obesity and diabetes induced by high-fat/high-carbohydrate diets. *Proc. Natl. Acad. Sci. USA*.100:10207-10212, 2003

[52] Abu-Elheiga L, Matzuk MM, Abo-Hashema KAH, Wakil SJ. Continuous fatty acid oxidation and reduced fat storage in mice lacking acetyl-CoA carboxylase 2. *Science*. 291:2613-2616, 2001

improvement in GSIS. We hypothesize that the more direct effect of CPTI on LC-CoA oxidation may allow the LCPTI M593S mutant to restore the impairment in GSIS.

Further research is needed on the aetiology of obesity and Type 2 diabetes and the potential use of CPTI as an effective drug target.

2. STABLE EXPRESSION OF LCPTI wt AND LCPTI M593S

We aimed to corroborate the results obtained with the adenoviruses encoding for LCPTI wt and LCPTI M593S cDNAs by generating INS-1 cells which stably expressed these constructs under the Tet-on system. This system allows temporary control of gene expression upon doxycycline treatment of the cells.

The functionality and correct protein expression of the construct were checked by transient expression in HEK 293 rtTA cells. However, when the INS-1 clones obtained were incubated with doxycycline, a lack of increase in LCPTI protein expression compared to endogenous LCPTI was correlated with a lack of increase in CPTI activity. We conclude that probably a slight basal overexpression of LCPTI even in the absence of doxycycline could be toxic for the cells, as a result of which only that cells which did not contain the LCPTI plasmids survived throughout cell passages. The presence of the LCPTI construct in the genome of the clones 26, 52 and 57, suggests that maybe the transgene may not have been well integrated into the genome, which caused non LCPTI overexpression.

These events could be compared with previous studies performed in our group[53], in which the effect of LCPTI *in vivo* was examined to investigate the involvement of LCPTI in obesity and diabetes. Six transgenic mouse lines were generated using the construct RIP-β-globin-LCPTI wt which conducted the LCPTI wt transgene to the pancreas of the mice under the rat insulin promoter (RIP). However, none of these mouse lines expressed the desired construct, indicating that LCPTI expression could lead to a defect in the development of the animals, preventing their survival. Therefore, these results along with that obtained in the present study with the LCPTI wt and LCPTI M593S stable cell lines, suggest that a tight control of lipid homeostasis is essential for development and survival.

[53] Rubi B. El glutamato y los ácidos grasos participan en la transducción de la señal para la liberación de insulina estimulada por glucosa en la célula β del páncreas. Thesis, 2001

3. STUDY OF THE INTERACTION BETWEEN C75 AND CPTI IN THE PANCREATIC β-CELL

The fatty acid synthase (FAS) synthetic inhibitor C75 has been described as the first pharmacological agonist of CPTI[54], identifying CPTI as a therapeutic target for obesity and Type 2 diabetes. Thus, these authors[54] explained the profound weigh loss peripherally seen in C75-treated mice by a C75-stimulation of CPTI activity and an increase in fatty acid oxidation. However, when FAS is inhibited by C75, the ensuing high content of malonyl-CoA should inhibit CPTI activity. However, paradoxically, in peripheral tissues, this effect seems to be overcome by C75-stimulated CPTI activity. On the other hand, cerulenin, a natural FAS inhibitor, has been reported to decrease CPTI activity[55,56] *in vivo* and *in vitro*, accompanied by a reduction in fatty acid oxidation.

Taking into account these paradoxical actions of C75 and the interesting fact that C75 could be a CPTI agonist with similar properties to our LCPTI M593S mutant, we decided to further investigate the effect of C75 on CPTI activity in pancreatic β-cells *in vitro* and *in vivo*. In the β-cell, the FAS expression is very low[6], thus allowing us to study the C75/CPTI interaction directly.

3.1 C75 INHIBITS CPTI ACTIVITY IN PANCREATIC β-CELLS

Recent studies by our group[57] have demonstrated that C75 itself neither inhibited nor activated mitochondrial LCPTI or MCPTI enzymes overexpressed in yeast. The same occurred with etomoxir itself. As it has been described[58] that the active inhibitory

---

[54] Thupari JN, Landree LE, Ronnett GV, Kuhajda FP. C75 increases peripheral energy utilization and fatty acid oxidation in diet-induced obesity. *Proc. Natl. Acad. Sci. USA.* 99**:**9498-9502, 2002

[55] Thupari JN, Pinn ML, Kuhajda FP. Fatty acid synthase inhibition in human breast cancer cells leads to malonyl-CoA-induced inhibition of fatty acid oxidation and cytotoxicity. *BBRC*. 285:217-223, 2001

[56] Jin YJ, Li SZ, Zhao ZS, An JJ, Kim RY, Kim YM, Baik JH, Lim SK. Carnitine palmitoyltransferase-1 (CPT-1) activity stimulation by cerulenin via sympathetic nervous system activation overrides cerulenin's peripheral effect. *Endocrinology*. 145:3197-3204, 2004

[57] Bentebibel A, Sebastián D, Herrero L, Serra D, Asins G, Hegardt FG. C75-CoA inhibits Carnitine Palmitoyltransferase I activity thus decreasing palmitate oxidation. Submitted.

[58] Weis BC, Cowan AT, Brown N, Foster DW, McGarry JD. Use of a selective inhibitor of liver carnitine palmitoyltransferase I (CPT I) allows quantification of its contribution to total CPT I activity in rat heart. Evidence that the dominant cardiac CPT I isoform is identical to the skeletal muscle enzyme. *J. Biol. Chem.* 269:26443-26448, 1994

form of etomoxir is its CoA-derivative, etomoxiryl-CoA, we also demonstrated that C75 was also converted to C75-CoA. The formation of both compounds, C75-CoA and etomoxiryl-CoA, was confirmed by MALDI-TOF analysis and indeed, only when C75 or etomoxir were transformed to their CoA derivatives could alter CPTI activity in yeast overexpressing L or M CPTI. In the case of pancreatic β-cells, mitochondrion-enriched cell fractions were incubated with C75-CoA for CPTI activity assays, but INS(832/13) cells were directly incubated with C75 as the activation to CoA could occur inside the cells *via* mitochondrial acyl-CoA synthase.

In pancreatic β-cells, surprisingly, we found that CPTI activity was not activated but inhibited by C75 in INS(832/13) cells and by C75-CoA in mitochondrion-enriched cell fractions. This inhibition was also seen in HEK 293 cells and in L6E9 muscle cells[57].

It is interesting to compare the present results where CPTI is inhibited, with those obtained by others[54,59,60] who observed CPTI activation. In the study of Yang *et al*.[59] human hepatocarcinoma cells (Hep G2) were directly incubated with C75 plus labelled carnitine and an increase in CPTI activity was found, as measured by the synthesis of palmitoylcarnitine. In the other studies[54,60], the authors observed a C75-stimulation of CPTI activity in human breast cancer cells (MCF-7) and in rodent adipocytes (3T3-L1) and primary hepatocytes and cortical neurons. The discrepancy may be explained by differences in the method used to measure CPTI activity. These authors[54,60] performed CPTI assays in digitonin-permeabilized cells, while in the present study isolated and purified mitochondria from tissues and cultured cells were used. Interestingly, when the experiments of digitonin permeabilization in L6E9 muscle cells were repeated in our laboratory following Thupari's protocol, it was also found that CPTI was activated. We hypothesized that digitonine permeabilization together with the C75 treatment might alter interactions between mitochondria and the cytoskeleton[17,61] which may either alter CPTI activity or disturb the assay. It has been suggested that

[59] Yang N, Kays JS, Skillman TR, Burris L, Seng TW, Hammond C. C75 activates carnitine palmitoyltransferase-1 in isolated mitochondria and intact cells without displacement of bound malonyl-CoA. *J. Pharmacol. Exp. Ther*. PMID: 15356215, 2004

[60] Landree LE, Hanlon AL, Strong DW, Rumbaugh G, Miller IM, Thupari JN, Connolly EC, Hunganir RL, Richardson C, Witters LA, Kuhajda FP, Ronnet GV. C75, a Fatty acid synthase inhibitor, modulates AMP-activated protein kinase to alter neuronal energy metabolism. *J. Biol. Chem*. 279:3817-3827, 2004

[61] Guzmán M, Velasco G, Geelen MJH. Do cytoskeletal components control fatty acid translocation into liver mitochondria? *Trends Endocrinol. Metab.* 11:49-53, 2000

changes in the lipid composition of the membrane microenvironment in which CPTI resides cause alteration of CPTI activity[62,63,64,65], indicating the importance of CPTI's interaction with the mitochondrial membrane for its activity and regulation. Numerous approaches[10,66,67,68,69] suggest that modulation of interdomain interactions, for instance by covalent modification (phosphorylation)[16] of the protein, may be also involved in changes of CPTI activity. These events may occur as a consequence of an indirect action of C75 on permeabilized cells.

3.2 C75 INHIBITS PALMITATE OXIDATION IN PANCREATIC β-CELLS

The experiments performed in the present study on palmitate oxidation on INS(832/13) cells reveal that C75 inhibits β-oxidation, in acute accordance with inhibition of CPTI. This inhibition was also seen in HEK 293 cells and in L6E9 muscle cells[57]. Again, we find a discrepancy between our results and those obtained by others[54,60] performed in rodent adipocytes and primary hepatocytes and cortical neurons, in which they reported an increase in fatty acid oxidation. However, a slightly decrease

---

[62] Zammit VA, Corstorphine CG, Kolodziej MP, Fraser F. Lipid molecular order in liver mitochondrial outer membranes, and sensitivity of carnitine palmitoyltransferase I to malonyl-CoA. *Lipids*. 33:371-376, 1998

[63] Mynatt RL, Greenhaw JJ, Cook GA. Cholate extracts of mitochondrial outer membranes increase inhibition by malonyl-CoA of carnitine palmitoyltransferase-I by a mechanism involving phospholipids. *Biochem. J*. 299:761-767, 1994

[64] Zammit VA. Carnitine acyltransferases: functional significance of subcellular distribution and membrane topology. *Progress in lipid research*. 38:199-224, 1999

[65] Fraser F, Padovese R, Zammit VA. Distinct kinetics of carnitine palmitoyltransferase in contact sites and outer membranes of rat liver mitochondria. *J. Biol. Chem*. 276:20182-20185, 2001

[66] Swanson ST, Foster DW, McGarry JD, Brown NF. Roles of the N- and C-terminal domains of carnitine palmitoyltransferase I isoforms in malonyl-CoA sensitivity of the enzymes: insights from expression of chimaeric proteins and mutation of conserved histidine residues. *Biochem. J*. 335:513-519, 1998

[67] Jackson VN, Zammit VA, Price NT. Identification of positive and negative determinants of malonyl-CoA sensitivity and carnitine affinity within the amino termini of rat liver- and palmitoyltransferase I. *J. Biol. Chem*. 275:38410-38416, 2000

[68] Jackson VN, Price NT, Zammit VA. Specificity of the interactions between Glu-3, Ser-24, and Gln-30 within the N-terminal segment of rat liver mitochondrial overt carnitine palmitoyltransferase (L-CPT I) in determining the malonyl-CoA sensitivity of the enzyme. *Biochemistry*. 40:14629-14634, 2001

[69] Shi J, Zhu H, Arvidson DN, Cregg JM, Woldegiorgis G. Deletion of the conserved first 18 N-terminal amino acid residues in rat liver carnitine palmitoyltransferase I abolishes malonyl-CoA sensitivity and binding. *Biochemistry*. 37:11033-11038, 1998

in palmitate oxidation has been described in rat islets treated with cerulenin[70]. It is difficult to explain these discrepancies, which could be attributed to differences in cell line or experimental conditions, or unknown effects of C75 on other cellular signalling pathways.

Recent data suggest that modulation of FAS activity by C75 in the hypothalamus can alter energy perception by reducing AMPK, enzyme that functions as a physiological energy sensor in the hypothalamus[71]. AMPK activates MCD and suppresses the synthesis of ACC, FAS and other enzymes of lipid biogenesis in many tissues by inhibiting the generation of the transcriptional factor SREBP-1c[72]. The net effect of AMPK activation is therefore to increase fatty acid oxidation (at least in part by lowering the concentration of malonyl-CoA) and to decrease their esterification and use in other non-β-oxidative pathways[73]. Thus, as C75 has been reported to reduce AMPK activity[71] this could lead to a decrease in fatty acid oxidation, which would reconcile the inhibition of β-oxidation seen in the present study in pancreatic β-cells.

In addition, it has been recently shown that inhibition of hypothalamic CPTI in rats causes a reduction in food intake and glucose production[74], suggesting that the increase in LC-CoAs due to CPTI inhibition represents a central signal of "nutrient abundance". Moreover, central delivery of the LCFA oleic acid also inhibits glucose production and food intake[75]. These findings support the idea that increased LC-CoAs function as a sensor of nutrient availability in hypothalamic neurons. Finally, endocannabinoids, which have potent orexigenic (appetite-stimulating) effects, stimulate CPTI activity and fatty acid oxidation in cultured astrocytes independently of

[70] Yajima H, Komatsu M, Yamada S, Straub SG, Kaneko T, Sato Y, Yamauchi K, Hashizume K, Sharp GWG, Aizawa T. Cerulenin, an inhibitor of protein acylation, selectively attenuates nutrient stimulation of insulin release. *Diabetes*. 49:712-717, 2000

[71] Kim EK, Miller I, Aja S, Landree LE, Pinn M, McFadden J, Kuhajda FP, Moran TH, Ronnett GV. C75, a fatty acid synthase inhibitor, reduces food intake via hypothalamic AMP-activated protein kinase. *J. Biol. Chem*. 279:19970-19976, 2004

[72] Ferre P, Azzout-Marniche D, Foufelle F. AMP-activated protein kinase and hepatic genes involved in glucose metabolism. *Biochem. Soc. Trans*. 31:220-223, 2003

[73] Ruderman N, Prentki M. AMP kinase and malonyl-CoA: targets for therapy of the metabolic syndrome. *Nature.* 3:340-351, 2004

[74] Obici S, Feng Z, Arduini A, Conti R, Rossetti L. Inhibition of hypothalamic carnitine palmitoyltransferase-1 decreases food intake and glucose production. *Nat Med*. 9:756-761, 2003

[75] Obici S, Feng Z, Morgan K, Stein D, Karkanias G, Rossetti L. Central administration of oleic acid inhibits glucose production and food intake. *Diabetes*. 51:271-275, 2002

malonyl-CoA and through interaction with CB_1 receptors[76,77]. All together, these studies support evidence in favour of the implication of CPTI inhibition in the loss of food intake.

However, this does not explain the increase in energy expenditure and the profound weight loss observed peripherally in mice[54]. One possible explanation of this increased energy production could be the C75-mediated up-regulation of UCPs. It has recently been reported that long-term treatment with C75 increases expression of UCP-3 mRNA in skeletal muscle of obese mice, suggesting that this up-regulation of UCP-3 may increase thermogenesis and thereby explain the increase in energy expenditure[78]. Nevertheless, further investigations are needed to clarify the effect of C75 on the whole metabolism.

It has been reported that C75 treatment of human cancer cells *in vitro* led to rapid inhibition of fatty acid synthesis, followed by inhibition of DNA replication, culminating in apoptosis[79,80]. Whereas induction of apoptosis appeared to be related to accumulation of the substrate, malonyl-CoA, after FAS inhibition, the cytostatic effects were independent of malonyl-CoA accumulation and may have resulted from product depletion[80]. To rule out the possibility that the inhibition of palmitate oxidation seen in INS(832/13) cells was due to cytotoxic effects of C75, viability assays were performed. They showed that in our conditions viability of pancreatic β-cells was above 98%. The sensitivity of the cell to the cytotoxic effect of C75 may depend on the lipid composition and metabolism. For instance, breast carcinoma cell line SKBR3, with higher lipid content, needs 6 h of C75-preincubation to show the cytotoxic effect[79]. However, in pancreatic β-cells, where the expression of FAS and fatty acid biosynthesis

---

[76] Blazquez C, Sanchez C, Daza A, Galve-Roperh I, Guzman M. The stimulation of ketogenesis by cannabinoids in cultured astrocytes defines carnitine palmitoyltransferase I as a new ceramide-activated enzyme. *J. Neurochem.* 72:1759-1768, 1999

[77] Di Marzo V, Goparaju SK, Wang L, Liu J, Batkai S, Jarai Z, Fezza F, Miura GI, Palmiter RD, Sugiura T, Kunos G. Leptin-regulated endocannabinoids are involved in maintaining food intake. *Nature.* 410:822-825, 2001

[78] Cha SH, Hu Z, Lane MD. Long-term effects of a fatty acid synthase inhibitor on obese mice: food intake, hypothalamic neuropeptides, and UCP3. *BBRC.* 317:301-308, 2004

[79] Pizer ES, Thupari J, Han WF, Pinn ML, Chrest FJ, Frehywot GL, Townsend CA, Kuhajda FP. Malonyl-coenzyme-A is a potential mediator of cytotoxicity induced by fatty acid synthase inhibition in human breast cancer cells and xenografts. *Cancer Res*. 60:213-218, 2000

[80] Li JN, Gorospe M, Chrest FJ, Kumaravel TS, Evans MK, Han WF, Pizer ES. Pharmacological inhibition of fatty acid synthase activity produces both cytostatic and cytotoxic effects modulated by p53. *Cancer Research*. 61:1493-1499, 2001

are low, more than 2h of C75-preincubation or concentrations of C75 higher than 40 µg/ml were toxic for the cells.

3.3 *IN VIVO* C75 INHIBITS CPTI ACTIVITY AT SHORT TIMES

The experiments *in vitro*, which consistently indicate that C75 inhibits CPTI activity and fatty acid oxidation, were also corroborated by the experiments *in vivo*. C75 produced short-term inhibition of CPTI activity in mouse liver and pancreas, with the maximum CPTI-inhibitory properties shown in the liver. The differential extent of inhibition of CPTI could be explained by differences in the rate of C75-CoA endogenous activation and pharmacokinetics in each tissue. Inhibition of CPTI by the drug may remain stable until the C75-modified CPTI is replaced by a new molecule. It is possible that the proteasome recognizes the drug-modified CPTI and promotes its disappearance. This time scale would be tissue dependent. This increased turnover of the CPTI protein or the unknown effects of C75 on other cellular signalling pathways of cellular fuel state, like that observed in UCP-3[78] or in hypothalamic AMPK[60,71], which in turn could affect CPTI activity, could explain the increases in energy expenditure observed by Thupary *et al*.[54].

Interestingly, cerulenin, a natural FAS inhibitor, has been reported to decrease CPTI activity[81,82]. In the former study[81], performed with human breast cancer cells cultured with cerulenin, the decrease in CPTI activity was correlated with a reduction in fatty acid oxidation and an increase in the cytotoxicity effect. In the latter study[82], the authors showed that the effect of cerulenin on CPTI activity in mice was biphasic in liver and muscle, with an early suppression followed by a late stimulation after intraperitoneal treatment. They concluded that the late stimulating effect of cerulenin on CPTI activity occurred *via* the sympathetic nervous system. C75 may behave like cerulenin in mice, producing a dual effect on CPTI: first inhibition and later activation. This would also be consistent with the increased peripheral fatty acid oxidation observed in mice after several hours of treatment.

---

[81] Thupari JN, Pinn ML, Kuhajda FP. Fatty acid synthase inhibition in human breast cancer cells leads to malonyl-CoA-induced inhibition of fatty acid oxidation and cytotoxicity. *BBRC*. 285:217-223, 2001

[82] Jin YJ, Li SZ, Zhao ZS, An JJ, Kim RY, Kim YM, Baik JH, Lim SK. Carnitine palmitoyltransferase-1 (CPT-1) activity stimulation by cerulenin via sympathetic nervous system activation overrides cerulenin's peripheral effect. *Endocrinology*. 145:3197-3204, 2004

3.4 FUTURE: FURTHER INVESTIGATION

The results presented in this thesis provide compelling evidence that C75 is a potent and direct inhibitor of LCPTI in pancreatic β-cells *in vitro* and *in vivo*. A summary of our results and the effects of C75 published in the literature is shown in Table. 1.

CENTRAL	PERIPHERAL			
Hypothalamus	**Adipocyte**	**Liver**	**Muscle**	**Pancreatic β-cell**
↑ Malonyl-CoA[83]	↓ Adipose tissue[78]	↓ Fatty liver[85]	↑ UCP-3[78]	↓ CPTI (Thesis)
↓ Food consumption[85]	↑ CPTI[54]	↑ CPTI[54]	↓ CPTI[57]	↓ Palmitate oxidation (Thesis)
↓ NYP, AgRP[84]	↑ Palmitate oxidation[54]	↑ Palmitate oxidation[54]		
↑ POMC, CART[84]		↓ CPTI[57]		
↑ ATP levels[71]				
↓ AMPK[71]				
↑ CPTI[60]				
↑ Palmitate oxidation[60]				

Table. 1. Central and peripheral effects of C75. Centrally (hypothalamus) C75 increases malonyl-CoA levels as a result of FAS inhibition[83]. Hypothalamic malonyl-CoA is an indicator of energy status and mediates feeding behaviour. C75 prevents the up-regulation of the orexigenic neuropeptides (NYP and AgRP) and down-regulation of the anorexigenic neuropeptides (POMC, CART)[84] thus decreasing food consumption[85]. In addition, C75 has been reported to inhibit AMPK[71] by increasing ATP levels[71] and to increase CPTI activity[60] and palmitate oxidation[60]. Peripherally, C75 reduces body weight (loss of adipose tissue[78] and resolution of hepatic steatosis[85]) by increasing energy expenditure as a result of CPTI activation and increased palmitate oxidation[54]. Long-term treatment with C75 results in increased expression of UCP-3 mRNA in skeletal muscle of obese mice[78]. This may increase thermogenesis and thereby explain the increase in energy expenditure. C75 inhibits CPTI activity in mitochondria isolated from rat liver and muscle[57]. Finally, in the present study we found that C75 inhibits CPTI activity both *in vitro* and *in vivo* in acute accordance with inhibition of palmitate oxidation. NPY; neuropeptide Y, AgRP; agouti-related protein, POMC; pro-opiomelanocortin, CART; cocaine-amphetamine-regulated transcript.

[83] Hu Z, Cha SH, Chohnan S, Lane MD. Hypothalamic malonyl-CoA as a mediator of feeding behavior, *Proc. Natl. Acad. Sci. USA.* 100:12624-12629, 2003

[84] Shimokawa T, Kumar MV, Lane MD. Effect of fatty acid synthase inhibitor on food intake and expression of hypothalamic neuropeptides. *Proc. Natl. Acad. Sci. USA.* 99:66-71, 2002

[85] Loftus TM, Jaworsky DE, Freywot GL, Townsend CA, Ronet GV, Lane MD, Kuhajda FP. Reduced food intake and body weight in mice treated with fatty acid synthase inhibitors. *Science* 288:2379-2381, 2000

Further investigation is needed to explain the stimulation of fatty acid oxidation of C75 observed by others in peripheral tissues and the loss of body weight. It would be interesting to perform a three-dimensional structural model for CPTI on which the position of C75 could be assigned by superposition and docking analysis. This study would help us to improve our knowledge of the interaction between CPTI and C75 and to discern between covalent and non-covalent interaction and activation or inhibition of the CPTI activity. In addition, octanoate oxidation experiments may rule out distant C75 effects on CPTI, as octanoate is a medium-chain fatty acid that does not require CPTI to enter the mitochondria and be oxidized.

CONCLUSIONS

CONCLUSIONS

1. CPTI activity is not inhibited by malonyl-CoA in INS(832/13) cells expressing LCPTI M593S. CPTI activity of INS(832/13) cells expressing LCPTI M593S is less sensitive to etomoxir than LCPTI wt-expressing cells.

2. Expression of LCPTI wt and LCPTI M593S in INS(832/13) cells increases enzymatic activity of CPTI, correlated with the amount of adenovirus used. CPTI activity increases in both cases to a plateau of 9-10 fold compared with the endogenous LCPTI. The increase in CPTI activity is correlated with similar levels of LCPTI protein in INS(832/13) cells and rat islets overexpressing LCPTI wt and LCPTI M593S.

3. Overexpression of LCPTI M593S increases palmitate oxidation rates in INS(832/13) cells at all glucose concentrations tested. Fat oxidation rates were much higher than in control Ad-LacZ-infected cells and still higher than in cells infected with Ad-LCPTI wt, even at high malonyl-CoA concentrations (high glucose).

4. Malonyl-CoA levels and glucose oxidation are not modified by LCPTI wt or LCPTI M593S overexpression, compared with LacZ control cells.

5. GSIS is reduced by 60% in INS(832/13) cells expressing LCPTI M593S, but not in response to a depolarizing concentration of KCl, indicating that exocytosis *per se* is preserved in those cells. GSIS is recovered completely in the presence of 0.25 mM palmitate only in the case of LCPTI wt, showing the strong metabolic influence of LCPTI M593S on fatty acid oxidation and insulin secretion in the pancreatic β-cell. The GSIS impairment is restored in both cases after 200 μM etomoxir incubation.

6. LCPTI wt and LCPTI M593S overexpression impairs K_{ATP} channel-independent GSIS in INS(832/13) cells, which is consistent with the view that malonyl-CoA/CPTI interaction is involved in the amplification arm of secretion.

7. In islets overexpressing LCPTI M593S GSIS was decreased by 40%, while no difference was seen in Ad-LCPTI wt-infected islets, suggesting preserved lipid signalling above a critical threshold of cytosolic FA-CoA.

8. Glucose-induced esterification processes are reduced in INS(832/13) cells expressing LCPTI wt and even more decreased in LCPTI M593S-expressing cells.

9. PKC activation is impaired in INS(832/13) cells expressing LCPTI M593S suggesting that enhanced β-oxidation by the LCPTI M593S mutant reduces GSIS as a result of a decrease in PKC activation.

10. The attempt to establish an LCPTI wt or an LCPTI M593S stable cell line by the Tet-on system was unsuccessful, probably because a slight basal overexpression of LCPTI, even in the absence of doxycycline, could be toxic to the cells.

11. CPTI activity is inhibited in INS(832/13) cells and in mitochondrion-enriched cell fractions incubated with C75. This is correlated with an inhibition of palmitate oxidation whereas viability of the cells was not affected by the drug.

12. A single intraperitoneal injection of C75 to mice produces short-term inhibition of CPTI activity *in vivo* in mitochondria from liver and pancreas, recovering upon time.

APPENDIX

APPENDIX

1. PRIMER SEQUENCES

PRIMER	**SEQUENCE (5'——3')**
Myc.for	GGC GAA TGG GTG AGT AAC ACG
Myc.rev	CGG ATA ACG CTT GCG ACC TAT
pTRE2.for	GGC CTA TAT AAG CAG AGC TCG
CPTI*Nco*I.rev	GCT GCC TGG ATA TGG GTT GG
COTH131A.for	GCA TAC TAC TGT GGG CCA AAC TTG AAC TAC TGG C
COT*Xba*I.rev	TCA TGT CTA GAG GAG TAT TTC C
rtTA.for	CTC GCC AGA AGC TTG GTG TAG
rtTA.rev	CTG AAT GTA CTT TTG CTC CAT TGC G

2. SEQUENCE OF THE RAT LIVER CARNITINE PALMITOYLTRANSFERASE I

Sequence of the rat liver carnitine palmitoyltransferase I (LCPTI), published by Esser V. *et al* in 1993, with accession number in GeneBank Data Libraries L00736.

DEFINITION: Rat carnitine palmitoyltransferase I mRNA, complete cDNAs.

ACCESSION NUMBER: L07736

EC NUMBER: 2.3.1.21

SOURCE: Rattus norvegicus (Norway rat) male adult liver cDNA to mRNA.

AUTHORS: Esser V, Britton CH, Weis BC, Foster DW and McGarry JD.

TITLE: Cloning, sequencing, and expression of a cDNA encoding rat liver carnitine palmitoyltransferase I. Direct evidence that a single polypeptide is involved in inhibitor interaction and catalytic function.

JOURNAL: *J. Biol. Chem.* 268: 5817-5822, 1993

CODIFYING SEQUENCE: 103..2424
translation="MAEAHQAVAFQFTVTPDGIDLRLSHEALKQICLSGLHSWKKKFIRF
KNGIITGVFPANPSSWLIVVVGVISSMHAKVDPSLGMIAKISRTLDTTGRMSSQT
KNIVSGVLFGTGLWVAVIMTMRYSLKVLLSYHGWMFAEHGKMSRSTKIWMA
MVKVLSGRKPMLYSFQTSLPRLPVPAVKDTVSRYLESVRPLMKEEDFQRMTAL
AQDFAVNLGPKLQWYLKLKSWWATNYVSDWWEEYIYLRGRGPLMVNSNYY
AMEMLYITPTHIQAARAGNTIHAILLYRRTLDREELKPIRLLGSTIPLCSAQWER
LFNTSRIPGEETDTIQHIKDSRHIVVYHRGRYFKVWLYHDGRLLRPRELEQQMQ
QILDDPSEPQPGEAKLAALTAADRVPWAKCRQTYFARGKNKQSLDAVEKAAFF
VTLDESEQGYREEDPEASIDSYAKSLLHGRCFDRWFDKSITFVVFKNSKIGINAE
HSWADAPIVGHLWEYVMATDVFQLGYSEDGHCKGDTNPNIPKPTRLQWDIPG

ECQEVIDASLSSASLLANDVDLHSFPFDSFGKGLIKKCRTSPDAFIQLALQLAHY
KDMGKFCLTYEASMTRLFREGRTETVRSCTMESCNFVQAMMDPKSTAEQRLK
LFKIACEKHQHLYRLAMTGAGIDRHLFCLYVVSKYLAVDSPFLKEVLSEPWRLS
TSQTPQQQVELFDFEKNPDYVSCGGGFGPVADDGYGVSYIIVGENFIHFHISSKF
SSPETDSHRFGKHLRQAMMDIITLFGLTINSKK"

BASES: 1109 a 1115 c 1121 g 1032 t

```
1    agtcggtcga ctccgagctc agtgaggacc taaagcagag gactgtggtg cggaggacag
61   tgcttgctcc ggggagtgca gagcaatagg tccccactca agatggcaga ggctcaccaa
121  gctgtggcct tccagttcac cgtcaccccc gatggcattg acctccgcct gagccacgaa
181  gccctcaaac agatctgcct gtcggggctg cactcctgga agaagaagtt catccggttc
241  aagaatggca tcatcactgg tgtgttcccc gcgaatccgt ccagctggct tatcgtggtg
301  gtgggtgtga tttcatccat gcatgccaaa gtggacccct ccctgggcat gatcgcaaag
361  atcagtcgga ccctagacac cactggccgc atgtcaagcc agacgaagaa cattgtgagc
421  ggcgtcctct ttggtacagg gctctgggtg gcagtcatca tgaccatgcg ctactcgctg
481  aaggtgctgc tctcctacca cggctggatg tttgcagaac acggcaaaat gagccgcagc
541  accaagatct ggatggctat ggtcaaggtc ctctcaggtc ggaagcccat gttgtacagc
601  ttccagacgt ctctgccacg cctgcctgtc ccagctgtca aagatactgt gagcaggtac
661  ctggaatctg taaggccact gatgaaggaa gaagacttcc agcgcatgac agcactggcc
721  caggattttg ctgtcaacct cggacccaaa ttgcagtggt atttgaagct aaaatcctgg
781  tgggccacaa attacgtgag tgactggtgg gaagaatata tctacctgcg gggccgaggg
841  ccgctcatgg tcaacagcaa ctactacgcc atggagatgc tgtacatcac cccaacccat
901  atccaggcag cgagagctgg caacaccatc cacgccatac tgctgtatcg tcgcacatta
961  gaccgtgagg aactcaaacc cattcgtctt ctgggatcca ccattccact ctgctcagcc
1021 cagtgggagc gactcttcaa tacttcccgg atccctgggg aggagacaga caccatccaa
1081 catatcaagg acagcaggca cattgttgtg taccacagag ggcggtactt caaggtctgg
1141 ctctaccacg atgggaggct gctgaggccc cgagagctgg agcagcagat gcagcagatc
1201 ctggatgatc cctcagagcc acagcctggg gaggccaagc tggccgccct cactgctgca
1261 gacagagtgc cctgggcaaa gtgtcggcag acctattttg cacgagggaa aaataagcag
1321 tccctggatg cggtggaaaa ggcagcgttc ttcgtgacgt tggacgaatc ggagcaggga
1381 tacagagagg aggatcctga ggcatccatc gacagctacg ccaaatccct gctgcatgga
1441 agatgctttg acaggtggtt tgacaagtcc atcacctttg ttgtcttcaa aaacagcaag
1501 ataggcataa atgcagagca ctcctgggcg gacgcgccca tcgtgggcca tttgtgggag
1561 tatgtcatgg ccaccgacgt cttccagctg ggttactcag aggatggaca ctgtaaagga
1621 gacaccaacc ccaacatccc taagcccaca aggctacaat gggacattcc aggagagtgc
1681 caggaggtca tagatgcatc cctgagcagc gccagtcttt tggcaaatga tgtggacctg
1741 cattccttcc catttgactc tttcggcaaa ggcttgatca agaagtgccg gacgagtccc
1801 gatgccttca tccagctggc gctgcagctc gcacattaca aggacatggg caagttctgc
1861 ctcacatatg aggcctccat gacccggctc ttccgagaag ggaggacaga gactgtacgc
1921 tcctgcacta tggagtcctg caactttgtg caggccatga tggaccccaa gtcaacggca
```

1981 gagcagaggc tcaagctgtt caagatagct tgtgagaagc accagcacct gtaccgcctc
2041 gccatgacgg gcgccggcat cgaccgccat ctcttctgcc tctatgtggt gtccaagtat
2101 cttgcagtcg actcaccttt cctgaaggag gtattgtctg agccatggag gttgtctacg
2161 agccagactc ctcagcagca ggtggagctc tttgactttg agaaaaaccc tgactatgtg
2221 tcctgtggag ggggctttgg gccggttgcc gatgacggct atggtgtctc ctacattata
2281 gtgggagaga atttcatcca cttccatatt tcttccaagt tctctagccc tgagacagac
2341 tcacaccgct ttgggaagca cttgagacaa gccatgatgg acattatcac cttgtttggc
2401 ctcaccatca attctaaaaa gtaaacccct gagccacacg gaaggaaaac ggaccctcgt
2461 gatacaaacc aaatgaatag atgttgctcc tgaccatagg acaggcagaa aattgctctt
2521 ataaaactca gttttccttc cagaaggttt accgtcagtc tccctagaac aacagtaggc
2581 ttcacgtgtg aattgtgacc ctactacatc cagagatgcc ttggctccag gaatattggg
2641 cacagtcccc tgatgtcttt tgaatcggct cctactggat aaagggattt aaatgctggt
2701 gaattcctgg attctggggg ttgtttcttc acatgtgttg gaggtgacag acttcctcag
2761 tggtgaccct gtgaatactt gggcgtctga ctccacccag gcagtgtgag catcaccttg
2821 tggaaagaga aagtgtcttc agagccagca gaggcaacag ctgtagctaa cacatctgta
2881 acacactaat ggaatggtta ggcctgggga ttaaggttct gctatgagtg acagccactg
2941 tccctttgga agttcacatt tccaggaagc agagtaccac ctccccagtg ccaccttcct
3001 cacacatctt caaaacccag tgccttaaag aaggggccca ttggcaagcg ggaccataga
3061 gaagacttag catctgtgaa gcctttgggt ggatatgtga ggatgctgct tccccttact
3121 ggttcctgca taaagatgtc cctaagtaag cacttccccc acccctagaa aatgaggtcc
3181 ttggtgaagg cagggatgct ggagtctcat tgcctgccag ttccattaag ccacaaaata
3241 gcagacatgt gtccacagag ggaggggctt ggtagtcaaa ggctgcatag ctggacaaca
3301 gcgggagagt gtggcttgct gtatttgaca gctgttggca agaggagtga gaccctggtc
3361 accaagtcag acatactgac acaggcagcc aaagctcacg gagccaggag atatagatag
3421 atactggctt gtattctggc agatacaccc ctgggcttat cttctaatcc cacccagtca
3481 gattccaacc agagtcaaat tccatagaag gctaggtcat tttggcgaca gactcaggga
3541 tctcaagtaa tgggtgcttt tacccacatg ccatccctca gtgggagtgc ctttcttgaa
3601 agcatccaat gggctaaagc agctctacca agtctgtttg gtatttaatg taaacattag
3661 cattaatgga gtggtctctc ctacctgtca ccatcctgtc ctgacaagct tagctctccg
3721 aggtttacat catgtattta ttttccagtg ccccctttggc cttgtttgat tcctgcccct
3781 gtgccagaag tggcccagaa gtgaggggtg gggtgaccag cagtgcagag aggtgctggc
3841 tgaacagttc atgtgtgtct tatgggtata catgtataaa ttttgtaatg taaaaaaaaa
3901 aatcatacct aaaagggcca aagtttttt ttttttact aaaaccaaga aaacaaaaga
3961 caacataaag acataagcag aaacaaactg ttgtaagtca gagcggcctg actctcgctg
4021 ctgtgaccac tcaccaacct gtgttactca gagtagcccg gctagtgccc gagtgggaca
4081 ttcctctctc aggtttccag tgtccttgct gctcctgagc agttaccaat gcaatttcgc
4141 attccttaca aggcagaaga gtgggctctc actgtatgtg ttcaaaggag gaggtaagac
4201 tattgtgtat ttaatttaat gtggaacaaa atatagtctt accgcagcca aggttcaaat
4261 ttggtgttct aatctgtcca ttgcatgtaa ataccatatc tgtttggata taaatcttag
4321 aagtgcatgt gtgagcgaat gtagctggcc attaataaaa cattaatact gtctact

PUBLICATIONS

Adenovirus-mediated overexpression of liver carnitine palmitoyltransferase I in INS1E cells: effects on cell metabolism and insulin secretion

Blanca RUBÍ*, Peter A. ANTINOZZI†, Laura HERRERO*, Hisamitsu ISHIHARA†, Guillermina ASINS*, Dolors SERRA*, Claes B. WOLLHEIM†, Pierre MAECHLER† and Fausto G. HEGARDT*[1]

*Department of Biochemistry and Molecular Biology, University of Barcelona, School of Pharmacy, Diagonal 643, E-08028 Barcelona, Spain, and †Department of Biochemistry, Centre Medical Universitaire, Michel Servet 1, 1211 Geneva-4, Switzerland

Lipid metabolism in the β-cell is critical for the regulation of insulin secretion. Pancreatic β-cells chronically exposed to fatty acids show higher carnitine palmitoyltransferase I (CPT I) protein levels, higher palmitate oxidation rates and an altered insulin response to glucose. We examined the effect of increasing CPT I levels on insulin secretion in cultured β-cells. We prepared a recombinant adenovirus containing the cDNA for the rat liver isoform of CPT I. The overexpression of CPT I in INS1E cells caused a more than a 5-fold increase in the levels of CPT I protein (detected by Western blotting), a 6-fold increase in the CPT activity, and an increase in fatty acid oxidation at 2.5 mM glucose (1.7-fold) and 15 mM glucose (3.1-fold). Insulin secretion was stimulated in control cells by 15 mM glucose or 30 mM KCl. INS1E cells overexpressing CPT I showed lower insulin secretion on stimulation with 15 mM glucose (-40%; $P < 0.05$). This decrease depended on CPT I activity, since the presence of etomoxir, a specific inhibitor of CPT I, in the preincubation medium normalized the CPT I activity, the fatty-acid oxidation rate and the insulin secretion in response to glucose. Exogenous palmitate (0.25 mM) rescued glucose-stimulated insulin secretion (GSIS) in CPT I-overexpressing cells, indicating that the mechanism of impaired GSIS was through the depletion of a critical lipid. Depolarizing the cells with KCl or intermediary glucose concentrations (7.5 mM) elicited similar insulin secretion in control cells and cells overexpressing CPT I. Glucose-induced ATP increase, glucose metabolism and the triacylglycerol content remained unchanged. These results provide further evidence that CPT I activity regulates insulin secretion in the β-cell. They also indicate that up-regulation of CPT I contributes to the loss of response to high glucose in β-cells exposed to fatty acids.

Key words: beta cells, etomoxir, fatty acid oxidation, glucose-stimulated insulin secretion, pancreas.

INTRODUCTION

Lipid metabolism in the β-cell is critical for the normal regulation of insulin secretion [1,2]. Depletion of lipid stores together with deprivation of non-esterified fatty acids (NEFA) alters glucose-stimulated insulin secretion (GSIS) in rats and humans [3–5]. NEFAs, presumably via long-chain acyl-CoA (LC-CoA), generate signals for insulin secretion [6].

Stimulation of insulin secretion by glucose alters the CoA derivatives in clonal pancreatic β-cells, especially malonyl-CoA and fatty acyl-CoA. The LC-CoA model of GSIS holds that during glucose stimulation, anaplerosis in the mitochondria increases citrate [7], which is exported and converted into malonyl-CoA, resulting in inhibition of carnitine palmitoyltransferase I (CPT I) [8] and fatty acid oxidation [2,6,9]. Therefore the increase in malonyl-CoA may be responsible for the accumulation of fatty acyl-CoAs in the cytosol [10]. Moreover cytosolic acyl-CoA content increases with the addition of exogenous fatty acids. In addition, glucose metabolism in the β-cell raises acyl-CoA levels, which, in combination with α-glycerophosphate, may increase the levels of triacylglycerols, phosphatidic acid and diacylglycerol [2]. Fatty acyl-CoAs may act as coupling factors in insulin secretion by stimulating several isoforms of protein kinase C [11,12], by overcoming malonyl-CoA inhibition of CPT I [13], by stimulating the ATP-sensitive K^+ channel [14], and by acetylating proteins to target them to appropriate membrane sites [15].

Both malonyl-CoA and LC-CoA participate in the signal transduction for insulin secretion: malonyl-CoA as a regulator and LC-CoA as an effector signal [16]. Systems that regulate both malonyl-CoA and LC-CoA appear to be involved in insulin secretion. Accordingly, acetyl-CoA carboxylase, which controls the synthesis of malonyl-CoA, and CPT I, which is regulated by it, are considered to integrate the circulating fuel stimuli. The fate of malonyl-CoA in the pancreatic β-cell, in contrast with other tissues, is not *de novo* synthesis of fatty acids, but the regulation of CPT I activity, due to the very low levels of fatty acid synthase in the β-cell [17]. The metabolism of several nutrients that converge to form malonyl-CoA and increase LC-CoA esters (carbohydrate, amino acids and ketoacids) might act as fuel sensors in the β-cell. Therefore stable expression of an acetyl-CoA carboxylase antisense construct in INS1 cells decreased malonyl-CoA levels and insulin secretion [18]. Moreover, hydroxycitrate, which inhibits ATP-citrate lyase, and consequently malonyl-CoA formation, inhibited GSIS from the perifused rat pancreas [19]. Inhibition of fatty acid oxidation by a CPT I-specific irreversible inhibitor, etomoxir [19], or non-metabolizable fatty acid analogues [20] stimulates GSIS in perfused pancreas and isolated islets.

In the present study the CPT I liver isoform, predominantly expressed in rat pancreatic islets, was overexpressed in rat insulinoma INS1E cells by a recombinant adenovirus vector. The transduced cells had increased CPT I protein levels, an increased palmitate oxidation rate and impaired GSIS, and these effects

Abbreviations used: AdCA, adeno-chicken actin promoter; CPT I, carnitine palmitoyltransferase I; DMEM, Dulbecco's modified Eagle's medium; DNA-TPC, DNA-terminal protein complex; FBS, fetal bovine serum; GSIS, glucose-stimulated insulin secretion; LC-CoA, long-chain acyl-CoA; NEFA, non-esterified fatty acids; TBS, Tris-buffered saline; KRBH buffer, Krebs–Ringer bicarbonate Hepes buffer; UCP2, uncoupling protein 2.

[1] To whom correspondence should be addressed (e-mail hegardt@farmacia.far.ub.es).

were overcome by incubation with etomoxir. Incubation of INS1E cells with KCl had no effect on insulin secretion in CPT I overexpressed cells. CPT I overexpression did not change glucose-induced ATP generation, glucose oxidation, or the triacylglycerol levels. These results show that an increase in fatty acid oxidation rate in the β-cell impairs GSIS, confirming data of other authors on the role of fatty acyl-CoA. They are also compatible with the hypothesis that an increase in CPT I [1], together with an increase in uncoupling protein 2 (UCP2) [21,22], could contribute to the altered insulin response to glucose in β-cells after fatty acid exposure.

MATERIAL AND METHODS

Cell culture and materials

INS1E cells [23] were chosen since they secrete more insulin in response to glucose in the range 5–20 mM than the parental INS-1 cells [24]. INS1E cells (passages 46–70) were cultured in a humidified atmosphere containing 5% CO_2 in a medium composed of RPMI 1640 supplemented with 10 mM Hepes, 5% (v/v) heat-inactivated fetal bovine serum (FBS), 2 mM glutamine, 100 units/ml penicillin, 100 μg/ml streptomycin, 1 mM sodium pyruvate and 50 μM 2-mercaptoethanol as originally described [24]. An antibody against rat insulin was purchased from LINCO (St. Louis, MO, U.S.A.). RPMI 1640, Dulbecco's modified Eagle's medium (DMEM) and FBS were obtained from Life Technologies, Inc. Reagents commonly used for the experiments were from Sigma Chemical Co. and Fluka Chemie AG. Secondary antibody and radioactively labelled compounds were obtained from Amersham Biosciences. Chemiluminescent reagent (Supersignal West Pico Chemiluminescent substrate) was obtained from Pierce.

Adenovirus construction

Recombinant adenovirus was constructed as described previously [25]. Briefly, the expression unit to be introduced into the recombinant adenovirus was first inserted into the unique *Swa*I site of the E1-substitution type full-length adenovirus genome cloned in a cassette cosmid. The cassette bearing the expression unit was then co-transfected into HEK-293 cells together with the adenovirus DNA-terminal protein complex (DNA-TPC) digested at several sites with *Eco*T22I.

The CPT I cDNA, containing the whole coding sequence, was obtained by reverse-transcriptase PCR from rat liver mRNA, subcloned in BlueScript and sequenced, revealing no change with the previously reported rat liver CPT I [26]. The CPT I cDNA was then digested, blunt-ended and subcloned into the cosmid pAdCA (where AdCA corresponds to adeno-chicken actin promoter) previously cut with *Swa*I and dephosphorylated. The CPT I insert (nt 58–2700 of the previously reported mRNA) contained the ATG codon and the stop codon. The presence of the insert was checked with the restriction enzyme *Cla*I and its correct orientation was checked with *Bgl*II. The cosmid containing the full coding sequence for rat liver CPT I was called pAdCA-CPT I. The adenovirus DNA-TPC of the parent adenovirus was prepared through a buoyant CsCl density gradient with 4 M guanidine hydrochloride [25]. Cassette cosmid pAdCA-CPT I (8 μg) and 1 μg of the *Eco*T22I-digested DNA-TPC were co-transfected in a 6-cm dish with calcium phosphate (Cellfect Transphection Kit; Pharmacia) in HEK-293 cells and 1 day later the cells were distributed in 96-well plates [27]. The desired recombinant adenovirus was generated by overlapping recombination. At 10 days after transfection, the cell lysate from the selected viral clones was used to infect 24-well dishes, the adenoviral DNA was extracted from these cells and the DNA was analysed by digestion with *Cla*I to check the CPT I insert.

To amplify and purify the selected virus the cell lysate containing the virus with full-length rat liver CPT I (AdCA-CPT I) was used to infect two 138-mm dishes of HEK-293 cells. The AdCA-CPT I and AdCA-LacZ viruses, which express the bacterial β-galactosidase [28] were amplified and purified by CsCl ultracentrifugation. Adenovirus amplification was performed in HEK-293 cells cultured in DMEM containing 5 or 10% (v/v) FBS.

Viral treatment of INS1E cells

INS1E cells (500000) were seeded in 12-well dishes (Falcon) and cultured for 48 h prior to infection. For infection, cells were incubated with 500 μl of medium containing 20 plaque-forming units of the recombinant adenovirus/cell for 90 min, washed once in the medium, and cultured in RPMI medium for 20 h before experiments to allow the transgenes to be expressed, before initiating metabolic studies or measurements of insulin secretion.

Immunoblot analysis

For detection of rat liver CPT I protein, infected INS1E cells were collected and dissolved in SDS sample buffer. Proteins were subjected to SDS/PAGE (10% gels) and transferred on to nitrocellulose membranes. The membranes were blocked for 1 h with Tris-buffered saline (TBS) containing 0.1% Tween-20 and 5% (w/v) non-fat dried milk. The membrane was washed three times in TBS/Tween at 22 °C. Membranes were probed with the CPT I-specific antibody [29] by overnight incubation, and then incubated for 1 h with anti-sheep IgG conjugated to horseradish peroxidase (1:5000 dilution). The signal was detected by chemiluminescence.

Determination of CPT I activity in INS1E cells

INS1E cells (12 million) were seeded in 15-cm dishes and cultured for 48 h prior to infection. For infection, cells were incubated with 10 ml of medium containing 20 plaque-forming units of the recombinant adenovirus (AdCA-LacZ and AdCA-CPT I)/cell for 90 min, washed once in the medium, and cultured in RPMI medium for 20 h. Prior to obtaining the mitochondria-enriched cell fraction, cells were preincubated for 30 min in Krebs–Ringer bicarbonate Hepes buffer (KRBH buffer; 140 mM NaCl, 3.6 mM KCl, 0.5 mM NaH_2PO_4, 0.5 mM $MgSO_4$, 1.5 mM $CaCl_2$, 2 mM $NaHCO_3$ and 10 mM Hepes) + 1% (w/v) BSA without glucose in the absence or the presence of etomoxir at 50 and 200 μM. After preincubation, the cells were washed with 10 ml of PBS and resuspended in 5 ml of the same solution. The cells were pooled at this point and sedimented by centrifugation at 1200 ***g*** for 5 min at 4 °C. After resuspension in 1 ml of 5 mM Tris/HCl (pH 7.2)/150 mM KCl (buffer A), they were broken with 10 cycles of a glass homogenizer fitted with a tight pestle. Further centrifugation was performed in a microfuge for 5 min at 4 °C at 16000 ***g***, and the final pellet was resuspended in the desired volume of buffer A. CPT I was assayed in these preparations where the mitochondria remain largely intact [30]. Carnitine acyltransferase activity of 10 μg of protein was determined by the radiometric method as previously described [31].

[1-^{14}C]Palmitate oxidation

At 20 h after infection, INS1E cells seeded in 12-well dishes were placed in a water bath at 37 °C, washed once in 1 ml of solution A, which contained KRBH + 0.1% BSA (essentially fatty acid

free). The cells were then preincubated for 30 min with 500 μl of KRBH containing 1 % (w/v) BSA (solution B), with or without 200 μM etomoxir and washed in 1 ml of KRBH.

The rate of fatty acid oxidation was measured essentially as described by Chen et al. [19]. Briefly, the cells were washed in 1 ml of solution A and harvested by resuspension in 300 μl of KRBH. Cell suspension (160 μl) was added to a centre well containing 20 μl of 2.5 mM palmitate complexed to 10 % (w/v) BSA, with 0.5 μCi of [1-^{14}C]palmitic acid as a tracer and 20 μl of a solution containing 25 or 150 mM D-(+)-glucose plus 8 mM carnitine, and the centre well was immediately placed in a sealed vial. After 2 h at 37 °C, the reaction was stopped by the addition of 100 μl of 7 % (w/v) perchloric acid. The rate of [1-^{14}C]palmitate oxidation was measured as released $^{14}CO_2$, which was trapped by 300 μl of benzethonium chloride, added to the bottom of the sealed vials. After 5 h, the centre wells and the rubber stoppers were discarded and 10 ml of scintillation mixture was added. Control incubations without INS1E cells were run with each series. Following overnight incubation at 22 °C, $^{14}CO_2$ production was counted in an LS6500 liquid scintillation counter (Beckman Instruments Inc.). Palmitate oxidation was expressed as nmol of palmitate oxidized/h per mg of cell protein.

ATP determinations

ATP was generated in 6-well plates following 30 min of preincubation in KRBH. Cells were incubated for 10 min in KRBH with 2.5 or 15 mM glucose before the stimulation was arrested on ice by washing with ice-cold KRBH and the addition of 0.4 M perchloric acid. ATP levels were determined using a bioluminescence assay kit (Roche, Rotkreuz, Switzerland).

Measurements of cellular insulin secretion and insulin content

Insulin was measured essentially as described previously [32]. INS1E cells (500000) were seeded in 12 wells. Two days after seeding the cells were treated with the recombinant adenovirus and 20 h later INS1E infected cells were placed in a water bath at 37°C, washed once in 1 ml of solution A, preincubated for 30 min with 500 μl of solution B, with or without 200 μM etomoxir, and washed again in solution A.

Insulin secretion was measured for 30 min. Briefly, 1 ml of solution A containing 2.5, 7.5 or 15 mM glucose, or 2.5 mM glucose plus 30 mM KCl, was added. After 30 min the solution was collected and centrifuged at 10000 rev./min in a microcentrifuge for 1 min to remove cell debris. To measure insulin content, INS1E cells remaining in the wells were extracted with 1 ml of 75 % ethanol/0.2 M HCl added to each well. The supernatant and cell insulin samples were immediately stored at −20 °C until insulin determination by RIA, using rat insulin as a standard and an antibody specific for rat insulin. The insulin secretion was expressed as a percentage of the cell insulin content.

[U-^{14}C]Glucose oxidation

Glucose oxidation was measured as $^{14}CO_2$ production from [U-^{14}C]glucose with the same experimental design as for the measurement of palmitate oxidation, except that cells were incubated for 1 h with [U-^{14}C]glucose in the absence or in the presence of 0.25 mM palmitate [32].

INS1E cells infected with recombinant adenovirus as described above were washed with 1 ml of solution A and harvested by light resuspension in 600 μl of KRBH; 180 μl of the cell suspension was added to a centre well containing 20 μl of 25 or 150 mM D-(+)-glucose with 0.5 μCi of [U-^{14}C]glucose as a tracer, and the centre well was placed immediately in a sealed vial. After 1 h at 37 °C, the reaction was stopped by the addition of 100 μl of 7 % (w/v) perchloric acid. The rate of [U-^{14}C]glucose oxidation was measured as released $^{14}CO_2$, which was trapped by 300 μl of benzethonium chloride at the bottom of the sealed vials to bind the liberated $^{14}CO_2$. Labelled CO_2 was measured as described above. The data were expressed as nmol of glucose oxidized/h per mg of cell protein.

Triacylglycerol content measurements

At 20 h after infection, INS1E cells seeded in 12-well dishes were placed in a water bath at 37 °C, washed once with 1 ml of solution A, preincubated for 30 min with 500 μl of solution B and washed with solution A.

Lipids were extracted as described elsewhere [33]. Briefly, 1 ml of methanol/PBS (2:3, v/v) was added to each well and the cells were gently collected in a pipette, centrifuged at 700 ***g*** for 5 min and washed with PBS; 200 μl of 0.2 M NaCl was then added to the pellet and the mixture was immediately frozen in liquid N_2. To separate aqueous and lipid phases, 750 μl of chloroform/methanol (2:1, v/v) and 50 μl of 0.1 M KOH were added and, after vigorous vortex-mixing, the phases were separated by 15 min of centrifugation at 2000 ***g***. The top aqueous phase was removed and the lipid phase was washed with 200 μl of methanol/water/chloroform (48:47:3, by vol.). After vortex-mixing and centrifugation, 400 μl of the lower phase was taken and dried. Triacylglycerols were measured in each sample using the Sigma 334 triacylglycerol kit. The method involves the hydrolysis of triacylglycerols by lipoprotein lipase and measures 'true triacylglycerols'.

Statistical analysis

Unless otherwise indicated data are represented as the means ± S.E.M. for at least three independent experiments performed in triplicate. Differences between groups are assessed by the Student's *t* test for unpaired data.

RESULTS

Assessment of adenovirus-mediated CPT I overexpression in INS1E cells

The capacity of AdCA-CPT I to direct expression of liver CPT I in insulinoma INS1E cells was evaluated by Western-blot analysis of extracts from cells infected with AdCA-CPT I and AdCA-LacZ as a control. The conditions of the infection are described in the Materials and methods section. Immunoblotting revealed a band of the expected size of 88 kDa and the signal increased according to the viral amount from 0 to 40 plaque-forming units/cell (Figure 1A). An infection titre of 20 plaque-forming units/cell was used for the rest of the experiments. There was a 6-fold increase in the CPT activity in the mitochondria-enriched fractions of the cells infected with AdCA-CPT I compared with the cells infected with AdCA-LacZ. In contrast, preincubation of the AdCA-CPT I-infected INS1E cells with increasing amounts of etomoxir diminished the CPT activity (60 and 9 % of the control with 50 and 200 μM etomoxir respectively) (Figure 1B).

Impact of recombinant CPT I adenovirus on palmitate oxidation in INS1E cells

We evaluated the metabolic effects of the AdCA-CPT I virus. [1-^{14}C]Palmitate oxidation was measured in adenovirus-treated INS1E cells for 2 h, after a 30 min preincubation in KRBH with no glucose and no fatty acids, in the absence or in the presence

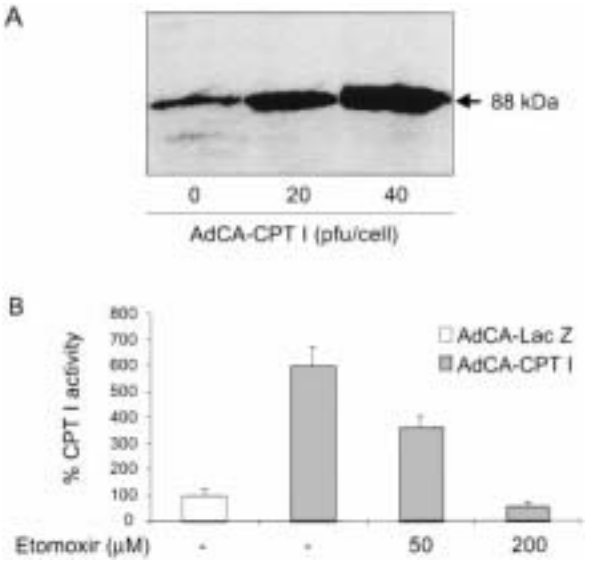

Figure 1 Immunoblot analysis of CPT I expressed in INS1E infected cells and CPT activity in mitochondria-enriched INS1E fractions

(**A**) Samples were prepared and analysed as described in the Materials and methods section. At 20 h after the infection of INS1E cells with 20 and 40 plaque-forming units (pfu) of recombinant adenovirus/cell, cells were collected and protein extracts (100 μg) were separated by SDS/PAGE (10% gels) and subjected to immunoblotting by using specific antibodies for CPT I from rat liver. A unique band corresponding to a protein of approx. 88 kDa was seen in control and AdCA-CPT I-infected cells. (**B**) CPT I activity was measured in mitochondrial-enriched fractions of LacZ and CPT I-overexpressing cells, before and after treatment with etomoxir. Results are the means of three experiments performed in duplicate.

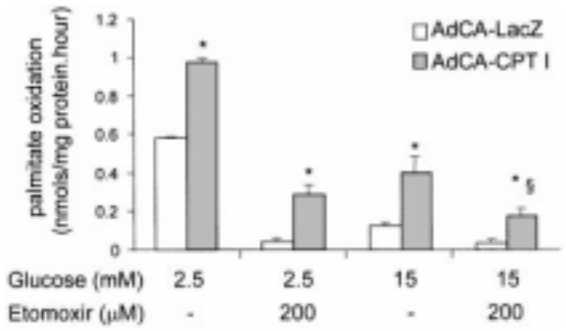

Figure 2 [1-^{14}C]Palmitate oxidation in INS1E infected cells

INS1E cells were treated with AdCA-LacZ or AdCA-CPT I. At 20 h after viral treatment, [1-^{14}C]palmitate oxidation was measured after 30 min of preincubation with either 2.5 or 15 mM glucose with or without etomoxir. Results are expressed as means $\pm$ S.E.M. for three independent experiments, which were performed in triplicate. $^*P < 0.01$ compared with AdCA-LacZ; §$P < 0.05$ compared with AdCA-CPT I without etomoxir.

of 200 μM etomoxir. Incubation with AdCA-LacZ at 15 mM glucose reduced the rate of palmitate oxidation to 20% in comparison with cells incubated with 2.5 mM glucose (Figure 2). This decrease in fatty acid oxidation rate has been reported previously and in similar fashion for rat islets [19] and INS1 cells [34]. According to these results [19,34], when glucose is raised from non-stimulatory to stimulatory concentration, INS1E cells (like INS1 cells and islet β-cells) increase glycolytic flux and decrease the rate of palmitate oxidation.

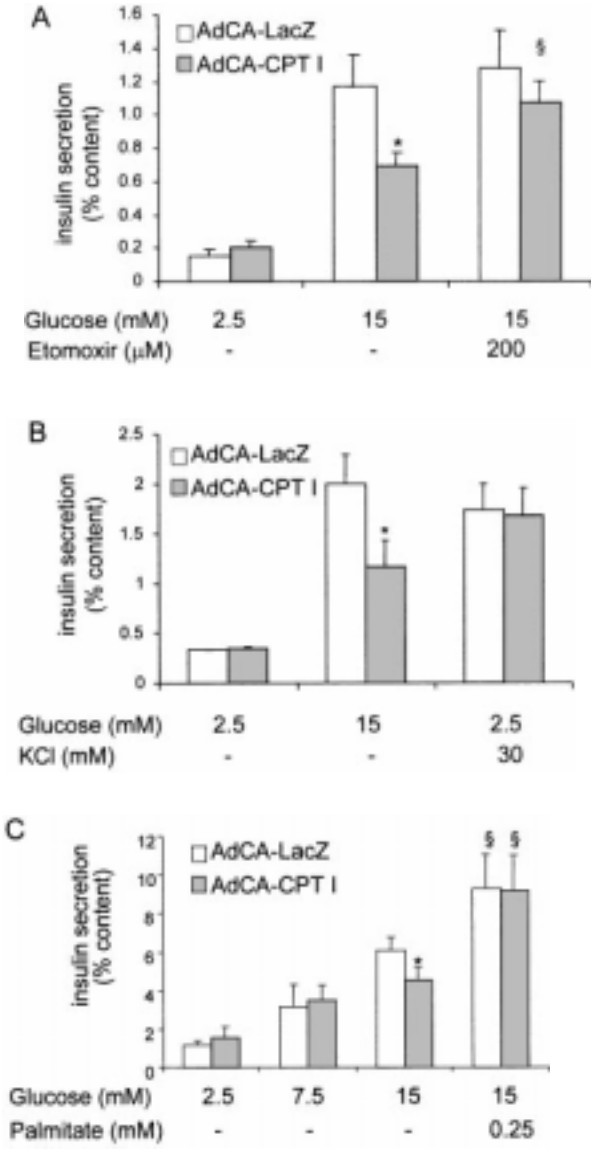

Figure 3 Effect of CPT I overexpression on GSIS in INS1E infected cells

(**A**) INS1E cells were treated with the indicated adenovirus and cultured for 20 h in regular medium. After a 30 min preincubation in KRBH solution without glucose and with or without 200 μM etomoxir, cells were washed and incubated in KRBH solution containing either 2.5 or 15 mM glucose for 30 min and insulin release was determined. Results represent the means $\pm$ S.E.M. for three independent experiments performed in triplicate. (**B**) A similar set of experiments was performed, in the absence of etomoxir preincubation, testing 2.5, 15 mM glucose and 2.5 mM glucose plus 30 mM KCl. Results are the means $\pm$ S.E.M. of one representative experiment out of three, performed in triplicate. $^*P < 0.05$ compared with AdCA-LacZ. (**C**) To test the effect of intermediate glucose concentrations and of 0.25 mM palmitate, cells were seeded on 24 wells and insulin secretion was measured in a 1 h period and expressed as a percentage of the content. Results are the means $\pm$ S.E.M. for three experiments performed in triplicate. $^*P < 0.05$ compared with AdCA-LacZ; §$P < 0.05$ compared with 15 mM glucose.

The overexpression of CPT I in INS1E cells increased palmitate oxidation at low (1.7-fold) and high (3.1-fold) glucose concentrations ($P < 0.01$). An increase in palmitate oxidation at high glucose was also described for INS1 and INS1-derived (832/13) β-cells overexpressing malonyl-CoA decarboxylase, the enzyme which eliminates malonyl-CoA, the CPT I physiological inhibitor [34,35]. Nevertheless the increase in fatty acid oxidation at low

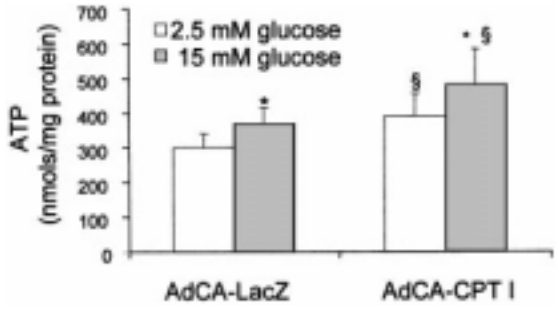

Figure 4 Glucose-induced ATP generation

Cytosolic ATP levels were measured in INS1E cells overexpressing LacZ or CPT I, preincubated for 30 min without glucose and exposed to 2.5 and 15 mM glucose for 10 min. Results represent the means ± S.E.M. *$P < 0.05$ compared with 2.5 mM glucose; §$P < 0.05$ AdCA-CPT I compared with AdCA-LacZ.

glucose concentration was not observed by these authors, since at low glucose the malonyl-CoA levels are low.

The stimulatory glucose concentration was more effective in suppressing fatty acid oxidation in control cells (20 % residual palmitate oxidation) than in CPT I-overexpressing cells, which showed a 40 % residual palmitate oxidation after the switch from low glucose to high glucose.

Control and CPT I-overexpressing INS1E cells treated with etomoxir showed a lower fatty acid oxidation rate, as expected from its capacity to inhibit CPT I irreversibly. The presence of etomoxir decreased the high oxidation rate in CPT I-overexpressing cells from 0.4 to 0.17 nmol/h per mg of protein ($P < 0.05$). The fatty acid oxidation rate in etomoxir-treated CPT I-overexpressing cells was similar to the control cells without etomoxir and high concentrations of glucose (0.176 compared with 0.128). This indicates that the treatment with etomoxir reversed the effect of CPT I overexpression.

Effect of CPT I overexpression on INS1E insulin secretion

Having established that AdCA-CPT I increases the rate of fatty acid oxidation in all the conditions studied we evaluated the effect of CPT I on insulin secretion. INS1E cells were maintained in culture for 2 days, infected with AdCA-LacZ and AdCA-CPT I and cultured for 20 h prior to the experiments. For insulin secretion experiments, cells were preincubated for 30 min in solution B with or without 200 μM etomoxir. After this treatment cells were washed to eliminate etomoxir, and insulin secretion was determined for 30 min with KRBH plus 2.5 mM glucose and 15 mM glucose.

In INS1E cells treated with the control virus AdCA-LacZ, 15 mM glucose caused an 8-fold increase in insulin secretion relative to secretion at 2.5 mM glucose, while cells treated with AdCA-CPT I exhibited only a 3.5-fold increase, indicating that the increase in lipid metabolism caused by the overexpression of CPT I affects GSIS (Figure 3A). In these conditions insulin secretion was reduced by 40 % ($P < 0.01$) in overexpressed CPT I cells in relation to control cells.

Control cells treated with 200 μM etomoxir gave the same response to glucose as non-treated control cells (8.5-fold compared with 8-fold) (Figure 3A). Moreover, AdCA-CPT I-infected cells pre-treated with etomoxir showed a significantly higher increase in insulin secretion (5.5-fold compared with 3.5-fold, $P < 0.05$). The treatment of the AdCA-CPT I-infected cells with etomoxir suggests a specific effect of CPT I on insulin secretion, since etomoxir partially restores the normal insulin secretion in these cells. Insulin secretion was also stimulated at basal 2.5 mM glucose with 30 mM KCl, as a Ca^{2+}-raising agent. As shown in Figure 3(B), the effects of 30 mM KCl on insulin exocytosis were similar in control cells and cells overexpressing CPT I. These results distinguish between the K^+–Ca^{2+} axis and the anaplerotic effects of glucose and fatty acid oxidation.

To test the effect of intermediate glucose concentrations and long-chain fatty acids in insulin secretion in INS1E cells, insulin secretion was performed over a 1 h period in infected INS1E cells seeded in 24 wells. In control cells (AdCA-LacZ-infected), raising glucose concentrations from a basal concentration of 2.5 mM to 7.5 and 15 mM stimulated insulin secretion 2.8-fold ($P < 0.05$) and 5.4-fold ($P < 0.01$) respectively (Figure 3C). Insulin release at basal (2.5 mM) or intermediate (7.5 mM) glucose concentration was not affected in cells overexpressing CPT I. In contrast, insulin secretion stimulated by 15 mM glucose (3-fold versus basal glucose, $P < 0.05$) was inhibited by 27 % ($P < 0.05$) compared with the corresponding control at high glucose. In the same experiments palmitate potentiated GSIS in control and CPT I-overexpressing cells (9.3 compared with 6.1 in control cells, and 9.3 compared with 4.5 in CPT I-overexpressing cells) (Figure 3C), emphasizing the role of fatty acids in the signal transduction of insulin secretion.

Effect of CPT I overexpression on glucose-induced ATP generation and ATP levels

Incubation of INS1E cells with glucose stimulated the synthesis of ATP by activation of the electron transport chain. The levels of ATP/mg of protein were measured following a 10 min incubation period, at low and high glucose. ATP levels at 15 mM glucose compared with 2.5 mM glucose were elevated by 23.1 % (367 ± 49 compared with 298 ± 42 respectively) in AdCA-LacZ control cells and by 23.3 % (481 ± 101 compared with 390 ± 66 respectively) ($P < 0.05$) in AdCA-CPT I cells (Figure 4). Therefore CPT I overexpression did not modify the glucose-induced ATP increase. However, there was a 31 % elevation in ATP levels in CPT I- versus Lac Z-overexpressing cells ($P < 0.05$) at low and high glucose concentrations.

Effect of CPT I expression on glucose utilization

To investigate whether the impaired GSIS in INS1E cells overexpressing CPT I could be due to a decrease in glucose utilization in INS1E cells we measured the release of $^{14}CO_2$ at the same glucose concentrations used for the insulin secretion experiments in INS1E cells overexpressing LacZ or CPT I and using [U-^{14}C]glucose. The use of [U-^{14}C]glucose allows the measurement of the CO_2 released not only at the steps in the tricarboxylic acid cycle but at the pyruvate dehydrogenase step.

The release of $^{14}CO_2$ was determined for 1 h in the presence of 2.5 and 15 mM glucose after a 30 min preincubation with or without 200 μM etomoxir. The presence of a stimulatory glucose concentration increased the rate of $^{14}CO_2$ release from 2.5 to 15 mM glucose by 5.2-fold both in cells overexpressing LacZ and in cells overexpressing CPT I (Figure 5). The treatment of the cells with etomoxir did not change the CO_2 formation from glucose in either LacZ- or CPT I- overexpressing cells. This result shows that, in the absence of external fatty acids, there is no difference in the rate of glucose utilization between control and CPT I-overexpressing cells. Etomoxir had no effect on glucose utilization in either control or CPT I-overexpressing cells. This result suggests that the mechanism by which the overexpression of CPT I decreases GSIS in INS1E cells is not a decrease in glucose oxidation. Glucose oxidation was determined in LacZ-

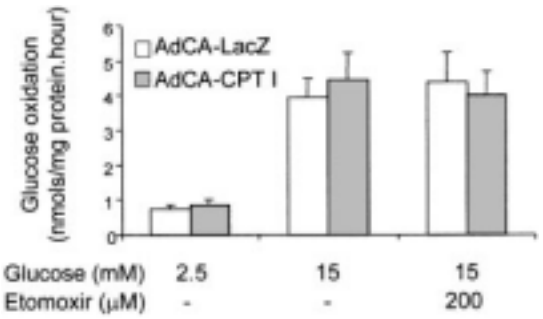

Figure 5 Glucose oxidation in INS1E infected cells

[U-^{14}C]Glucose oxidation was measured in INS1E cells overexpressing LacZ or CPT I. After a 30 min preincubation in KRBH solution without glucose and with or without 200 μM etomoxir, cells were washed and resuspended in KRBH with [U-^{14}C]glucose at the indicated concentrations for 1 h and the CO_2 released was measured as described in the Materials and methods section. Data are the means $\pm$ S.E.M. for three independent experiments performed in triplicate and are expressed as nmol of oxidized glucose/h per mg of protein.

and CPT I-overexpressing cells and the effect of 0.25 mM palmitate was tested. The addition of 0.25 mM palmitate had no significant effect on glucose oxidation in control or CPTI-overexpressing cells over a 1 h period (results not shown). Comparison of Figures 2 and 5 shows that at high glucose concentration, glucose oxidation in INS1E cells is much higher (32 times) than fatty acid oxidation, these results agreeing with those described in INS1 cells [1] and in islets [36,37]; therefore it appears unlikely that accelerated fatty acid oxidation influences glucose metabolism.

Effect of CPT I overexpression on triacylglycerol levels

It has been shown that a depletion of β-cell lipids, measured as triacylglycerols [5], blocks insulin secretion in response to glucose and other secretagogues, and that perifusion with a mixture of fatty acids restored insulin responses to supranormal levels. To address the question of whether the impaired insulin response to glucose seen in INS1E cells overexpressing CPT I was due to a decrease in triacylglycerol levels, we measured triacylglycerol content in INS1E cells infected with either the control virus AdCA-LacZ or AdCA-CPT I. The cells were infected and 20 h later incubated in KRBH without glucose for 30 min as previously described. After this incubation cells were washed and collected for the triacylglycerol measurement. The triacylglycerol content was not significantly different between LacZ- and CPT I-overexpressing cells (14.8 ± 1.2 compared with 13.6 ± 1.3 ng of triacylglycerols/mg of protein). Thus a decrease in triacylglycerols does not seem to account for the lower insulin secretion at stimulatory glucose concentrations seen in CPT I-overexpressing cells.

DISCUSSION

Many studies implicate NEFAs in type II diabetes [2,38,39]. Long term exposure of β-cells to NEFAs *in vitro* has several effects: (1) it increases basal insulin release and strongly decreases secretion in response to glucose [2]; (2) it alters the coupling of glucose metabolism to insulin secretion by acting on the expression of specific genes, such as that for UCP2 [21,22]; and (3) it increases the expression of CPT I, which is considered to be the rate-limiting step in fatty acid oxidation [1]. CPT I up-regulation may contribute to the change in insulin secretion. The aim of the present study was to evaluate the capacity of CPT I overexpression to alter the insulin response to glucose in β-cells. In view of the interest in the LC-CoA model of GSIS, which is still under discussion [40], we examined this effect in a β-cell-derived cell line, which is more sensitive at physiological glucose concentrations than the parenteral INS1 cell line.

Recent advances in adenoviral vector technology have facilitated the transfer of multiple foreign genes into well-differentiated cell lines. The chicken actin promoter [25,41] allows the use of low adenoviral infection titres, with high levels of protein expression. The rat liver CPT I is the only isoform present in both the β-cell and INS1E cells. Therefore, since the muscle CPT I isoform has different malonyl-CoA inhibition properties, we used the rat liver isoform to construct the adenovirus.

The overexpression of CPT I increased fatty acid oxidation rates in the INS1E cells, as expected. However, the percentage increase in ATP (23%) in CPT I-overexpressing cells and in controls was identical when glucose was increased from 2.5 to 15 mM, showing that CPT I overexpression had no effect on the electron transport chain. Stimulation of fatty acid oxidation by CPT I was higher than that induced by malonyl-CoA decarboxylase or acetyl-CoA carboxylase [18,34]. These enzymes modulate CPT I activity indirectly through changes in malonyl-CoA, whereas CPT I controls the fatty acid oxidation flux directly. Interestingly, the overexpression of CPT I increased the rate of fatty acid oxidation not only at high glucose, but also at low glucose concentrations. INS1E cells overexpressing CPT I secreted less insulin in response to high glucose concentration, but not in response to intermediate glucose concentrations or non-nutrient secretagogues, such as KCl. Thus exocytosis was preserved, since the effect of the cytosolic [Ca^{2+}]-raising agent (30 mM KCl) was not altered by CPT I overexpression. The increase in fatty acid oxidation may be responsible for the change in the insulin response. This indicates that lipid homoeostasis is necessary for the correct insulin response to glucose.

The specificity of the CPT I effect on insulin secretion was tested by the use of etomoxir, an irreversible inhibitor of CPT I activity. Etomoxir reversed the CPT I effect on fatty acid oxidation and insulin secretion, which indicates that the effect on insulin response is due to the increase in fatty acid oxidation [42]. Only preincubation of the INS1E cells with 200 μM etomoxir abolished the higher CPT I activity after infection with AdCA-CPT I (Figure 1B). To avoid any non-specific effect on the secretory machinery, etomoxir was eliminated after the preincubation and the cells were washed prior to the experiments. Under these conditions we consider that the only effect of etomoxir was the inhibition of CPT I through direct and irreversible covalent binding of CPT I and not as a fatty acid analogue. Under these conditions our control INS1E cells did not show any enhancement of GSIS, in contrast with what has been shown previously [19]. In the work of Chen et al. [19], 200 μM etomoxir, added with the glucose in rat perfusion experiments stimulated GSIS. This discrepancy could be explained by the presence of etomoxir throughout all the secretion experiments. Palmitate, which potentiates insulin secretion in HIT cells [6] and islets [43], increased insulin secretion to the same extent in control and CPT I-overexpressing INS1E cells. This could indicate the mechanism by which CPT I diminishes insulin secretion, that is, the depletion of a critical lipid which could act as a signal molecule. In fact, palmitate has been shown to increase the long chain acyl-CoA ester content in HIT cells [6].

Some authors did not find a correlation of cell malonyl-CoA levels with insulin secretion since the reduction of malonyl-

CoA levels by overexpression of malonyl-CoA decarboxylase in an INS1 cell-derived clone had no effect on insulin secretion [34, 35]. However, malonyl-CoA depletion incompletely reverses the glucose-induced suppression of fatty acid oxidation. The authors attribute this to the regulation of CPT I activity by factors derived from glucose metabolism other than malonyl-CoA in the β-cell [35]. Interestingly, a regulation of CPT I that is independent of malonyl-CoA has been demonstrated in rat hepatocytes [44]. Another explanation for this lack of correlation between malonyl-CoA levels and fatty acid oxidation could be the presence of different pools of malonyl-CoA in the cell. There are two acetyl-CoA carboxylases, one in the cytosol the other in the mitochondria, the latter directly modulating the malonyl-CoA levels accessible to CPT I [45].

INS1 cells overexpressing CPT I show higher rates of palmitate oxidation at low and high glucose concentrations (Figure 2) than control cells, yet the rates of glucose oxidation were nearly identical in the CPT I-non-expressing and expressing cells. This would mean that the excess of CPT I activity would increase fatty acid oxidation, without affecting the oxidation of glucose. This excess of fatty acid oxidation under CPT I overexpression would explain the 31% increase in ATP generation observed in these cells, which therefore would be exclusively produced by the overactivity of CPT I under the conditions of the assay. The increased CPT I, in addition, slightly decreased the triacylglycerol content, indicating that the pool of fatty acyl-CoA present in the cell was responsible for generation of ATP, without the need to hydrolyse triacylglycerols.

In conclusion, the present study shows that the overexpression of CPT I increases the fatty acid oxidation rate at high and low glucose concentrations. The increase in fatty acid oxidation affected insulin response to high glucose but not to intermediate glucose concentrations and non-metabolizable secretagogues, like KCl, while other cell parameters remained unchanged. The effect of CPT I was reverted by the use of etomoxir and by the exogenous addition of fatty acids. These results show that CPT I activity regulates insulin secretion, probably allowing a certain level of fatty acids to be available for exocytosis of insulin [46]. These results also favour the hypothesis that up-regulation of CPT I [1] contributes to the early loss of glucose responsiveness seen in β-cells chronically exposed to high concentrations of fatty acids.

We are grateful to Ms G. Chaffard for her expert technical assistance. We thank Dr Victor Zammit for kindly supplying anti-(liver rat CPT I) antibody and Mr Robin Rycrof of the Language Service for valuable assistance in the preparation of the English manuscript. This study was supported by Grants PB95-0012 and BMC2001-3048 from the Dirección General de Investigación Científica y Técnica, Spain, and by Ajuts de Suport als Grups de Recerca de Catalunya, 1999SGR0075 and 2001/SGR/0129 and from the Marató de TV3. B.R. is a recipient of a fellowship from the University of Barcelona.

REFERENCES

1 Assimacopoulos-Jeannet, F., Thumelin, S., Roche, E., Esser, V., McGarry, J. D. and Prentki, M. (1997) Fatty acids rapidly induce the carnitine palmitoyltransferase I gene in the pancreatic β-cell line INS1. J. Biol. Chem. **272**, 1659–1664

2 Prentki, M. and Corkey, B. E. (1996) Are the β-cell signaling molecules malonyl-CoA and cytosolic long-chain acyl-CoA implicated in multiple tissue defects of obesity and NIDDM? Diabetes **45**, 273–283

3 Stein, D. T., Esser, V., Stevenson, B. E., Lane, K. E., Whiteside, J. H., Daniels, M. B., Chen, S. and McGarry, J. D. (1996) Essentiality of circulating fatty acids for glucose-stimulated insulin secretion in the fasted rat. J. Clin. Invest. **97**, 2728–2735

4 Dobbins, R. L., Chester, M. W., Daniels, M. B., McGarry, J. D. and Stein, D. T. (1998) Circulating fatty acids are essential for efficient glucose-stimulated insulin secretion after prolonged fasting in humans. Diabetes **47**, 1613–1618

5 Koyama, K., Chen, G., Wang, M. Y., Lee, Y., Shimabukuro, M., Newgard, C. B. and Unger, R. H. (1997) β-cell function in normal rats made chronically hyperleptinemic by adenovirus-leptin gene therapy. Diabetes **46**, 1276–1280

6 Prentki, M., Vischer, S., Glennon, M. C., Regazzi, R., Deeney, J. T. and Corkey, B. E. (1992) Malonyl-CoA and long chain acyl-CoA esters as metabolic coupling factors in nutrient-induced insulin secretion. J. Biol. Chem. **267**, 5802–5810

7 Schuit, F., De Vos, A., Farfari, S., Moens, K., Pipeleers, D., Brun, T. and Prentki, M. (1997) Metabolic fate of glucose in purified islet cells. Glucose-regulated anaplerosis in β cells. J. Biol. Chem. **272**, 18572–18579

8 McGarry, J. D. and Brown, N. F. (1997) The mitochondrial carnitine palmitoyltransferase system. From concept to molecular analysis. Eur. J. Biochem. **244**, 1–14

9 Corkey, B. E., Glennon, M. C., Chen, K. S., Deeney, J. T., Matschinsky, F. M. and Prentki, M. (1989) A role for malonyl-CoA in glucose-stimulated insulin secretion from clonal pancreatic β-cells. J. Biol. Chem. **264**, 21608–21612

10 Liang, Y. and Matschinsky, F. M. (1991) Content of CoA-esters in perifused rat islets stimulated by glucose and other fuels. Diabetes **40**, 327–333

11 Yaney, G. C., Korchak, H. M. and Corkey, B. E. (2000) Long-chain acyl-CoA regulation of protein kinase C and fatty acid potentiation of glucose-stimulated insulin secretion. Endocrinology **141**, 1989–1998

12 Deeney, J. T., Gromada, J., Hoy, M., Olsen, H. L., Rhodes, C. J., Prentki, M., Berggren, P. O. and Corkey, B. E. (2000) Acute stimulation with long chain acyl-CoA enhances exocytosis in insulin-secreting cells (HIT T-15 and NMRI β-cells). J. Biol. Chem. **275**, 9363–9368

13 Mills, S. E., Foster, D. W. and McGarry, J. D. (1983) Interaction of malonyl-CoA and related compounds with mitochondria from different rat tissues. Relationship between ligand binding and inhibition of carnitine palmitoyltransferase I. Biochem. J. **214**, 83–91

14 Gribble, F. M., Proks, P., Corkey, B. E. and Ashcroft, F. M. (1998) Mechanism of cloned ATP-sensitive potassium channel activation by oleoyl-CoA. J. Biol. Chem. **273**, 26383–26387

15 Schmidt, M. F. G. (1989) Fatty acid acylation of proteins. Biochim. Biophys. Acta **988**, 411–426

16 Corkey, B. E., Deeney, J. T., Yaney, G. C., Tornheim, K. and Prentki, M. (2000) The role of long-chain fatty acyl-CoA esters in β-cell signal transduction. J. Nutr. **130**, 299S–304S

17 Brun, T., Roche, E., Assimacopoulos-Jeannet, F., Corkey, B., Kim, K. H. and Prentki, M. (1996) Evidence for an anaplerotic/malonyl-CoA pathway in pancreatic β-cell nutrient signaling. Diabetes **45**, 190–198

18 Zhang, S. and Kim, K. H. (1998) Essential role of acetyl-CoA carboxylase in the glucose-induced insulin secretion in a pancreatic β-cell line. Cell. Signalling **10**, 35–42

19 Chen, S., Ogawa, A., Ohneda, M., Unger, R. H., Foster, D. and McGarry, J. D. (1994) More direct evidence for a malonyl-CoA-carnitine palmitoyltransferase I interaction as a key event in pancreatic β-cell signalling. Diabetes **43**, 878–883

20 Bliss, C. R. and Sharp, G. W. (1992) Glucose-induced insulin release in islets of young rats: time dependent potentiation and effects of 2-bromostearate. Am. J. Physiol. **263**, E890–E896

21 Lameloise, N., Muzzin, P., Prentki, M. and Assimacopoulos-Jeannet, F. (2001) Uncoupling protein 2: a possible link between fatty acid excess and impaired glucose-induced insulin secretion? Diabetes **50**, 803–809

22 Zhang, C. Y., Baffy, G., Perret, P., Krauss, S., Peroni, O., Grujic, D., Hagen, T., Vidal-Puig, A. J., Boss, O., Kim, Y. B. et al. (2001) Uncoupling protein-2 negatively regulates insulin secretion and is a major link between obesity, beta cell dysfunction, and type 2 diabetes. Cell (Cambridge, Mass.) **105**, 745–755

23 Janjic, D., Maechler, P., Sekine, N., Bartley, C., Annen, A. S. and Wollheim, C. B. (1999) Free radical modulation of insulin release in INS1-E cells exposed to alloxan. Biochem. Pharmacol. **57**, 639–648

24 Asfari, M., Janjic, D., Meda, P., Li, G., Halban, P. A. and Wollheim, C. B. (1992) Establishment of 2-mercaptoethanol-dependent differentiated insulin-secreting cell lines. Endocrinology **130**, 167–178

25 Miyake, S., Makimura, M., Kanegae, Y., Harada, S., Sato, Y., Takamori, K., Tokuda, C. and Saito, I. (1996) Efficient generation of recombinant adenoviruses using adenovirus DNA-terminal protein complex and a cosmid bearing the full-length virus genome. Proc. Natl. Acad. Sci. U.S.A. **93**, 1320–1324

26 Esser, V., Britton, C. H., Weis, B. C., Foster, D. W. and McGarry, J. D. (1993) Cloning, sequencing, and expression of a cDNA encoding rat liver carnitine palmitoyltransferase I. Direct evidence that a single polypeptide is involved in inhibitor interaction and catalytic function. J. Biol. Chem. **268**, 5817–5822

27 Graham, F. L., Smiley, J., Russell, W. C. and Nairn, R. (1977) Characteristics of a human cell line transformed by DNA from human adenovirus type 5. J. Gen. Virol. **36**, 59–74

28 Herz, J. and Gerard, R. D. (1993) Adenovirus-mediated transfer of low density lipoprotein receptor gene acutely accelerates cholesterol clearance in normal mice. Proc. Natl. Acad. Sci. U.S.A. **90**, 2812–2816
29 Kolodziej, M. P., Crilly, P. J., Corstorphine, C. G. and Zammit, V A. (1992) Development and characterization of a polyclonal antibody against rat liver mitochondrial overt carnitine palmitoyltransferase (CPT I). Distinction of CPT I from CPT II and of isoforms of CPT I in different tissues. Biochem. J. **282**, 415–421
30 Swanson, S. T., Foster, D. W., McGarry, J. D. and Brown, N. F. (1998) Roles of the N- and C-terminal domains of carnitine palmitoyltransferase I isoforms in malonyl-CoA sensitivity of the enzymes: insights from expression of chimaeric proteins and mutation of conserved histidine residues. Biochem J. **335**, 513–519
31 Morillas, M., Clotet, J., Rubí, B., Serra, D., Asins, G., Ariño, J. and Hegardt, F. G. (2000) Identification of the two histidine residues responsible for the inhibition by malonyl-CoA in peroxisomal carnitine octanoyltransferase from rat liver. FEBS Lett. **466**, 183–186
32 Rubí, B., Ishihara, H., Hegardt, F. G., Wollheim, C. B. and Maechler, P. (2001) GAD65-mediated glutamate decarboxylation reduces glucose-stimulated insulin secretion in pancreatic beta cells. J. Biol. Chem. **276**, 36391–36396
33 Folch, J., Lees, M. and Stanley, G. H. S. (1957) A simple method for the isolation and purification of total lipids from animal tissues. J. Biol. Chem. **226**, 497–509
34 Antinozzi, P. A., Segall, L., Prentki, M., McGarry, J. D. and Newgard, C. B. (1998) Molecular or pharmacologic perturbation of the link between glucose and lipid metabolism is without effect on glucose-stimulated insulin secretion. A reevaluation of the long-chain acyl-CoA hypothesis. J. Biol. Chem. **273**, 16146–16154
35 Mulder, H., Lu, D., Finley, J., An, J., Cohen, J., McGarry, J. D. and Newgard, C. B. (2000) Overexpression of a modified human malonyl-CoA decarboxylase blocks the glucose induced increase in malonyl-CoA level but has no impact on insulin secretion in INS-1-derived (832/13) β-cells. J. Biol. Chem. **276**, 6479–6484
36 Alcazar, O., Qiu-yue, Z., Gine, E. and Tamarit-Rodriguez, J. (1997) Stimulation of islet protein kinase C translocation by palmitate requires metabolism of the fatty acid. Diabetes **46**, 1153–1158
37 Malaisse, W. J., Malaisse-Lagae, F., Sener, A. and Hellerstrom, C. (1985) Participation of endogenous fatty acids in the secretory activity of the pancreatic β-cell. Biochem. J. **227**, 995–1002
38 McGarry, J. D. (1992) What if Minkowski had been ageusic? An alternative angle on diabetes. Science (Washington, D.C.) **258**, 766–770
39 Unger, R. H. (1995) Lipotoxicity in the pathogenesis of obesity-dependent NIDDM. Genetic and clinical implications. Diabetes **44**, 863–870
40 Henquin, J. C. (2000) Triggering and amplifying pathways of insulin secretion by glucose. Diabetes **49**, 1751–1760
41 Niwa, H., Yamamura, K. and Miyazaki, J. (1991) Efficient selection for high-expression transfectants with a novel eukaryotic vector. Gene **108**, 193–200
42 Spurway, T. D., Pogson, C. I., Sherratt, H. S. and Agius, L. (1997) Etomoxir, sodium 2-[6-(4-chlorophenoxy)hexyl] oxirane-2-carboxylate, inhibits triacylglycerol depletion in hepatocytes and lipolysis in adipocytes. FEBS Lett. **404**, 111–114
43 Malaisse, W. J. and Malaisse-Lagae, F. (1968) Stimulation of insulin secretion by noncarbohydrate metabolites. J. Lab. Clin. Med. **72**, 438–448
44 Velasco, G., Geelen, M. J., del Pulgar, T. G. and Guzman, M. (1998) Malonyl-CoA-independent acute control of hepatic carnitine palmitoyltransferase I activity. J. Biol. Chem. **273**, 21497–21504
45 Ha, J., Lee, J. K., Kim, K. S., Witters, L. A. and Kim, K. H. (1996) Cloning of human acetyl-CoA carboxylase-β and its unique features. Proc. Natl. Acad. Sci. U.S.A. **93**, 11466–11470
46 Yajima, H., Komatsu, M., Yamada, S., Straub, S. G., Kaneko, T., Sato, Y., Yamauchi, K., Hashizume, K., Sharp, G. W. and Aizawa, T. (2000) Cerulenin, an inhibitor of protein acylation, selectively attenuates nutrient stimulation of insulin release: a study in rat pancreatic islets. Diabetes **49**, 712–717

Received 6 September 2001/6 February 2002; accepted 20 February 2002

THE JOURNAL OF BIOLOGICAL CHEMISTRY
Vol. 278, No. 19, Issue of May 9, pp. 16622–16629, 2003

Printed in U.S.A.

The Transcription Factor SREBP-1c Is Instrumental in the Development of β-Cell Dysfunction*

Received for publication, December 9, 2002, and in revised form, February 21, 2003
Published, JBC Papers in Press, February 24, 2003, DOI 10.1074/jbc.M212488200

Haiyan Wang‡, Pierre Maechler§, Peter A. Antinozzi¶, Laura Herrero‖, Kerstin A. Hagenfeldt-Johansson, Anneli Björklund‡‡, and Claes B. Wollheim**

From the Division of Clinical Biochemistry, Department of Internal Medicine, University Medical Centre, Geneva-4 CH-1211, Switzerland

Accumulation of lipids in non-adipose tissues is often associated with Type 2 diabetes and its complications. Elevated expression of the lipogenic transcription factor, sterol regulatory element binding protein-1c (SREBP-1c), has been demonstrated in islets and liver of diabetic animals. To elucidate the molecular mechanisms underlying SREBP-1c-induced β-cell dysfunction, we employed the Tet-On inducible system to achieve tightly controlled and conditional expression of the nuclear active form of SREBP-1c (naSREBP-1c) in INS-1 cells. Controlled expression of naSREBP-1c induced massive accumulation of lipid droplets and blunted nutrient-stimulated insulin secretion in INS-1 cells. K^+-evoked insulin exocytosis was unaltered. Quantification of the gene expression profile in this INS-1 stable clone revealed that naSREBP-1c induced β-cell dysfunction by targeting multiple genes dedicated to carbohydrate metabolism, lipid biosynthesis, cell growth, and apoptosis. naSREBP-1c elicits cell growth-arrest and eventually apoptosis. We also found that the SREBP-1c processing in β-cells was irresponsive to acute stimulation of glucose and insulin, which was distinct from that in lipogenic tissues. However, 2-day exposure to these agents promoted SREBP-1c processing. Therefore, the SREBP-1c maturation could be implicated in the pathogenesis of β-cell glucolipotoxicity.

The lipogenic transcription factors, sterol regulatory element binding proteins (SREBPs)[1] are transmembrane proteins of the endoplasmic reticulum (ER). In response to low sterol and other unidentified factors, SREBP cleavage-activating protein escorts SREBPs from the ER to the Golgi, where SREBPs are sequentially cleaved by Site-1 protease and Site-2 protease. The processed mature SREBPs enter the nucleus and transactivate target genes (1). Three SREBP isoforms have been identified: SREBP-1a and -1c (alternatively known as adipocyte determination and differentiation factor-1 (ADD1)) (2), which are derived from the same gene through alternative splicing, and SREBP-2, which is encoded by a distinct gene (1). SREBPs play an essential role in regulation of lipid homeostasis in animals and have been shown to directly activate the expression of more than 30 genes dedicated to the biosynthesis of cholesterol, fatty acids, triglycerides, and phospholipids (3). SREBP-1 preferentially regulates genes implicated in fatty acid synthesis, whereas SREBP-2 preferentially activates genes involved in cholesterol synthesis (1). In particular, SREBP-1c mediates insulin effects on lipogenic gene expression in both adipocytes and liver (4, 5).

Type 2 diabetes mellitus is a common disorder that affects ~5% of the population worldwide, especially in industrialized countries (6). Affected patients are usually obese with accumulation of lipids in non-adipose tissues such as the pancreatic islets, liver, heart, skeletal muscle, and blood vessels (7–9). This is associated with impaired glucose-stimulated insulin secretion, increased hepatic glucose production, peripheral insulin resistance, and late complications in various organs (10, 11). The ultimate precipitating process responsible for the development of Type 2 diabetes is the failure of the pancreatic β-cells to compensate for insulin resistance (7, 10, 11). However, the mechanism by which the β-cells become unable to meet increased insulin demands remains to be established.

Elevated expression of SREBP-1c has been demonstrated in islets or liver of diabetic animals, such as Zucker diabetic fatty rats, *ob/ob* mice, insulin receptor substrate-2-deficient mice, and a transgenic mouse model of lipodystrophy (7, 12–16). On the other hand, preventing SREBP-1c overexpression is a common function of leptin, metformin, and PPARγ agonists, which is well correlated with their antidiabetic effects (7, 12–15). An important function of leptin in the regulation of fatty acid homeostasis is to restrict the lipid storage in adipocytes and to limit lipid accumulation in non-adipocytes, thereby protecting them from lipotoxicity (7, 9). Infusion of recombinant leptin reverses insulin resistance and hyperglycemia in the transgenic model of congenital generalized lipodystrophy and in *ob/ob* mice (13). Adenovirus-mediated hyperleptinemia also decreases the expression of SREBP-1c and lipogenic genes in liver

* This work was supported by Swiss National Science Foundation Grant 32-49755.96 (to C. B. W.) and the Leenaards Foundation (to P. M.). The costs of publication of this article were defrayed in part by the payment of page charges. This article must therefore be hereby marked "*advertisement*" in accordance with 18 U.S.C. Section 1734 solely to indicate this fact.

‡To whom correspondence should be addressed. Tel.: 41-22-702-5548; Fax: 41-22-702-5543; E-mail: Haiyan.Wang@medicine.unige.ch.
§Fellow of the Dr. Max Cloetta Foundation.
¶ Present address: Cellular Biochemistry and Biophysics, Memorial Sloan-Kettering Cancer Center, 1275 York Ave., Box 251, New York, NY 10021.
‖ Present address: Dept. of Biochemistry, School of Pharmacy, University of Barcelona, E-08028 Barcelona, Spain.
** Present address: Swiss Institute for Experimental Cancer Research (ISREC), CH-1066 Epalinges, Switzerland.
‡‡Present address: Rolf Luft Center of Diabetes Research, Endocrine and Diabetes Unit, Dept. of Molecular Medicine, Karolinska Institute, Karolinska Hospital, Stockholm, Sweden.

[1] The abbreviations used are: SREBP, sterol regulatory element-binding protein; ER, endoplasmic reticulum; ADD1, adipocyte determination and differentiation factor-1; PPAR, peroxisome proliferator-activated receptor; naSREBP, nuclear active form of SREBP-1c; PBS, phosphate-buffered saline; BSA, bovine serum albumin; KRBH, Krebs-Ringer-bicarbonate-HEPES buffer; UCP, uncoupling protein; FCCP, carbonyl cyanide 4-trifluoromethoxyphenylhydrazone; Pdx, pancreas duodenum homeobox; HNF, hepatocyte nuclear factor; IRS, insulin receptor substrate; TNF, tumor necrosis factor.

and islets of wild-type *fa/fa* rats (12). Leptin also prevents the SREBP-1c overexpression in insulin receptor substrate (IRS)-2-null mice (15). It is noteworthy that metformin, an oral antihyperglycemic agent, also corrects fatty liver disease in *ob/ob* mice by inhibition of obesity-related induction of SREBP-1c (14). The inhibitory effects of metformin on hepatic SREBP-1c expression involves activation of AMP-activated protein kinase (17). Similarly, Troglitazone, an antidiabetic agent and a high-affinity ligand for the PPARγ, prevents SREBP-1c overexpression in Zucker diabetic fatty rats (12). In addition, it has recently been reported that adenovirus-mediated overexpression of SREBP-1c in MIN6 cells results in impaired glucose-stimulated insulin secretion (18). Therefore, these studies suggest that overexpression of SREBP-1c may be the cause of both liver steatosis and islet β-cell dysfunction.

The present study was designed to evaluate the direct correlation between SREBP-1c overexpression and β-cell dysfunction and to elucidate the underlying molecular mechanism. The Tet-On system was employed in INS-1 cells to achieve tightly controlled and inducible expression of a nuclear active form of SREBP-1c (naSREBP-1c; N-terminal 1–403 amino acids) (19). Quantification of the gene expression profile in this INS-1 stable cell line revealed that naSREBP-1c induced β-cell dysfunction by targeting multiple genes implicated in carbohydrate metabolism, lipid biosynthesis, cell growth, and eventually apoptosis.

EXPERIMENTAL PROCEDURES

Establishment of INS-1 Cells Permitting Inducible Expression of naSREBP-1c—Rat insulinoma INS-1 cell-derived clones were cultured in RPMI 1640 containing 11.2 mM glucose (20), unless otherwise indicated. The first step stable clone INS-rβ cell line, which carries the reverse tetracycline/doxycycline-dependent transactivator (21) was described previously (22, 23). The plasmid used in the secondary stable transfection were constructed by subcloning the cDNA encoding the nuclear active form of SREBP-1c (naSREBP-1c/ADD1-(1–403) (19), kindly supplied by Dr. B. M. Spiegelman) into the expression vector PUHD10–3 (21) (a generous gift from Dr. H. Bujard). The procedures for stable transfection, clone selection and screening were described previously (22).

Immunofluorescence and Western Blotting—For immunofluorescence, cells grown on polyornithine-treated glass coverslips were treated for 24 h with or without 500 ng/ml doxycycline. Cells were then washed, fixed in 4% paraformaldehyde, permeabilized with 0.1% Triton X-100 in phosphate-buffered saline containing 1% BSA (PBS-BSA). The preparation was then blocked with PBS-BSA before incubating with the first antibody, anti-SREBP-1 (Santa Cruz, Basel, Switzerland) (1:100 dilution), followed by the second antibody labeling.

For Western blotting cells were cultured with 0, 75, 150, and 500 ng/ml doxycycline for 24 h. Rat islets were isolated by collagenase digestion as described (24), and their nuclear proteins were extracted as previously reported (25). Total cell proteins were prepared by lysis and sonication of naSREBP-1c#233 and INS-1E cells in buffer containing 20 mM Tris-HCl, pH 7.4, 2 mM EDTA, 2 mM EGTA, 1% Triton X-100, and 1 mM phenylmethylsulfonyl fluoride. Nuclear extracts and total cellular proteins were fractionated by 9% SDS-PAGE. The dilution for SREBP-1 antibody is 1:1,000. Immunoblotting procedures were performed as described previously (26) using enhanced chemiluminescence (Pierce) for detection.

Staining of Lipid Accumulation by Oil Red O and Measurements of Triglyceride Content—Cells were cultured with 0, 75, 150, and 500 ng/ml doxycycline for 24 h. Cells were fixed and stained as previously reported (19). Lipid droplets were visualized using phase-contrast microscopy (Nikon Diaphot). Cellular triglyceride content was determined using Triglyceride (GPO-TRINDER) kit (Sigma) according to the manufacturer's protocol.

Measurements of Insulin Secretion and Cellular Insulin Content—Insulin secretion in naSREBP-1c#233 cells was measured in 12-well plates over a period of 30 min, in Krebs-Ringer-bicarbonate-HEPES buffer (KRBH, 140 mM NaCl, 3.6 mM KCl, 0.5 mM NaH_2PO_4, 0.5 mM $MgSO_4$, 1.5 mM $CaCl_2$, 2 mM $NaHCO_3$, 10 mM HEPES, 0.1% BSA) containing indicated concentrations of glucose. Insulin content was determined after extraction with acid ethanol following the procedures of Wang *et al.* (26). Insulin was detected by radioimmunoassay using rat insulin as a standard (26).

Total RNA Isolation and Northern Blotting—Cells were cultured with or without 500 ng/ml doxycycline in 2.5 mM glucose medium for 16 h and then incubated for a further 8 h at 2.5, 6, 12, and 24 mM glucose concentrations. Alternatively, naSREBP-1c#233 cells were cultured with or without 75 ng/ml doxycycline in standard medium (11.2 mM glucose) for 0, 24, 48, and 96 h. Total RNA was extracted and blotted to nylon membranes as described previously (22). The membrane was prehybridized and then hybridized to ^{32}P-labeled random primer cDNA probes according to Wang and Iynedijian (22). To ensure equal RNA loading and even transfer, all membranes were stripped and re-hybridized with a "housekeeping gene" probe cyclophilin. cDNA fragments used as probes for SREBP-1c, hepatocyte nuclear factor (HNF)-1α, HNF-4α, glucokinase, Glut-2, insulin, Sur1, Kir6.2, and pancreas duodenum homeobox (Pdx-1) mRNA detection were digested from the corresponding plasmids. cDNA probes for rat islet amyloid polypeptide, Nkx6.1, adenine nucleotide translocator 1 and 2, mitochondrial uncoupling protein 2 (UCP2), mitochondrial glutamate dehydrogenase, citrate synthase, glyceraldehydes-3 phosphate dehydrogenase, fatty acid synthase, acetyl-CoA carboxylase, glycerol-phosphate acyltransferase, carnitine palmitoyltransferase-1, acyl-CoA oxidase, 3-hydroxy-3-methylglutaryl-CoA reductase, $P21^{WAF1/CIP1}$, $P27^{KIP1}$, Bax, Bad, APO-1, Cdk-4, IRS-2, and glucagon-like peptide-1 receptor were prepared by reverse transcription-PCR and confirmed by sequencing.

Mitochondrial Membrane Potential ($\Delta\psi_m$)—Cells seeded in 24-well plates were cultured with or without 500 ng/ml doxycycline in 11.2 mM glucose medium for 24, 48, and 96 h (day 1, day 2, and day 4, respectively). Cells were then maintained for 2 h in 2.5 mM glucose medium at 37 °C before loading with 10 μg/ml rhodamine-123 for 20 min at 37 °C in KRBH (28). The $\Delta\psi_m$ was monitored in a plate-reader fluorimeter (Fluostar Optima, BMG Labtechnologies, Offenburg, Germany) with excitation and emission filters set at 485 and 520 nm, respectively, at 37 °C with automated injectors for glucose (addition of 13 mM on top of basal 2.5 mM) and carbonyl cyanide 4-trifluoromethoxyphenylhydrazone (FCCP).

Cell Proliferation/Viability and Apoptosis—Quantification of cell proliferation/viability was measured by a Quick Cell Proliferation Assay Kit (LabForce/MBL, Nunningen, Switzerland) according to the manufacturer's protocol. This assay is based on the reduction of a tetrazolium salt WST-1 to formazan by cellular mitochondrial dehydrogenases. Expansion in the number of viable cells results in an increase in the overall activity of the mitochondrial dehydrogenases and subsequently an augmentation in the amount of formazan dye formed. The formazan dye produced by viable cells was quantified with a multiwell spectrophotometer by measuring the absorbance at 440 nm.

Experiments for DNA fragmentation were performed using a Quick Apoptosis DNA Ladder Detection Kit (LabForce/MBL) following the manufacturer's protocol. Detection of mitochondrial cytochrome *c* release into cytosol was performed as described previously (29). Briefly, cells in 15-cm dishes were harvested and suspended in Buffer A (20 mM HEPES-KOH, pH 7.5, 10 mM KCl, 1.5 mM $MgCl_2$, 1 mM EDTA, 1 mM EGTA, 1 mM dithiothreitol, 250 mM sucrose, 1 mM phenylmethylsulfonyl fluoride) and homogenized by a Dounce homogenizer. Cell debris and nuclei were removed by centrifugation at 1000 × *g* for 10 min at 4 °C. The supernatant was further centrifuged at 10,000 × *g* for 20 min. The cytosolic proteins (supernatant fractions) were separated by 15% SDS-PAGE and analyzed by Western blotting with a specific antibody against cytochrome *c* (LabForce/MBL).

RESULTS

Establishment of a Stable INS-1 Cell Line Permitting Inducible Expression of naSREBP-1c—A rat insulinoma INS-1-derived stable cell line, INSrβ (23), which expresses the reverse tetracycline-dependent activator (21), was used for the secondary stable transfection with an expression vector, PUHD10–3 (21), carrying the naSREBP-1c and a plasmid pTKhygro containing the hygromycin-resistant marker. Five-round stable transfection experiments were performed, and a total of 400 hygromycin-resistant clones were screened by Northern blotting for clones positively expressing naSREBP-1c after doxycycline induction. Our persistent effort was rewarded. Only one clone, termed naSREBP-1c#233, which actually represented undetectable background expression under non-induced conditions, showed remarkable expression of naSREBP-1c mRNA

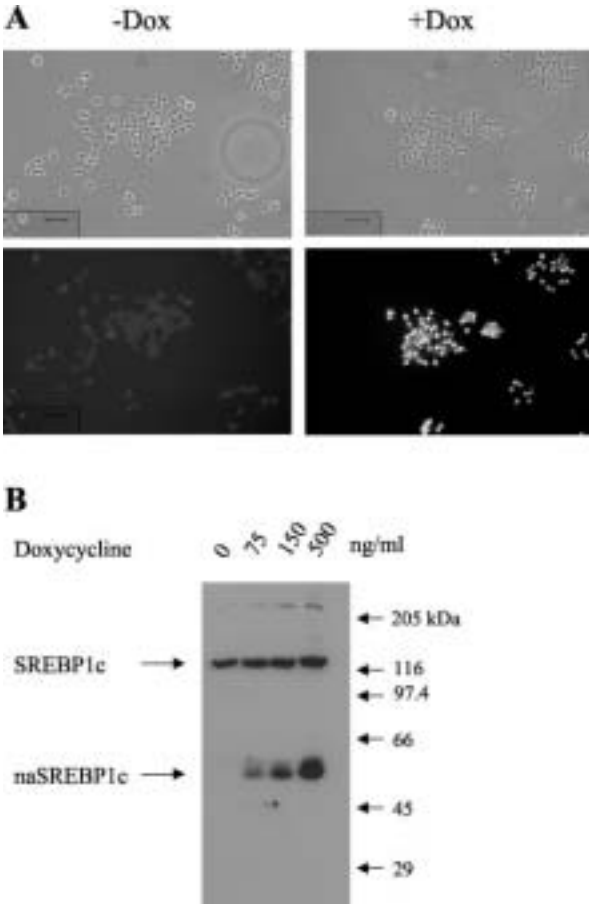

FIG. 1. **Induction of naSREBP-1c protein in a dose-dependent and an all-or-none manner.** *A*, immunofluorescence staining with an antibody against the N terminus of SREBP-1c. The phase contrast image is shown in the *upper panel*. The naSREBP-1c#233 cells were cultured with (+Dox) or without (−Dox) 500 ng/ml doxycycline for 24 h. *B*, Western blotting of total cell extracts (100 μg) with the same antibody. Cells were cultured with 0, 75, 150, and 500 ng/ml doxycycline for 24 h.

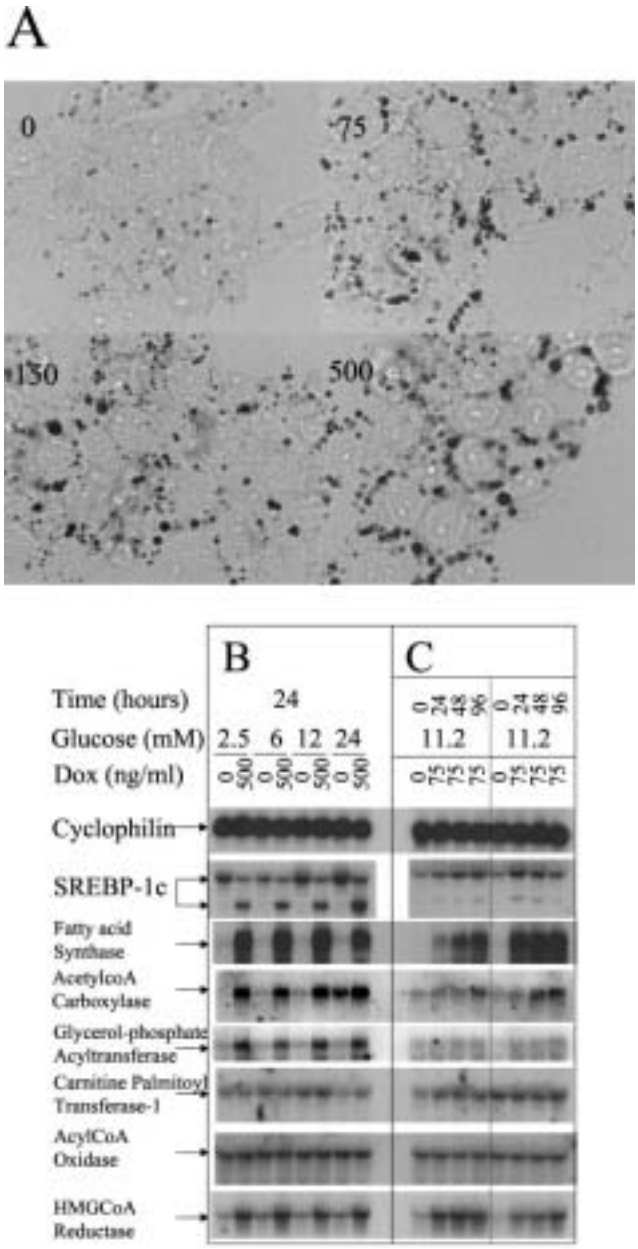

FIG. 2. **Accumulation of lipid droplets and increased lipogenic gene expression are shown in INS-1 cells expressing naSREBP-1c.** *A*, Oil Red O staining naSREBP-1c#233 cells cultured with 0, 75, 150, and 500 ng/ml doxycycline for 24 h. *B*, Northern blotting was performed using total RNA isolated from cells cultured with 500 ng/ml doxycycline in 2.5 mM glucose medium for 16 h and continued in 2.5, 6, 12, and 24 mM glucose medium for a further 8 h. The experiments were repeated two times with similar results. *C*, Northern blotting was conducted using total RNA isolated from cells cultured in standard glucose medium (11.2 mM glucose) with 75 ng/ml doxycycline for 0, 24, 48, and 96 h. Two independent experiments are shown side by side to demonstrate the consistency of the results.

after doxycycline induction. From experience, we would have anticipated that 10–20% of hygromycin-resistant clones should positively express the transgene. The unexpected results indicate that expression of naSREBP-1c even at leakage level was sufficient to cause "β-cell toxicity." The INS-1 stable cell line naSREBP-1c#233 provided a unique chance to study the impact of naSREBP-1c expression on β-cell function.

All Cells Uniformly Express the Nuclear Localized naSREBP1c Protein in a Doxycycline Dose-dependent Manner—Immunofluorescence (Fig. 1*A*) with an antibody against the N terminus of SREBP1c illustrated that nuclear localized naSREBP1c protein was induced homogeneously in naSREBP-1c#233 cells cultured with 500 ng/ml doxycycline for 24 h. Western blotting (Fig. 1*B*) with the same antibody demonstrated that naSREBP-1c#233 cells expressed the transgene-encoded protein in a doxycycline dose-dependent manner. As predicted, naSREBP-1c#233 cells did not show detectable expression of naSREBP-1c protein under non-induced conditions (Fig. 1). The protein levels of naSREBP-1c in cells cultured with 75, 150, and 500 ng/ml were ~10%, 25%, and 150%, respectively, of endogenous level of SREBP-1c precursor protein (Fig. 1*B*).

Induction of naSREBP-1c Causes Rapid Accumulation of Lipid Droplets by Increasing Lipogenic Gene Expression—Oil Red O staining showed that induction of naSREBP-1c with 75, 150, and 500 ng/ml doxycycline for 24 h resulted in accumulation of lipid droplets in INS-1 cells cultured in standard medium (10% fetal calf serum) (Fig. 2*A*). Cellular triglyceride content was increased by 39% (−Dox: 0.536 ± 0.08; +Dox: 0.745 ± 0.10 mg/mg protein, $p < 0.001$, $n = 14$) after 24 h of induction with 500 ng/ml doxycycline. Similar results were obtained in cells cultured in serum-free medium (data not shown), suggesting that the naSREBP-1c-induced lipid accumulation was not due to uptake of fatty acids by the cells. This contention was supported by results of quantitative Northern blotting. Induction of naSREBP-1c significantly increased the

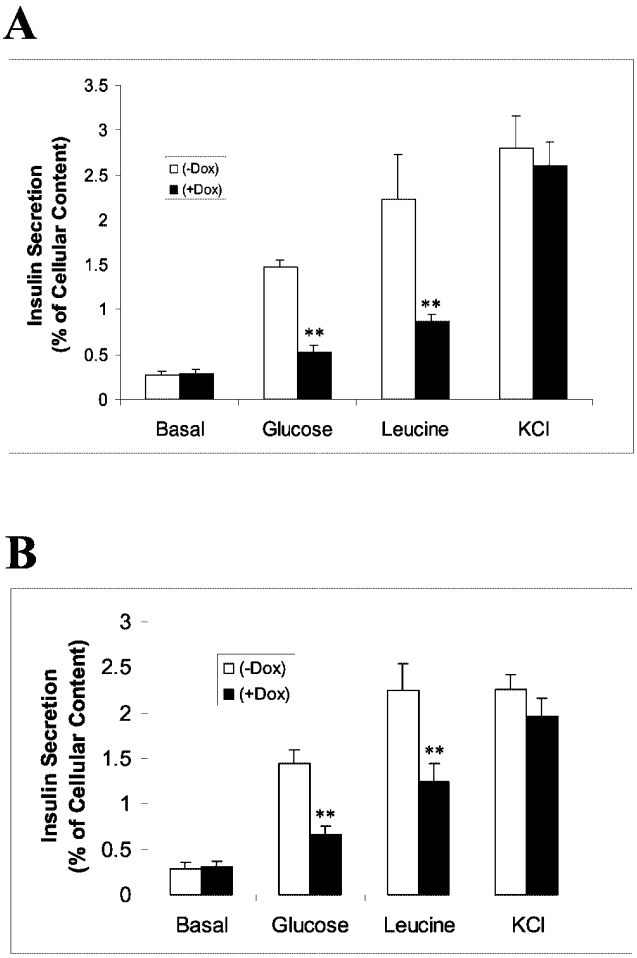

FIG. 3. **Induction of naSREBP-1c results in impaired nutrient-stimulated insulin secretion.** *A*, cells were cultured with (+Dox) or without (−Dox) 500 ng/ml doxycycline in standard medium (11.2 mM glucose) for 19 h and then equilibrated in 2.5 mM glucose medium for a further 5 h. *B*, cells were cultured with (+Dox) or without (−Dox) 75 ng/ml doxycycline in standard glucose medium (11.2 mM) for 91 h followed by an additional 5 h of equilibration in 2.5 mM glucose medium. Cellular insulin content in *A* and *B* was reduced, respectively, by 24.6 ± 4.8 ($n = 6$) and 21 ± 5.3 ($n = 6$) after naSREBP-1c induction. Insulin release from naSREBP-1c#233 cells stimulated by 21.5 mM glucose, 20 mM leucine, and 20 mM KCl in KRBH buffer (140 mM NaCl, 3.6 mM KCl, 0.5 mM NaH_2PO_4, 0.5 mM $MgSO_4$, 1.5 mM $CaCl_2$, 2 mM $NaHCO_3$, 10 mM HEPES, 0.1% BSA) containing 2.5 mM glucose (*Basal*) was quantified by radio-immunoassay and normalized by cellular insulin content. Data represent mean ± S.E. of six independent experiments. **, $p < 0.0001$.

expression of genes dedicated to biosynthesis of fatty acids and cholesterol but did not alter the expression of genes involved in β-oxidation of fatty acids (Fig. 2, *B* and *C*). The increased mRNA levels of fatty acid synthase, acetyl-CoA carboxylase, glycerol-phosphate acyltransferase, and 3-hydroxy-3-methyl-glutaryl-CoA reductase would explain the naSREBP-1c-induced lipid accumulation. In addition, the increased lipogenesis did not raise the transcript levels of carnitine palmitoyltransferase-1 and acyl-CoA oxidase, which are important for fatty acid metabolism.

Induction of naSREBP-1c Impairs Nutrient-stimulated Insulin Secretion—Induction of naSREBP1c with 500 ng/ml doxycycline for 24 h (Fig. 3*A*) or 75 ng/ml doxycycline for 96 h (Fig. 3*B*) caused blunted glucose- and leucine-stimulated but not K^+-depolarization-induced insulin secretion. Glucose generates ATP and other metabolic-coupling factors important for insulin exocytosis through glycolysis and mitochondrial oxidation (30). Leucine stimulates insulin release through direct uptake and metabolism by the mitochondria, thereby providing substrates for the tricarboxylic acid cycle (30). K^+ causes insulin secretion by depolarization of the β-cell membrane, resulting in increased cytosolic Ca^{2+} (30). To explore the molecular targets of naSREBP-1c responsible for the impaired metabolism-secretion coupling, we examined the gene expression profile in naSREBP-1c#233 cells.

Induction of naSREBP-1c Alters the Expression of Genes Important for Glucose Metabolism and β-Cell Function—Quantitative Northern blotting revealed that similar induction of naSREBP1c also caused marked down-regulation of glucokinase and Glut2 but up-regulation of mitochondrial UCP-2 (Fig. 4, *A* and *B*). In contrast, naSREBP-1c did not alter the mRNA levels of glyceraldehydes-3-phosphate dehydrogenase, mitochondrial adenine nucleotide translocator-1 and -2, glutamate dehydrogenase, citrate synthase, K_{ATP} channel subunits SUR1 and KIR6.2 (Fig. 4, *A* and *B*). Glucokinase is the rate-limiting enzyme for glycolysis and thereby determines β-cell glucose sensing (22, 31). The effect of naSEBP-1c on β-glucokinase expression is opposite to its action on liver glucokinase, which is transcribed from a distinct liver-specific promoter (5, 32). UCP-2 may act as a protonophore and dissipate the mitochondrial membrane potential, thereby uncoupling respiration from ATP synthesis (33–36).

Induction of naSREBP1c also suppressed the expression of Pdx-1, HNF-4α, and CCAAT/enhancer-binding protein-β in a dose- and time-dependent manner (Fig. 4, *C* and *D*). The HNF-1α expression was unaffected, whereas the mRNA level of a β-cell transcription factor Nkx6.1 was increased by naSREBP-1c (Fig. 4, *C* and *D*). High-level induction of naSREBP-1c also decreased the transcript levels of insulin and islet amyloid polypeptide (Fig. 4*C*).

Induction of naSREBP-1c Disrupts Mitochondrial Membrane Potential—Mitochondrial membrane potential ($\Delta\psi_m$), reflecting electron transport chain activity, was measured in attached cells by monitoring rhodamine-123 fluorescence. In non-induced control cells, the addition of 13 mM glucose (15.5 mM final) hyperpolarized $\Delta\psi_m$ and 1 μM the protonophore FCCP deploarized $\Delta\psi_m$. After induction of naSREBP1c, glucose-induced mitochondrial hyperpolarization was markedly inhibited as early as day 1 (24 h of induction) and completely abolished at days 2 and 4 (Fig. 5). Basal activity of the electron transport chain was progressively lost, as indicated by the dissipation of $\Delta\psi_m$ by FCCP, and completely abrogated at day 4 (Fig. 5). The mitochondrion is not only the powerhouse for cell growth and survival but also the arsenal for cell apoptosis (37). Disruption of mitochondrial membrane potential is an essential event that commits a cell to undergo apoptosis (38, 39). Consistently, we also found that expression of naSREBP-1c even at leakage level was sufficient to cause "cell toxicity" during the screening procedure for naSREBP-1c-positive clones. To elucidate the molecular mechanism underlying naSREBP-1c-induced cell toxicity, we investigated the effect of naSREBP-1c on the expression of genes important for cell proliferation and apoptosis.

SREBP-1c Targets Multiple Genes Implicated in β-Cell Growth and Survival—As shown in Fig. 6, induction of naSREBP-1c decreased the expression of cyclin-dependent kinase 4 and IRS-2 in a dose- and time-dependent manner. In contrast, the mRNA level of glucagon-like polypeptide-1 receptor was barely changed (Fig. 6). Both cyclin-dependent kinase 4 and IRS-2 have been reported to promote β-cell development, proliferation, or survival (40, 41). In addition, the mRNA level of $P21^{WAF1/CIP1}$ was dramatically increased by naSREBP-1c induction, whereas the $P27^{KIP1}$ remained constant (Fig. 6). The increased expression of the $P21^{WAF1/CIP1}$, a cyclin-dependent kinase inhibitor, could also lead to INS-1 cell growth arrest. Furthermore, as demonstrated in Fig. 6, naSREBP-1c up-reg-

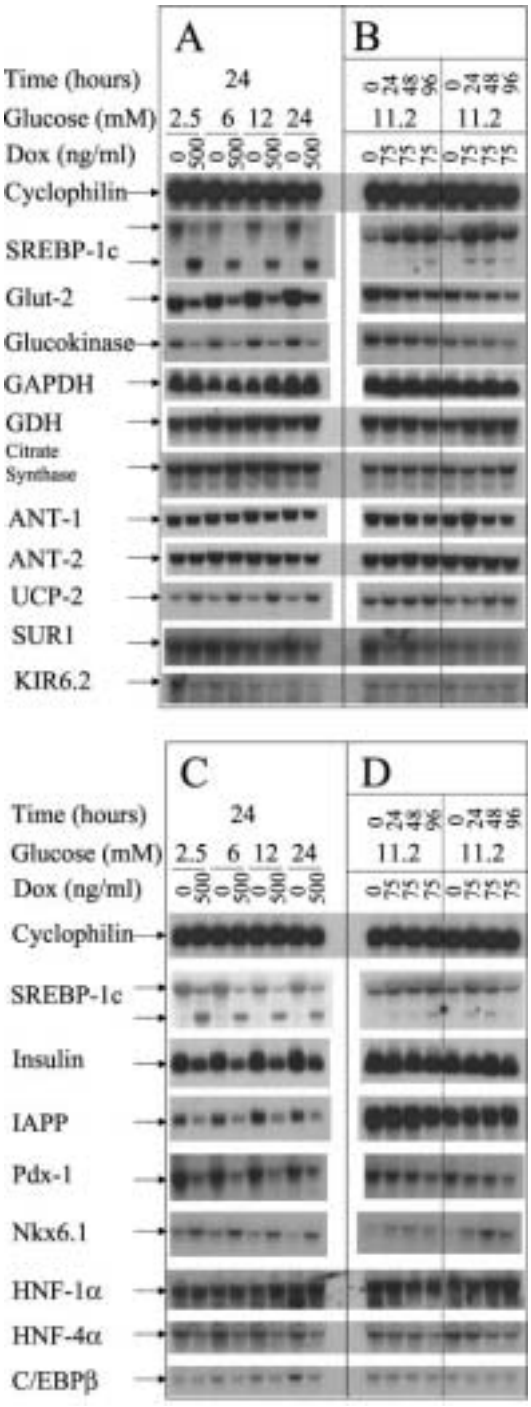

FIG. 4. **Induction of naSREBP-1c causes defective expression of genes implicated in glucose metabolism and β-cell function.** *A* and *C*, cells were cultured with or without 500 ng/ml doxycycline in 2.5 mM glucose medium for 16 h and then incubated for a further 8 h at indicated glucose concentrations. The experiments were repeated two times with similar results. *B* and *D*, cells were cultured with or without 75 ng/ml doxycycline in standard medium (11.2 mM glucose) for 0, 24, 48, and 96 h. Two independent experiments are shown side by side to demonstrate the consistency of the results. The gene expression patterns in naSREBP-1c#233 cells were quantified by Northern blotting. Total RNA samples (20 μg/lane) were analyzed by hybridizing with indicated cDNA probes.

ulated the expression of proapoptotic genes, APO-1/Fas/CD95 and Bax (37, 38), but did not alter the mRNA levels of Bad and tumor necrosis factor (TNF)-1α. The up-regulation of APO-1 and Bax could contribute to the naSREBP-1c-induced INS-1 cell apoptosis (see below).

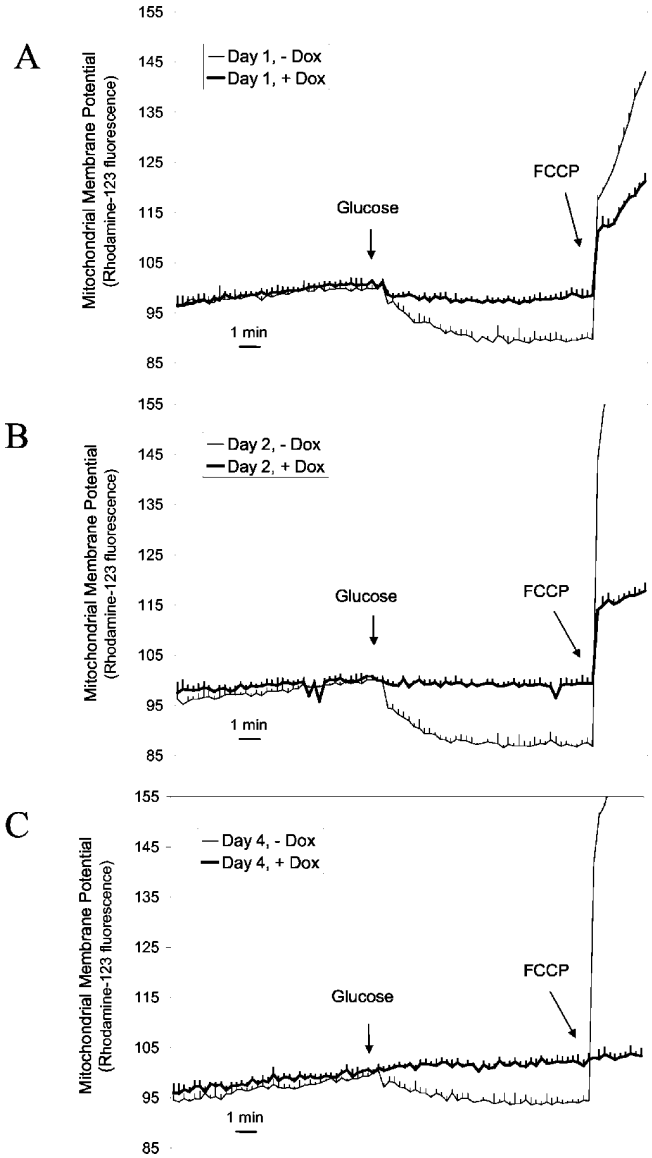

FIG. 5. **Induction of naSREBP-1c dissipates mitochondrial membrane potential ($\Delta\psi_m$) in naSREBP-1c#233 cells.** Cells were cultured without (−Dox) or with (+Dox) 500 ng/ml doxycycline for 24, 48, and 96 h (day 1, day 2, and day 4, respectively). The $\Delta\psi_m$ was measured on attached cells in KRBH containing basal 2.5 mM glucose using rhodamine-123 fluorescence. Electron transport chain activation observed as hyperpolarization of $\Delta\psi_m$ was induced by the addition of 13 mM glucose (15.5 mM final), followed by the complete depolarization of $\Delta\psi_m$ using 1 μM of the uncoupler FCCP. Values are means plus standard deviations ($n = 4$) of one of a total of four to six independent experiments.

Induction of naSREBP-1c Results in Cell Growth Arrest and Apoptosis in INS-1 Cells—To assess the impact of naSREBP-1c on INS-1 cell growth and viability, we performed the WST-1 assay. This assay is based on the reduction of a tetrazolium salt WST-1 to formazan by cellular mitochondrial dehydrogenases. Expansion in the number of viable cells results in an increase in the overall activity of the mitochondrial dehydrogenases and subsequently an augmentation in the amount of formazan dye formed. Induction of naSREBP-1c with 500 ng/ml doxycycline for 24 h or with 75 ng/ml doxycycline for 4 days in naSREBP-1c#233 cells significantly inhibited INS-1 cell growth/viability. The measurements of optical density at 440 nM were reduced by, respectively, 31.6 ± 4.2% and 36.3 ± 5.5% relative to non-induced cells ($n = 4, p < 0.001$). Mitochondrial cytochrome *c* release and DNA fragmentation are characteristic hallmarks

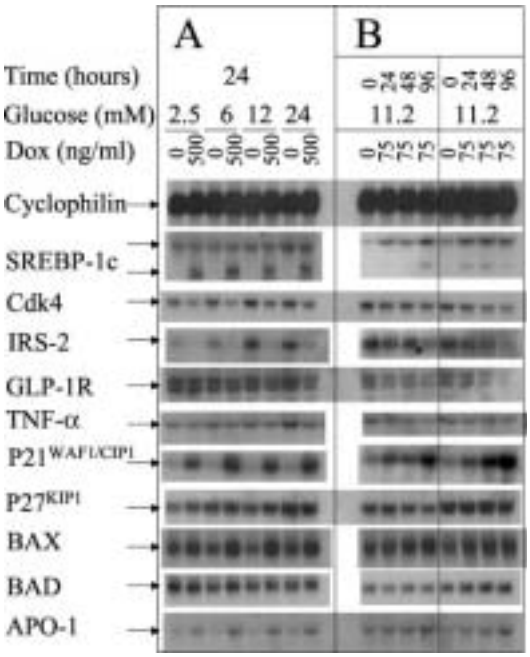

FIG. 6. **Induction of naSREBP-1c alters the expression of genes important for β-cell growth and survival.** *A*, cells were cultured with or without 500 ng/ml doxycycline in 2.5 mM glucose medium for 16 h and then incubated for a further 8 h at indicated glucose concentrations. The experiments were repeated two times with similar results. *B*, cells were cultured with or without 75 ng/ml doxycycline in standard medium (11.2 mM glucose) for 0, 24, 48, and 96 h. Two separate experiments are demonstrated in parallel. The gene expression profile in naSREBP-1c#233 cells was quantified by Northern blotting. Total RNA samples (20 μg/lane) were analyzed by hybridizing with indicated cDNA probes.

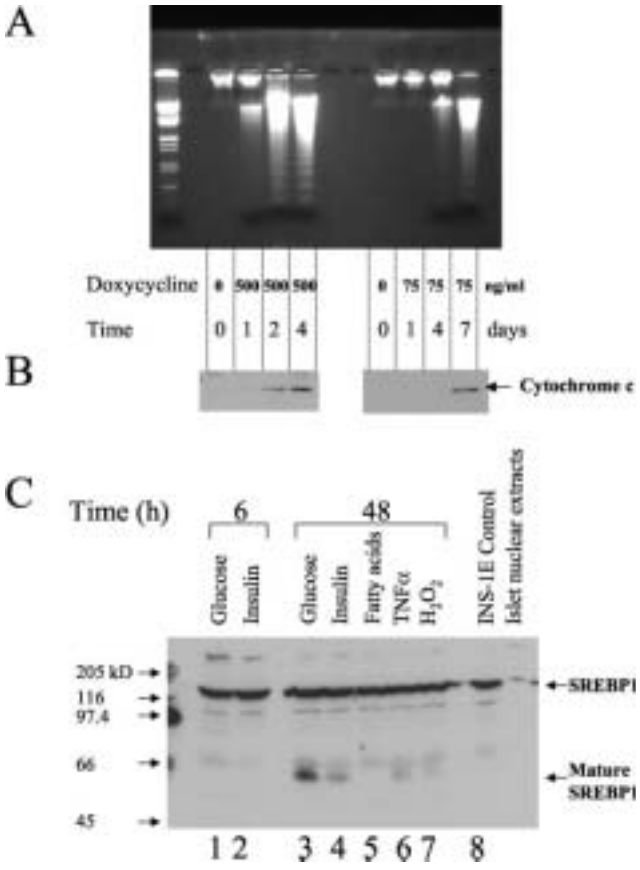

FIG. 7. **Apoptosis in INS-1 cells induced by naSREBP-1c and maturation of SREBP-1 protein in INS-1E cells regulated by factors causing β-cell dysfunction.** *A*, DNA fragmentation in naSREBP-1c#233 cells cultured either with 500 ng/ml doxycycline for 1, 2, and 4 days (*left panel*) or with 75 ng/ml doxycycline for 1, 4, and 7 days (*right panel*). *B*, cytochrome *c* released in cytosolic fractions isolated from naSREBP-1c#233 cells cultured either with 500 ng/ml doxycycline for 1, 2, and 4 days (*left panel*) or with 75 ng/ml doxycycline for 1, 4, and 7 days (*right panel*). Cytosolic proteins (100 mg/lane) were separated with 15% SDS-PAGE and analyzed by immunoblotting with an anti-cytochrome *c* antibody. *C*, immunoblotting with antibody against the N terminus of SREBP-1. Total cell extracts (100 μg of protein/lane) from INS-1E cells (*lanes 1–8*) or nuclear proteins (50 μg of protein) from freshly isolated rat islets (*lane 9*) were separated by 9% SDS-PAGE. INS-1E cells were treated for either 6 h (*lanes 1* and 2) or 48 h (*lanes 3* and *4*) with 30 mM glucose or 100 nM exogenous insulin as indicated. *Lanes 5–7* represent, respectively, total cell extracts from INS-1E cultured for 48 h in standard medium (11.2 mM glucose) containing 1.5 mM long-chain free fatty acids (2:1 oleate/palmitate), 10 ng/ml TNF-α, and 10 μM H_2O_2. Total cell lysates from INS-1E cells under standard culture conditions are shown in *lane 8* as control.

of cells undergoing apoptosis (37, 42). Extensive DNA fragmentation was observed in naSREBP-1c#233 cells cultured with 500 ng/ml doxycycline for 48 h or with 75 ng/ml doxycycline for a week (Fig. 7*A*). Consistently, similar induction of naSREBP-1c also induced mitochondrial cytochrome *c* release (Fig. 7*B*). These results suggest that naSREBP-1c induces INS-1 cell apoptosis in a dose- and time-dependent manner.

SREBP-1c Processing in β-Cells Is Distinct from Lipogenic Tissues—Unlike liver and adipose tissue, pancreatic β-cells have evolved to secrete insulin rather than store energy in response to rising blood glucose and nutrient levels. The released insulin subsequently promotes the lipogenic gene expression in liver and adipocytes through up-regulation of SREBP-1 expression and increase of its processing (4, 5, 43). The molecular mechanism by which β-cells restrict lipogenesis in response to physiological glucose and insulin stimulation remains undefined. We performed Western blotting using an antibody specific for the N terminus of SREBP-1, which should recognize both precursor and mature SREBP-1. As shown in Figure 7*C*, the mature nuclear form of SREBP-1 was not detectable in nuclear extracts from freshly isolated rat islets. Consistently, only the precursor but not the mature nuclear form of SREBP-1 protein was detected in total cell extracts from native INS-1E cells (Fig. 7*C*). Similar results were obtained in INS-1E cells treated for 6 h with 30 mM glucose and 100 nM exogenous insulin (Fig. 7*C*).

Low sterol-mediated cleavage of SREBP precursor proteins is not the only mechanism for the processing of SREBPs. It has been suggested that insulin and cytokines stimulate phosphorylation and transcriptional activity of SREBPs via the mitogen-activated protein kinase cascade (44–48). Caspase-3/CPP32, a cysteine protease and mediator of apoptosis, also induces cleavage of SREBPs and release of their transactive N-terminal fragments (42). In addition, TNF-α stimulates the maturation of SREBP-1c in human hepatocytes (49). Furthermore, hyperglycemia in animal models of diabetes causes increased SREBP-1 maturation and renal lipid accumulation leading to diabetic nephropathy (50). Moreover, ethanol, ER stress, shear stress, and cytokines have been reported to up-regulate the lipogenic gene expression in hepatocytes and/or vascular endothelial cells by activation of SREBPs (14, 49, 51–54).

Hyperglycemia, hyperlipidemia, elevated TNF-α, and increased oxidative stress have been linked to β-cell dysfunction in Type 2 diabetes (9, 55–63). We therefore studied the SREBP-1 maturation in native INS-1E cells, the most differentiated INS-1 cell clone (64). The cells were exposed for 48 h to 30 mM glucose, 100 nM insulin, 1.5 mM long-chain free fatty acids (2:1 oleate/palmitate), 10 ng/ml TNF-α, and 10 μM H_2O_2 (Fig. 7*C*). The mature nuclear form of SREBP-1 was detected in

INS-1E cells treated for 48 h with glucose, insulin, TNF-α, or H_2O_2 (Fig. 7*C*). In contrast, free fatty acids were without effects (Fig. 7*C*). The level of the mature form of SREBP-1 in INS-1E cells treated with high glucose for 48 h is ~10% of that of the endogenous precursor protein (Fig. 7*C*). This corresponds to the induction observed with 75 ng/ml doxycycline in naSREBP-1c#233 cells (Fig. 1*B*).

DISCUSSION

Intracellular lipid accumulation, termed lipotoxicity (metabolic syndrome X), in skeletal muscle, myocardium, blood vessels, kidney, liver, and pancreatic islets has been speculated to cause, respectively, insulin resistance, cardiac dysfunction, vascular complications, nephropathy, fatty liver (hepatic steatosis), and β-cell dysfunction in Type 2 diabetes (9, 50). However the molecular mechanism underlying the pathogenesis of lipotoxicity in pancreatic β-cells and other non-adipose tissues remains undefined. In fact, lipotoxicity is a confusing concept. Some investigators refer to lipotoxicity as the consequence of increased circulating free fatty acids and cellular lipid accumulation (7–9), whereas others suggest that glucotoxicity is the prerequisite for lipotoxicity, at least in β-cells (58, 59, 65–68). The present study and other observations[2] support the latter (see bellow). In creased expression of SREBP-1c has been demonstrated in islets and/or liver in several animal models of diabetes (7, 12–16). Overexpression of SREBP-1 has been suggested to be the cause of hepatic steatosis (14, 16, 51, 53, 69, 70) and diabetic nephropathy (50). The present study provides direct and strong evidence proving that the transcriptional activity of SREBP-1c also mediates β-cell dysfunction.

Conditional expression of naSREBP-1c, a nuclear localized N-terminal form of SREBP-1c with intact transcriptional activity, results in massive accumulation of lipid-droplets in INS-1 cells, a clonal β-cell line. This could be explained by marked increases in lipogenic gene expression and unaltered mRNA levels of genes involved in fatty acid β-oxidation. The lipogenic transcription factor naSREBP-1c also induces impairment of nutrient-induced insulin secretion, suggesting defective glucose metabolism. This could be caused by the down-regulation of glucokinase, up-regulation of UCP-2, and disrupted mitochondrial membrane potential observed in these INS-1 cells expressing naSREBP-1c. In addition, we also show that naSREBP-1c suppresses the expression of insulin, Pdx-1, and HNF-4α. Induction of naSREBP-1c also leads to INS-1 cell growth arrest and apoptosis possibly by both suppressing the expression of cyclin-dependent kinase 4 and IRS-2 and promoting the expression of $P21^{WAF1/CIP1}$, APO-1/Fas/CD95, and Bax. Since the SREBP-1c precursor is a known substrate for caspase 3, we postulate that SREBP-1c may function as a proapoptotic gene in β-cells. Similarly, lipid accumulation, impaired glucose-stimulated insulin secretion, defective β-cell gene expression (insulin, Pdx-1, glucokinase, and Glut-2), disorganized mitochondrial ultrastructure, and "lipoapoptosis" have been reported in islet β-cells of diabetic animals (7, 71–73). We have, therefore, not only established an *in vitro* cellular model for β-cell glucolipotoxicity but also elucidated the underlying mechanism.

In addition, the present study also suggests that, in contrast to hepatocytes and adipocytes, islet β-cells have evolved to limit the lipogenic gene expression in response to acute stimulation of glucose and insulin by restricting the SREBP-1c processing. Our data are in disagreement with a previous study, claiming that SREBP-1c maturation in MIN-6 cells is acutely regulated by glucose (18). Whereas 6 h of stimulation with glucose had no effect in the present study, we could indeed detect the mature form of SREBP-1c in INS-1E cells after 48 h of exposure to high concentrations of glucose or insulin. In contrast, 48 h of treatment with free fatty acids did not increase the levels of the active form of SREBP-1c. Glucotoxicity, a phenomenon occurring after prolonged exposure to high concentrations of glucose, has been reported to induce lipid accumulation in INS-1 cells by raising lipogenic gene expression (58). Our study may have established a link between glucotoxicity and lipotoxicity and provided an explanation for the predominant role of high glucose in β-cell dysfunction (59, 65). A similar effect may account for the increased apoptosis and subsequent decreased β-cell mass in Type 2 diabetic patients compared with obese subjects (27). We also found that a 48-h culture of INS-1E cells with 30 mM glucose caused cell apoptosis and defective gene expression similar to naSREBP-1c induction, whereas 72 h of incubation with 1.5 mM free fatty acids (2:1 oleate/palmitate) did not have such deleterious effects.[2] Therefore, naSREBP-1c may induce β-cell dysfunction independent of lipid accumulation. Hyperglycemia and hyperinsulinemia are characteristics of Type 2 diabetes. We hypothesize that as a result of the persistent hyperglycemia and hyperinsulinemia present in diabetes, SREBP-1c protein is processed and modified to an active form. Activated SREBP-1c alters the expression of various target genes that contribute to β-cell dysfunction and therefore exacerbates the progression of Type 2 diabetes. Furthermore, our results suggest that the SREBP-1c maturation regulated by cytokines and oxidative stress may also play a role in β-cell dysfunction in Type 2 diabetes. It should be noted that the present work was performed in a rat insulinoma cell line and therefore may not entirely reflect the situation in native β-cells, necessitating caution in the interpretation.

We hypothesize that SREBPs have evolved to allow animals adapting to starvation by mediating insulin action on energy storage and promoting cell survival by maintaining constant lipid composition of membranes. Overnutrition and sedentary life-style in industrialized modern society may lead to lipotoxicity in non-adipose tissue. The important contribution of our study is that the transcription factor SREBP-1c is instrumental in the pathogenesis of β-cell lipotoxicity by targeting multiple genes implicated in carbohydrate metabolism, lipid biosynthesis, cell growth, and apoptosis. Similar mechanisms may also apply to the lipotoxicity in other non-adipose tissues. Development of chemical compounds acting like leptin, PPARγ agonists, and metformin through suppression of SREBP-1c function should have therapeutic potential in the treatment of Type 2 diabetes and its complications.

Acknowledgments—We are grateful to D. Cornut-Harry, D. Nappey, Y. Dupré, S. Polti, and V. Calvo for expert technical assistance. We are indebted to Drs. B. M. Spiegelman (SREBP-1c/ADD1-(1–403) cDNA), H. Bujard (PUHD10–3 vector), and N. Quintrell (pTKhygro plasmid).

REFERENCES

1. Brown, M. S., and Goldstein, J. L. (1997) *Cell* **89,** 331–340
2. Tontonoz, P., Kim, J. B., Graves, R. A., and Spiegelman, B. M. (1993) *Mol. Cell. Biol.* **13,** 4753–4759
3. Horton, J. D., Goldstein, J. L., and Brown, M. S. (2002) *J. Clin. Invest.* **109,** 1125–1131
4. Kim, J. B., Sarraf, P., Wright, M., Yao, K. M., Mueller, E., Solanes, G., Lowell, B. B., and Spiegelman, B. M. (1998) *J. Clin. Invest.* **101,** 1–9
5. Foretz, M., Guichard, C., Ferre, P., and Foufelle, F. (1999) *Proc. Natl. Acad. Sci. U. S. A.* **96,** 12737–12742
6. Zimmet, P., Alberti, K. G., and Shaw, J. (2001) *Nature* **414,** 782–787
7. Unger, R. H., Zhou, Y. T., and Orci, L. (1999) *Proc. Natl. Acad. Sci. U. S. A.* **96,** 2327–2332
8. Friedman, J. (2002) *Nature* **415,** 268–269
9. Unger, R. H. (2002) *Annu. Rev. Med.* **53,** 319–336
10. Cavaghan, M. K., Ehrmann, D. A., and Polonsky, K. S. (2000) *J. Clin. Invest.* **106,** 329–333
11. Saltiel, A. R. (2000) *J. Clin. Invest.* **106,** 163–164
12. Kakuma, T., Lee, Y., Higa, M., Wang, Z., Pan, W., Shimomura, I., and Unger, R. H. (2000) *Proc. Natl. Acad. Sci. U. S. A.* **97,** 8536–8541
13. Shimomura, I., Hammer, R. E., Ikemoto, S., Brown, M. S., and Goldstein, J. L. (1999) *Nature* **401,** 73–76

[2] H. Wang and C. B. Wollheim, unpublished data.

14. Lin, H. Z., Yang, S. Q., Chuckaree, C., Kuhajda, F., Ronnet, G., and Diehl, A. M. (2000) *Nat. Med.* **6,** 998–1003
15. Tobe, K., Suzuki, R., Aoyama, M., Yamauchi, T., Kamon, J., Kubota, N., Terauchi, Y., Matsui, J., Akanuma, Y., Kimura, S., Tanaka, J., Abe, M., Ohsumi, J., Nagai, R., and Kadowaki, T. (2001) *J. Biol. Chem.* **276,** 38337–38340
16. Shimomura, I., Bashmakov, Y., and Horton, J. D. (1999) *J. Biol. Chem.* **274,** 30028–30032
17. Zhou, G., Myers, R., Li, Y., Chen, Y., Shen, X., Fenyk-Melody, J., Wu, M., Ventre, J., Doebber, T., Fujii, N., Musi, N., Hirshman, M. F., Goodyear, L. J., and Moller, D. E. (2001) *J. Clin. Invest.* **108,** 1167–1174
18. Andreolas, C., da Silva Xavier, G., Diraison, F., Zhao, C., Varadi, A., Lopez-Casillas, F., Ferre, P., Foufelle, F., and Rutter, G. A. (2002) *Diabetes* **51,** 2536–2545
19. Kim, J. B., and Spiegelman, B. M. (1996) *Genes Dev.* **10,** 1096–1107
20. Asfari, M., Janjic, D., Meda, P., Li, G., Halban, P. A., and Wollheim, C. B. (1992) *Endocrinology* **130,** 167–178
21. Gossen, M., Freundlieb, S., Bender, G., Muller, G., Hillen, W., and Bujard, H. (1995) *Science* **268,** 1766–1769
22. Wang, H., and Iynedjian, P. B. (1997) *Proc. Natl. Acad. Sci. U. S. A.* **94,** 4372–4377
23. Wang, H., Maechler, P., Ritz-Laser, B., Hagenfeldt, K. A., Ishihara, H., Philippe, J., and Wollheim, C. B. (2001) *J. Biol. Chem.* **276,** 25279–25286
24. Rubi, B., Ishihara, H., Hegardt, F. G., Wollheim, C. B., and Maechler, P. (2001) *J. Biol. Chem.* **276,** 36391–36396
25. Schreiber, E., Matthias, P., Muller, M. M., and Schaffner, W. (1988) *EMBO J.* **7,** 4221–4229
26. Wang, H., Maechler, P., Hagenfeldt, K. A., and Wollheim, C. B. (1998) *EMBO J.* **17,** 6701–6713
27. Butler, A. E., Janson, J., Bonner-Weir, S., Ritzel, R., Rizza, R. A., and Butler, P. C. (2003) *Diabetes* **52,** 102–110
28. Maechler, P., Kennedy, E. D., Pozzan, T., and Wollheim, C. B. (1997) *EMBO J.* **16,** 3833–3841
29. Yang, J., Liu, X., Bhalla, K., Kim, C. N., Ibrado, A. M., Cai, J., Peng, T. I., Jones, D. P., and Wang, X. (1997) *Science* **275,** 1129–1132
30. Wollheim, C. B. (2000) *Diabetologia* **43,** 265–277
31. Matschinsky, F. M. (1996) *Diabetes* **45,** 223–241
32. Magnuson, M. A., Andreone, T. L., Printz, R. L., Koch, S., and Granner, D. K. (1989) *Proc. Natl. Acad. Sci. U. S. A.* **86,** 4838–4842
33. Boss, O., Muzzin, P., and Giacobino, J. P. (1998) *Eur. J. Endocrinol.* **139,** 1–9
34. Lameloise, N., Muzzin, P., Prentki, M., and Assimacopoulos-Jeannet, F. (2001) *Diabetes* **50,** 803–809
35. Wang, H., Antinozzi, P. A., Hagenfeldt, K. A., Maechler, P., and Wollheim, C. B. (2000) *EMBO J.* **19,** 1–8
36. Zhang, C. Y., Baffy, G., Perret, P., Krauss, S., Peroni, O., Grujic, D., Hagen, T., Vidal-Puig, A. J., Boss, O., Kim, Y. B., Zheng, X. X., Wheeler, M. B., Shulman, G. I., Chan, C. B., and Lowell, B. B. (2001) *Cell* **105,** 745–755
37. Hengartner, M. O. (2000) *Nature* **407,** 770–776
38. Gross, A., McDonnell, J. M., and Korsmeyer, S. J. (1999) *Genes Dev.* **13,** 1899–1911
39. Vander Heiden, M. G., Chandel, N. S., Williamson, E. K., Schumacker, P. T., and Thompson, C. B. (1997) *Cell* **91,** 627–637
40. Rane, S. G., Dubus, P., Mettus, R. V., Galbreath, E. J., Boden, G., Reddy, E. P., and Barbacid, M. (1999) *Nat. Genet.* **22,** 44–52
41. Withers, D. J., Gutierrez, J. S., Towery, H., Burks, D. J., Ren, J. M., Previs, S., Zhang, Y., Bernal, D., Pons, S., Shulman, G. I., Bonner-Weir, S., and White, M. F. (1998) *Nature* **391,** 900–904
42. Wang, X., Zelenski, N. G., Yang, J., Sakai, J., Brown, M. S., and Goldstein, J. L. (1996) *EMBO J.* **15,** 1012–1020
43. Shimomura, I., Bashmakov, Y., Ikemoto, S., Horton, J. D., Brown, M. S., and Goldstein, J. L. (1999) *Proc. Natl. Acad. Sci. U. S. A.* **96,** 13656–13661
44. Streicher, R., Kotzka, J., Muller-Wieland, D., Siemeister, G., Munck, M., Avci, H., and Krone, W. (1996) *J. Biol. Chem.* **271,** 7128–7133
45. Kotzka, J., Muller-Wieland, D., Koponen, A., Njamen, D., Kremer, L., Roth, G., Munck, M., Knebel, B., and Krone, W. (1998) *Biochem. Biophys. Res. Commun.* **249,** 375–379
46. Kotzka, J., Muller-Wieland, D., Roth, G., Kremer, L., Munck, M., Schurmann, S., Knebel, B., and Krone, W. (2000) *J. Lipid Res.* **41,** 99–108
47. Roth, G., Kotzka, J., Kremer, L., Lehr, S., Lohaus, C., Meyer, H. E., Krone, W., and Muller-Wieland, D. (2000) *J. Biol. Chem.* **275,** 33302–33307
48. Muller-Wieland, D., and Kotzka, J. (2002) *Ann. N. Y. Acad. Sci.* **967,** 19–27
49. Diomede, L., Albani, D., Bianchi, M., and Salmona, M. (2001) *Eur. Cytokine Netw.* **12,** 625–630
50. Sun, L., Halaihel, N., Zhang, W., Rogers, T., and Levi, M. (2002) *J. Biol. Chem.* **277,** 18919–18927
51. Werstuck, G. H., Lentz, S. R., Dayal, S., Hossain, G. S., Sood, S. K., Shi, Y. Y., Zhou, J., Maeda, N., Krisans, S. K., Malinow, M. R., and Austin, R. C. (2001) *J. Clin. Invest.* **107,** 1263–1273
52. Lawler, J. F., Jr., Yin, M., Diehl, A. M., Roberts, E., and Chatterjee, S. (1998) *J. Biol. Chem.* **273,** 5053–5059
53. You, M., Fischer, M., Deeg, M. A., and Crabb, D. W. (2002) *J. Biol. Chem.* **277,** 29342–29347
54. Liu, Y., Chen, B. P., Lu, M., Zhu, Y., Stemerman, M. B., Chien, S., and Shyy, J. Y. (2002) *Arterioscler. Thromb. Vasc. Biol.* **22,** 76–81
55. Tanaka, Y., Tran, P. O., Harmon, J., and Robertson, R. P. (2002) *Proc. Natl. Acad. Sci. U. S. A.* **99,** 12363–12368
56. Jonas, J. C., Sharma, A., Hasenkamp, W., Ilkova, H., Patane, G., Laybutt, R., Bonner-Weir, S., and Weir, G. C. (1999) *J. Biol. Chem.* **274,** 14112–14121
57. Tanaka, Y., Gleason, C. E., Tran, P. O., Harmon, J. S., and Robertson, R. P. (1999) *Proc. Natl. Acad. Sci. U. S. A.* **96,** 10857–10862
58. Roche, E., Farfari, S., Witters, L. A., Assimacopoulos-Jeannet, F., Thumelin, S., Brun, T., Corkey, B. E., Saha, A. K., and Prentki, M. (1998) *Diabetes* **47,** 1086–1094
59. Poitout, V., and Robertson, R. P. (2002) *Endocrinology* **143,** 339–342
60. Newgard, C. B., and McGarry, J. D. (1995) *Annu. Rev. Biochem.* **64,** 689–719
61. Hostens, K., Pavlovic, D., Zambre, Y., Ling, Z., Van Schravendijk, C., Eizirik, D. L., and Pipeleers, D. G. (1999) *J. Clin. Invest.* **104,** 67–72
62. Greenberg, A. S., and McDaniel, M. L. (2002) *Eur. J. Clin. Invest.* **32,** 24–34
63. Maechler, P., Jornot, L., and Wollheim, C. B. (1999) *J. Biol. Chem.* **274,** 27905–27913
64. Maechler, P., and Wollheim, C. B. (1999) *Nature* **402,** 685–689
65. Harmon, J. S., Gleason, C. E., Tanaka, Y., Poitout, V., and Robertson, R. P. (2001) *Diabetes* **50,** 2481–2486
66. Weir, G. C. (1982) *Am. J. Med.* **73,** 461–464
67. Bonner-Weir, S., Trent, D. F., and Weir, G. C. (1983) *J. Clin. Invest.* **71,** 1544–1553
68. Weir, G. C., Laybutt, D. R., Kaneto, H., Bonner-Weir, S., and Sharma, A. (2001) *Diabetes* **50,** S154–S159
69. Shimano, H., Horton, J. D., Shimomura, I., Hammer, R. E., Brown, M. S., and Goldstein, J. L. (1997) *J. Clin. Invest.* **99,** 846–854
70. Shimano, H., Horton, J. D., Hammer, R. E., Shimomura, I., Brown, M. S., and Goldstein, J. L. (1996) *J. Clin. Invest.* **98,** 1575–1584
71. Unger, R. H., and Zhou, Y. T. (2001) *Diabetes* **50,** S118–S121
72. Wang, M. Y., Koyama, K., Shimabukuro, M., Mangelsdorf, D., Newgard, C. B., and Unger, R. H. (1998) *Proc. Natl. Acad. Sci. U. S. A.* **95,** 11921–11926
73. Zhou, Y. T., Shimabukuro, M., Lee, Y., Koyama, K., Higa, M., Ferguson, T., and Unger, R. H. (1998) *Diabetes* **47,** 1904–1908

Diabetes, October 2004

Alteration of the malonyl-CoA/carnitine palmitoyltransferase I interaction in the β cell impairs glucose-induced insulin secretion

Laura Herrero[1], Blanca Rubí[2], David Sebastián[1], Dolors Serra[1], Guillermina Asins[1], Pierre Maechler[2], Marc Prentki[3], and Fausto G. Hegardt[1]

Short running title: Fatty acid oxidation, malonyl-CoA and insulin secretion

[1]Department of Biochemistry and Molecular Biology, University of Barcelona, School of Pharmacy, Diagonal 643, E-08028 Barcelona, Spain; [2]Department of Cell Physiology and Metabolism, University Medical Centre, Michel Servet 1, 1211 Geneva-4, Switzerland; [3]Molecular Nutrition Unit, Department of Nutrition, University of Montreal and the Montreal Diabetes Research Center, 1560 Sherbrooke Est, Montreal H2L 4M1, Quebec, Canada.

Abbreviations used: LCPTI, liver carnitine palmitoyltransferase I; NEFA, non-esterified fatty acids; GSIS, glucose-stimulated insulin secretion; LC-CoA, long-chain fatty acyl-CoA; KRBH buffer, Krebs–Ringer Bicarbonate HEPES buffer; PKC, protein kinase C.

Address correspondence to:
Fausto G. Hegardt, Department of Biochemistry and Molecular Biology, School of Pharmacy, Diagonal 643, E-08028 Barcelona, Spain
Phone: +34 93 402 4523; Fax: +34 93 402 1896; E-mail: fgarciaheg@ub.edu

ABSTRACT

Carnitine palmitoyltransferase I, which is expressed in the pancreas as the liver isoform (LCPTI), catalyzes the rate-limiting step in the transport of fatty acids into the mitochondria for their oxidation. Malonyl-CoA derived from glucose metabolism regulates fatty acid oxidation by inhibiting LCPTI. To directly examine whether the availability of long-chain fatty acyl-CoA (LC-CoA) affects the regulation of insulin secretion in the β-cell and whether malonyl-CoA may act as a metabolic coupling factor in the β-cell, we infected INS(832/13) cells and rat islets with an adenovirus encoding a mutant form of LCPTI (Ad-LCPTI M593S) that is insensitive to malonyl-CoA. In Ad-LCPTI M593S infected INS(832/13) cells LCPTI activity increased six-fold. This was associated with enhanced fatty acid oxidation, at any glucose concentration, and a 60% suppression of glucose-stimulated insulin secretion (GSIS). In isolated rat islets in which LCPTI M593S was overexpressed, GSIS decreased 40%. The impairment of GSIS in Ad-LCPTI M593S infected INS(832/13) cells was not recovered when cells were incubated with 0.25 mM palmitate, indicating the deep metabolic influence of a non-regulated fatty acid oxidation system. At high glucose concentration, overexpression of a malonyl-CoA-insensitive form of LCPTI reduced partitioning of exogenous palmitate into lipid esterification products, and decreased PKC activation. Moreover, LCPTI M593S expression impaired K_{ATP} channel-independent GSIS in INS(832/13) cells. The LCPTI M593S mutant caused more pronounced alterations in GSIS and lipid partitioning (fat oxidation, esterification, the level of non-esterified palmitate) than LCPTI wt in INS(832/13) cells transduced with these constructs. The results provide direct support for the hypothesis proposing that the malonyl-CoA/CPTI interaction is a component of a metabolic signalling network that controls insulin secretion.

INTRODUCTION

Lipid metabolism in the ß-cell is critical for the regulation of insulin secretion (1, 2). Depletion of lipid stores together with deprivation of non-esterified fatty acids (NEFA) alters glucose-stimulated insulin secretion (GSIS) in rats and humans (3-5). NEFAs, presumably via long-chain fatty acyl-CoA (LC-CoA), generate signals for insulin secretion (6).

Stimulation of insulin secretion by glucose alters CoA derivatives levels in clonal pancreatic β-cells, in particular malonyl-CoA and LC-CoAs. The malonyl-CoA/LC-CoA model of GSIS holds that during glucose stimulation, anaplerosis increases citrate (7), which is exported and finally converted to malonyl-CoA, resulting in inhibition of carnitine palmitoyltransferase I (CPTI) (8) and fatty acid oxidation (6, 9). Therefore, the increase in malonyl-CoA may be responsible for the accumulation of LC-CoAs in the cytosol (10). Moreover, the β-cell LC-CoA content increases with the supplement of exogenous NEFA. In addition, glucose metabolism in the β–cell raises cytosolic LC-CoA levels, which in combination with α-glycerophosphate may increase the levels of triglycerides, phosphatidic acid and diacylglycerol (1). LC-CoA may act as coupling factors in insulin secretion by stimulating several isoforms of protein kinase C (11, 12), through acylation of exocytotic proteins or by generating complex lipid signalling molecules such as diacylglycerol and phosphatidate (1).

Both malonyl-CoA and LC-CoA are thought to participate in the signal transduction for insulin secretion: the former as a regulator and the latter as an effector (13). Systems that regulate both malonyl-CoA and LC-CoA appear to be involved in insulin secretion. Accordingly, acetyl-CoA carboxylase (ACC), which controls the synthesis of malonyl-CoA, malonyl-CoA decarboxylase (MCD), which catalyzes malonyl-CoA degradation, and CPTI which is regulated by malonyl-CoA, are components of a metabolic signalling network that senses the level of fuel stimuli (1, 8). The physiological role of malonyl-CoA in the endocrine pancreas, unlike many other tissues, is not *de novo* synthesis of fatty acids but rather the regulation of CPTI activity, since the level of fatty acid synthetase in normal β-cells is very low (14). The metabolism of several nutrients that converge to form malonyl-CoA and increase LC-CoA esters (carbohydrate, amino acids and ketoacids) might play a key role in fuel regulated-insulin secretion in the β-cell (2). Thus, for example, stable expression of an ACC-antisense construct in INS1 cells (15) or overexpression of MCD in rat insulinoma

INS(832/13) cells (16) decreased malonyl-CoA levels, increased LC-CoA oxidation and decreased insulin secretion.

The overexpression of native LCPTI in clonal INS-1E β-cells increased beta oxidation of fatty acids and decreased insulin secretion at high glucose (17). The effect of LCPTI was reverted by etomoxir, an irreversible inhibitor of CPTI, and by the exogenous addition of fatty acids. However, using this approach glucose-derived malonyl-CoA is still able to inhibit LCPTI in cells overexpressing the enzyme and consequently fat oxidation is moderately altered (17). To directly test the hypothesis that the CPTI/malonyl-CoA interaction is involved in GSIS we chose to overexpress LCPTI M593S, a mutant enzyme that is insensitive to malonyl-CoA (18). The LCPTI mutant and the native LCPTI were overexpressed in INS(832/13) cells and rat islets using recombinant adenoviruses.

INS(832/13) cells transduced with the M593S mutant had increased CPTI activity and protein levels, a markedly increased palmitate oxidation rate and a more impaired GSIS than cells transduced with LCPTI wt. At high glucose, esterification products and protein kinase C activation were decreased in cells expressing the mutated CPTI. Overall, the data provide direct support for the view that the malonyl-CoA/CPTI interaction is involved in glucose-regulated insulin secretion.

RESEARCH DESIGN AND METHODS

Materials. The collagenase used to isolate rat pancreatic islets was from Serva Electrophoresis (Heidelberg, Germany). Protran nitrocellulose membranes for protein analysis were from Schleicher & Schuell and the Bradford solution for protein assay was from Bio-Rad Laboratories. The enhanced chemifluorescence (ECF) reagent pack from Amersham Biosciences was used for Western blot analysis. TLC plates were purchased from Merck. Defatted bovine serum albumin (BSA), palmitic acid (sodium salt) and the migration standards phosphatidyl-serine, dipalmitoyl-glycerol, glyceryl tripalmitate and cholesteryl palmitate were from Sigma-Aldrich. Radioactive compounds, [1-^{14}C]palmitic acid, [U-^{14}C]glucose, [1-^{14}C]acetyl-CoA and L-[*methyl*-^{3}H]carnitine were from Amersham Biosciences.

Construction of recombinant adenoviruses. Ad-LCPTI wt encoding LCPTI wt was constructed as previously described (17). Ad-LacZ, which expresses bacterial β-galactosidase, was used as a control adenovirus. Ad-LCPTI M593S, encoding the malonyl-CoA-insensitive LCPTI M593S cDNA under the chicken actin (CA) promoter, was constructed using the Adenovirus Expression Vector Kit (Takara, Biomedicals). Briefly, blunt-ended LCPTI M593S cDNA (18) was subcloned into the cosmid pAdCA previously cut with *Swa*I and dephosphorylated. The resulting cosmid was packaged using the Gigapack III Plus Packaging Extract (Stratagene). The presence and right orientation of the insert were checked by restriction enzyme digestions using *Cla*I and *Bgl*II and the presence of the mutation by sequencing. The cosmid was cotransfected with DNA-TPC (adenovirus DNA of terminal protein complex) in a 10-cm dish with calcium phosphate (CellPhect, Amersham Pharmacia Biotech) in human embryonic kidney (HEK 293) cells (17). Cell lysate from selected viral clones was analyzed by Western Blot and probed with a LCPTI-specific antibody. The adenovirus was amplified, purified by CsCl ultracentrifugation and carefully titrated using the Adeno-X Rapid Titer kit (Clontech Laboratories, Inc.).

INS cell culture. The clonal β−cell line INS(832/13) (19), derived and selected from the parental rat insulinoma INS-1 (20) was cultured (passages 48-60) in a 5% CO_2 humidified atmosphere in complete medium composed of RPMI 1640 (Life Technologies, Inc) containing 11 mM glucose and supplemented with 10% (v/v) heat-inactivated fetal bovine serum (Wisent Inc, USA), 10 mM HEPES (pH 7.4), 2 mM glutamine, 1 mM sodium pyruvate, 50 μM 2-mercaptoethanol, 100 U/ml penicillin and 100 μg/ml streptomycin. The maintenance culture

was passaged once a week by gentle trypsinization, cells were seeded in Falcon dishes and medium was changed every 2-3 days.

Pancreatic islet isolation. Islets were prepared from male Wistar rats weighing 250–350 g by collagenase digestion and handpicking (21). At the end of the isolation step, islets were maintained in culture in regular RPMI 1640 medium containing 11 mM glucose supplemented with 10% (v/v) fetal bovine serum, 100 U/ml penicillin and 100 µg/ml streptomycin at 37ºC in a humidified atmosphere containing 5% CO_2.

Viral treatment. INS(832/13) cells were seeded in 12-well plates (0.5 x 10^6 cells/well), 25-cm^2 flasks (2 x 10^6 cells), 10-cm dishes (7 x 10^6 cells) or 15-cm dishes (10 x 10^6 cells) and cultured 48 h before infection. For infection cells were incubated for 90 min with complete RPMI medium containing 4.1 pfu/cell of Ad-LacZ, 1.7 pfu/cell of Ad-LCPTI wt or 4.1 pfu/cell of Ad-LCPTI M953S. Cells were cultured for 24 h before experiments to allow the transgenes to be expressed before initiating metabolic studies or measurements of insulin secretion. One day after the isolation, batches of 100-200 islets were infected in 1 ml of RPMI 1640 medium for 1 h with 10-150 x 10^4 pfu/islet (22) of the recombinant adenoviruses and further cultured for 24 h before experiments were performed. At these incubation times no toxicity effects were seen.

Western blot analysis. For detection of LCPTI protein, infected INS(832/13) cells or islets were resuspended directly in SDS sample buffer and sonicated. Proteins obtained from cell extracts were analyzed by SDS/PAGE (8% gels) and transferred onto nitrocellulose membranes using a Mini Trans-Blot Electrophoretic Cell according to the manufacturer's instructions (Bio-Rad). Immunoblots were developed by incubation with the LCPTI-specific polyclonal antibody against amino acids 317-430 of the rat liver CPTI (23) (1/6,000 dilution) and the anti-rabbit IgG alkaline phosphatase goat antibody (1/10,000 dilution). Detection was carried out with the enhanced chemifluorescence (ECF) immunoblotting detection system (Amersham Biosciences). For detection of PKC protein, cytosolic or membrane proteins of infected INS(832/13) cells were separated on an 8% SDS/PAGE gel and transferred to a nitrocellulose membrane as described above. Membranes were incubated with mouse anti-PKC monoclonal antibody (MC5, Santa Cruz Biotechnology, Santa Cruz, CA) (1/100 dilution) followed by incubation with an anti-mouse IgG + IgM alkaline phosphatase goat antibody (1/10,000 dilution). Antibody binding was visualized using the ECF system as described above

and band intensities were quantified using a Storm 840 Laser scanning system (Molecular dynamics, Amersham Pharmacia Biotech). Intensities of the spots were expressed as arbitrary optical units.

CPTI activity assay. INS(832/13) cells (10 x 10^6) were seeded in 15-cm dishes and cultured for 48 h prior to infection with the different adenoviruses. 24h later cells were pretreated as follows: cells were washed in Krebs-Ringer Bicarbonate HEPES buffer (KRBH buffer; 135 mM NaCl, 3.6 mM KCl, 0.5 mM NaH_2PO_4, 0.5 mM $MgSO_4$, 1.5 mM $CaCl_2$, 2 mM $NaHCO_3$ and 10 mM HEPES, pH 7.4) containing 0.1% (w/v) deffatted BSA, preincubated at 37ºC for 30 min in KRBH plus 1% BSA without glucose in the absence or presence of etomoxir at 200 µM and washed again in KRBH 0.1% BSA. Mitochondrion-enriched cell fractions were obtained as previously described (17). LCPTI was assayed in those preparations where the mitochondria remain largely intact. CPTI activity in 8 µg of protein was determined by the radiometric method as previously described (24) with minor modifications. The substrates were L-[*methyl*-^{3}H]carnitine and palmitoyl-CoA. Enzyme activity was assayed for 5 min at 30ºC in a total volume of 200 µl. For malonyl-CoA inhibition assays 8 µg of mitochondrion-enriched cell fractions were preincubated for 1 min at 30ºC with different amounts of malonyl-CoA prior to CPTI activity assay.

Fatty acid oxidation. Fatty acid oxidation to CO_2 and acid soluble products (ASP), essentially ketone bodies (25), were measured in INS(832/13) cells cultured in 25-cm^2 flasks. Cells were pretreated as described above and incubated for 2 h at 37ºC with fresh KRBH containing 2.5, 7.5 or 15 mM glucose in the presence of 0.8 mM carnitine plus 0.25 palmitate and 1 µCi/ml [1-^{14}C]palmitic acid complexed to 1% (w/v) BSA. Oxidation to CO_2 and ASP were measured as previously described (16).

Fatty acid esterification. Fatty acid esterification to complex lipids was measured in INS(832/13) cells cultured in 12-well plates and pretreated as described above. Cells were incubated for 2 h at 37ºC with fresh KRBH containing 2.5 or 15 mM glucose in the presence of 0.8 mM carnitine plus 0.25 palmitate and 1 µCi/ml [1-^{14}C]palmitic acid complexed to 1% (w/v) BSA. Cells were washed in cold PBS and lipids were extracted as described in (17). Total lipids dissolved in 30 µl of chloroform were separated by thin layer chromatography to measure the incorporation of labeled fatty acid into phospholipids (PL), diacylglycerol (DAG),

triacylglycerols (TG), non-esterified labeled palmitate (NE palm) and cholesterol esters (CE) as described before (16). Phosphatidyl-serine, dipalmitoyl-glycerol, glyceryl tripalmitate, cholesteryl palmitate and labeled control palmitate were used as migration references. Plates were developed with hexane:diethylether:acetic acid (70:30:1, v/v/v) as described before (26) and quantified with a Storm 840 Laser scanning system (Molecular dynamics, Amersham Pharmacia Biotech).

Triglyceride content. For the cellular triglyceride content measurement, INS(832/13) cells were cultured in 12-well plates and pretreated as described above. Total lipids were extracted as described in (17) and dissolved in 30 µl of chloroform. 10 µl of Thesit (Sigma-Aldrich) 20% (v/v) in chloroform were added, samples were air dried, dissolved in 50 µl of water and triglyceride content was measured with triolein as a standard using the Sigma 337 triacylglycerol kit.

Malonyl-CoA assay. INS(832/13) cells were cultured in 10-cm dishes and pretreated as described above. Cells were then incubated for 30 min at 37ºC with fresh KRBH containing 2.5 or 15 mM glucose. Malonyl-CoA was extracted as described in (27) and assayed with a radioenzymatic method (28) using [1-^{14}C] acetyl-CoA. The fatty acid synthetase required for the assay was isolated from rat liver as described in (29).

Insulin secretion. Insulin secretion was measured as previously described with minor changes (30). INS(832/13) cells (0.5 x 10^6) seeded in 12-well plates were pretreated as described above. Insulin secretion was measured during a 1 h incubation at 37ºC in 1 ml of KRBH 0.1% BSA in the presence of either 2.5 mM glucose, 15 mM glucose, 15 mM glucose plus 0.25 mM palmitate complexed to 1% (w/v) BSA or 2.5 mM glucose plus 30 mM KCl. After this time insulin content, obtained as described in (17), was determined by radioimmunoassay using rat insulin standards with the Coated Tube Insulin RIA kit (Insulin-CT, Schering).

For studies of K_{ATP} channel-independent insulin secretion, assays were performed as described above except that 35 mM KCl (depolarizing K^+) was included; consequently, the Na^+ concentration in the KRBH was reduced from 135 to 89.9 mM to maintain osmolarity, and 250 µM diazoxide was added.

Isolated rat islets were transduced with Ad-LCPTI wt, Ad-LCPTI M593S or Ad-LacZ and used after 24 h for insulin secretion experiments. Batches of 10 islets each were incubated for 30

min in KRBH 0.1% BSA containing 2.8 or 16.7 mM glucose. Insulin was determined by radioimmunoassay (30)

PKC translocation assay. INS(832/13) cells (7 x 10^6) seeded in 10-cm dishes were infected and pretreated as described above. To promote PKC translocation cells were incubated for 30 min at 37ºC in 2 ml of KRBH 0.1% BSA in the presence of 15 mM glucose. For the control situation, cells were incubated at low (2.5 mM) glucose. Then, cells were washed in cold PBS and used directly for preparation of membrane and cytosol fractions as described in (12). Western blot of membrane and cytosol proteins was performed using a specific antibody (MC5, Santa Cruz Biotechnology, Santa Cruz, CA) against the pancreatic β-cell isoforms of PKC (α, β and γ) as described above. Band intensities were assessed using a Storm 840 Laser scanning system.

Glucose oxidation. Glucose oxidation to CO_2 was measured in INS(832/13) cells cultured in 25-cm^2 flasks, infected and pretreated as described above. Cells were incubated for 2h at 37ºC with fresh KRBH 1% BSA containing 2.5 or 15 mM glucose in the presence of 0.5 μCi/ml [U-^{14}C]glucose. Oxidation to CO_2 was measured as previously described (16).

Statistical analysis. Data are expressed as means ± SE for at least four independent experiments performed in triplicate. Different experimental groups were compared with one-way ANOVA followed by Bonferroni's test for comparisons post hoc. A probability level of $P<0.05$ was considered to be statistically significant.

RESULTS

CPTI activity is not inhibited by malonyl-CoA in INS(832/13) cells expressing LCPTI M593S. In a previous study we documented a LCPTI M593S mutant which was insensitive to malonyl-CoA (18). The capacity of LCPTI M593S to show enzyme activity despite the presence of malonyl-CoA was evaluated in pancreatic β-cells. INS(832/13) cells were infected with Ad-LCPTI wt and Ad-LCPTI M593S. Mitochondrion-enriched fractions of cells were incubated with different amounts of malonyl-CoA and CPTI activity assay was performed. In the presence of malonyl-CoA (100 μM) mitochondrion-enriched fractions of cells infected with Ad-LCPTI M593S retained 80% of their activity while that of the LCPTI wt was almost completely inhibited (Fig. 1).

CPTI protein and activity in INS(832/13) cells infected with Ad-LCPTI wt and Ad-LCPTI M593S. INS(832/13) cells were infected with different amounts of Ad-LCPTI wt (Fig. 2A) and Ad-LCPTI M593S (Fig. 2B). CPTI activity assay was performed with mitochondrion-enriched cell fractions. In both cases CPTI activity increased to a plateau of 9-10 fold compared with the endogenous LCPTI, calculated from Ad-LacZ infected cells (5.0 ± 1.8 $nmol.mg^{-1}$ $prot.min^{-1}$, mean ± SE of 6 experiments). For subsequent experiments we used the amount of adenovirus LCPTI wt (1.7 pfu/cell) and LCPTI M593S (4.1 pfu/cell) that increased CPTI activity 6-fold (30 $nmol.\ mg^{-1}prot.\ min^{-1}$) with respect to the control Ad-LacZ. In an additional experiment, as a control, cells were also incubated for 30 min with or without 200 μM of etomoxir. This irreversible CPTI inhibitor blocked CPTI activity in Ad-LacZ and Ad-LCPTI wt infected cells, but left 65% CPTI activity in Ad-LCPTI M593S infected cells (Fig. 2C). LCPTI protein expression was measured by Western blot. Total protein was isolated from INS(832/13) cells infected with the amounts of adenoviruses that gave a 6-fold increase in CPTI activity. Consistent with the activity assays, Western blots showed similar amounts of protein in Ad-LCPTI wt and Ad-LCPTI M593S-infected cells (Fig. 2D) and fold increase over the control situation (Ad-LacZ). Similar results were obtained in Western blots performed with infected rat islets (Fig. 2E). Thus, expression of LCPTI wt and LCPTI M593S in the β-cell was successful in markedly increasing the protein and enzymatic activity of CPTI.

Effect of LCPTI M593S expression on palmitate oxidation in INS(832/13) cells. To evaluate the metabolic effects of the Ad-LCPTI wt and Ad-LCPTI M593S constructs we

measured fatty acid oxidation in pancreatic β-cells. [1-^{14}C]palmitate oxidation was determined in adenovirus-treated INS(832/13) cells. Fatty acid oxidation was highest in cells infected with Ad-LCPTI M593S at all tested glucose concentrations (Fig. 3). At high glucose (15 mM) fatty acid oxidation to CO_2, acid soluble products (ASP), and their sum were increased by 8.3, 3.4 and 4.4 fold respectively, compared with Ad-LacZ infected cells. These oxidation rates were higher than those obtained when overexpression was performed with Ad-LCPTI wt (3.3, 1.5 and 1.8 fold, respectively). Malonyl-CoA levels were not modified following LCPTI wt or LCPTI M593S overexpression, compared with LacZ control cells, either at 2.5 or 15 mM glucose (Fig. 4A). These findings confirm that even at high malonyl-CoA concentrations (high glucose), fatty acid oxidation in LCPTI M593S overexpressing cells is much higher than in the control Ad-LacZ adenovirus-infected cells and still higher than in cells infected with Ad-LCPTI wt. Since LCPTI M593 is resistant to malonyl-CoA, beta oxidation to CO_2 and ketone bodies (acid soluble compounds) is accelerated in cells overexpressing the mutated enzyme. Glucose oxidation at low (2.5 mM) and high (15 mM) glucose remained unaltered in cells expressing both the wt and mutated LCPTI constructs (Fig. 4B). This is in accordance with the view that a Randle cycle is inoperative in the β-cell (31).

GSIS is reduced in INS(832/13) cells and rat islets expressing LCPTI M593S. GSIS was reduced by 60% in INS(832/13) cells infected with Ad-LCPTI M593S and by 40% in Ad-LCPTI wt-infected cells, both with respect to the control Ad-LacZ (Fig. 5A). GSIS was recovered completely in the presence of 0.25 mM palmitate only in the case of LCPTI wt, suggesting that at high glucose, the provision of exogenous FFA was not matched with a rise in intracellular FFA (non esterified palmitate) in cells overexpressing the mutated enzyme due to the dramatically enhanced fatty acid oxidation. The results in Fig. 6D are in total accordance with this view.

As a control of the insulin secretion mechanism, incubation at low glucose in the presence of 30 mM KCl was performed and insulin release was similar in the three cases of adenovirus-infected cells indicating that the exocytotic machinery is preserved in cells transduced with the various constructs. Insulin secretion was also studied in the presence of 35 mM K^+ plus 250 μM diazoxide, a condition revealing the K_{ATP} channel-independent pathway of glucose sensing (32). The expression of LCPTI wt and LCPTI M593S led to a decrease in insulin release (the difference between 15 and 2.5 mM glucose) of 55 ± 12% and 85 ± 17% (n=3) respectively, compared with Ad-LacZ-infected cells. This is consistent with the view that

K_{ATP}-independent signalling (also referred as the amplification pathway) was affected in cells overexpressing the LCPTI construct (Fig. 5B).

Isolated rat islets infected with Ad-LCPTI wt or Ad-LCPTI M593S showed increased levels of LCPTI protein in Western blots analysis compared with Ad-LacZ-infected islets (Fig. 2C). In control islets, raising glucose from 2.8 mM to 16.7 mM resulted to a 6.8-fold insulin secretion. In islets overexpressing LCPTI M593S, GSIS was decreased by 40% compared to the Ad-LacZ control, while no difference was seen with Ad-LCPTI wt-infected islets (Fig. 5C). To explain the difference in the results between INS(832/13) cells and islets we hypothesize that normal β-cells are more protected than INS cells against lipid depletion due to enhanced fat oxidation, such that only the more efficient LCPTI M593S construct is active in rat islets.

Effect of LCPTI M593S on glucose-induced changes in lipid partitioning. To examine whether the increase in fatty acid oxidation could reduce the availability of LC-CoA for lipid signalling we measured esterification processes in INS(832/13) cells infected with Ad-LCPTI wt and Ad-LCPTI M593S. The levels of [1-^{14}C]palmitate incorporated to phospholipids (PL), diacylglycerol (DAG), triacylglycerides (TG), cholesterol esters (CE) as well as the levels of non-esterified palmitate (NE Palm) were measured. Glucose-induced palmitate esterification into the different complex lipid species was expressed as the differences (ΔG) between high (15 mM) and low (2.5 mM) glucose (Fig. 6). The glucose-induced rise in PL, DAG, TG and NE Palm was decreased by 20%, 25%, 35% and 38% respectively for Ad-LCPTI wt-infected cells and by 37%, 58%, 59% and 71% respectively, for Ad-LCPTI M593S-infected cells (Fig. 6 A, B, C, D), both compared to Ad-LacZ-infected cells. Palmitate esterification to CE was reduced by 23% and 50% for Ad-LCPTI wt and Ad-LCPTI M593S respectively at low glucose and by 42% and 60% for Ad-LCPTI wt and Ad-LCPTI M593S respectively at high glucose, compared to the Ad-LacZ control (Fig. 6E). Fig. 6D also shows that the glucose-induced rise in NE Palm, an indirect measurement of cytosolic LC-CoA (16), was markedly curtailed in cells expressing the LCPTI construct and that the CPTI mutant was most effective in this respect. Changes in the cellular TG content were not observed by the expression of LCPTI wt nor LCPTI M593S (Fig. 6F). This is probably due to the fact that differences in the incorporation of LC-CoA into TG are not reflected in the large and stable total TG pool.

PKC activation is impaired in INS(832/13) cells expressing LCPTI M593S. DAG and LC-CoA activate many PKC enzymes (11, 12). To assess whether the decrease of the glucose-induced rise in DAG and NE Palm seen in Ad-LCPTI wt and Ad-LCPTI M593S-infected cells

is associated with alteration in PKC activity in the β-cell, we measured PKC activation as estimated by its translocation from cytosol to membranes. Western blot carried out on membrane and cytosol proteins of INS(832/13) cells incubated at high (15 mM) glucose showed that PKC translocation of Ad-LCPTI wt and Ad-LCPTI M593S-infected cells was decreased by 63% and 78%, respectively, in comparison with Ad-LacZ-infected cells. No difference in the partitioning of PKC enzyme between the cytosolic and membrane compartments was noted in Ad-LacZ, Ad-LCPTI wt and Ad-LCPTI M593S-infected cells incubated at low glucose (2.5 mM) (Fig. 7).

DISCUSSION

Many studies implicate NEFAs in type II diabetes (33, 34). Long-term exposure of β-cells to NEFAs *in vitro* has several effects: 1) it increases basal insulin release and decreases secretion in response to glucose (35); 2) it alters the coupling of glucose metabolism to insulin secretion by acting on the expression of specific genes, such as UCP2 (36, 37); 3) it increases the expression of CPTI, which is considered the rate-limiting step in fatty acid oxidation (38). CPTI upregulation following chronic NEFA exposure of the β-cell may contribute to reduced GSIS. In an earlier study we evaluated the capacity of LCPTI wt overexpression to alter the insulin response to glucose in ß-cells (17). The results showed that overexpression of a cDNA encoding LCPTI using an adenovirus not only increased beta-oxidation in INS-1E cells but also decreased GSIS by 40%. In the search for a malonyl-CoA insensitive LCPTI we found that the M593S LCPTI mutant was almost completely refractory to malonyl-CoA (18). In view of the interest in the malonyl-CoA/LC-CoA model of GSIS, which is still under discussion (27, 39), we directly tested the hypothesis that the malonyl-CoA/CPTI interaction is implicated in GSIS using a β-cell derived cell line overexpressing the malonyl-CoA insensitive LCPTI. Since liver CPTI is the only isoform present in the β-cell, we used the rat liver isoform of CPTI to construct the adenovirus.

Overexpression of the malonyl-CoA-insensitive form of LCPTI increased fatty-acid oxidation rates in INS(832/13) at all glucose concentrations. Fat oxidation rates were much higher than in control Ad-LacZ-infected cells or in cells overexpressing malonyl-CoA-sensitive LCPTI wt. INS(832/13) cells overexpressing LCPTI M593S secreted less insulin in response to high glucose concentration (approximately 60% reduction) but not in response to a depolarizing concentration of KCl. Thus, exocytosis *per se* was preserved in cells overexpressing the mutated LCPTI, since the effect of the Ca^{2+} raising agent (30 mM KCl) was unaltered. The utilization of elevated K^+ and diazoxide to discern between the K_{ATP} channel-dependent and -independent pathways of glucose sensing showed that LCPTI M593S overexpression affected the K_{ATP}-independent pathway of GSIS, thus providing direct support for the view that the malonyl-CoA/CPTI interaction is involved in the amplification arm of secretion. In isolated rat islets, similar results were obtained, i.e. reduced secretory responses to high glucose upon LCPTI M593S expression. Interestingly, overexpression of LCPTI wt did not affect GSIS in islets, suggesting preserved lipid signalling above a critical threshold of cytosolic LC-CoA.

Incubation of LCPTI M593S transduced cells with 0.25 mM palmitate did not completely restore GSIS, showing the strong metabolic influence of LCPTI M593S on fatty acid oxidation and insulin secretion in the pancreatic β-cell. This points to a possible mechanism by which increased metabolic flux through LCPTI diminishes insulin secretion via the depletion of a critical lipid synthesized at or near the mitochondrial outer membrane that would act as a signal molecule.

It is interesting to compare the present results with those of Roduit et al. (16) who overexpressed malonyl-CoA decarboxylase (MCD) in the cytosol (MCDc) by infecting INS(832/13) cells and rat islets with an adenovirus containing the cDNA for MCD devoid of its mitochondrial and peroxysomal targeting sequences. The authors found that MCDc overexpression in the absence of exogenous FFA had no effect on GSIS and that MCDc overexpression suppressed the additional secretion in response to glucose provided by the presence of exogenous FFA (16). In the present study exogenous fatty acids had no effect on GSIS at 15 mM glucose, perhaps because we used a relatively low concentration of fatty acids (0.25 mM bound to 1% BSA) or possibly because lipolysis was higher in the current study. Nonetheless it is interesting to note that altering β-cell lipid partitioning with the malonyl-CoA-insensitive mutant of LCPTI had more profound consequence than with the overexpression of cytosolic MCD on both GSIS and lipid partitioning with more enhanced fat oxidation and reduced esterification processes at both low and elevated glucose. In other studies (27), the lack of correlation between malonyl-CoA levels and β-oxidation has been remarked on, suggesting that glucose might regulate cytosolic LC-CoA in a manner not entirely dependent of malonyl-CoA. Whatever is the explanation for the differences in alterations in GSIS in the absence or presence of exogenous FFA when MCDc (16) or CPTI (present study) are overexpressed, both studies show a reduction of GSIS when the malonyl-CoA/CPTI interaction is perturbed.

The data of the current study in cells overexpressing a malonyl-CoA insensitive CPTI together with previous results obtained in INS cells or islets overexpressing MCDc in the cytoplasm provide evidence that malonyl-CoA acts as a glucose-driven coupling factor that regulates the partitioning of fatty acids into effector molecules in the insulin secretory pathway. The nature of these molecules (NE palm, LC-CoA, PL and/or DAG) and their mechanisms of action on insulin secretion are poorly understood. Overexpression of LCPTI M593S altered lipid partitioning of exogenous palmitate from oxidation into esterification products at high glucose. The incorporation of palmitate into PL, DAG, TG, NE palm and CE were reduced

compared to controls. Determination of PKC translocation from cytosol to membrane showed that PKC activation in Ad-LCPTI wt and Ad-LCPTI M593S-infected cells was decreased compared with Ad-LacZ-infected cells. This suggests that enhanced beta oxidation of fatty acids by the LCPTI M593S mutant reduces GSIS as a result of a decrease in PKC activation. The lower values of DAG and NE Palm (an indirect determination of LC-CoA levels) observed in the LCPTI M593S-overexpressing cells support this view since both DAG and LC-CoA activate a number of PKC enzymes (11, 12).

In conclusion, this study shows directly for the first time that when the malonyl-CoA/CPTI interaction is altered glucose-induced insulin release is impaired. Together with the results obtained in previous studies in which MCDc was overexpressed (16) or ACC expression was reduced (15), the data point out to a critical role of the malonyl-CoA/CPTI metabolic signalling network in the coupling mechanism of insulin secretion. These results also favor the hypothesis that upregulation of CPTI (33) contributes to the early loss of glucose responsiveness seen in β-cells chronically exposed to high concentrations of fatty acids and provide direct support for the malonyl-CoA/LC-CoA model of fuel-induced insulin secretion.

ACKNOWLEDGMENTS

We thank Dr. Prip-Buus for supplying anti-rat liver CPTI antibody. This study was supported by Grants BMC2001-3048 from the Dirección General de Investigación Científica y Técnica, by grant C3/08 from the Fondo de Investigación Sanitaria of the Instituto de Salud Carlos III, Red de Centros RCMN from the Ministry of Health, Madrid, Spain, and by the Ajut de Suport als Grups de Recerca de Catalunya (2001SGR-00129), Spain. This work was also supported by grants to P.M. from the Swiss National Science Foundation and the Max Cloetta Foundation. L.H. and D.S. are recipients of fellowships from the Ministry of Education and Science, and the University of Barcelona, Spain, respectively. This work was supported by grants from the Canadian Institute of Health Research and the Juvenile Diabetes Research Foundation (to M.P.). We are also grateful to Robin Rycroft of the Language Service for valuable assistance in the preparation of the manuscript.

LEGENDS TO FIGURES

Fig.1. **CPTI activity of INS(832/13) cells infected with Ad-LCPTI M593S is insensitive to malonyl-CoA.** INS(832/13) cells were infected with Ad-LCPTI wt or Ad-LCPTI M593S and 24 h later CPTI activity assay was performed with 8 µg of mitochondrion-enriched cell fractions incubated with different amounts of malonyl-CoA. Data are the mean ± SE of 6 experiments.

Fig. 2. **CPTI activity and immunoblot analysis of LCPTI expressed in infected INS(832/13) cells and rat islets.** INS(832/13) cells were infected with different pfu/cell of Ad-LCPTI wt (**A**) or Ad-LCPTI M593S (**B**), 24 h later mitochondrion-enriched cell fractions were obtained and 8 µg of protein were used for the CPTI activity assay. The amount of both viruses which increased CPTI activity 6-fold, compared with Ad-LacZ (0 pfu/cell), were chosen for further experiments (1.7 pfu/cell for Ad-LCPTI wt and 4.1 pfu/cell for Ad-LCPTI M593S). Insert: expanded dose-response curve. (**C**) INS(832/13) cells infected with Ad-LacZ, Ad-LCPTI wt or Ad-LCPTI M593S were incubated for 30 min in KRBH 1% BSA with or without etomoxir (200 µM). After that, mitochondrion-enriched cell fractions were obtained and CPTI activity assay was performed. (**D**) INS(832/13) cells infected with Ad-LacZ, Ad-LCPTI wt or Ad-LCPTI M593S were collected and protein extracts were separated by SDS/PAGE (8% gels) and subjected to immunoblotting by using specific antibodies for CPTI from liver. A unique band corresponding to a protein of approx. 88 kDa was seen in control, Ad-LCPTI wt and Ad-LCPTI M593S infected cells. (**E**) Rat islets (batches of 100-200) were infected with the different adenoviruses as described in RESEARCH DESIGN AND METHODS and 24 h later LCPTI protein expression was determined by Western blot. Data in A, B and C are the mean ± SE of 4 experiments. *P<0.05 *vs* Ad-LCPTI M593S without etomoxir; **P<0.001 *vs* Ad-LacZ.

Fig.3. **Fatty acid oxidation is increased in INS(832/13) cells expressing LCPTI M593S.** INS(832/13) were infected with Ad-LacZ, Ad-LCPTI wt or Ad-LCPTI M593S. 24 h after viral treatment cells were preincubated for 30 min at 37ºC in KRBH medium containing 1% BSA and then incubated for 2 h at 2.5, 7.5 or 15 mM glucose in the presence of 0.8 mM carnitine, 1 µCi/ml [1-^{14}C]-palmitic acid and 0.25 mM unlabeled palmitate complexed to 1% (w/v) BSA. Palmitate oxidation to CO_2 (**A**), acid soluble products (ASP) (**B**), and total palmitate oxidation

(CO_2 + ASP) (**C**) was measured as described in RESEARCH DESIGN AND METHODS. Data are the mean ± SE of 5 experiments. *P<0.05 *vs* Ad-LacZ; #P<0.05 *vs* Ad-LCPTI wt.

Fig. 4. **Malonyl-CoA content and glucose oxidation are unaltered in INS(832/13) cells expressing LCPTI M593S.** INS(832/13) cells were infected with Ad-LacZ, Ad-LCPTI wt or Ad-LCPTI M593S and 24 h later, they were preincubated for 30 min at 37ºC in KRBH medium containing 1% BSA. (**A**) For the malonyl-CoA content measurements, cells were incubated for 30 min with KRBH containing 2.5 or 15 mM glucose and malonyl-CoA was extracted and assayed with a radioactive method using purified fatty acid synthetase as detailed in RESEARCH DESIGN AND METHODS. (**B**) Glucose oxidation to CO_2 was measured after a 2 h incubation of the cells at 2.5 or 15 mM glucose in the presence of 0.5 µCi/ml [U-^{14}C]-glucose as described in RESEARCH DESIGN AND METHODS. Data are the mean ± SE of 4 experiments. *P<0.05 *vs* 2.5 mM glucose.

Fig. 5. **Glucose-induced insulin release is impaired in INS(832/13) cells and in isolated rat islets expressing LCPTI M593S.** INS(832/13) cells or rat islets were infected with Ad-LacZ, Ad-LCPTI wt or Ad-LCPTI M593S as detailed in RESEARCH DESIGN AND METHODS. (**A**) After a 30 min preincubation in KRBH 1% BSA without glucose, INS(832/13) cells were washed and incubated for 1 h in KRBH 0.1% BSA containing either 2.5, 15 mM glucose, 15 mM glucose plus 0.25 mM palmitate complexed to 1% (w/v) BSA or 2.5 mM glucose plus 30 mM KCl. Insulin release was determined by RIA. (**B**) Experiments conducted in the presence of depolarizing K^+ (35 mM) and 250 µM diazoxide to measure K_{ATP} channel-independent glucose sensing. (**C**) Batches of 10 islets each were washed and incubated for 30 min in KRBH 0.1% BSA containing 2.8 or 16.7 mM glucose and insulin release was determined by RIA. Data are the mean ± SE of 4 experiments. *P<0.05 *vs* Ad-LacZ and #P<0.05 *vs* Ad-LCPTI wt.

Fig. 6. **Glucose-induced fatty acid esterification processes are reduced in INS(832/13) cells expressing LCPTI.** INS(832/13) infected with Ad-LacZ, Ad-LCPTI wt or Ad-LCPTI M593S were preincubated for 30 min at 37ºC in KRBH medium containing 1% BSA and then incubated for 2 h at 2.5 or 15 mM glucose in the presence of 0.8 mM carnitine, 1 µCi/ml [1-^{14}C]-palmitic acid and 0.25 mM unlabeled palmitate complexed to 1% (w/v) BSA. Fatty acid esterification into phospholipids (**A**), diacylglycerol (**B**), triglyceride (**C**), non-esterified palmitate (**D**) and cholesterol esters (**E**) were assessed using thin layer chromatography after

lipid extraction. ΔG is the difference between the incorporation of palmitate in the particular lipid classes at 15 mM *vs* 2.5 mM glucose. (**F**) total triglyceride content. Data are the mean ± SE of 4 experiments. *P<0.05 *vs* Ad-LacZ.

Fig. 7. **PKC activation is impaired in Ad-LCPTI wt and Ad-LCPTI M593S-infected cells.** Ad-LacZ, Ad-LCPTI wt and Ad-LCPTI M593S INS(832/13)-infected cells were incubated for 30 min at low (2.5 mM) (**A**) or high (15 mM) (**B**) glucose. Western blot of membrane (M) and cytosolic (C) fractions was performed using a specific antibody against the PKC isoforms expressed in pancreatic β-cells (α, β and γ) giving a unique band of 80 KDa. The intensity of the PKC bands were quantified using a Laser scanning system. The lower panels in A and B show mean results ± SE of 3 experiments. (A.U.; arbitrary optical units). *P<0.05 *vs* Ad-LacZ.

REFERENCES

1. Prentki M, Corkey BE: Are the β-cell signaling molecules malonyl-CoA and cytosolic long-chain acyl-CoA implicated in multiple tissue defects of obesity and NIDDM? *Diabetes* 45: 273-283, 1996
2. Yaney GC, Corkey BE: Fatty acid metabolism and insulin secretion in pancreatic beta cells. *Diabetologia* 46:1297-1312, 2003
3. Stein DT, Esser V, Stevenson BE, Lane KE, Whiteside JH, Daniels MB, Chen S, McGarry JD: Essentiality of circulating fatty acids for glucose-stimulated insulin secretion in the fasted rat. *J. Clin. Invest.* 97:2728-2735, 1996
4. Dobbins RL, Chester MW, Daniels MB, McGarry JD, Stein DT: Circulating fatty acids are essential for efficient glucose-stimulated insulin secretion after prolonged fasting in humans. *Diabetes* 47:1613-1618, 1998
5. Koyama K, Chen G, Wang MY, Lee Y, Shimabukuro M, Newgard CB, Unger RH: β-cell function in normal rats made chronically hyperleptinemic by adenovirus-leptin gene therapy. *Diabetes* 46:1276-1280, 1997
6. Prentki M, Vischer S, Glennon MC, Regazzi R, Deeney JT, Corkey BE: Malonyl-CoA and long chain acyl-CoA esters as metabolic coupling factors in nutrient-induced insulin secretion. *J. Biol. Chem.* 267:5802-5810, 1992
7. Schuit F, De Vos A, Farfari S, Moens K, Pipeleers D, Brun T and Prentki M: Metabolic fate of glucose in purified islet cells. Glucose-regulated anaplerosis in β cells. *J. Biol. Chem.* 272:18572-18579, 1997
8. McGarry JD, Brown NF: The mitochondrial carnitine palmitoyltransferase system. From concept to molecular analysis. *Eur. J. Biochem.* 244:1-14, 1997
9. Corkey BE, Glennon MC, Chen KS, Deeney JT, Matschinsky FM, Prentki M: A role for malonyl-CoA in glucose-stimulated insulin secretion from clonal pancreatic β-cells. *J. Biol. Chem.* 264:21608-21612, 1989
10. Liang Y, Matschinsky FM: Content of CoA-esters in perifused rat islets stimulated by glucose and other fuels. *Diabetes* 40:327-333, 1991
11. Yaney GC, Korchak HM, Corkey BE: Long-chain acyl-CoA regulation of protein kinase C and fatty acid potentiation of glucose-stimulated insulin secretion. *Endocrinology* 141:1989-1998, 2000
12. Alcázar O, Qiu-yue Z, Giné E, Tamarit-Rodriguez J: Stimulation of islet protein kinase C translocation by palmitate requires metabolism of the fatty acid. *Diabetes* 46:1153-1158, 1997
13. Corkey BE, Deeney JT, Yaney GC, Torheim, Prentki M: The role of long-chain fatty acyl-CoA esters in β-cell signal transduction. *J. Nutr.* 130:299S-304S, 2000
14. Brun T, Roche E, Assimacopoulos-Jeannet F, Corkey B, Kim KH, Prentki M: Evidence for an anaplerotic/malonyl-CoA pathway in pancreatic β-cell nutrient signaling. *Diabetes* 45:190-198, 1996
15. Zhang S, Kim K H: Essential role of acetyl-CoA carboxylase in the glucose-induced insulin secretion in a β-cell line. *Cell Signal.* 10:35-42, 1998
16. Roduit R, Nolan C, Alarcon C, Moore P, Barbeau A, Delghingaro-Augusto V, Przybykowski E, Morin J, Masse F, Massie B, Ruderman N, Rhodes C, Poitout V, Prentki M: A Role for the Malonyl-CoA/Long-Chain Acyl-CoA Pathway of Lipid Signaling in the Regulation of Insulin Secretion in Response to Both Fuel and Nonfuel Stimuli. *Diabetes* 53:1007-1019, 2004
17. Rubi B, Antinozzi PA, Herrero L, Ishihara H, Asins G, Serra D, Wollheim CB, Maechler P, Hegardt FG: Adenovirus-mediated overexpression of liver carnitine palmitoyltransferase I

in INS1E cells: effects on cell metabolism and insulin secretion. *Biochem. J.* 364:219-226, 2002
18. Morillas M, Gomez-Puertas P, Bentebibel A, Selles E, Casals N, Valencia A, Hegardt FG, Asins G, Serra D: Identification of conserved amino acid residues in rat liver carnitine palmitoyltransferase I critical for malonyl-CoA inhibition. Mutation of methionine 593 abolishes malonyl-CoA inhibition. *J. Biol. Chem*. 278:9058-9063, 2003
19. Hohmeier HE, Mulder H, Chen G, Henkel-Rieger R, Prentki M, Newgard CB: Isolation of INS-1-derived cell lines with robust ATP-sensitive K+ channel-dependent and -independent glucose-stimulated insulin secretion. *Diabetes* 49:424-430, 2000
20. Asfari M, Janjic D, Meda P, Li G, Halban PA, Wollheim CB: Establishment of 2-mercaptoethanol-dependent differentiated insulin-secreting cell lines. *Endocrinology* 130:167-178, 1992
21. Gotoh M, Maki T, Satomi S, Porter J, Bonner-Weir S, O'Hara Cj, Monaco AP: Reproducible high yield of rat islets by stationary in vitro digestion following pancreatic ductal or portal venous collagenase injection. *Transplantation* 43:725-730, 1987
22. Baetens D, Malaisse-Lagae F, Perrelet A, Orci L: Endocrine pancreas: three-dimensional reconstruction shows two types of islets of langerhans. *Science* 206:1323-1325, 1979
23. Prip-Buus C, Cohen I, Kohl C, Esser V, McGarry JD, Girard J: Topological and functional analysis of the rat liver carnitine palmitoyltransferase 1 expressed in Saccharomyces cerevisiae. *FEBS Lett.* 429:173-178, 1998
24. Morillas M, Clotet J, Rubi B, Serra D, Asins G, Arino J, Hegardt FG: Identification of the two histidine residues responsible for the inhibition by malonyl-CoA in peroxisomal carnitine octanoyltransferase from rat liver. *FEBS Lett*. 466:183-186, 2000
25. Fulgencio JP, Kohl C, Girard J, Pegorier JP: Troglitazone inhibits fatty acid oxidation and esterification, and gluconeogenesis in isolated hepatocytes from starved rats. *Diabetes* 45:1556-1562, 1996
26. Montell E, Turini M, Marotta M, Roberts M, Noé V, Ciudad CJ, Macé K, Gómez-Foix AM: DAG accumulation from saturated fatty acids desensitizes insulin stimulation of glucose uptake in muscle cells. *Am. J. Physiol. Endocrinol. Metab.* 280:E229-E237, 2001
27. Mulder H, Lu D, Finley IV J, An J, Cohen J, Antinozzi PA, McGarry JD, Newgard CB: Overexpression of a modified human malonyl-CoA decarboxylase blocks the glucose-induced increase in malonyl-CoA level but has no impact on insulin secretion in INS-1-derived (832/13) β-cells. *J. Biol. Chem*. 276: 6479-6484, 2001
28. McGarry JD, Stark MJ, Foster DW: Hepatic malonyl-CoA levels of fed, fasted and diabetic rats as measured using a simple radioisotopic assay. *J. Biol. Chem.* 253:8291-8293, 1978
29. Linn TC: Purification and crystallization of rat liver fatty acid synthetase. *Arch. Biochem. Biophys.* 209:613-619, 1981
30. Rubi B, Ishihara H, Hegardt FG, Wollheim CB, Maechler P: GAD65-mediated glutamate decarboxylation reduces glucose-stimulated insulin secretion in pancreatic beta cells. *J. Biol. Chem*. 276: 36391-36396, 2001
31. Segall L, Lameloise N, Assimacopoulos-Jeannet F, Roche E, Corkey P, Thumelin S, Corkey BE, Prentki M: Lipid rather than glucose metabolism is implicated in altered insulin secretion caused by oleate in INS-1 cells. *Am. J. Physiol.* 277:E521-528, 1999
32. Henquin JC: Triggering and amplifying pathways of regulation of insulin secretion by glucose. *Diabetes*. 49:1751-1769, 2000
33. Unger RH: Lipotoxicity in the pathogenesis of obesity-dependent NIDDM. Genetic and clinical implications. *Diabetes* 44:863-870, 1995
34. McGarry JD: Dysregulation of fatty acid metabolism in the etiology of type 2 diabetes. *Diabetes* 51:7-18, 2002

35. Zhou YP, Grill V: Long-term exposure of rat pancreatic islets to fatty acids inhibits glucose-induced insulin secretion and biosynthesis through a glucose fatty acid cycle. *J. Clin. Invest.* 93:870-876, 1994
36. Lameloise N, Muzzin P, Prentki M, Assimacopoulos-Jeannet F: Uncoupling protein 2: a possible link between fatty acid excess and impaired glucose-induced insulin secretion? *Diabetes* 50:803-809, 2001
37. Zhang CY, Baffy G, Perret P, Krauss S, Peroni O, Grujic D, Hagen T, Vidal-Puig AJ, Boss O, Kim YB, Zheng XX, Wheeler MB, Shulman GI, Chan CB, Lowell BB: Uncoupling protein-2 negatively regulates insulin secretion and is a major link between obesity, beta cell dysfunction and type 2 diabetes. *Cell* 105:745-755, 2001
38. Assimacopoulos-Jeannet F, Thumelin S, Roche E, Esser V, McGarry JD, Prentki M: Fatty acids rapidly induce the carnitine palmitoyltransferase I gene in the pancreatic β-cell line INS1. *J. Biol. Chem*. 272:1659-1664, 1997
39. Boucher A, Lu D, Burgess SC, Telemaque-Potts S, Jensen MV, Mulder H, Wang MY, Unger RH, Sherry AD, Newgard CB: Biochemical mechanism of lipid-induced impairment of glucose-stimulated insulin secretion and reversal with a malate analogue. *J. Biol. Chem*. 279:27263-27271, 2004

Final word count: 7,436

Figure 1

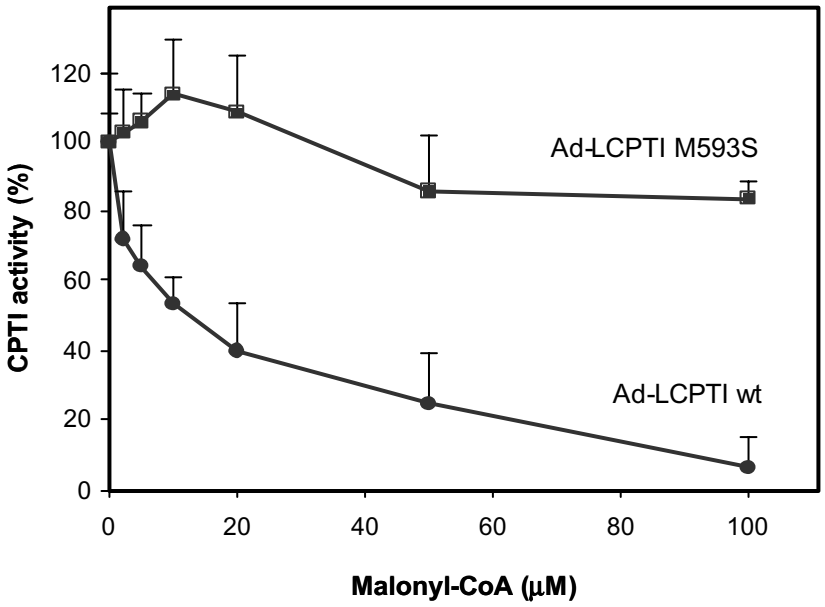
CPTI activity (%)
120
100
80
60
40
20
0
0
20
40
60
80
100
Malonyl-CoA (μM)
Ad-LCPTI M593S
Ad-LCPTI wt

Figure 2

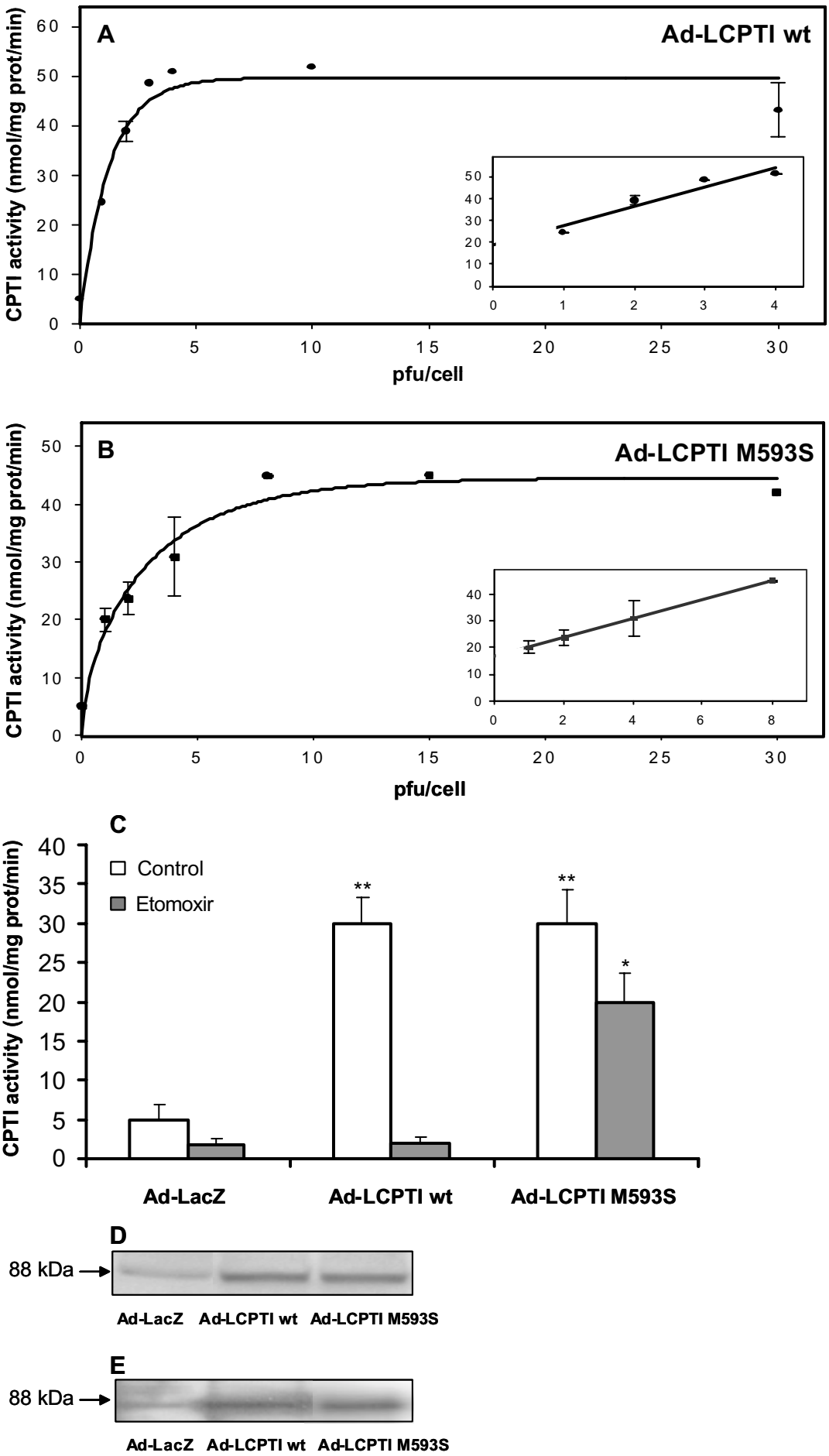
A
Ad-LCPTI wt
CPTI activity (nmol/mg prot/min)
pfu/cell
B
Ad-LCPTI M593S
CPTI activity (nmol/mg prot/min)
pfu/cell
C
Control
Etomoxir
CPTI activity (nmol/mg prot/min)
**
**
*
Ad-LacZ
Ad-LCPTI wt
Ad-LCPTI M593S
D
88 kDa
Ad-LacZ
Ad-LCPTI wt
Ad-LCPTI M593S
E
88 kDa
Ad-LacZ
Ad-LCPTI wt
Ad-LCPTI M593S

Figure 3

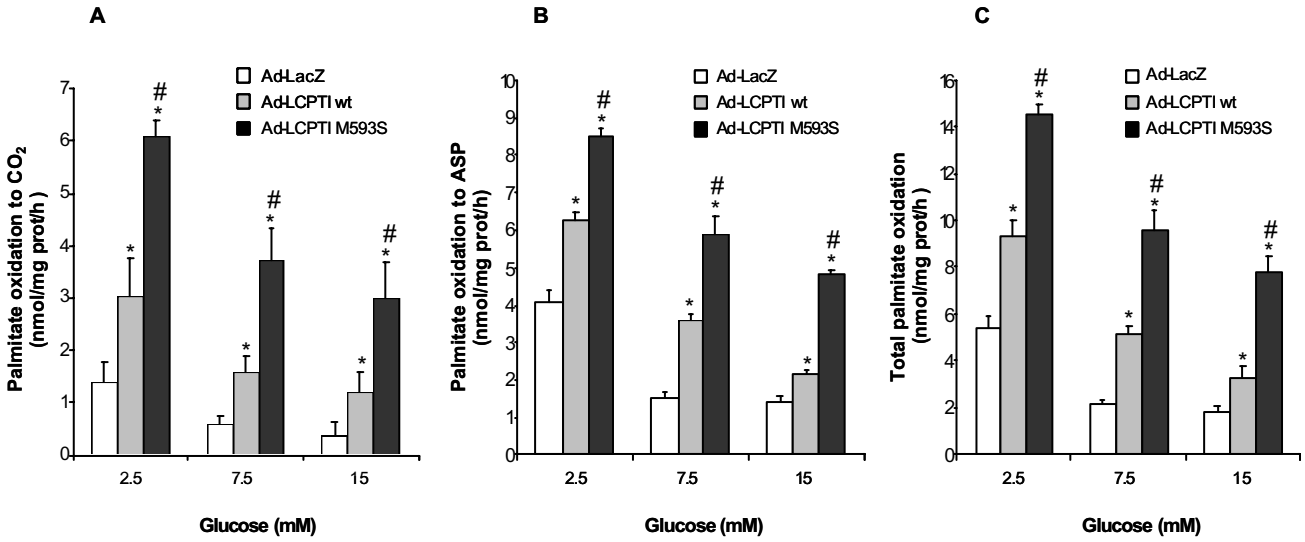
A
B
C
Ad-LacZ
Ad-LCPTI wt
Ad-LCPTI M593S
Palmitate oxidation to CO_2 (nmol/mg prot/h)
Palmitate oxidation to ASP (nmol/mg prot/h)
Total palmitate oxidation (nmol/mg prot/h)
2.5
7.5
15
Glucose (mM)

Figure 4

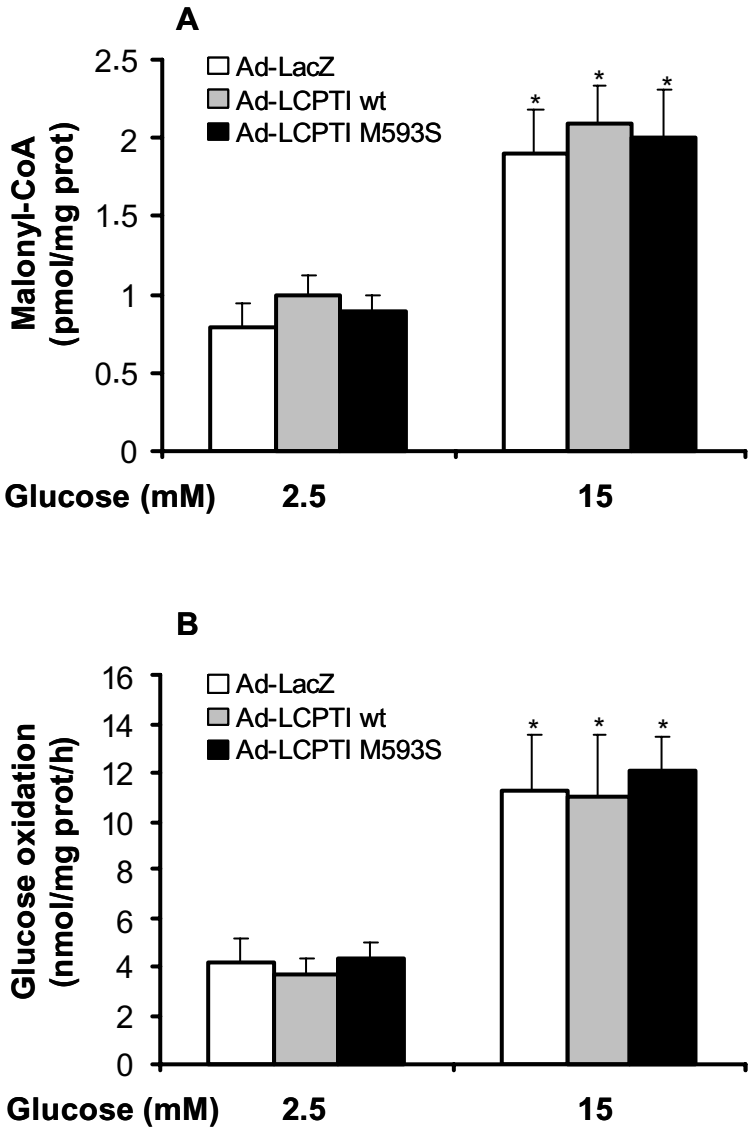
A
Ad-LacZ
Ad-LCPTI wt
Ad-LCPTI M593S
Malonyl-CoA (pmol/mg prot)
2.5
2
1.5
1
0.5
0
*
*
*
Glucose (mM)
2.5
15
B
Ad-LacZ
Ad-LCPTI wt
Ad-LCPTI M593S
Glucose oxidation (nmol/mg prot/h)
16
14
12
10
8
6
4
2
0
*
*
*
Glucose (mM)
2.5
15

Figure 5

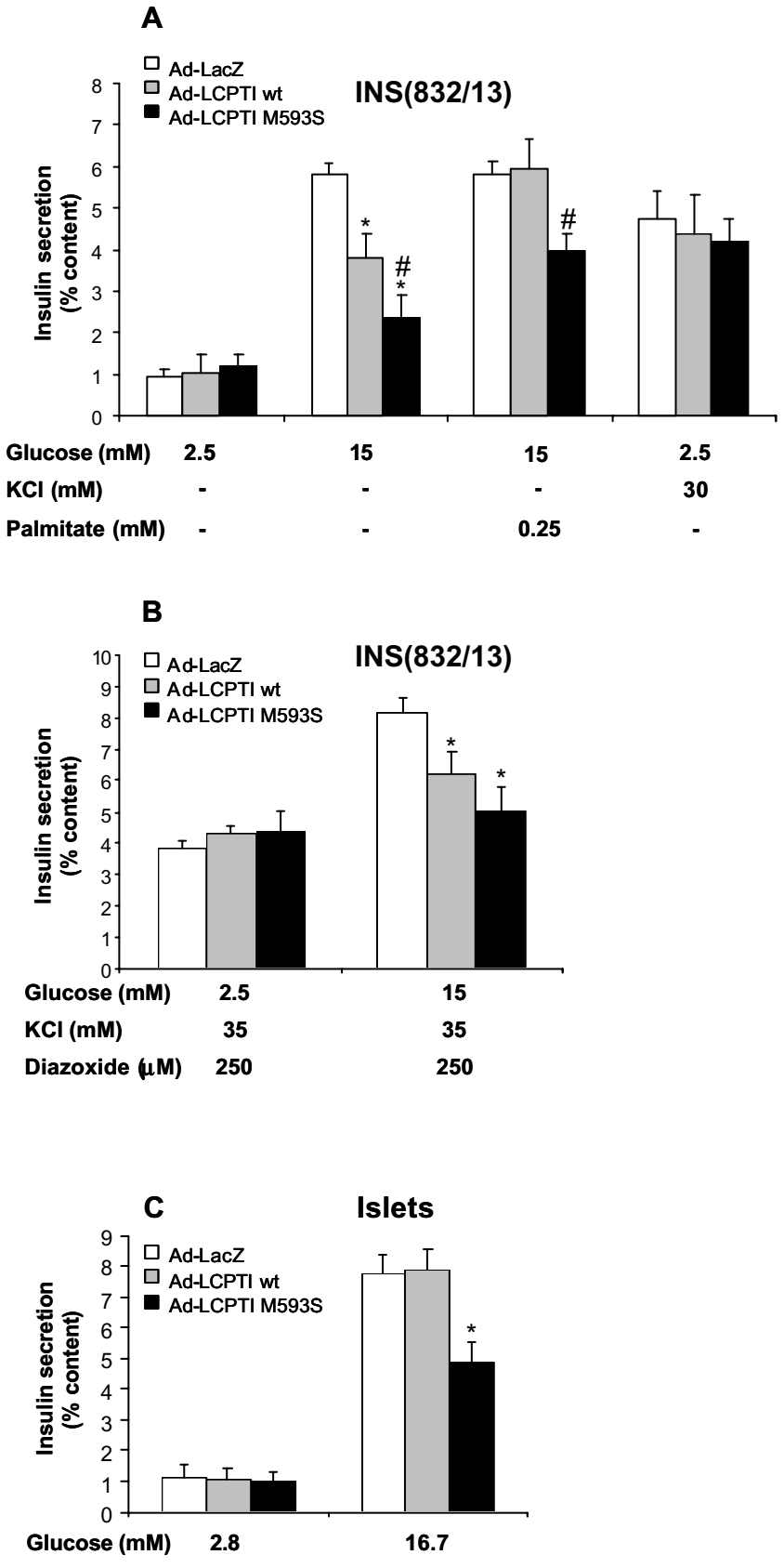
A
Ad-LacZ
Ad-LCPTI wt
Ad-LCPTI M593S
INS(832/13)
Insulin secretion (% content)
Glucose (mM) 2.5 15 15 2.5
KCl (mM) - - - 30
Palmitate (mM) - - 0.25 -
B
INS(832/13)
Ad-LacZ
Ad-LCPTI wt
Ad-LCPTI M593S
Insulin secretion (% content)
Glucose (mM) 2.5 15
KCl (mM) 35 35
Diazoxide (μM) 250 250
C
Islets
Ad-LacZ
Ad-LCPTI wt
Ad-LCPTI M593S
Insulin secretion (% content)
Glucose (mM) 2.8 16.7

Figure 6

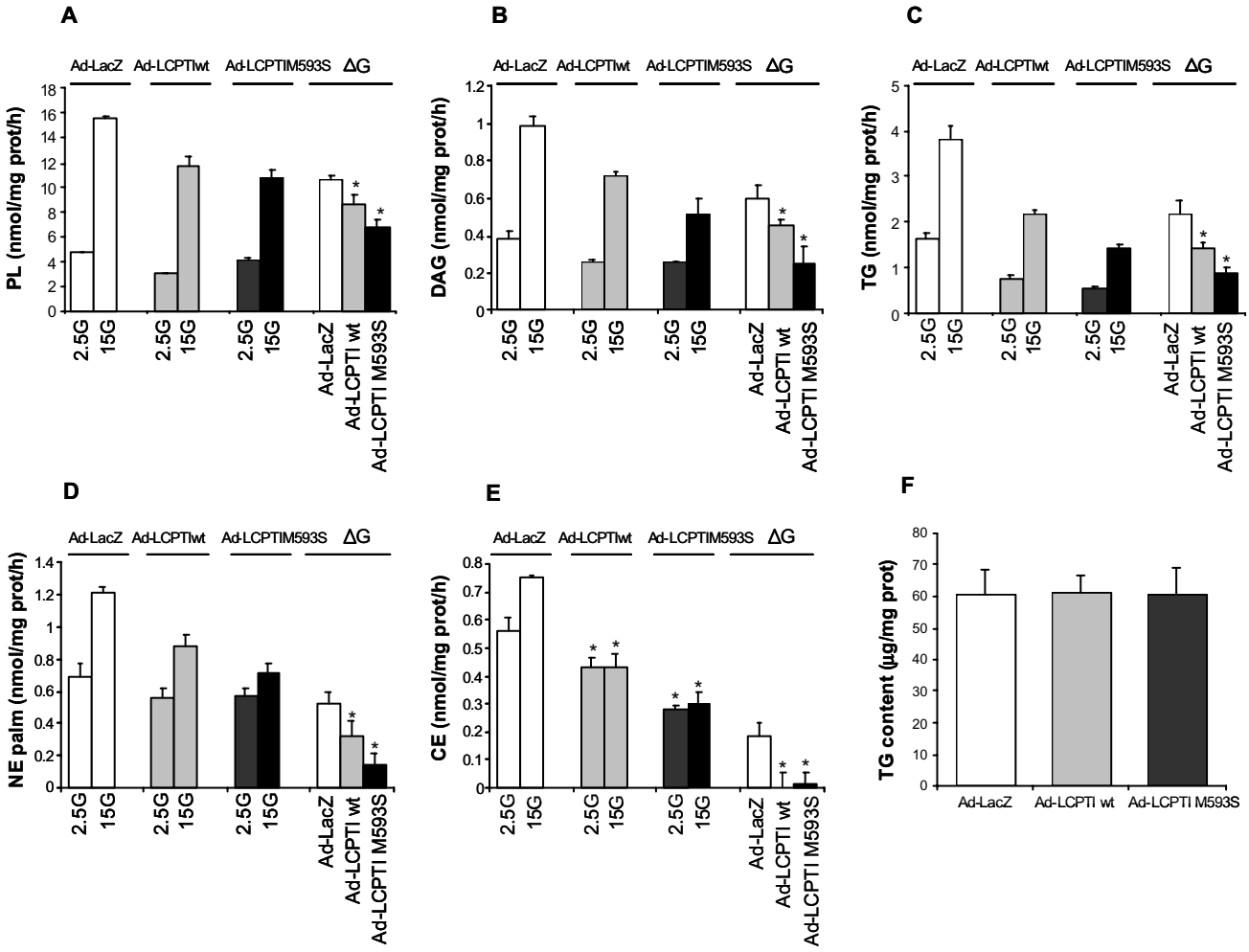
A
Ad-LacZ
Ad-LCPTIwt
Ad-LCPTIM593S
ΔG
PL (nmol/mg prot/h)
2.5G
15G
Ad-LacZ
Ad-LCPTI wt
Ad-LCPTI M593S
B
DAG (nmol/mg prot/h)
C
TG (nmol/mg prot/h)
D
NE palm (nmol/mg prot/h)
E
CE (nmol/mg prot/h)
F
TG content (µg/mg prot)

Figure 7

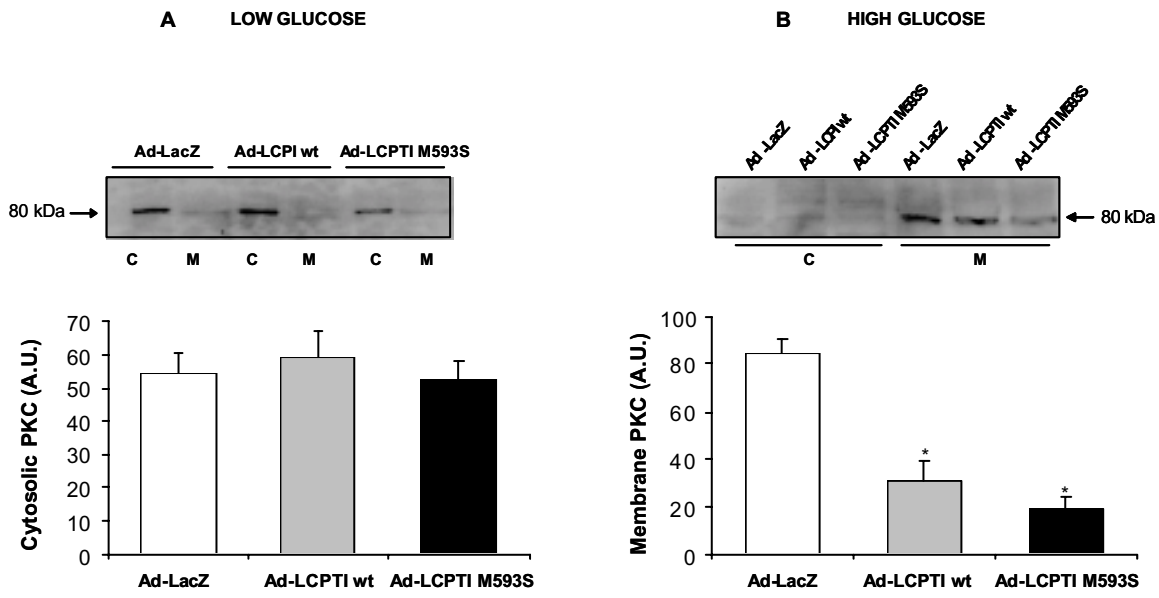
A
LOW GLUCOSE
Ad-LacZ
Ad-LCPI wt
Ad-LCPTI M593S
80 kDa
C
M
C
M
C
M
Cytosolic PKC (A.U.)
70
60
50
40
30
20
10
0
Ad-LacZ
Ad-LCPTI wt
Ad-LCPTI M593S
B
HIGH GLUCOSE
Ad-LacZ
Ad-LCPI wt
Ad-LCPTI M593S
Ad-LacZ
Ad-LCPI wt
Ad-LCPTI M593S
80 kDa
C
M
Membrane PKC (A.U.)
100
80
60
40
20
0
*
*
Ad-LacZ
Ad-LCPTI wt
Ad-LCPTI M593S

Submitted

C75-CoA inhibits Carnitine Palmitoyltransferase I activity thus decreasing palmitate oxidation

Assia Bentebibel*, David Sebastián*, Laura Herrero*, Dolors Serra, Guillermina Asins and Fausto G. Hegardt

Department of Biochemistry and Molecular Biology, School of Pharmacy, University of Barcelona, E-08028, Spain

Running title: C75-CoA is an inhibitor of CPT I activity

Keywords: C75, fatty acid oxidation, carnitine palmitoyltransferase I, etomoxir, obesity.

Author to whom correspondence should be addressed:

Prof. Fausto G. Hegardt

Department of Biochemistry and Molecular Biology, School of Pharmacy, University of Barcelona, Diagonal 643, E-08028, Spain

Phone: +34 93 4024523

Fax: +34 93 4024520

e-mail: fgarciaheg@.ub.edu

* these authors contributed equally to the work

ABSTRACT

C75 is described as a potential drug for treatment of obesity and type II diabetes. First known as a synthetic inhibitor of fatty acid synthase (FAS), it has been also described as an activator of carnitine palmitoyltransferase I (CPT I), increasing peripheral energy utilization and fatty acid oxidation in mice. To further investigate the C75/CPT I interaction, we have characterized the effects of C75 on CPT I *in vitro* and *in vivo*. C75 itself has no effect on either yeast-overexpressed L- and M- CPT I isoforms or in purified mitochondria from rat liver and muscle. However, the CoA derivative, C75-CoA, strongly inhibits yeast-overexpressed L- and M- CPT I isoforms, as does etomoxiryl-CoA, a potent inhibitor of CPT I. The binding of CPT I to C75-CoA is irreversible. Moreover, C75-CoA inhibits CPT I activity in purified mitochondria from rat liver and muscle. The IC50 values for either L- or M-CPT I isoforms fall in a similar micromolar range to those observed for etomoxiryl-CoA. When INS(823/13), L6E9 or HEK293 cell lines are incubated with C75, CPT I activity is inhibited, as is fatty acid oxidation. *In vivo*, a single intraperitoneal injection of C75 to mice produces a short-term inhibition of CPT I activity in mitochondria from liver, soleus and pancreas, suggesting that in cellular models and in lean mice, C75 is transformed into its C75-CoA derivative, which directly inhibits CPT I activity. Overall, these findings provide compelling evidence that C75, through its activated form C75-CoA, is a potent inhibitor of CPT I.

Abbreviations used: FAS: Fatty acid synthase; L-CPT I: carnitine palmitoyltransferase I, liver isoform; M-CPT I: carnitine palmitoyltransferase I, muscle isoform; KRBH buffer: Krebs-Ringer Bicarbonate Hepes buffer

INTRODUCTION

C75 is a chemically stable synthetic inhibitor of fatty acid synthase (FAS) derived from cerulenin, a natural product obtained from the fungus *Cephalosporium caerulens*. It binds irreversibly to the catalytic site of both type I (mammalian and yeast) and type II (bacterial) FAS, by covalent modification of the β-ketoacyl-acyl carrier protein synthase domain (1, 2). Structurally, C75 is a cell-permeable α-methylene-γ-butyrolactone, designed to be less reactive and potentially safer than cerulenin. It lacks the reactive epoxide present on cerulenin, which enhances chemical stability and specificity (Fig. 1). C75 inhibits purified mammalian FAS with the characteristics of a slow-binding inhibitor (3), inducing cytostatic and cytotoxic effects in cultured tumour cells, and exhibiting significant growth inhibitory effects on human breast cancer xenografts (4, 5).

C75 has several other interesting properties. It decreases food intake and fat mass and results in a strong loss of weight in both lean and fat mice (leptin-deficient (*ob/ob*) or diet-induced obese (DIO) mice) (6-10). It has been hypothesized that C75 may alter the metabolism of neurons in the hypothalamus that regulate feeding behaviour. Recent evidence (6, 11, 12) has implicated malonyl-CoA, an intermediate in fatty acid biosynthesis, as a possible mediator in the hypothalamic pathway that indicates energy status and mediates the feeding behaviour of mice. Intra-cerebroventricular administration of C75 increases cellular malonyl-CoA in the hypothalamus (12), caused by inhibition of FAS, and blocks fasting-induced up-regulation of hypothalamic neuropeptide Y, thus reducing food intake (6). Furthermore, it appears that C75 exerts its short and long-term effects on food intake by preventing the up-regulation of the orexigenic neuropeptides and down-regulation of the anorexigenic neuropeptides (9, 13).

In addition to the hypothalamic actions, it has been described that C75 decreases fat mass in peripheral tissues by increasing fatty acid oxidation through the stimulation of carnitine palmitoyltransferase (CPT) I (7, 8). This enzyme is the main regulatory mitochondrial step of fatty acid oxidation (14) and it facilitates the transport of long-chain acyl-CoA into mitochondria, thus leading to the release of energy by β-oxidation of fatty acids. Mammalian tissues express three isoforms of CPT I: liver (L-CPT I) (15, 16) muscle (M-CPT I) (17, 18) and brain (CPT I-C) (19). CPT I is tightly regulated by

its physiological inhibitor malonyl-CoA, and thus it confers to CPT I the ability to signal the availability of lipid and carbohydrate fuels to the cell (14). The malonyl-CoA sensitivity of L-CPT I in the adult rat depends on the physiological state. It is increased by re-feeding carbohydrates to fasted rats, by obesity or after insulin administration to diabetic rats, whereas it is decreased by starvation and diabetes (20, 21)

When C75 is given to mice, the inhibition of FAS produces an increase of cellular malonyl-CoA content which should decrease CPT I activity. Paradoxically, however, *in vivo*, the inhibitory effect on CPT I, caused by the high content of malonyl-CoA in peripheral tissues, is overcome by C75-stimulated CPT I activity (7, 8). In order to examine this paradox we tested the direct effect of C75 on CPT I activity. We show that C75 itself neither inhibits nor activates CPT I. In contrast, C75-CoA inhibits both L- and M-CPT I isoforms with similar kinetics to etomoxiryl-CoA, a well-known inhibitor of CPT I. The inhibition of CPT I activity is also observed in pancreas, muscle and kidney cell cultures incubated with C75. These effects were followed by a decrease of fatty acid oxidation. Finally, in mice treated with a single intraperitoneal (i.p.) injection of C75, CPT I activity decreased but later recovered.

EXPERIMENTAL PROCEDURES

Animals

Six-week-old C57BL/6J male mice were purchased from Harlam Co. Animals were maintained under a 12-h dark/light cycle at 23ºC with free access to food and water. After a 1-week acclimatization, experiments with animals were performed. Male Sprague Dawley rats (180-200 g) bred in our laboratory were used to obtain liver and soleus. All the experimental protocols were approved by the Animal Ethics Committee at the University of Barcelona.

Materials

L-[*methyl*-^{3}H]carnitine hydrochloride and [1-^{14}C]palmitic acid were purchased from Amersham Biosciences. C75 was purchased from Alexis Biochemicals and etomoxir was provided by Dr. H.P.O. Wolf (GMBH, Allensbach, Germany). Yeast culture media products were from Difco. Bradford solution for protein assay was from Bio-Rad. Dulbecco's modified Eagle's medium (DMEM), RPMI 1640 and antibiotics were from Gibco-Invitrogen Corporation. Defatted bovine serum albumin (BSA), palmitate, malonyl-CoA and other chemicals were purchased from Sigma-Aldrich. Acyl-CoA synthase from *Pseudomonas sp*. was obtained from Fluka.

Activation of C75 and etomoxir to C75-CoA and etomoxiryl-CoA

Etomoxir and C75 were activated to CoA derivatives in the presence of CoA-SH (22). The reaction was performed with 1 µmol of each drug separately in a total volume of 1 ml of a buffer containing 0.1% (w/v) Triton X-100, 5 mM CoA-SH, 10 mM ATP, 1 mM DTT, 10 mM $MgCl_2$, 100 mM MOPS-NaOH pH 7.5 and 0.25 U of Acyl-CoA synthase from *Pseudomonas sp*. The reaction was carried out at 35 ºC for 2 h. We assumed that the conversion of C75 and etomoxir to their CoA derivatives was complete. Stock aliquots, where the final concentration of each CoA derivative was 1 mM, were stored at –20ºC and diluted in 100 mM MOPS-NaOH pH 7.5 for activity assays.

Mass spectrometry

The MALDI-TOF mass spectra of C75-CoA and etomoxiryl-CoA were obtained on a Voyager DE-RP (Applied Biosystems) mass spectrometer equipped with a nitrogen

laser (337 nm, 3 ns pulse). The acceleration voltage was set to 20 kV. Data were acquired in the reflector mode with delay times of 320 ns for both the positive and negative polarities. Spectra were calibrated externally using a calibration mixture (Calibration Mixture 1, Applied Biosystems): CHCA, des-Arg^1-Bradykinin, Angiotensin I, Glu^1-Fibrinopeptide B, Neurotensin m/z 300-1700.

Samples were prepared by diluting 1 µl of each drug in the activation buffer to 100 µl with H_2O, and mixing 1 µl of this diluted solution with 1 µl of matrix solution (10 mg/ml of 2,5-dihydroxybenzoic acid (2,5-DHB, Aldrich) in methanol:water 1:1). One microliter of the sample:matrix mixture was spotted onto the stainless steel sample plate, allowed to evaporate to dryness in air and introduced into the mass spectrometer. Spectra were acquired in the positive and negative ion mode. MALDI-TOF spectra were performed by the Mass Spectrometry Service (SCT, University of Barcelona).

Expression of CPT I in Saccharomyces cerevisiae

Saccharomyces cerevisiae was chosen as a heterologous expression system because it does not express endogenous CPT activity. The plasmid, pYES2-L-CPT I encoding the liver isoform of CPT I was obtained as previously described (23). The plasmid pYES-M-CPT I was obtained from the plasmid DS112-36 (18) containing the coding cDNA of rat muscle CPT I isoform. The fragment that encompassed nucleotides 27-2432, including the coding region of M-CPT I, was subcloned into the *S. cerevisiae* expression plasmid pYES2 (Invitrogen). A *Hin*dIII site (underlined) was introduced by PCR immediately 5' of the ATG start codon of M-CPT I to enable cloning into the unique *Hin*dIII site of plasmid pYES2. A consensus sequence (in boldface type), optimized for efficient translation in yeast, was also introduced in the same PCR, using the forward primer CPT I *Hin*dIII.for (5'-TCG AT<u>A AGC TT</u>**A TAA A**AT GGC GGA AGC ACA CCA GGC AG-3') and the reverse primer CPT I *Hin*dIII.rev (5'-GGA AGC TTG GGC AGT GAT GT-3'). The resulting fragment of 550 pb obtained after the digestion of PCR products with *Hin*dIII, was ligated on pYES2 plasmid digested with the same restriction enzyme, yielding the plasmid pYES2-M-CPT I-ATG. This plasmid was digested with *Sal*I (in cDNA of M-CPT I) and *Sph*I (in plasmid pYES2) and ligated with the CPT I fragment *Sal*I - *Sph*I (purified band of 2351 bp), producing pYES2-M-CPT Ipre. The sequence TTTTTTA (387-393 nt) present in the M-CPT I cDNA, which resembles a known yeast polyadenylation signal (24), was subsequently changed by PCR in order to increase expression levels in yeast without changing the amino acid

sequence, producing pYES-M-CPT I. The appropriate substitutions and the absence of unwanted mutations were confirmed by sequencing the inserts in both directions with an Applied Biosystems 373 automated DNA sequencer. The expression of the plasmids pYES-L-CPT I and pYES-M-CPT I in yeast was performed as described in (23).

Cell culture

The clonal β cell line INS(832/13) (25), derived and selected from the parental rat insulinoma INS-1 (26), was kindly given by Dr. M. Prentki (Montreal, Canada). Cells were cultured (passages 48-60) in a humidified atmosphere containing 5% CO_2 in complete medium composed of RPMI 1640 containing 11 mM glucose and supplemented with 10% heat inactivated FBS (Wisent Inc, USA), 10 mM HEPES, 2 mM glutamine, 1 mM sodium pyruvate, 50 mM 2-mercaptoethanol, 100 U/ml penicillin and 100 μg/ml streptomycin. The maintenance culture was passaged once a week by gentle trypsinization and cells were grown until confluence in Falcon dishes.

The L6E9 rat skeletal muscle cell line was kindly provided by Dr. A. Zorzano (University of Barcelona). Cells were cultured in a humidified atmosphere containing 5% CO_2 in complete medium composed of DMEM containing 10% FBS (Gibco-Invitrogen Corporation), 100 units/ml penicillin, 100 μg/ml streptomycin and 25 mM HEPES pH 7.4 (Growth Medium). Pre-confluent myoblasts (80-90%) were induced to differentiate by lowering FBS to a final concentration of 2% (Differentiation Medium). All the experiments were performed with completely differentiated myotubes (after 4 days in Differentiation Medium).

Human Embryonic Kidney (HEK) 293 cells obtained from ECACC (European Collection of Cell Cultures) were cultured in a humidified atmosphere containing 5% CO_2 in complete medium composed of DMEM containing 10% FCS (Biological Industries), 100 units/ml penicillin and 100 μg/ml streptomycin. For experiments cells were grown until 80% confluence.

Preparation of mitochondrial fractions

Mitochondria-enriched fractions from yeast overexpressing L- and M-CPT I were obtained as described previously (23). Mitochondria-enriched cell fractions from INS(832/13), L6E9 and HEK293 cells cultured in 15-cm dishes, were obtained with a glass homogenizer as previously described (27). The pellet, in which the mitochondria

remain largely intact, was used directly for CPT I activity assay.

To obtain mitochondria-enriched fractions from rat and mice muscle, two soleus muscle samples of each animal were homogenized separately in 250 mM sucrose buffer using an omni mixer and then centrifuged at 1,000 x*g* for 15 min. The pellet was homogenized and centrifuged at 600 x*g* for 10 min. The resulting supernatant was centrifuged at 15,000 x*g* for 15 min and the pellet was resuspended in 100 µl of 250 mM sucrose and 150 mM KCl solution (28). Mitochondria-enriched fractions from rat and mouse liver were obtained and mechanically homogenized in a buffer containing 250 mM sucrose, 1 mM EDTA and 10 mM Tris/HCl, pH 7.4. Liver suspension was centrifuged at 560 x*g* for 15 min and the supernatant was further centrifuged at 12,000 x*g* for 20 min. Pellet was resuspended in 2 ml of homogenization buffer, centrifuged for 10 min at 7,000 x*g*, washed and resuspended in 1 ml of the same buffer (28). To obtain mitochondria-enriched fractions from mice pancreas, tissue was homogenized in a buffer containing 250 mM sucrose, 20 mM Tris/HCl pH 7.4, 0.5 mM EDTA, 0.5 mM EGTA, 1 mM DTT, 10 µg/ml leupeptine, 4 µg/ml aprotinin, 2 µg/ml pepstatin and 100 µM PMSF. The homogenate was subjected to differential centrifugation at 900 x*g* for 10 min and at 5,500 x*g* for 10 min. The pellet was resuspended with a Dounce homogenizer and centrifuged at 2,000 x*g* for 2 min and at 4,000 x*g* for 8 min. Finally, the pellet was resuspended in 250 µl of 250 mM sucrose (29). All the processes were performed at 4 ºC and fractions were assayed immediately for determination of CPT I activity.

Determination of CPT I activity

CPT I activity was measured in mitochondria-enriched fractions obtained from yeast, cells or tissues as described above. CPT I activity in 3-4 µg of yeast protein extracts, 10-15 µg of mitochondria-enriched cell fractions or 20 µg of mitochondria fractions from tissues was determined by the radiometric method as previously described (23). Extracts were preincubated at 30 ºC for different times in the presence or absence of drugs. Enzyme activity was assayed for 4 min at 30 °C in a total volume of 200 µl. The substrates were 50 µM palmitoyl-CoA and 400 µM or 1000 µM L-[methyl-^{3}H]carnitine for L- and M- CPT I isoforms respectively. In yeast extracts only the overexpressed L-CPT I or M-CPT I activity is present. In tissues and cell culture extracts both CPT I (sensitive to malonyl-CoA) and CPT II (insensitive to malonyl-CoA) are present, therefore in these

fractions CPT I activity was determined as the malonyl-CoA/etomoxiryl-CoA sensitive CPT activity. CPT II activity was always subtracted from total activity to calculate specific CPT I activity. The presence of CPT activity sensitive to malonyl-CoA in cell cultures is less than 5% and thus it was not taken into consideration. Concentrations of drugs ranging from 0.02 to 50 μM were used to estimate the IC_{50} value. 50 μM malonyl-CoA was used for malonyl-CoA inhibition assay. All protein concentrations were determined using the Bio Rad protein assay with bovine albumin as standard.

Binding assays

To evaluate the binding of CoA derivatives to CPT I, experiments were performed based on the procedures described in (30) with some modifications. Yeast mitochondria preincubated for 5 min at 30 ºC with 50 μM of each derivative-CoA were directly used for the CPT I activity assay (unwashed) or centrifuged at 13,000 xg for 5 min at 4 ºC and resuspended (washed) in buffer 5 mM Tris/HCl pH 7.2, 150 mM KCl, 10 μg/ml leupeptine, 500 μM benzamidine, 1 μg/ml pepstatin and 100 μM PMSF before the assay. CPT I activity assay was performed for 4 min at 30 ºC as described above.

C75 treatment of cell cultures and administration to mice

Cells were incubated with either C75 at 10, 20, 30 or 40 μg/ml or etomoxir at 30 or 40 μg/ml in the culture medium. Stock solutions of C75 and etomoxir were prepared at 100 mM in DMSO. Control cells were incubated with the same amount of DMSO. L6E9 myotubes were incubated for 2 h at 37 ºC and INS(832/13) and HEK293 cells were incubated for 1 h at 37ºC. After this time, cells were washed in PBS and either the CPT I activity, palmitate oxidation or cell viability were measured.

Mice were given a single i.p. injection of C75, dissolved in RPMI 1640 medium, at 20 mg/kg body weight or medium alone for control. Animals were sacrificed at different times post-injection and mitochondria-enriched fractions from liver, soleus and pancreas were obtained as described above. Fractions were assayed immediately for determination of CPT I activity.

Measurement of fatty acid oxidation

Palmitate oxidation to CO_2 was measured in culture cells grown in 12-well plates. On the day of the assay cells were washed in KRBH plus 0.1% defatted BSA, preincubated at 37 ºC for 30 min in KRBH 1% BSA and washed in KRBH 0.1% BSA. Cells were then incubated for 2 h at 37 ºC with fresh KRBH containing 2.5 mM glucose in the presence of 0.8 mM carnitine plus 0.25 mM palmitate and 1 μCi/ml [1-^{14}C]palmitic acid bound to 1% (w/v) BSA. Oxidation measurements were performed by a CO_2-capture system assay as previously described (31).

Viability cell culture assay

To evaluate the cytotoxic effect of the drugs, the MTT [3-(4,5-dimethylthiazol-2-yl)-2,5-diphenyltetrazolium bromide] assay was performed (32). Cells were seeded in 12-well plates and incubated with drugs as described above. After this, 200 μl of 0.25% (w/v) MTT was added to each well and cells were further incubated for 2 h. After that, the formazan crystals formed were solubilized by adding 1 ml of MTT lysis solution (10% (w/v) SDS and 1 mM acetic acid in DMSO) and the absorbance at 570 nm was measured. The results are expressed as the percentage of absorbance related to control cells.

Statistical Analysis

Data are expressed as means ± SE for at least three independent experiments. The significance of differences was assessed by unpaired Student's *t* test.

RESULTS

Effect of C75 and C75-CoA on yeast-expressed L- and M-CPT I activity

Yeast-overexpressed mitochondrial L-CPT I and M-CPT I were incubated independently with different concentrations of C75 (Fig. 1). The drug neither inhibited nor activated CPT I from either L- or M- isoform (Fig. 2A and 2B). In parallel, we also determined the inhibition of both CPT I isoforms with etomoxir, a well-known inhibitor of CPT I activity. Etomoxir did not inhibit either form of CPT I (Fig. 2C and 2D).This is in agreement with the fact that the active inhibitory form of etomoxir is its CoA-derivative, etomoxiryl-CoA (33). To test whether C75 needs to be converted to C75-CoA derivative to be pharmacologically active, both drugs were transformed to their CoA derivatives in the presence of CoA by the action of acyl-CoA synthase as described in EXPERIMENTAL PROCEDURES. The CoA derivatives of both drugs strongly inhibited both CPT I isoforms with similar kinetics (Fig. 2). IC_{50} values for C75-CoA were 0.24 and 0.36 μM for L- and M-CPT I isoforms respectively (Table I).

To confirm that C75 reacted with CoA to produce a stable derivative, a MALDI-TOF analysis was carried out. Figure 3A shows the peak of 1020.4 Da corresponding to the molecular mass of the product formed by the reaction of the two compounds C75 and CoA. A similar analysis for etomoxiryl-CoA (Fig. 3B) shows the peak of 1064.0 Da. Other peaks correspond to products derived from either CoA, C75 or etomoxir.

The binding of C75-CoA to CPT I is stable

To assess whether binding of C75-CoA to CPT I is stable, yeast mitochondrial enriched fractions overexpressing L-CPT I were incubated with 50 μM C75-CoA, etomoxiryl-CoA or malonyl-CoA, or with buffer alone as a control. After 5 min of preincubation, extracts were assayed directly (unwashed samples) or centrifuged and resuspended in buffer (washed samples) (see EXPERIMENTAL PROCEDURES) and assayed for CPT I activity. As shown in Figure 4, malonyl-CoA inhibition was reversible, and CPT I activity was recovered at 91% after washing with respect to control washed fractions. However, both C75-CoA and etomoxiryl-CoA produced a permanent inhibition, 75% and 79% respectively with respect to control washed fractions. The experiments with C75-CoA show that it is tightly bound to CPT I, as is etomoxiryl-CoA, a well-known irreversible covalently-bound inhibitor of CPT I.

C75-CoA inhibits CPT I activity from rat liver and muscle mitochondria

Since it had been reported that C75 activated but did not inhibit CPT I (7), we carried out additional experiments with isolated mitochondria from rat liver and muscle. C75 did not inhibit nor activated liver or muscle CPT I activity. However, both C75-CoA and etomoxiryl-CoA inhibited CPT I activity from mitochondria with similar kinetics (Fig. 5A and 5B). At 50 μM of each product, CPT I was almost completely inhibited. IC_{50} values for C75-CoA and etomoxiryl-CoA were respectively 0.37 μM and 0.56 μM for L-CPT I and 0.015 and 0.71 μM for M-CPT I (Table I). C75-CoA appears to be a stronger inhibitor for M- than L-CPT I.

C75-CoA inhibits CPT I activity of mitochondrial-enriched fractions from pancreatic and muscle cultured cells.

The inhibitory effect of C75-CoA and etomoxiryl-CoA was also tested on purified mitochondria from cultured cells from pancreas (INS(832/13)) and muscle (L6E9). In all cases CPT I activity was strongly inhibited at increasing concentrations of both CoA-derivatives (Fig. 5C and 5D). The IC_{50} values for C75-CoA were 0.25 μM and 0.46 μM for INS(812/13) and L6E9 cells respectively. The IC_{50} values for etomoxiryl-CoA were 1.21 μM and 2.87 μM for INS(823/13) and L6E9 cells, respectively (Table I). Again, C75-CoA was a slightly more potent CPT I inhibitor than etomoxiryl-CoA.

Effects of C75 on CPT I activity and fatty acid oxidation in cultured cells

To assess whether CPT I inhibition by C75-CoA is followed by a similar decrease in fatty acid oxidation, three cultured cell lines INS(812/13), L6E9 and HEK293 were incubated with C75, and etomoxir as a control. It was not necessary in this case to transform the drugs to their CoA derivatives, since this conversion occurs inside the cells *via* the mitochondrial long-chain acyl-CoA synthase. CPT I activity decreased at increasing C75 concentrations. CPT I activity was reduced by 49%, 62% and 62% respectively in pancreatic INS(832/13), muscle L6E9 and kidney HEK293 cells at maximal C75 concentrations of 30, 40 and 30 μg/ml respectively. In parallel, [1-^{14}C]palmitate oxidation decreased at increasing concentrations of C75 in all cultured cells. Palmitate oxidation was reduced by 62%, 84% and 68% respectively in pancreatic

INS(832/13), muscle L6E9 and kidney HEK293 cells at maximal C75 concentrations of 30, 40 and 30 μg/ml respectively (Fig. 6). Etomoxir also decreased CPT I activity and palmitate oxidation in all cell types assayed. CPT I activity was reduced by 80%, 52% and 71% respectively in pancreatic INS(832/13), muscle L6E9 and kidney HEK293 cells, and palmitate oxidation was consequently reduced by 71%, 78% and 77% respectively, with respect to control. To rule out the possibility that the inhibition of palmitate oxidation was due to an increase in cell death caused by C75, we performed viability experiments using the MTT assay. In all cases cell viability was higher than 98% of control.

Effect of C75 treatment on whole animal

We examined the effect of C75 on CPT I activity *in vivo*. Mice were injected (i.p.) with a single dose of C75 (20 mg/kg body weight) and sacrificed at different time points thereafter. Tissue samples (liver, soleus and pancreas) were taken to isolate mitochondria as described in EXPERIMENTAL PROCEDURES. CPT I activity decreased in all tissues assayed at short times (Fig. 7), but then recovered, the kinetics depending on the tissue. Inhibition of liver CPT I decreased by 59% at 1 h and by 70% after 3 h of treatment, and at 5 h CPT I values were similar to control. Muscle CPT I was inhibited by 61% at 30 min of treatment and recovered faster than the liver isoform. In pancreas CPT I activity decreased by 35% of control after 30 min of C75 treatment but recovered thereafter. In no case did CPT I activation exceed control.

DISCUSSION

In this study we investigate the interaction between C75 and CPT I. Recently, it has been published that C75 activated CPT I and fatty acid oxidation in primary cortical neurones, hypothalamus (34) and peripheral tissues (7) contributing to the weight loss observed in mice treated with C75. To further investigate this action, we choose the *S. cerevisiae* heterologous overexpression system of CPT I , which allows the separate expression of each CPT I isoforms (L- and M-), thus avoiding the occurrence of other carnitine acyltransferases like carnitine palmitoyltransferase II (CPT II), carnitine octanoyltransferase (COT) or carnitine acetyltransferase (CrAT), which are present in all mammals systems. This procedure has been used successfully by ourselves (35, 36) and others (37, 38) to study the kinetic characteristics of the various carnitine acyltransferases.

In the present study, yeast-overexpressed CPT I was clearly inhibited by C75-CoA, in a dose-dependent manner. We never observed any activation of CPT I by either C75 or C75-CoA in spite of the large number of experiments we carried out. It is important to emphasize that the drug is not active unless it is transformed to its CoA derivative. This was also observed with etomoxir, whose activated CoA derivative was identified as the active inhibitory form (33). MALDI-TOF analysis clearly showed that C75-CoA is formed when C75 is incubated with CoA in the presence of acyl-CoA synthase and ATP. As a control, etomoxiryl-CoA was also produced under the same conditions. As observed for etomoxiryl-CoA, C75-CoA binds stably to CPT I, at variance with malonyl-CoA, which releases CPT I when its concentration is decreased (by dilution).

C75-CoA, but not C75, also inhibited mitochondrial CPT I from rat liver and muscle. Isolation of mitochondrial fractions provides an excellent source of CPT I. The kinetics of inhibition were quite similar to those of etomoxiryl-CoA and malonyl-CoA (data not shown). The IC_{50} observed for CPT I from liver mitochondrial fractions (L-CPT I isoform) is 25-fold higher than that observed for M-CPT I isoform (from muscle mitochondria). M-CPT I isoform is more sensitive to C75-CoA than L-CPT I isoform. However, these differences were not observed in overexpressed yeast extracts.

The experiments performed in the present study on CPT I activity and palmitate oxidation in cultured pancreatic, muscle and kidney cells reveal a strong correlation between inhibition of CPT I activity and decrease of palmitate β−oxidation. These cells

were directly incubated with etomoxir or C75, which could enter the cell where they are converted to their CoA derivatives by endogenous acyl-CoA synthase and intracellular ATP. It is interesting to compare the present results, where CPT I is inhibited, with those obtained by others (7, 39), who observed CPT I activation in primary hepatocytes, adipocytes and in MCF-7 cells after C75 treatment. The discrepancy may be explained by differences in the method used to measure CPT I activity. Thupari *et al.* (7) performed CPT I assays in permeabilized cells, while we isolated and purified mitochondria from tissues and cultured cells. When we repeated the experiments of digitonin permeabilization in muscle cells following Thupari's protocol, we also found that CPT I is activated. However, when mitochondria were purified from these cells, we found CPT I to be inhibited. We hypothesise that digitonin permeabilization together with the C75 treatment might alter interactions between mitochondria and the cytoskeleton (40), which may either alter CPT I activity or disturb the assay. It has been suggested that changes in the lipid composition of the membrane microenvironment in which CPT I resides are important for alteration of CPT I activity (41-45). Numerous approaches (36, 38, 46-49) suggest that modulation of inter-domain interactions, for instance by covalent modification (phosphorylation) (50) of the protein, may also be involved in changes of CPT I activity. All these events may occur as a consequence of an indirect action of C75 on permeabilized cells.

It has been reported that C75 treatment of human cancer cells *in vitro* led to rapid inhibition of fatty acid synthesis, followed by inhibition of DNA replication culminating in apoptosis (4, 5). Whereas induction of apoptosis appeared related to accumulation of the substrate, malonyl-CoA, after FAS inhibition, the cytostatic effects were independent of malonyl-CoA accumulation and may have resulted from product depletion (4). To rule out the possibility that the decrease of palmitate oxidation could be produced by C75 cytotoxicity, viability studies were performed. In our conditions, viability of the three cellular models is higher than 98%. Each clonal cellular type shows characteristics distinctive of viability. For instance, pancreatic β-cells INS(832/13) and kidney HEK293 were incubated at shorter times and lower C75 concentrations than L6E9 myotubes. Depending on the lipid composition and metabolism, each cell line may be more sensitive to the cytotoxic effect of C75. For instance, breast carcinoma cell line SKBR3, with higher lipid content, needs 6 h of C75-preincubation to achieve the cytotoxic effect (5). Therefore, the decrease on palmitate oxidation, could be produced only by the inhibition of CPT I.

The *in vitro* experiments are also corroborated by the experiments *in vivo*. A single intraperitoneal C75 injection produced a short-term inhibition of CPT I in liver, muscle (soleus) and pancreas in mice. The differential extent of inhibition of CPT I seen in the different tissues could be explained by differences in the rate of C75-CoA endogenous activation and pharmacokinetics in each tissue. It is important to stress that C75 shows its maximum CPT I-inhibitory properties in the liver. As binding of C75-CoA to CPT I appears to be irreversible, inhibition of CPT I by the drug may remain stable until the modified CPT I is replaced by a new molecule. This time scale would be tissue dependent (Fig. 7). This increased turnover of the CPT I protein or different effects of C75 on other cellular signalling pathways of cellular fuel state, like the up-regulation of the expression of skeletal muscle UCP-3 (51) a protein involved cellular fatty acid metabolism, may increase the energy expenditure observed by Thupari *et al.* (7) as a consequence of a long-term action of C75.

The effects of cerulenin on CPT I activity and on fatty acid oxidation also support the present study. Cerulenin, the natural FAS inhibitor on the basis of which C75 was designed, has been shown to be an inhibitor of CPT I *in vitro* (52) and *in vivo* (53). Moreover, rat pancreatic islets treated with cerulenin did not increase palmitate oxidation (54). *In vivo*, cerulenin inhibits liver and muscle CPT I in mice after i.p. injection (53), being recovered and slightly activated after a few hours. These authors concluded that the late stimulating effect of cerulenin on CPT I activity occurred *via* the sympathetic nervous system. C75 may behave like cerulenin in mice, producing a biphasic effect on CPT I (an initial inhibition followed by recovery). This would also be consistent with he increased peripheral fatty acid oxidation observed in mice after several hours of treatment.

In conclusion, all the results presented here provide compelling evidence that C75-CoA is a potent and direct inhibitor of both isoforms L- and M-CPT I *in vitro* and *in vivo,* and suggest that in cellular models and in lean mice, C75 is transformed into its C75-CoA derivative, which directly inhibits CPT I activity. Further investigation is needed to explain the stimulation of fatty acid oxidation of C75 observed by others in peripheral tissues and the loss of body weight.

ACKNOWLEDGMENTS

We thank Dr. Yamazaki for supplying plasmid DS112-36 containing the cDNA from rat M-CPT I. This study was supported by Grants BMC2001-3048 from the Dirección General de Investigación Científica y Técnica, by grant C3/08 from the Fondo de Investigación Sanitaria of the Instituto de Salud Carlos III, Red de Centros en Metabolismo y Nutrición (RCMN) from the Ministry of Health, Madrid, Spain and by the Ajut de Suport als Grups de Recerca de Catalunya (2001SGR-00129), Spain. A.B., D.S. and L.H. are recipients of fellowships from the Ministry of Science and Technology, the University of Barcelona and the Ministry of Education, Spain, respectively. We are also grateful to Robin Rycroft of the Language Service for valuable assistance in the preparation of the manuscript.

LEGENDS TO FIGURES

Fig.1. Structure of compounds affecting CPT I activity

Fig. 2. Effect of C75, etomoxir and their derivative-CoAs on the activity of liver (L) and muscle (M) isoforms of CPT I overexpressed in yeast *S. cerevisiae*.

L-CPT I (A and C) and M-CPT I (B and D) were overexpressed in yeast and preincubated for 5 min with increasing concentrations of etomoxir (open triangles), C75 (black triangles), etomoxiryl-CoA (open circles) and C75-CoA (black circles). CPT I activity was measured and data are expressed relative to control values in the absence of drugs (100%) as the mean of three independent experiments.

Fig. 3. MALDI-TOF spectra of C75-CoA and etomoxiryl-CoA.

Spectra were directly obtained from the activation reaction product of C75-CoA and etomoxiryl-CoA using a Voyager-DE-RP from Applied Biosystems with DHB (10 mg/ml in water: methanol, 1:1). The detection was done with a reflector and in the negative mode. The product C75-CoA (A) is confirmed by the peak at 1020.4 Da and etomoxiryl-CoA (B) by the peak at 1064.0 Da.

Fig. 4. Effect of C75-CoA, etomoxiryl-CoA and malonyl-CoA on CPT I activity overexpressed in yeast *S. cerevisiae*.

3 μg of mitochondria from yeast overexpressing L-CPT I was preincubated for 5 min with 50 μM of C75-CoA, etomoxiryl-CoA and malonyl-CoA, washed or not with buffer as described in EXPERIMENTAL PROCEDURES. Specific activity was represented as the mean of three independent experiments.

Fig. 5. Effect of C75-CoA and etomoxiryl-CoA on CPT I activity.

Mitochondria isolated from rat liver (*A*), rat muscle (*B*), INS(823/13) cells (*C*) or L6E9 myotubes (*D*) were preincubated for 1 min with increasing concentrations of C75-CoA (black circles) or etomoxiryl-CoA (open circles) and CPT I activity was assayed as described in EXPERIMENTAL PROCEDURES. Rat liver and muscle mitochondria were also incubated with increasing concentrations of C75 (black triangles). Data are the mean for at least three independent experiments and are expressed relative to control

values in the absence of inhibitor (100%). Insert: expanded dose-response curve for the two inhibitors.

Fig. 6. CPT I activity and palmitate oxidation in cell cultures.

Cells were incubated for 2 h (L6E9) or 1 h (INS(832/13) and HEK293) with complete medium containing either 0, 10, 20, 30 and 40 μg/ml of C75 or 30 and 40 μg/ml of etomoxir. Mitochondria-enriched cell fractions were obtained and 10 μg of protein were used for the CPT I activity assay. In palmitate oxidation assays, cells were preincubated for 30 min at 37 ºC with KRBH 1% BSA and then incubated for 2 h at 2.5 mM glucose in the presence of 0.8 mM carnitine, 0.25 mM palmitate and 1 μCi/ml [1-^{14}C]-palmitate. Palmitate oxidation to CO_2 was measured as described in EXPERIMENTAL PROCEDURES. Data are presented as the mean ± SE of three independent experiments. *P<0.05; **P<0.01 and ***P<0.001 compared with control without inhibitors.

Fig. 7. C75 effect on the whole animal.

C75 was injected i.p. in mice and animals were sacrificed at 0, 0.5, 1, 3, and 5 h after injection. Mitochondria-enriched fractions from liver, soleus, and pancreas were obtained and CPT I activity was assayed. Results are the mean ± SE of data obtained from 6 mice. *P<0.05 *v.s*. control (0 h).

Table I. IC_{50} values of CPT I for C75-CoA and etomoxiryl-CoA.

Mitochondrial fractions obtained from yeast overexpressing CPT I, rat liver, rat muscle and cultured cells were assayed for CPT I activity in the presence of C75-CoA and etomoxiryl-CoA. IC_{50} values were calculated as described in EXPERIMENTAL PROCEDURES.

BIBLIOGRAPHY

1. Moche, M., Schneider, G., Edwards, P., Dehesh, K., and Lindqvist, Y. (1999) *J. Biol. Chem*. **274**, 6031-6034
2. Price, A.C., Choi, K-H., Heath, R.J., Li, Z., White, S.W., and Rock, C.O. (2001) *J. Biol. Chem*. **276**, 6551-6559
3. Kuhajda, F.P., Pizer, E.S., Li, J.N., Mani, N.S., Frehywot, G.L., and Townsend C.A. (2000) *Proc. Natl. Acad. Sci. USA* **97**, 3450-3454
4. Li, J-N., Gorospe, M., Chrest, F.J., Kumaravel, T.S., Evans, M.K., Han, W.F., and Pizer, E.S. (2001) *Cancer Res.* **61**, 1493-1499
5. Pizer, E.S., Thupari, J., Han, W.F., Pinn, M.L., Chrest, F.J., Frehywot, G.L., Townsend, C.A., and Kuhajda, F.P. (2000) *Cancer Res*. **60**, 213-218
6. Loftus, T.M., Jaworsky, D.E., Frehywot, G.L., Townsend, C.A., Ronnett, G.V., Lane, M.D., and Kuhajda, F.P. (2000) *Science* **288**, 2379-2381
7. Thupari, J.N., Landree, L.E., Ronnett, G.V., and Kuhajda F.P. (2002) *Proc. Natl. Acad. Sci. USA* **99**, 9498-9502
8. Thupari, J.N., Kim, E-K., Moran, T.H., Ronnett, G.V., and Kuhajda, F.P. (2004) *Am. J. Physiol. Endocrinol. Metab*. **287**, E97-E104
9. Shimokawa, T., Kumar, M.V., and Lane, M.D. (2002) *Proc. Natl. Acad. Sci. USA* **99**, 66-71
10. Kumar, M.V., Shimokawa, T., Nagy, T.R., and Lane, M.D. (2002) *Proc. Natl. Acad. Sci. USA* **99**, 1921-1925
11. Gao, S., and Lane, M.D. (2003) *Proc. Natl. Acad. Sci. USA* **100**, 5628-5633
12. Hu, Z., Cha, S.H., Chohnan, S., and Lane, M.D. (2003) *Proc. Natl. Acad. Sci. USA* **100**, 12624-12629
13. Kim, E-K., Miller, I., Landree, L.E., Borisy-Rudin, F.F., Brown, P., Tihan, T., Townsend, C.A., Witters, LA., Moran, T.H., Kuhajda, F.P., and Ronnett, G.V. (2002) *Am. J. Physiol. Endocrinol. Metab*. **283**, E867-E879
14. McGarry, J.D., and Brown, N.F. (1997) *Eur. J. Biochem.* **244**, 1-14
15. Esser, V., Britton, C.H., Weis, B.C., Foster, D.W., and McGarry, J.D. (1993) *J. Biol. Chem.* **268**, 5817-5822
16. Britton, C.H., Schultz, R.A., Zhang, B., Esser, V., Foster, D.W., and McGarry J.D. (1995) *Proc. Natl. Acad. Sci. USA* **92**, 1984-1988

17. Yamazaki, N., Shinohara, Y., Shima, A., and Terada, H. (1995) *FEBBS Lett.* **363**, 41-45
18. Yamazaki, N., Shinohara, Y., Shima, A., Yamanaka, Y., and Terada, H. (1996) *Biochim. Biophys. Acta.* **1307**, 157-161
19. Price, N., van der Leij, F., Jackson, V., Corstorphine., C, Thomson, R., Sorensen, A., and Zammit, V.A. (2002) *Genomics* **80**, 433-442.
20. Grantham B.D., Zammit V.A. (1986) *Biochem. J.* **239**, 485-488
21. Grantham B.D., Zammit V.A. (1988) *Biochem. J.* **249**, 409-414
22. Taylor, DC., Weber, N., Hogge, LR., Underhill, EW. (1990) *Anal. Biochem.* **184**, 311-316
23. Morillas, M., Gómez-Puertas, P., Roca, R., Serra, D., Asins, G., Valencia, A., and Hegardt, F.G. (2001) *J. Biol. Chem*. **276**, 45001-45008
24. Jackson, V.N., Cameron, J.M., Fraser, F., Zammit, V.A., and Price N.T. (2000) *J. Biol. Chem*. **275**, 19560-19566
25. Hohmeier, H.E., Mulder, H., Chen, G., Henkel-Rieger, R., Prentki, M., and Newgard, C.B. (2000) *Diabetes* **49**, 424-430
26. Asfari, M., Janjic, D., Meda, P., Li, G., Halban, P.A., and Wollheim, C.B. (1992) *Endocrinology* **130**, 167-178
27. Rubí, B., Antinozzi, P.A., Herrero, L., Ishihara, H., Asins, G., Serra, D., Wollheim, C.B., Maechler, P., and Hegardt, F.G. (2002) *Biochem. J.* **364**, 219-226
28. Saggerson, E.D., and Carpenter, C.A. (1986) *Biochem. J.* **236**, 137-141
29. Li, G., Kowluru, A., and Metz, S.A. (1996) *Biochem. J.* **316**, 345-351
30. Tutwiler, GF., Ryzlak, MT. (1980) *Life Sciences* **26**, 393-397
31. Collins, C.L., Bode, B.P., Souba, W.W., and Abcouwer, S.F. (1998) *Biotechniques* **24**, 803-808
32. Mosmann, T. (1983) *J. Immunol. Methods* **65**, 55-63
33. Weis, B.C., Cowan, A.T., Brown, N., Foster, D.W., and McGarry, J.D. (1994) *J Biol Chem.* **269**, 26443-26448
34. Landree, L.E., Hanlon, A.L., Strong, D.W., Rumbaugh, G., Miller, I.M., Thupari, J.N., Connolly, E.C., Hunganir, R.L., Richardson, C., Witters, L.A., Kuhajda, F.P., and Ronnet, G.V. (2004) *J. Biol. Chem*. **279**, 3817-3827
35. Morillas, M., Gómez-Puertas, P., Rubí, B., Clotet, J., Arino, J., Valencia, A., Hegardt, F.G., Serra, D., and Asins, G. (2002) *J. Biol. Chem*. **277**, 11473-11480

36. Morillas, M., Gómez-Puertas, P., Bentebibel, A., Selles, E., Casals, N., Valencia, A., Hegardt, F.G., Asins, G., and Serra, D. (2003) *J. Biol. Chem.* **278**, 9058-9063
37. Brown, N.F., Esser, V., Foster, D.W., and McGarry, J.D. (1994) *J. Biol. Chem*. **269**, 26438-26442
38. Swanson, S.T., Foster, D.W., McGarry, J.D., and Brown, N.F. (1998) *Biochem J.* **335**, 513-519
39. Yang, N., Kays, J.S., Skillman, T.R., Burris, L., Seng, T.W., Hammond, C. (2004) *J. Pharmacol. Exp. Ther*. Sep 8. *In press*
40. Guzmán, M., Velasco, G., and Geelen, M.J.H. (2000) *Trends Endocrinol. Metab.* **11**, 49-53
41. Zammit, V.A., Corstorphine, C.G., Kolodziej, M.P., and Fraser, F. (1998) *Lipids* **33**, 371-376
42. Mynatt, R.L., Greenhaw, J.J., and Cook, G.A. (1994) *Biochem. J*. **299**, 761-767
43. Brady, L.J., Silverstein. L.J., Hoppel, C.L., and Brady, P.S. (1985) *Biochem J.* **232**, 445-450
44. Zammit, V.A (1999) *Prog. Lipid. Res*. **38**, 199-224
45. Fraser, F., Padovese, R., and Zammit, V.A. (2001) *J. Biol. Chem.* **276**, 20182-20185
46. Jackson, VN., Zammit, VA., and Price, NT. (2000) *J. Biol. Chem*. **275**, 38410-38416
47. Jackson, V.N., Price, N.T., and Zammit, V.A. (2001) *Biochemistry* **40**, 14629-14634
48. Shi, J., Zhu, H., Arvidson, DN., Cregg, JM., and Woldegiorgis, G. (1998) *Biochemistry* **37**, 11033-11038
49. Shi, J., Zhu, H., Arvidson, D.N., and Woldegiorgis, G. (2000) *Biochemistry* **39**, 712-717
50. Kerner, J., Distler, A.M., Minkler, P.E., Parland, W., Peterman, S.M., and Hoppel, C.L. (2004) *J. Biol.Chem*. **279**, 41104-41113
51. Cha, S.H., Hu, Z., and Lane, M.D. (2004) *Biochem Biophys Res Commun*. **317**, 301-308
52. Thupari, J.N., Pinn, M.L., and Kuhajda, F.P. (2001) *Biochem Biophys Res Commun*. **285**, 217-23
53. Jin, Y-J., Li, S-Z., Zhao, Z-S., An, J.J., Kim, R.Y., Kim, Y.M., Baik, J-H., and Lim, S-K. (2004) *Endocrinology* **145**, 3197-3204

54. Yajima, H., Komatsu, M., Yamada, S., Straub, S.G., Kaneko, T., Sato, Y., Yamauchi, K., Hashizume, K., Sharp, GW., and Aizawa, T. (2000) *Diabetes* **49**,712-717

Fig. 1

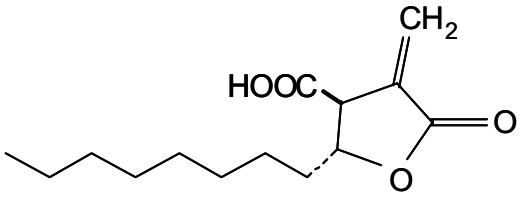

C75

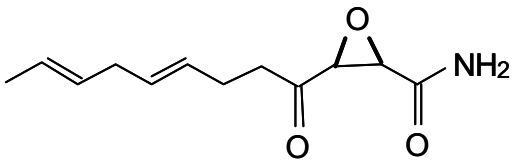

cerulenin

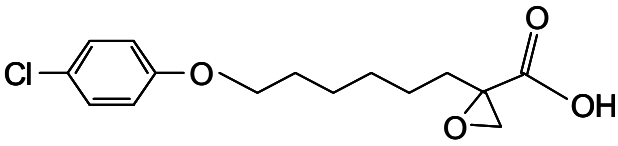

etomoxir

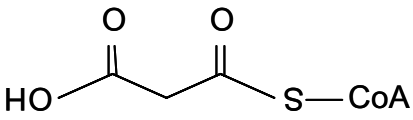

malonyl-CoA

Fig. 2

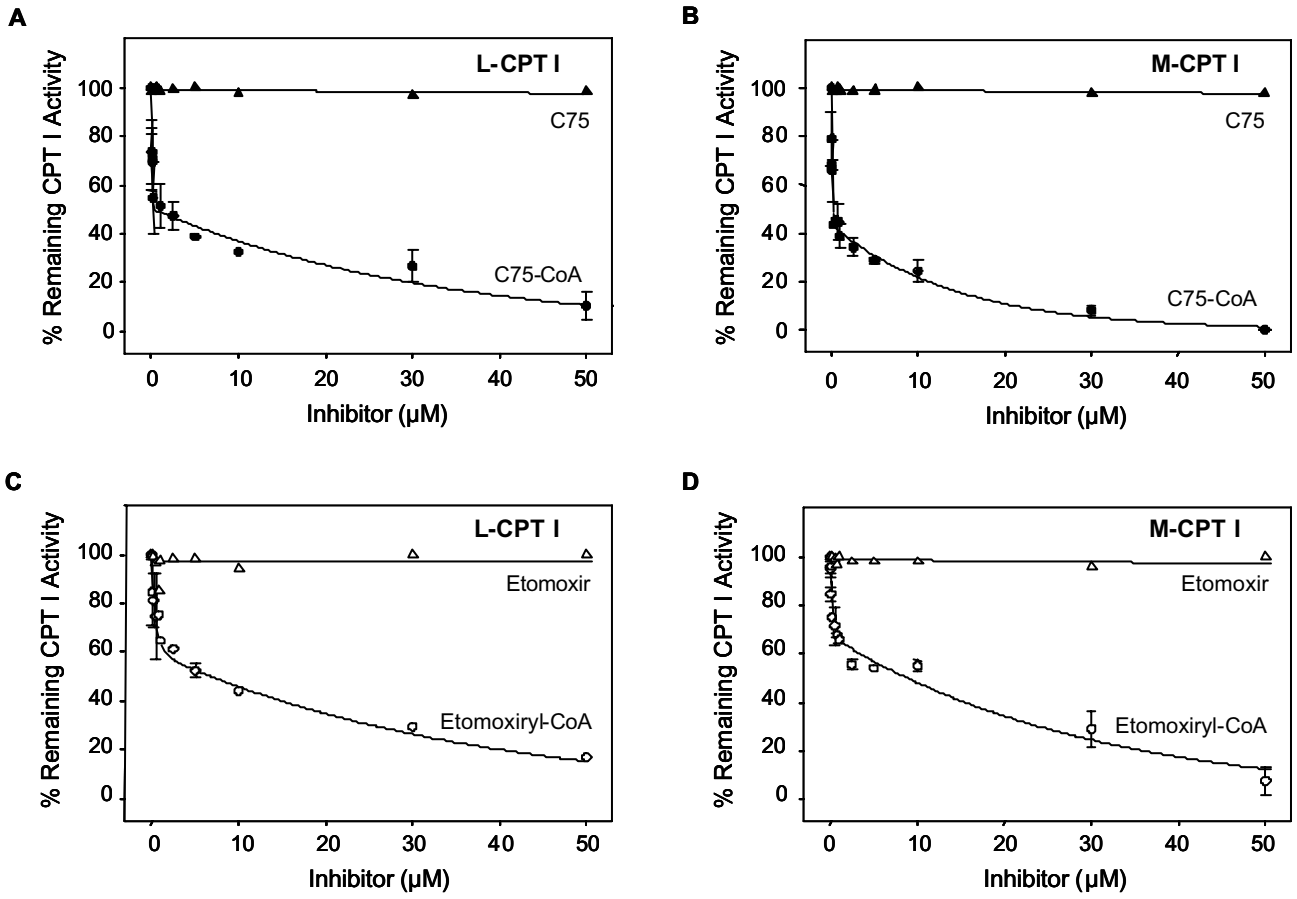
A
L-CPT I
C75
C75-CoA
% Remaining CPT I Activity
Inhibitor (μM)
B
M-CPT I
C75
C75-CoA
% Remaining CPT I Activity
Inhibitor (μM)
C
L-CPT I
Etomoxir
Etomoxiryl-CoA
% Remaining CPT I Activity
Inhibitor (μM)
D
M-CPT I
Etomoxir
Etomoxiryl-CoA
% Remaining CPT I Activity
Inhibitor (μM)

Fig. 3

A

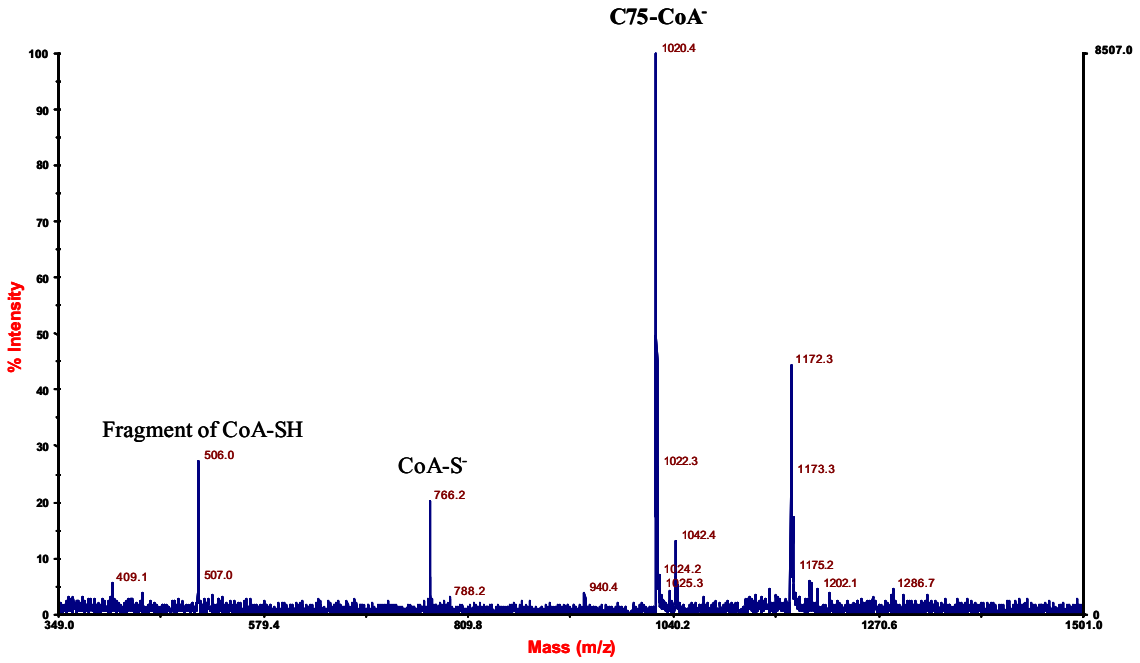
C75-CoA-
1020.4
8507.0
% Intensity
Fragment of CoA-SH
506.0
CoA-S-
766.2
1022.3
1172.3
1173.3
1042.4
409.1
507.0
788.2
940.4
1024.2
1025.3
1175.2
1202.1
1286.7
349.0
579.4
809.8
1040.2
1270.6
1501.0
Mass (m/z)

B

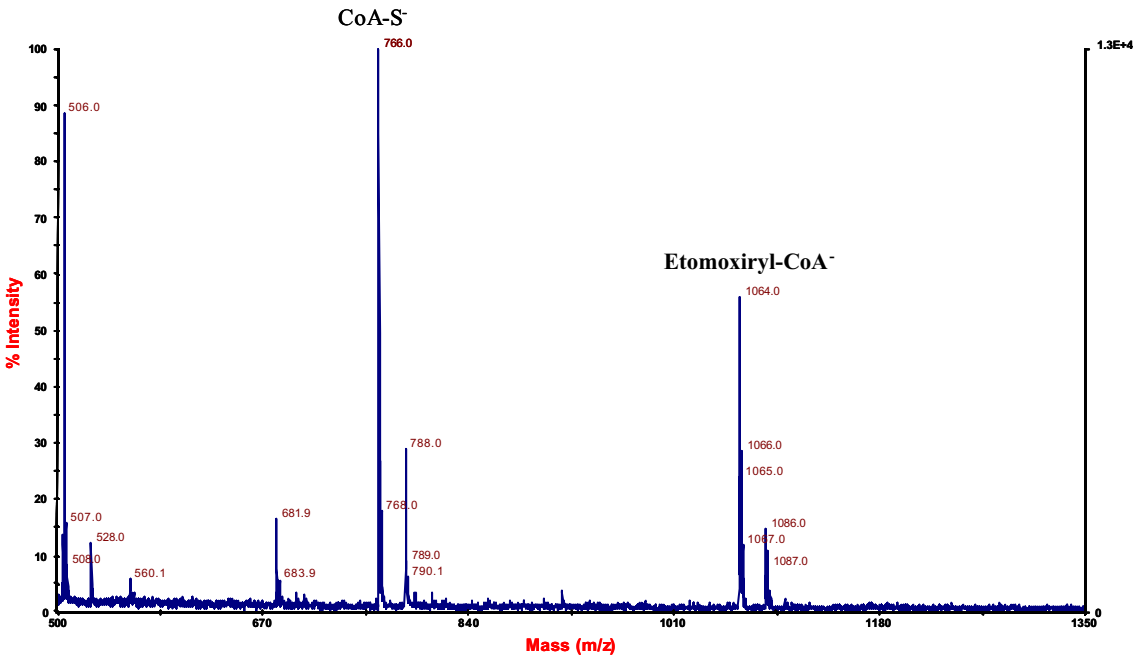
CoA-S-
766.0
1.3E+4
506.0
Etomoxiryl-CoA-
1064.0
% Intensity
788.0
1066.0
1065.0
768.0
681.9
507.0
528.0
1086.0
1067.0
508.0
560.1
683.9
789.0
790.1
1087.0
500
670
840
1010
1180
1350
Mass (m/z)

Fig. 4

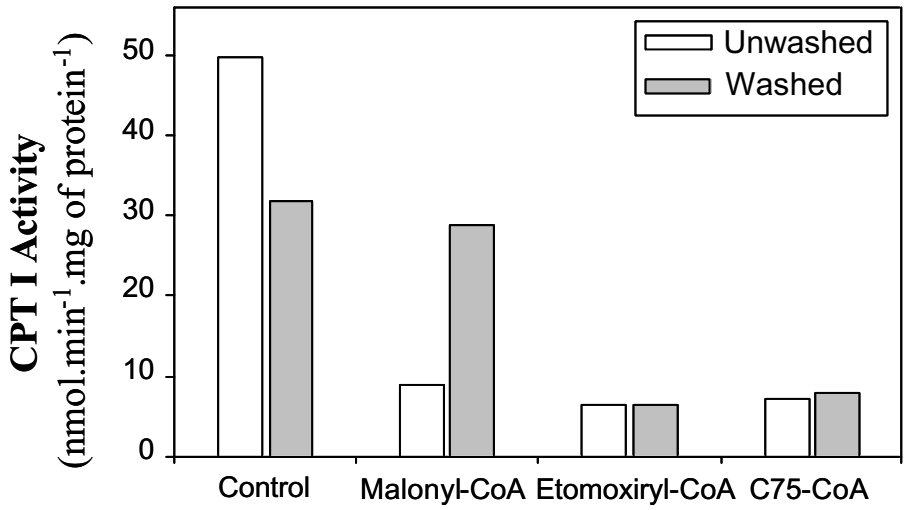
CPT I Activity
(nmol.min-1.mg of protein-1)
50
40
30
20
10
0
Unwashed
Washed
Control
Malonyl-CoA
Etomoxiryl-CoA
C75-CoA

Fig. 5

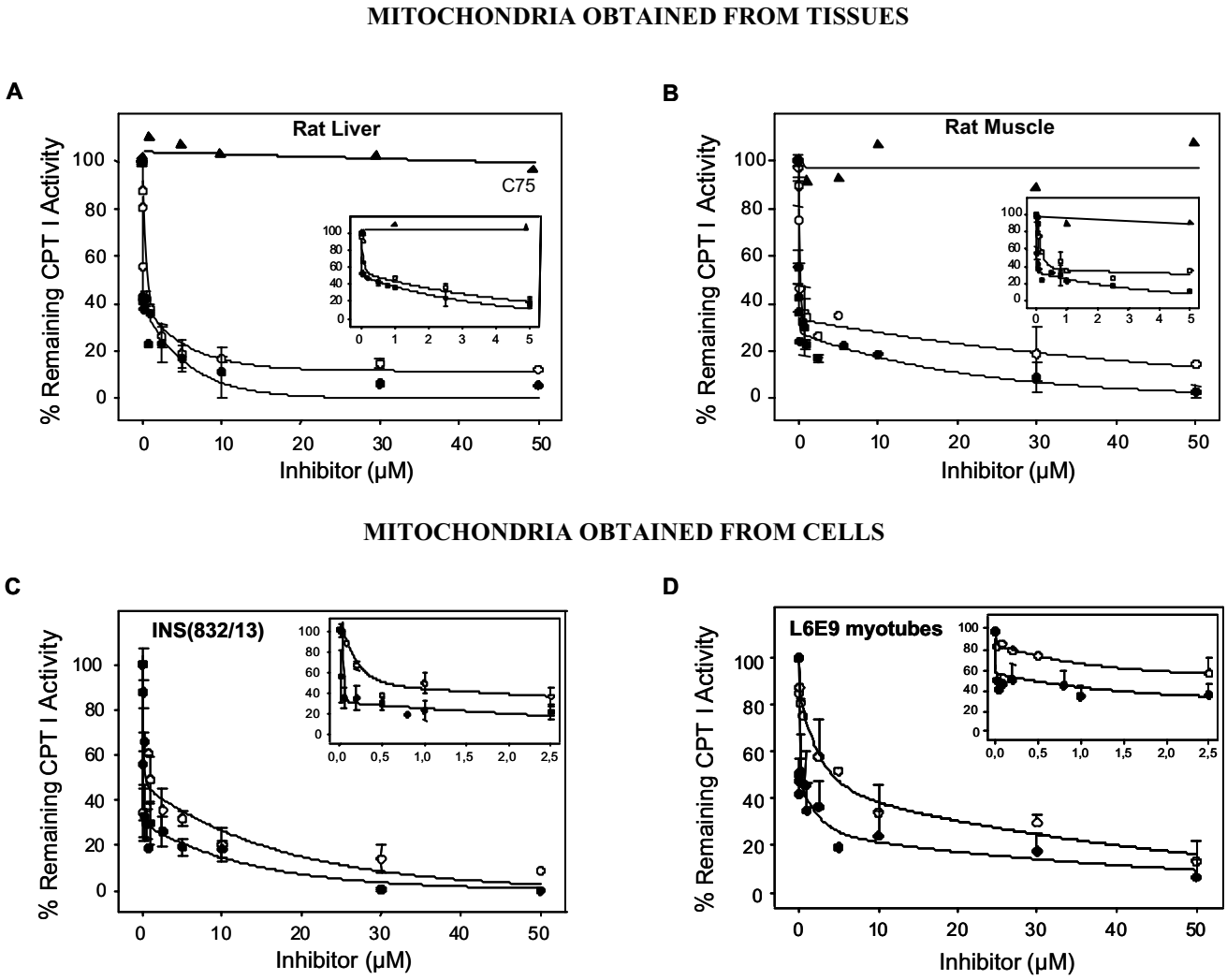
MITOCHONDRIA OBTAINED FROM TISSUES
A
Rat Liver
C75
% Remaining CPT I Activity
Inhibitor (μM)
B
Rat Muscle
% Remaining CPT I Activity
Inhibitor (μM)
MITOCHONDRIA OBTAINED FROM CELLS
C
INS(832/13)
% Remaining CPT I Activity
Inhibitor (μM)
D
L6E9 myotubes
% Remaining CPT I Activity
Inhibitor (μM)

Fig. 6

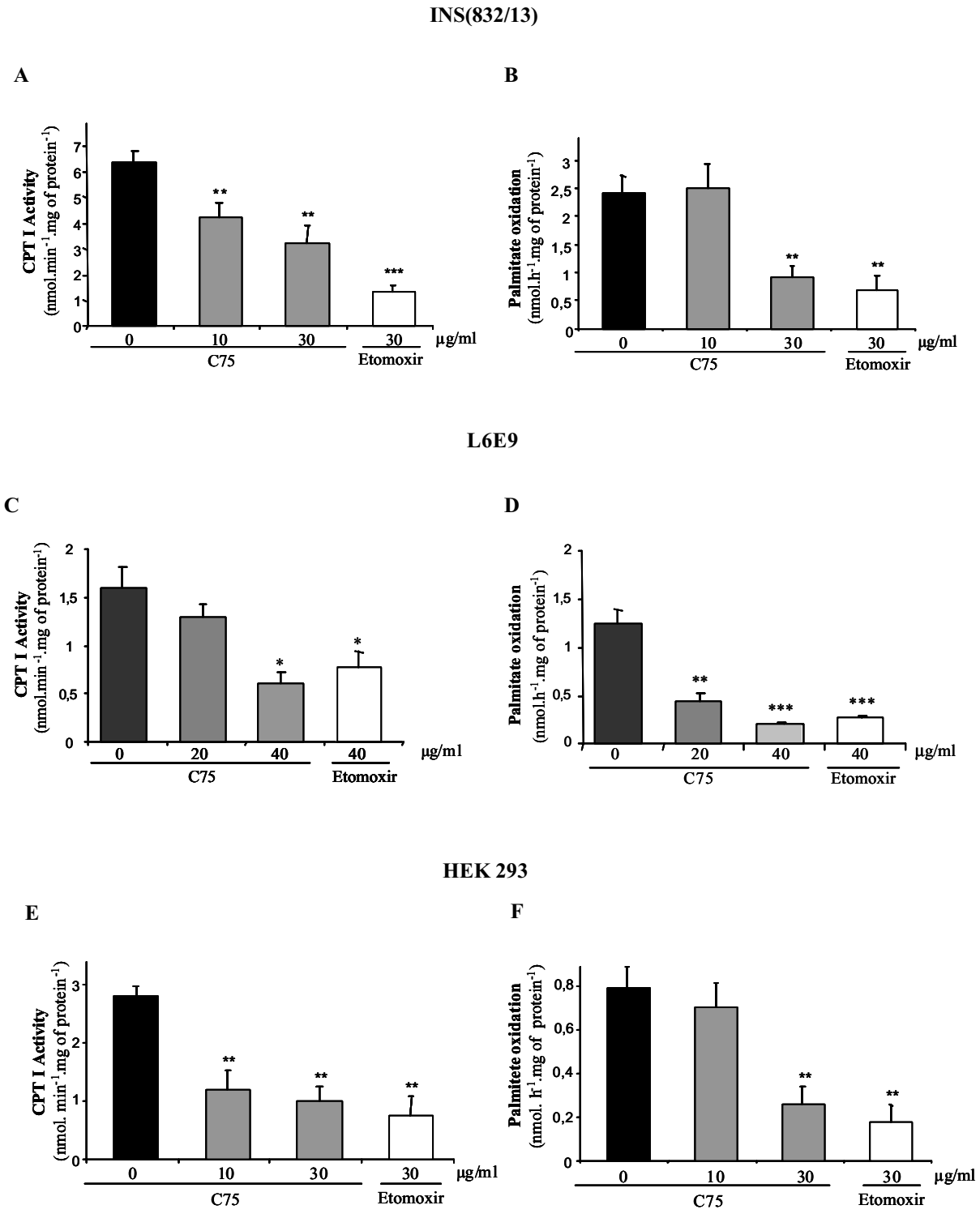
INS(832/13)
A
CPT I Activity
(nmol.min-1.mg of protein-1)
0
1
2
3
4
5
6
7
**
**
***
0
10
30
30
µg/ml
C75
Etomoxir
B
Palmitate oxidation
(nmol.h-1.mg of protein-1)
0
0,5
1
1,5
2
2,5
3
**
**
0
10
30
30
µg/ml
C75
Etomoxir
L6E9
C
CPT I Activity
(nmol.min-1.mg of protein-1)
0
0,5
1
1,5
2
*
*
0
20
40
40
µg/ml
C75
Etomoxir
D
Palmitate oxidation
(nmol.h-1.mg of protein-1)
0
0,5
1
1,5
2
**
***
***
0
20
40
40
µg/ml
C75
Etomoxir
HEK 293
E
CPT I Activity
(nmol. min-1.mg of protein-1)
0
1
2
3
**
**
**
0
10
30
30
µg/ml
C75
Etomoxir
F
Palmitete oxidation
(nmol. h-1.mg of protein-1)
0
0,2
0,4
0,6
0,8
**
**
0
10
30
30
µg/ml
C75
Etomoxir

Fig. 7

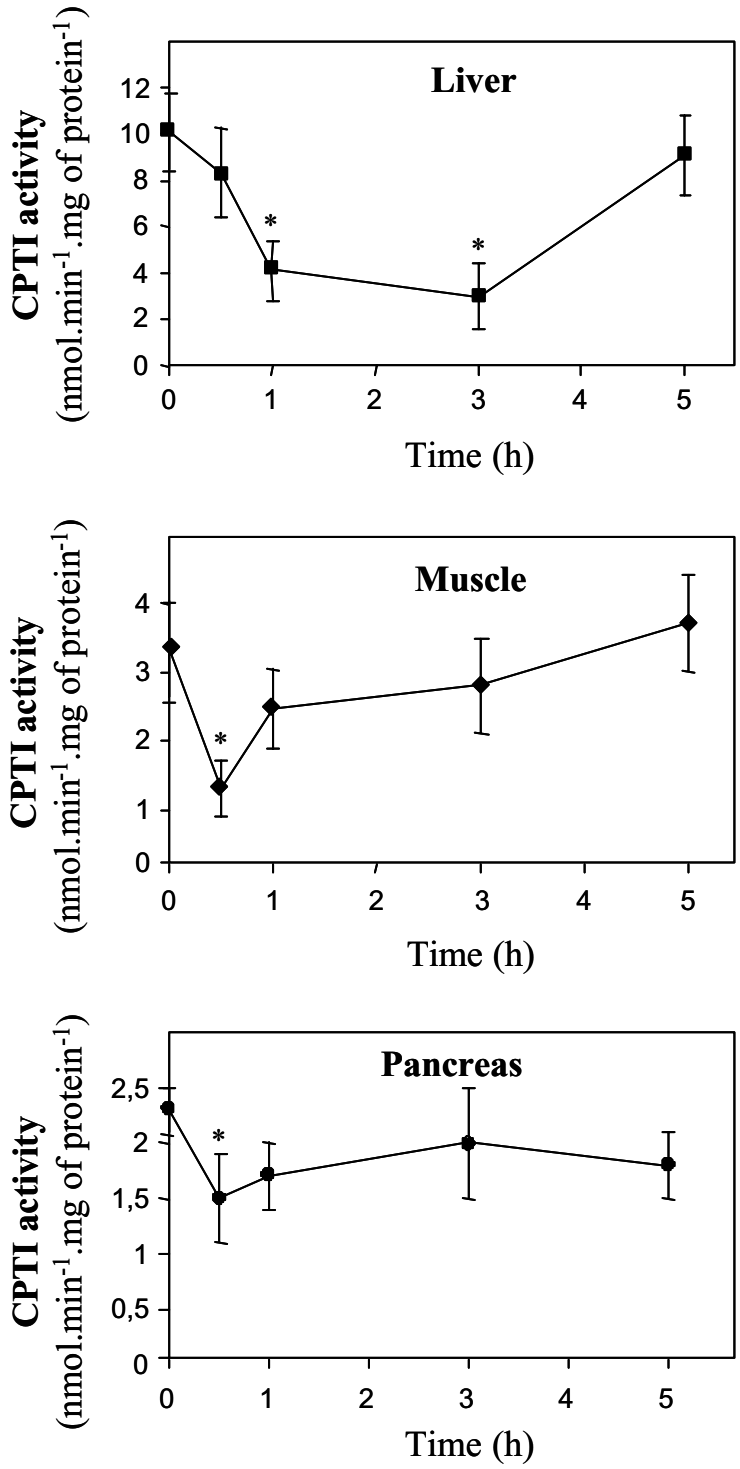
Liver
CPTI activity
(nmol.min-1.mg of protein-1)
Time (h)
Muscle
CPTI activity
(nmol.min-1.mg of protein-1)
Time (h)
Pancreas
CPTI activity
(nmol.min-1.mg of protein-1)
Time (h)

Table I

	IC_{50} *(μM)*	
	C75-CoA	etomoxiryl-CoA
Yeast overexpressing L-CPT I	0,24 ± 0,01	4,06 ± 0,78
Yeast overexpressing M-CPT I	0,36 ± 0,18	3,10 ± 0,06
Rat liver	0,37 ± 0,23	0,56 ± 0,04
Rat Muscle	0,015 ± 0,005	0,71 ± 0,05
INS(832/13) cells	0,25 ± 0,16	1,21 ± 0,35
L6E9 myotubes	0,46 ± 0,21	2,87 ± 0,87